

**The  
University  
Of  
Sheffield.**

**Department Of  
Materials Science and  
Engineering**

# **INVESTIGATING THE CLEANING EFFICACY OF NOVEL ORAL CARE FORMULATIONS**

**Raisa Karolia**

September 2015

**Thesis submitted for the Degree of Doctor of  
Philosophy**

# **Investigating the cleaning efficacy of novel oral care formulations**

*Raisa Karolia*

## **Summary**

Dentinal wear is a complex event system that is dependent on the quality of the dentinal surface and that of the toothbrush and toothpaste used. The wear properties of toothpaste mixtures are commonly characterised by the dentine abrasion it causes. This thesis aims to investigate not only this macroscopic wear but also to further analyse in detail the behaviour of the abrasive particles within toothpaste by analysing the microscopic tribological scratches caused by these abrasive particles to determine the mechanisms of their cleaning behaviour.

This project uses quantitative micro-tribological investigative methods on three different aspects of oral care:

- Calcium Carbonate particles - currently ground calcium carbonates (GCC) are the predominant abrasive particles in many commercial toothpastes. This investigation determines whether the use of uniform precipitated calcium carbonates within these mixtures is advantageous.
- Citrus fibres - citrus fibres are currently a waste product in the food industry, and sometimes used as a thickening agent in low-fat mayonnaise. Testing was done to show how the addition of these dietary fibres into toothpaste mixtures affects overall and microscopic abrasivity of the paste.
- Silica particles with polymer binders - Carbopol polymer binders are currently used in a number of commercially available toothpastes in the market today. Testing was done to determine how differing chemistries of these pastes or the method of addition of them to toothpaste mixtures affects the overall cleaning efficacy of the pastes.

Tribological testing was done to discern the wear characteristics of each paste on dentine and dentine models. Micro-visualisation techniques were then used to understand the scratch characteristics of each abrasive. Nano-manipulation techniques were employed to characterise dynamic primary movement traits. This was employed to directly observe the particles when moved, rather than only assuming dynamic movement from wear tracks.

It was found particle size is not the key factor in determining overall wear or individual scratch tenacity of particles. Instead factors such as geometry and interaction with other particles are most significant in determining how a particle operates and removes substrate material.

This research was carried out to develop an understanding of the abrasive efficacy of abrasive particles within oral care and to help further develop the next generation of toothpaste for Unilever Plc.



## **Acknowledgments**

For Salma and Seraj Karolia.

With added thanks to all those who helped make this work possible; Prof. Beverley Inkson, Prof. Rob Dwyer-Joyce, Dr. Chris Rose, Dr. Kevin Briston, Dr. Alexander Ashcroft, Unilever and the EPSRC.

## **Abbreviations**

AFM	Atomic Force Microscopy
CaCO <sub>3</sub>	Calcium Carbonate
DCJ	Dentinoenemental Junction
DEJ	Dentine Enamel Junction
ESEM	Environmental Secondary Electron Microscopy
GPa	Gigapascals (1 GPa = 1,000,000,000 Pa)
kV	Kilovolt
N	Newtons
PDL	Periodontal Ligament
PMMA	Poly(methyl methacrylate) more commonly know as acrylic
Ra	Surface Roughness
RDA	Relative Dentine Abrasion
REA	Relative Enamel Abrasion
SEM	Scanning Electron Microscopy
TEM	Transition Electron Microscopy
UMT	Universal Mechanical Tester
WD	Working Distance (distance at which microscope is focused – also the distance between the final pole piece of the lens and the sample)

## Table of Contents

Investigating the cleaning efficacy of oral care formulations.....	i
Summary.....	i
Acknowledgments.....	ii
Glossary.....	ii
CHAPTER 1 - LITERATURE REVIEW .....	1
1.1.1. The Importance of Good Dental Care.....	1
1.1.2. A Brief History of Toothpaste .....	2
1.1.3. Formulation of Toothpaste.....	3
1.1.4. Overview of Abrasives in Oral Care .....	6
1.1.4.1. Particle Types.....	7
1.1.4.1.1. Perlite.....	7
1.1.4.1.2. Hydroxyapatite.....	8
1.1.4.1.3. Silica.....	8
1.1.4.1.4. Calcium Carbonate .....	9
1.1.5. Dental Care and Unilever .....	10
1.1.6 Conclusions .....	10
1.2. Dental Substrates .....	11
1.2.1. The Structure of Teeth .....	11
1.2.1.1. Gingiva (gums).....	11
1.2.1.2. Enamel .....	12
1.2.1.3. Dentine .....	13
1.2.2. Testing Substrates .....	15
1.2.2.1. Dentine .....	15
1.2.2.2. Perspex and Copper.....	16
1.2.3. Imaging Techniques of Dental Substrates .....	16
1.2.3.1. Light Microscopy .....	16
1.2.3.2. Scanning Electron Microscopy (SEM).....	16
1.2.3.3. Environmental Scanning Electron Microscopy (ESEM).....	17
1.2.3.4. Transmission Electron Microscopy (TEM) .....	18

1.2.3.5. Focused Ion Beam (FIB) .....	18
1.2.3.6. Summary .....	19
1.2.4. Conclusions .....	19
1.3. Tribology and Toothpaste.....	19
1.3.1. Experimental Techniques .....	19
1.3.2. Mechanisms of Wear.....	20
1.3.2.1. Surface Fatigue .....	21
1.3.2.2. Abrasive Wear .....	21
1.3.3. Studies Relating to Toothbrush Interaction with Particles.....	22
1.3.4. A Review of Past Studies Concerning Tribology of Dental Abrasives ..	23
1.3.4.1. Effect of Particle Size on Dental Tribology .....	24
1.3.4.2. Effect of Loading on Dental Tribology.....	24
1.3.4.3. Effect of Co-efficient of Friction on Dental Tribology .....	25
1.3.4.4. Effect of Particle Hardness on Dental Tribology.....	26
1.3.4.5. Effect of Particle Shape on Dental Tribology.....	26
1.3.5. Summary .....	28
1.4. PhD Objectives .....	28
1.5. Thesis Layout.....	28
CHAPTER 2 - MATERIALS AND METHODS .....	30
2.1. Calcium Carbonates .....	30
2.2. Citrus Fibres.....	33
2.3. Binders with Silica Particles .....	34
2.3.1. Overview of Silica Particles Used .....	34
2.3.2. Overview of Carbopol Binders .....	34
2.4. Methods .....	36
2.4.1. Particle Sizing.....	36
2.4.2. SEM Imaging.....	37
2.4.3. Nano-manipulation .....	38
2.4.4. Preparation Process for Dental Samples. ....	40
2.4.5. Dentine Wear Trials .....	41
2.4.6. Profiling .....	42

2.2.7. Toothbrush Trials.....	43
2.2.8. Atomic Force Microscopy (AFM).....	44
2.2.9. Hardness Testing .....	44
2.3. Summary .....	45
CHAPTER 3 - CALCIUM CARBONATES AS ABRASIVES IN ORAL CARE.....	46
3.1. Determining particle characteristics .....	46
3.1.1. Evolution of Particles .....	47
3.2. Particle Agglomeration - Analysis by Particle Division .....	52
3.2.1. Experimental Procedure.....	52
3.3. Hardness Characterisation .....	53
3.3.1. Hardness Characterisation Conclusions and Discussion.....	58
3.4. Summary .....	58
CHAPTER 4 - SCRATCH ANALYSIS OF CALCIUM CARBONATE PARTICLES USING LINEAR RECIPROCATION .....	60
4.1. Introduction .....	60
4.2. Experimental Results .....	60
4.3. Conclusions .....	65
CHAPTER 5 - HUMAN DENTINE WEAR BY CALCIUM CARBONATES .....	66
5.1. Wear Testing Using Reciprocating Tribometer Experimental Approach.....	66
5.2. Results .....	66
5.2.1. Wear Depth Comparisons Through Scenarios.....	67
5.2.2. Effect of Load .....	70
5.2.3. Effect of Frequency .....	73
5.2.4. Imaging of Dentine Damage.....	72
5.2.4.1. Discussion and Conclusion of Imaging of Dentine Damage.....	80
5.2.5. Profilometry of Scratches. ....	81
5.2.6. Particle Mixtures .....	85
CHAPTER 6 - PARTICLE NANO-MANIPULATION .....	91
6.1. Background Information .....	91
6.2. Results .....	91
6.2.1. Motion of S2E.....	92

6.2.2. Motion of Sturcal L .....	94
6.2.3. Motion of Sturcal F.....	97
6.2.4. Motion of Omya 5AV.....	100
6.2.5. Motion of Rods.....	102
6.2.6. Motion of Albafil.....	102
6.3. Discussion.....	107
6.4. Conclusions .....	110
CHAPTER 7 - INTRODUCING NATURAL CITRUS FIBRES TO TOOTHPASTE FORMULATIONS TO AID IN ABRASIVE CLEANING.....	113
7.1. Overview of Fibres and Usefulness in Toothpastes.....	113
7.1.1. Citrus Fibre Characterisation.....	113
7.2. Dentinal Wear Testing with Citrus Fibres.....	114
7.3. Results .....	115
7.3.1. Experiment A .....	115
7.3.1.1. Effect of Frequency.....	122
7.3.2. Experiment B.....	122
7.3.3. Experiment C.....	128
7.3.4. Nano-manipulation .....	130
7.4. Discussion.....	130
CHAPTER 8 - SILICA AND CARBOPOL PASTES.....	133
8.1. Background .....	133
8.2. Formulation Information .....	134
8.3.1. Optical Imaging of Pastes .....	136
8.3.2. SEM Imaging of Brushed Pastes .....	139
8.3.3. Particle Sizing.....	145
8.3.4. Perspex Scratch Testing.....	146
8.3.5. Dentine Wear Testing .....	147
8.3.6. SEM Analysis of Dentine Wear Tracks.....	151
8.3.7. Nanomanipulation Trials .....	153
8.4. Discussion.....	155
8.4.1. Discussion of Imaging and Microstructure .....	155

8.4.2. Discussion of Composition and Processing .....	156
8.4.3. Discussion on Key Wear and Link to Microstructure .....	156
8.5. Conclusions .....	157
CHAPTER 9 - CONCLUSIONS .....	158
9.1. Industrial Applications and Future Recommendations .....	160
10. REFERENCES .....	161
11. APPENDICES .....	167
11.1. Appendix A .....	167
11.2. Appendix B .....	168
11.3. Appendix C .....	170
11.4. Appendix D .....	170

## **LITERATURE REVIEW**

### **CHAPTER 1**

The following chapter provides a review of relevant literature and research regarding this project. This includes an overview on dental abrasives, a review on the function and structure of teeth and the role of tribology in oral care.

#### **1.1 Overview of Oral Care**

The need for good oral care products has been documented throughout history. Good oral care products are established via research and development of toothpastes and the evolution of dental particles within them. Further detail about the importance of efficient dentifrices and a review of the common abrasives found in modern toothpastes is provided in this section of Chapter 1.

##### **1.1.1 The Importance of Good Dental Care**

The maintenance of teeth and gums is key in the prevention of dental problems [1-3]. There are three prevalent problems in terms of oral care. The first being erosion; caused by grinding, excessive brushing or, most commonly, an acidic diet. These cause a thinning of the outer enamel layer of teeth, exposing the more sensitive dentine layer leading to hypersensitivity (seen in Figure 1a). Secondly, periodontal/gum disease; caused by a build-up of plaque in gingival grooves - the space between the tooth and gum - calcifying on the tooth surface over time resulting in localized bacteria within these 'plaque traps' leading to destruction of gingival tissues (seen in Figure 1b). And lastly, dental cavities; otherwise known as caries or tooth decay, this is the breakdown of hard tooth tissues by bacteria from acid from debris on teeth (seen in Figure 1c).



**Figure 1: Photos showing a) severe acid erosion b) periodontal disease c) dental caries [1, 2]**

Both periodontal disease and decay can be prevented by the removal of plaque layers on teeth. Plaque is essentially a biofilm that forms on teeth if left. It is usually white/pale yellow in colour but can progress to a

deeper yellow when built up. It is able to adhere to the surface of teeth by Van der Waals and electrostatic forces and boosts further buildup by forming intermolecular bonds with secondary colonisers [3, 4].

This plaque can harden in as little as 24 hours (though normally takes around 10 to 20 days for the average person) into calculus (also known as tartar). Its removal requires the attention of a dental professional further highlighting the necessity of daily dental debridement.

Plaque formation cannot be prevented but it is the build up of plaque over time and its progression that leads to oral disease, which is why it is essential to remove it daily. The removal of plaque in toothpaste is done by the addition of abrasive particles within the formulation [5].

It is also important to note that though the swift removal of plaque is vital, the use of abrasives in oral care can be damaging to the dental substrate surface.

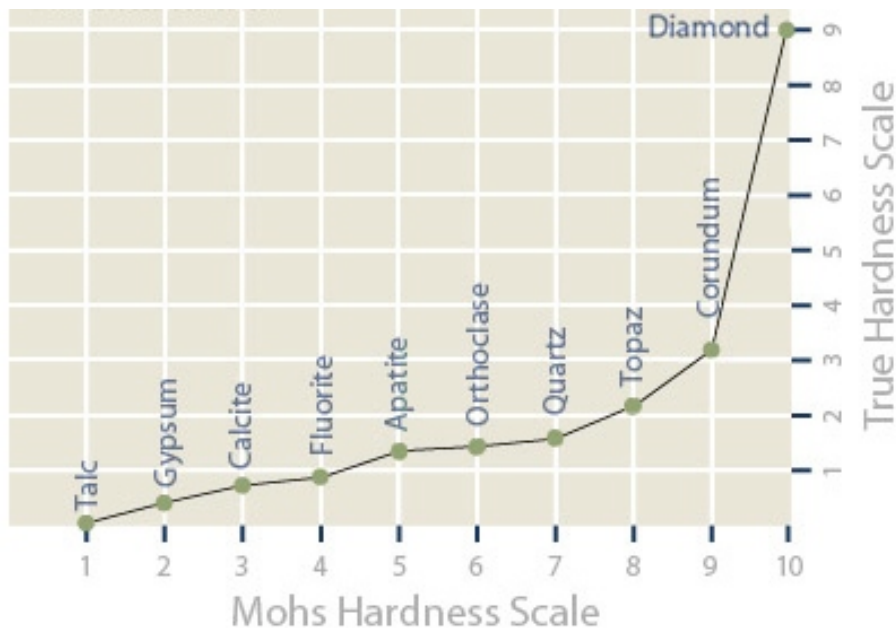
### **1.1.2. A Brief History of Toothpaste**

Dental care products have been in use for more than four thousand years, with the worlds oldest documented formula for toothpaste created by the Egyptians in 4AD (a mixture of crushed rock salt, dried iris flowers, mint and pepper). However it is only since the 18<sup>th</sup> century that inorganic products have been in use in oral hygiene products like tooth powders. Colgate first developed toothpaste in a tube in the USA; though products similar to this were available in Germany under the name Chlorodont and Kalodont. The basic substances in toothpastes have remained virtually the same since then; highly soluble, inorganic minerals suspended in water and thickened into a stable paste with appropriate binders along with aromatic substances such as peppermint oil and detergents or tensides to produce foam [6, 7].

In order for the abrasive mineral to be entirely undamaging to teeth, yet suitable for cleaning, its hardness must be between that of tooth dentine and stained pellicle in order to produce maximum abrasion on the stain while not damaging the tooth itself [8] .

The basic abrasivity of a material is usually measure in Mohs hardness. Mohs hardness is a scale that runs from 1 to 10. With 10 being the hardest material, diamond (See Figure 2).





**Figure 2: Mohs Mineral Hardness Scale [9]**

On this scale enamel has a hardness of 5 Mohs and dentine (which is less mineralized and less brittle) between 3 and 4 Mohs, dependent on the person's age and health. Normal plaque has a hardness of 1 Mohs (rendering an ideal dental abrasive to be around 2 Mohs) but can develop to 3-5 if left to calcify and develop to tartar [10].

Along with this, the paste must also have a low density and the highest relative volume so it can bind well to, not only aromatics and water, but also microorganisms and odours within the mouth. Few substances fulfilled these criteria in the early 20<sup>th</sup> century apart from black active carbon, some exotic materials (coral powder, marble dust and ground oyster shells) and chalk (calcium carbonate). Since the toothpaste had to be white and cheap for easy marketing, chalk was the obvious choice, which this thesis concentrates on predominately [7].

### **1.1.3. Formulation of Toothpaste**

Though the formulation of each 21<sup>st</sup> century toothpaste will differ from company to company the ingredients of a typical mixture are given in Table 1 [11];

**Table 1: A review of the composition of general toothpastes [9, 12, 13]**

Component	Proportion	Further information
Abrasive	10-40%	<p>As discussed earlier abrasives are used to provide the mechanical shear to abrade away the pellicle layer and provide efficient cleaning.</p> <p>The most commonly used abrasive particles used in dentifrices are calcium carbonate, silica, perlite and hydroxyapatite. These are discussed further in Section 1.1.4.1 - though there are other, less used abrasives, on the market currently.</p> <p>It is important to note here that though the swift removal of surface plaque they can be harmful to dental surfaces.</p>
Binder	1-2%	<p>Binders (also called hydrophilic colloids) will disperse or swell in the presence of water, preventing the separation between the liquid and solid phases. Mostly the derived from natural gums (Arabic gum and karaya) or seaweed colloids (Irish moss extract and gum carrageenan) or synthetically produced (carboxymethyl cellulose and hydroxyethyl cellulose)</p>
Humectant	20-70%	<p>Humectants prevent the loss of water in the formulations and therefore slow down the drying of process. In toothpastes on market today glycerol and sorbitol are the most common humectants used.</p>
Detergent	1-3%	<p>Initially added to produce foam, a characteristic many consumers find desirable from their oral care product it also aids cleaning by loosening pellicle</p>

		layers and emulsifies detritus removed by abrasive particles. Sodium lauryl sulphate is the most commonly added detergent.
Preservative	0.05-5%	Preservatives are normally added antibacterial agents to prevent the spoiling of other added ingredients. Most commonly used is triclosan or zinc chloride.
Flavour	1-2%	Normally only a small part of the mixture but essential for consumer satisfaction. This will vary in many formulations but most commonly peppermint, spearmint and wintergreen oils are used.
Therapeutic agent	0.1-0.5%	In most dentrifices the therapeutic agent added will be fluoride. Fluoride has been proven through research to prevent tooth decay and harden minerals in the outer layers of dental substrates. It inhibits acid-producing ability of plaque and therefore the subsequent growth of dental plaque. Fluoride has been shown to encourage remineralisation by increasing the strength of teeth by re-depositing lost minerals on the surfaces of teeth and producing a fluoro-hydroxyapatite composite which is harder and more acid-resistant; which can also aid in the repair of early dental caries.

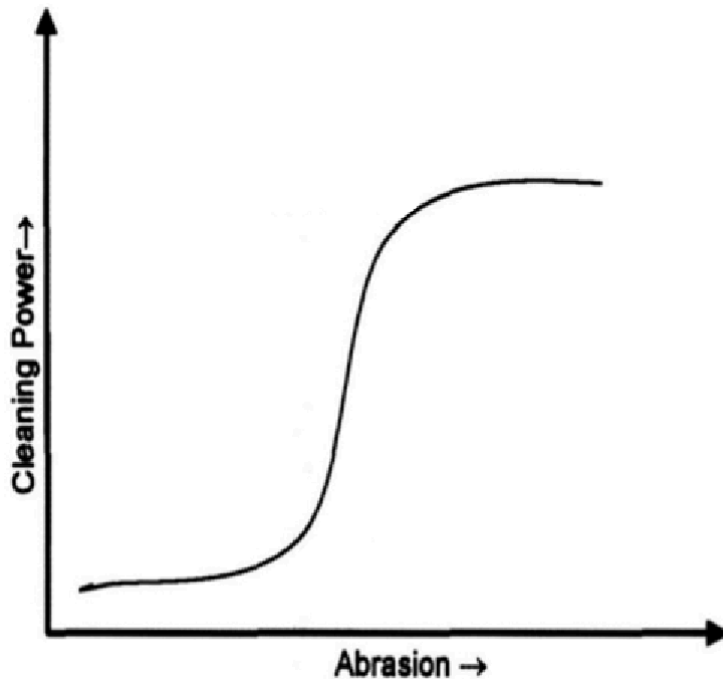
Bleaching, using peroxides, is restricted in the EU [1] and many of the studies and theoretical models found in the results chapters have minimally considered chemical effects. Though there is clearly a further need for studies on the effects of chemical cleaning products on teeth, data available does show that only a small number of 'whitening' toothpaste products have a good chemical stain removal promise [12, 13].

#### **1.1.4. Overview of Abrasives in Oral Care**

As explained earlier in this chapter the main purpose of all toothpastes is the removal of staining and plaque on tooth surfaces and in between gingival regions. It is also important to remove the initial plaque layer as this will prevent further calcification of the layer leading to a build up of harder tartar. This is done primarily by the addition of insoluble abrasive particles suspended in the pastes. The abrasive should get trapped between toothbrush bristles and against the dental surface. This mechanism will only affect the surface layer and will not change natural tooth colour or any underlying problems. Since the abrasives added are harder than the plaque/staining, the surface layer can be removed through mechanical stimulus [8, 14].

In industry a toothpaste abrasivity is recorded using either a REA (Relative Enamel Abrasion) or a RDA (Relative Dentine Abrasion) scale. These are normalized scales with only acknowledged standard materials being accepted as a benchmark [15]. Tests will vary from laboratory to laboratory but ISO 11609 Toothpaste Specification sets basic industry standards. Briefly summarised, clean polished radioactively marked dentine is brushed and worn in a 2 to 1 water to toothpaste slurry. The radioactivity of the end sample then noted and compared to that of a standard ADA reference toothpaste containing calcium pyrophosphate (which is set at 100 and the test paste results then calibrated to this relative scale). In general a low abrasive paste will have an RDA of 0-70, a medium abrasive paste an RDA of 70-100, a highly abrasive paste a RDA of 100 - 150 and a harmful paste one of 150-250 [15, 16].

This abrasivity does not linearly correlate with cleaning. In 1997, whilst studying how to achieve maximum cleaning with minimum abrasion Wülknitz found there is a peak cleaning point that can be reached and increasing RDA beyond this results in to additional cleaning (seen in Figure 3). The method of cleaning Wülknitz used in this study was the Indiana Power Cleaning method. Which is primarily a mechanical cleaning of 1000 cyclic toothbrush strokes with calcium pyrophosphate used as a reference.



**Figure 3: Wülkmit's Cleaning power as a function of abrasivity [17]**

It can be seen that particles will not clean more effectively after they reach a peak RDA. Instead a highly large RDA will instead just cause unnecessary tooth loss [17, 18]

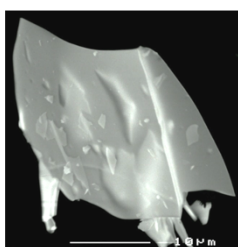
Many studies have shown dentifrice abrasives can be damaging to the substrate surface.

#### **1.1.4.1. Particle Types**

This study looks more extensively into specific calcium carbonate and silica particles, both currently on market and novel particles. Though it is important not to lose sight of the other abrasive particles currently used today.

##### **1.1.4.1.1. Perlite**

Perlite is made up largely of silica, aluminium oxide and sodium oxide. It is flat in shape with an average width of 20µm (though particles do go up to 100µm) and a thickness of 2µm.



**Figure 4: Perlite Particle**

Its main advantage is that it is softer than silica and therefore less harsh an abrasive but this does mean it is less effective as a tooth whitener. However, it has shown to give extremely low wear rates of dentine and enamel and therefore has been incorporated into calcium carbonate based toothpastes and has been proven to successfully remove external tooth stains [8, 19]

#### **1.1.4.1.2. Hydroxyapatite**

Hydroxyapatite is considered to be the most biocompatible dental abrasive material as nano-hydroxyapatite is the main composite of mineral bone. Conventional hydroxyapatite did not succeed in the toothpaste market but modifications of the mineral composite such as zinc carbonate hydroxyapatite or calcium carbonate hydroxyapatite have shown good promise in this field as they are better at remineralizing dental structure. Both these derivatives have a hardness of 5 Mohs which can lead to high dentine abrasion in larger size particles or large concentration of particles.

Nano-hydroxyapatite is said to provide a protective film layer on hydroxyapatite, penetrating into dentine canals of teeth [21, 22]. There, they can serve as crystallisation germs which take up further minerals and close the canals (also referred to as re-mineralisation), thus defusing the problem of sensitive teeth and aiding in enamel hardness repair. But there is no research to suggest this for existing dentine lesions [8, 20, 21].

#### **1.1.4.1.3 Silica**

Silica particles are granular in nature. Silica generally has a hardness of 5.9 Moh but recent developments have found a version of “soft” silica which has a hardness of 4.2 Moh. It has been found a combination of the two of these gives a better overall cleaning performance [8, 21]. Along with this silica is optically transparent, making it attractive in gel pastes.

Silica found in toothpastes is usually hydrated silica, which is a kind of silicon dioxide of which the water content is variable. Amorphous silica acids are used in a fine gel for toothpaste but their slightly higher hardness makes silica cause more aggressive and therefore cause more tooth erosion than its counterpart calcium carbonate and so are currently commonly used in a variety of toothpastes; both alone and in conjunction with calcium carbonate.

Silica particles found in toothpastes brands on today's markets can vary between 0.5-8  $\mu\text{m}$  in diameter but shall have agglomerate sizes of up to 25  $\mu\text{m}$  [8, 20, 22]

#### **1.1.4.1.4 Calcium Carbonate**

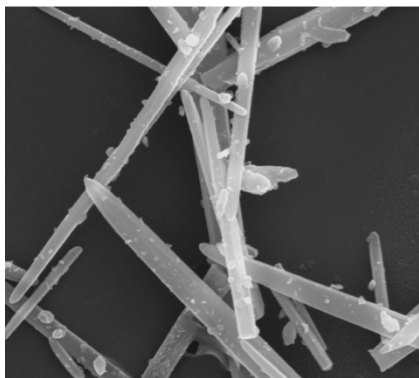
Chalk or Calcium Carbonate ( $\text{CaCO}_3$ ) is naturally found in three crystal modifications: Valerite, Calcite and Aragonite; of which calcite is clearly the most dominant in nature.

Aragonite was perfectly suitable for use as an abrasive particle within toothpaste as its hardness is lower than that of calcite but it is very rare in nature so precipitated calcium carbonate was considered [7].

#### **Aragonite**

Aragonite is calcium carbonate crystallised in orthorhombic form. The most common characteristic is a twin crystal (where 3 prism shaped crystals are grouped together to form a pseudo-hexagonal prism with deep vertical ribs). Aragonite has a hardness of 3.5-4 Mohs.

Aragonite crystal structure can be seen below in Figure 5.



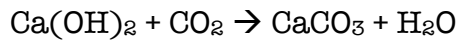
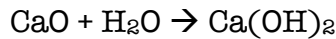
**Figure 5: Aragonite at 200 magnification**

Aragonite is not stable at a geological scale so is very rare but it is the main component in calcareous shells in organisms such as tridacnas; pearls are a mixture of lamella aragonite and organic material in changing composition. Due to this precipitated calcium carbonate was used instead [9].

#### **Precipitated Calcium Carbonate (PCC)**

PCC (also of hardness 3.5-4 Mohs) was quick to be used for toothpastes as the crystal modification of the product could be quickly determined by selecting the optimum precipitation settings; it was also certain to always be pure or of controllable chemistry.

Water is added to CaO to give calcium hydroxide. Carbon dioxide is then passed through this solution to precipitate the desired calcium carbonate, referred to in the industry as precipitated calcium carbonate (PCC):



PCC was the dominant mineral used in the toothpaste abrasive mineral market in the 1930's and was only replaced in the 1960's when fluorine was added to toothpaste as small amounts of the calcium carbonate would precipitate into insoluble calcium fluoride making it useless. This problem was later rectified by adding fluoride in other forms, such as sodium fluoride [7, 22]

Calcium carbonate particles used currently can vary from 0.7-18  $\mu\text{m}$  in diameter, usually in crushed calcite form or a smaller rounded PCC, dependent on the properties desired for the product.

Calcium carbonate is insoluble in water so can only be used in opaque pastes, unlike silica, which can be used in gels.

Amorphous synthetic silica acids now dominate the North American and Europe market but these are pricier and less bulky so PCC is still preferred in Africa and Asia.

#### **1.1.5. Dental Care and Unilever**

Signal and Close-up are Unilever's leading toothpaste brands world-wide, making them number two in toothpaste globally. Both use a mixture of crushed calcium carbonate and silica in their formulations as their primary abrasive. Signal is currently Unilever's leading brand (originally called stripe, as there was a red stripe which incorporated mouthwash into the paste. It was first launched in the US in 1957). Their strongest market place is held in France, Indonesia, India, Nigeria, Brazil and China; it is also known as Pepsodent (in Asia and Latin America), Menadent (in Italy), Zhong Hua (in China), Aim (in Greece) and P/S (in Vietnam).



## 1.2. Dental Substrates

Section 1.2. and its subsections look further into the structure of teeth and how the different layers must be considered and prepared for effective wear analysis and imaging. Wear experiments within this project are primarily undertaken on dentine samples so its function and structure are of particular importance. This section aims to highlight why this tissue is of significance with the field of oral care.

### 1.2.1. The Structure of Teeth

Teeth have four main parts (as can be seen in Figure 6); enamel, dentine, pulp and the root. Enamel and dentine are both classed as hard tissues in a tooth. Enamel is the outermost layer of a tooth and dentine the inner layer. Dentine is also the main part of a tooth.

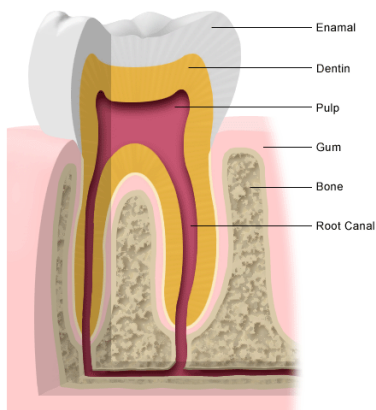
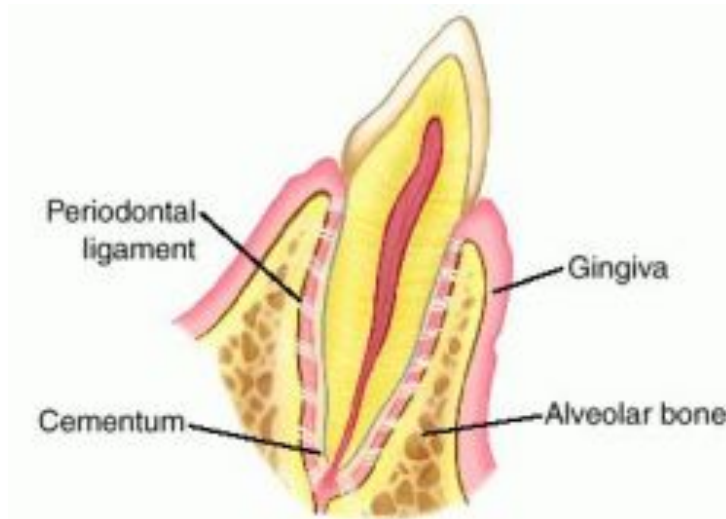


Figure 6: Anatomy of a tooth [23]

#### 1.2.1.1. Gingiva (gums)

The periodontium is the soft tissue that surrounds the teeth and provides a seal around teeth. It is made up of four parts; gingiva (gums), periodontal ligament (PDL), cementum and alveolar bone.



**Figure 7: Anatomy of the periodontium [24]**

Gums or gingiva are the mucosal tissue that lines the lower jaw (mandible) and upper jaw and palate (maxilla). Gums are normally coral pink in colour, a darkening of the gums usually indicates a problem with a build-up of plaque and bacteria around the gum-tooth margin.

The periodontium is subject to many external forces, from brushing to chewing to grinding, it is designed to reabsorb pressure to keep teeth in place but as gingiva is a soft tissue it is susceptible to wear as well as receding, leading to dentine exposure of teeth [25, 26].

### **1.2.1.2. Enamel**

Enamel covers the crown of the tooth providing the intense hard outer layer needed in teeth to combat the forces exerted during chewing and grinding, and often referred to as the protective layer around softer dentine. The hardness of enamel is approximately 5 Moh, making it the hardest substance in the human body.

The thickness of enamel is dependent on the type and part of the tooth it is found. It is thickest on the cusp of molars where it can be 4mm thick and thinnest on the incisal (cutting) edge of incisors where it is between 2-3mm thick. This affects the colour of enamel (thin enamel is yellow-white whereas thicker areas will appear a blueish white or grey).

The density of enamel is 2.84-3.0 g/ml and has a low tensile strength and is therefore extremely brittle. Structurally enamel has a hierarchical structure, and is made up of rods (of average diameter 4  $\mu\text{m}$ ), rod sheaths and interprismatic substance between the rods. The rods comprise of many hydroxyapatite crystals of size 8  $\mu\text{m}$  long and 4  $\mu\text{m}$  wide and hexagonal in shape.

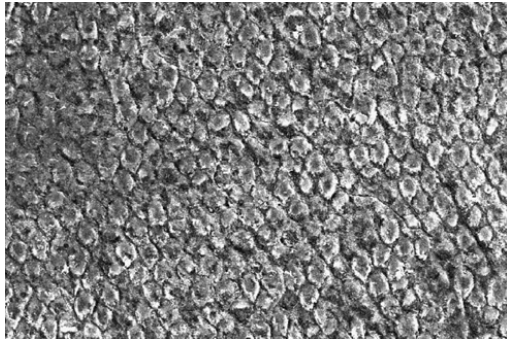


Figure 8: 800 x magnification showing the structural prism on the surface of enamel [27]

Enamel is not a living tissue as it has no cells or vessels and subsequently any damage done to it cannot be repaired. The main damage cause to enamel is the thinning of enamel via acid erosion but enamel can also be damaged via harsh abrasives in brushing, leading to hypersensitivity and dentine exposure [6, 28].

### 1.2.1.3. Dentine

As stated before, dentine forms the bulk of the tooth and therefore determines the shape of teeth. Unlike enamel, dentine is considered a living tissue and can react to physiological and pathological stimuli.

The hardness of dentine is lower than that of enamel (3-4 Mohs) but more than that of bone and a density of 22.1g/ml. Being a softer material makes it more vulnerable to decay and cavities but its elastic properties make it good support preventing the fracture of brittle enamel. It is largely made up of hydroxyapatite (around 70%), it is then around 20% collagen and 10% water. Dentine is also sensitive and formed constantly throughout life.

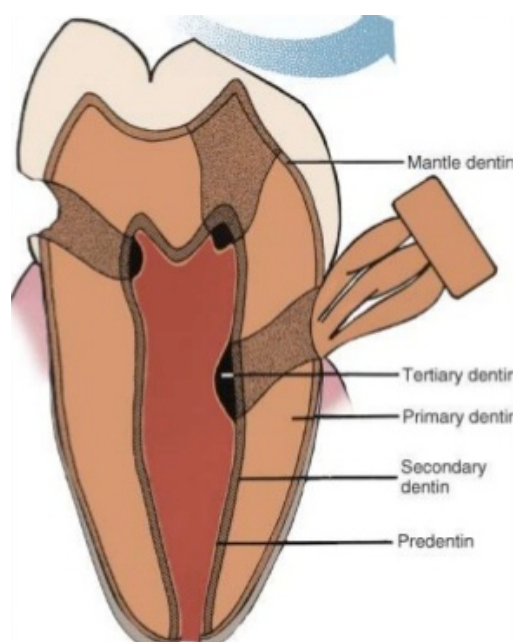
Dentine is a specialised type of bone that mainly composes of small, parallel tubules in a mineralised collagen matrix, making it an elastic tissue. This combined with the hardness found in enamel make teeth a perfect structure for, not only ripping and tearing food, but also for resisting abrasion and fracture.

Dentine contains a high density of tubules, which essentially are microscopic channels that radiate outwards from the centre (pulp) to the exterior (either the dentinoenamel junction at the outer surface - DEJ - or the dentinocemental junction - DCJ - at the root) [3, 6, 23].

Tubules near the pulp are the greatest in density and size (76,000 per square millimeter and 2.5  $\mu\text{m}$ ). In the middle of the dentine the density drops to 59,00 per square millimeter which decreases all the way to the

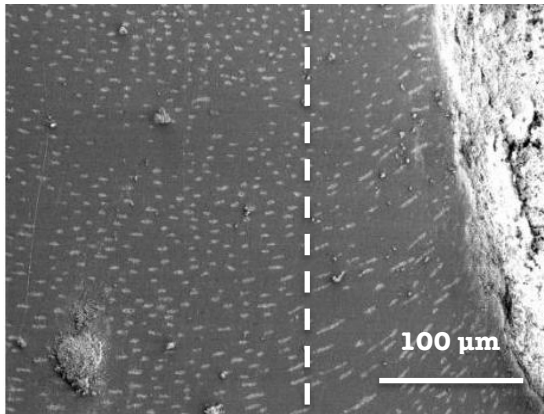
DEJ, where it can be as low as 35,000 per square millimeter. Tubule size also drops from 1.2  $\mu\text{m}$  in the center of the dentine to 0.9  $\mu\text{m}$  at the DEJ.

There are also three different classifications of dentine; primary tertiary and secondary. This is largely defined by the location of the dentine in the tooth. Figure 9 shows the locations of the three types of dentine and the most abundant in teeth. Primary dentine is found between the pulp and enamel edge of the dentine section, secondary dentine is found at the DCJ at the root and tertiary dentine only found when there is an external stimuli (such as caries forming). Primary dentine is strongly affected by abrasive wear, and is the substrate used in the laboratory testing done for this study.



**Figure 9: Cross section of the types of dentine [29]**

Primary dentine consists of mantle and circumpulpal dentine. Mantle dentine is less mineralized and found at the outer layer and only 150  $\mu\text{m}$  thick. The circumpulpal is the most prominent type of dentine and forms the inner dentine. There are subtle variations in the tubule orientation throughout a tooth due to how the dentine was formed (as can be seen in Figure 10). Dentine tubule size between the two types of primary dentine only range between 0.9-1.2 $\mu\text{m}$ , which is representative of those seen everyday in a typical healthy human adult tooth [30].



**Figure 10: Electron micrograph showing variation of tubule orientation in mantle and circumpulpal dentine**

All tribological wear tests done in this study were done on mantle and circumpulpal dentine as they have similar hardness, mechanical and frictional properties.

### **1.2.2. Testing Substrates**

#### **1.2.2.1. Dentine**

This study only uses human dental tissue in all laboratory experiments. Healthy adult teeth, which were extracted purely for cosmetic reasons, were provided by a dental practice with patient permissions (see Appendix B). Tissue (teeth) collection, destruction and storage was approved in June 2011 under the project ‘Dental de-scaling and surface cleaning’; the ethics approval document can be seen in Appendix B. Previous work for oral care investigations has shown though bovine dentine is more commercially available it is significantly different to human dentine and enamel tissue; in terms of tubule geometry and density [2].

All dental substrates used in this study were only removed due to cosmetic reasons, such as overcrowding. Any samples that had any dental disease or caries were discarded.

Some reported mechanical changes in the dental tissue can occur if dental tissue is left to dry due to the change in water content. It has been reported the hardness of dental tissue increases with drying time as does the co-efficient of friction, but elastic modulus decreased. Re-immersing the dentine in water can help restore the previous hardness of dentine tissue but only partially the elastic modulus [31, 32]. For this reason all teeth were stored in water and tested within 48 hours of preparation.

### **1.2.2.2. Perspex and Copper**

An alternative substrate model to dentine in many research studies is perspex or copper. This is due to the similar Mohs hardness of both substrates (3 Mohs), the ease of gaining a completely smooth surface before testing and ease of availability [5, 33-35].

In this study both copper and perspex substrates were used in scratch analysis.

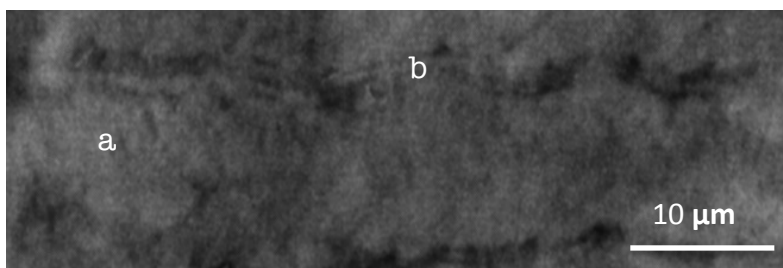
### **1.2.3. Imaging Techniques of Dental Substrates**

Both dentine and enamel are similarly difficult to prepare for imaging, both due to their composition and high hardness. In the last few years numerous approaches and techniques have been used to provide imaging of microscopic features of these two tooth layers.

#### **1.2.3.1. Light Microscopy**

Prior to further investigations, light microscopy is often used as a preliminary imaging technique to observe the macro tubules on the surface of teeth. This often only requires the tooth sample to be sawed to shape with a blade with a diamond edge, and then manually ground to an appropriate smoothness using rough paper. These samples are then washed in distilled water in order to remove any excess debris [36, 37].

Major and minor dentine branching can be seen using this method (as can be seen in the figures below) but light microscopy is certainly unsuitable for differentiating microstructural features at a micro level as this is below the resolution of light microscopy [37].



**Figure 11: Light microscopy image showing dentine tubules (a) and fine branching (b) [38]**

#### **1.2.3.2. Scanning Electron Microscopy (SEM)**

In order to produce clear images of the microstructure of dentine with a SEM, the sections of teeth must be dried due to the necessary high vacuum conditions of SEM. There are a number of different methods used to carry this out from soaking the specimen in acetone to achieve chemical

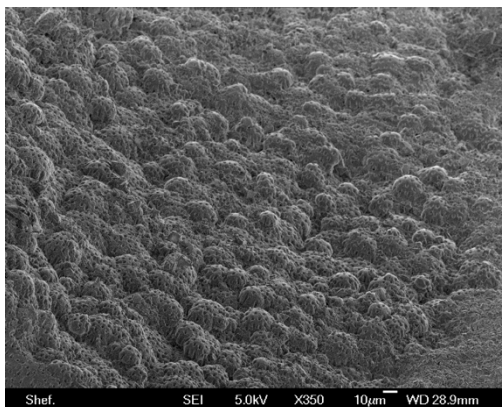


dehydration, or freeze drying the dentine, to simply placing the sample in a vacuum chamber. This causes a reported 10-35% shrinkage in the volume of the sample [37-39].

Most literature also demineralise the dentine squares by either soaking within 5.2% nitric acid or 10% EDTA (Edetic acid) prior to examination, to expose the collagen fibres to better observe the dentine layers bonding properties. This demineralisation process is the chief cause of shrinkage of the samples. It is reported without the demineralisation process the dentine would only reduce in volume by 5% but cause a change in the minerals mechanical properties, such as hardness and fictional properties [38, 40]

It is recommended to use vacuum chambers to dry dentine to its critical point, at which it is safe to place in a SEM chamber, and coated in a conductive film (such as gold or carbon).

Using this process an image of the following nature can be obtained:-

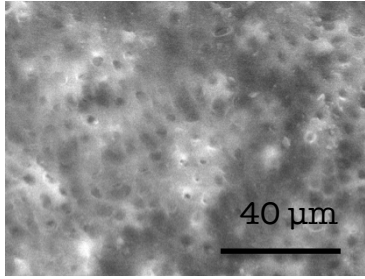


**Figure 12: 350 x magnification SEM image of pulp chamber dentine**

### **1.2.3.3. Environmental Scanning Electron Microscopy (ESEM)**

ESEM has the advantage over regular SEM as there is less constraint with regards to the high vacuum within the sample environment; enabling wet samples to be examined. The detectors used are not heat-sensitive so temperature related studies can be easily carried out and dynamic processes (such as heating, freezing, setting, dehydration, heating and tension-compression) can be recorded as they happen [41].

Using this method eliminates the need for sample dehydration. So ESEM can have the advantages of SEM (high magnification, depth of field and resolution) under wet conditions [41, 42]



**Figure 13: 500 x magnification of dentine tubules using ESEM**

The drying process required for SEM can cause a reported shrinkage of 10-35%. However, sample within ESEM still causes some reported shrinkage, even with the lower vacuum conditions [36, 39].

#### **1.2.3.4. Transmission Electron Microscopy (TEM)**

Due to the high hardness of both enamel and dentine it is difficult to prepare thin sections of teeth for observation under TEM. Early TEM preparation techniques involved simple sawing using a diamond knife and then wet polished to a high grit finish (around 600) until the sections were 0.5-1 $\mu$ m thick [39, 42]. This produced images such as the one seen in Figure 14.



**Figure 14: TEM image of an ultrathin section of dentine sample showing crystals [36].**

#### **1.2.3.5. Focused Ion Beam (FIB)**

Developments in techniques saw a focused ion beam used to section samples. This removes surface mechanical damage done by saw cutting techniques [37].

In order to produce this, thin sections of mechanically sawn or ground dentine were further thinned used a FIB. This is reportedly a lengthy process that can produce ultrathin sections [36, 43].

These sections can then be looked at under TEM to image the microstructure of dentine.



### **1.2.3.6. Summary**

Teeth can be imaged in a number of methods, especially when using electron microscopy, as can be seen from the review in this section. It can also be seen that considerable progress has been made in the preparation of dentine samples. However many important problems related to the effect on dentine structure and physiology under these techniques need further investigation.

### **1.2.4. Conclusions**

Section 1.2 and its subsections evaluate the various layers of teeth and provides an overview of the main dental substrates used in this study. Dentine is the softer dental tissue, more susceptible to wear and sensitivity, and therefore used as the main substrate for abrasion testing in this thesis.

Within this section it was seen the region of dentine most likely to be exposed is that closest to the gingival regions due to gums receding. Therefore general tribological testing done in this work are done on mantle dentine due to its availability and the similar nature, in mechanical and frictional properties, to that of the dentine most likely to be exposed.

## **1.3. Tribology and Toothpaste**

### **1.3.1. Experimental Techniques**

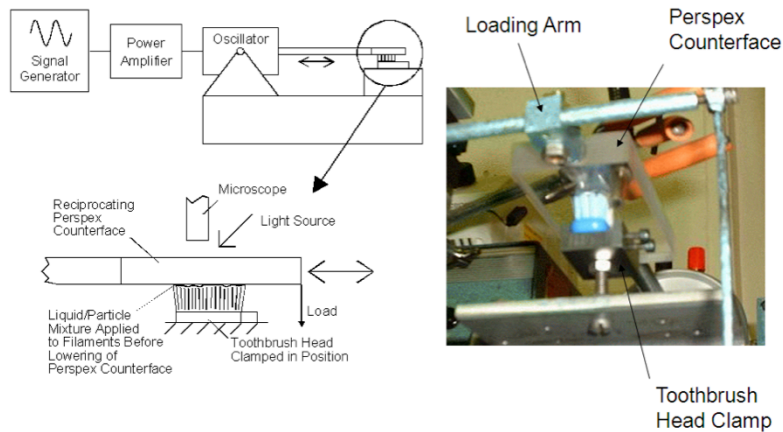
There are many methodologies used to test the behaviour of abrasive particles in dental care products. According to a British Standard of toothpaste and ISO documentation [2], in vitro tests can be conducted on standard materials to serve as a reference to measure the RDA (Relative Dentine Abrasion) or REA (Relative Enamel Abrasion) to prevent toothpastes being manufactured that can potentially harm teeth. The RDA ratio scale starts at 0 and is open ended but it is noted that toothpaste with an RDA of over 150 is not recommended for daily use [12].

Many in vivo, in vitro and in situ testing evaluations have been done to assess the cleaning efficiency of toothpastes.

In vivo testing usually requires giving volunteers controlled brushing techniques and apparatus as well as diet. This has been done and described in a number of papers [1, 12, 44], with the residual teeth

staining assessed usually using multiple observers; but clearly in this kind of testing it is hard to gain a good level of control.

With in vitro testing, a mechanical loading rig is used usually with perspex or bovine dental sections; an example of this can be seen below in Figure 15.



**Figure 15: Particle Observation Apparatus [45]**

Figure 15 shows a mechanical loading rig used to study toothbrush and toothpaste particles in the University of Sheffield Mechanical Engineering department. A visualisation apparatus was set up alongside abrasion tests – which was measured first by noting the scratches formed on the perspex (used as a replacement for teeth) by silica and perlite particles, and secondly by its removal properties of a stain layer and the rate of this removal [1, 45]. An organic dye was used to produce the stain and its thickness was measured by a profilometer (and found to be an average thickness of  $1\mu\text{m}$ ). Though this method offers a high level of control the main negative of this kind of testing is its lack of exposure to ‘real-life’ oral conditions [1, 34, 44].

Finally during in situ tests patches of dentine or enamel are worn in a volunteers mouth and then removed for ex vivo testing – though there are currently few papers using this method [34, 35], especially concerning the interactions of toothpaste particles with dentine/enamel.

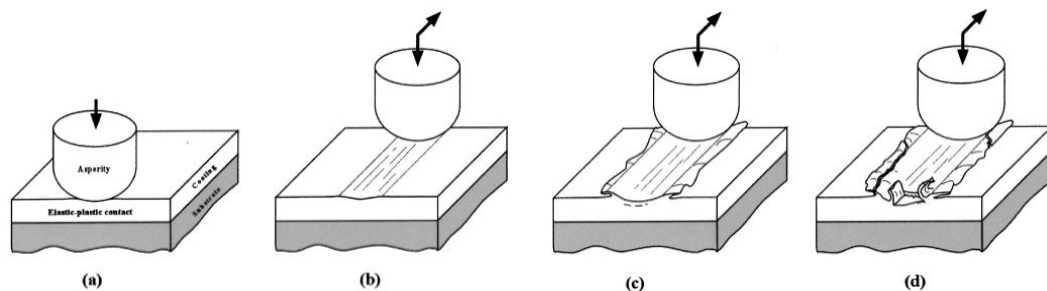
### **1.3.2. Mechanisms of Wear**

Tribology; the science and technology of friction, wear and lubrication, the study of interacting surfaces in relative motion is the primary theme of this project [46]. Wear (or the loss of material from a tooth surface) due to particle interaction with the toothbrush and tooth surface is the main study in this thesis.

General mechanisms and the nature of particle interaction during wear can be characterized by the wear scars left after surface contact.

### 1.3.2.1. Surface Fatigue

Surface fatigue, also called delamination wear, has been seen in dentine and enamel (most likely due to their laminar structures [47]). Surface delamination is found when a contact point is subject to repeated normal and tangential loads, which builds up subsurface damage until delamination occurs [48, [48]. The sequence of which can be seen in Figure 16.

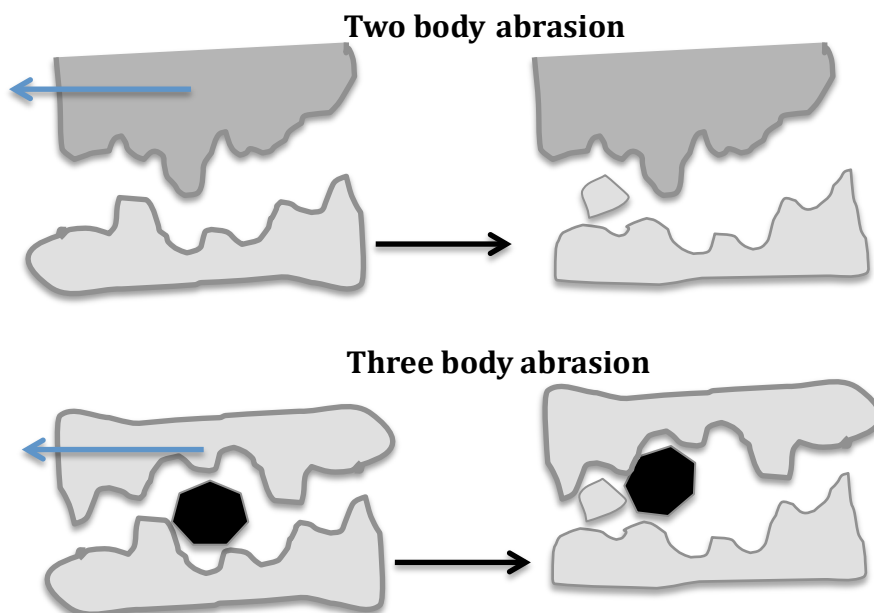


**Figure 16: Surface fatigue a) Loading b) Smooth plane formed by asperities c) Subsurface deformation d) Surface removal by shear [49].**

### 1.3.2.2. Abrasive Wear

Abrasive wear is surface removal when mechanical forces act between two hard and rough surfaces.

There are two main classifications of abrasive wear; two-body abrasive wear and three-body abrasive wear.

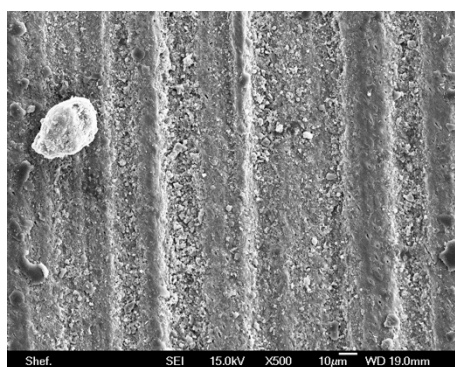


**Figure 17: Mechanism of Abrasive Wear.**

Two body abrasive wear, seen at the top of Figure 17 is when the asperities of two surfaces collide and the asperities of the softer surface are removed.

Three body abrasion occurs when particles (often the remnants of two body abrasion) are trapped in the contact area and cause the removal of material.

Abrasive wear is characterised by long parallel grooves in the tangential force direction (Figure 18). There are many parameters that affect the appearance of these grooves; including hardness, speed, particle shape (in third body abrasion), loading and ductility, these factors will determine whether light scratches or heavy gouging is seen. These will also determine whether plowing, cutting or fragmentation signs are observed [1, 3, 8, 33].



**Figure 18: Third body abrasion grooves, with loading occurring left to right.**

### **1.3.3. Studies relating to Toothbrush Interaction with Particles**

Though recent reviews [14, 34] have shown that typical brushing (twice a day) has little overall effect on dentine, it has been shown that the role of a toothbrush and toothpaste wear particles have great impact on hypersensitivity and has also been linked to gingival recession [15], and leaving an exposed dentine region.

Toothbrush design is primarily important for the entrapment of toothpaste particles. There are many factors that contribute to this, namely the stiffness of bristles, filament tip shape, brushing motion, loading, filament direction and length of use.

Studies have shown that stiffer filaments on a toothbrush head deflect less under load and therefore retain more tip contact region at the tooth allowing for better cleaning, and that rounded filament tips give better

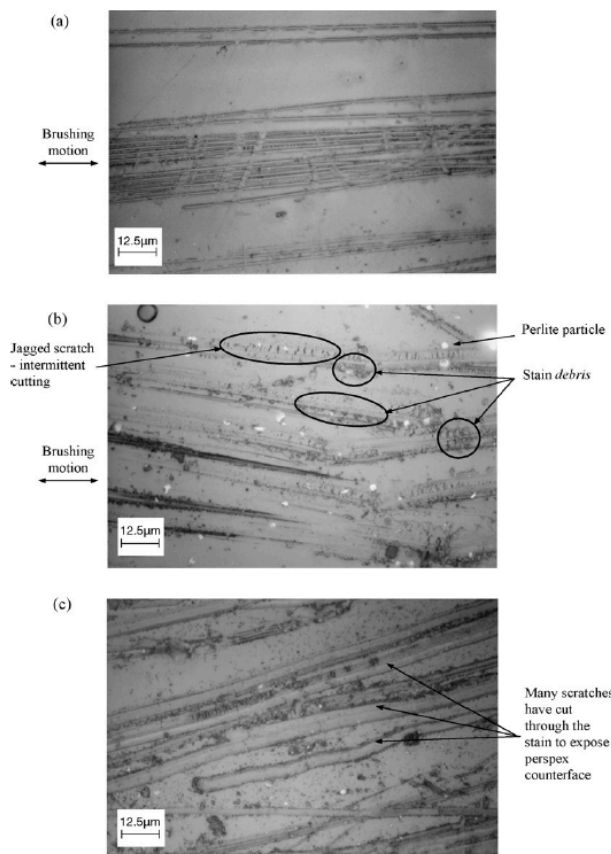
cleaning than flat ends as flattened ends have a tendency to cause soft tissue damage due to the sharper ends [33, 45].

Brushing with a toothbrush alone has no or negligible wear effects [14, 18].

#### 1.3.4. A Review of Past Studies Concerning Tribology of Dental Abrasives

In reciprocating wear research, similar to that seen above, it was seen that with larger particles, especially when at higher loads, only a few or no particles would reach the tip contact region and instead would be trapped under the bend in filaments. At low loads the larger particles would be trapped amongst the filaments and only a few would reach the contact regions [12, 33]. Works done on household cleaning products also has a similar philosophy and have found the same conclusion with regards to particle size [49].

In a test comparing the abrasiveness of silica and perlite [1, 44] it was seen silica was more abrasive but in both cases the counter face damage done was low. Though perlite scratches were less uniform than silica ones; most likely due to the fact that perlite particles have more of a tendency to scratch with their edges unlike silica where point scratches occur.



**Figure 19: Scratches formed a) with no particles b) with perlite particles c) with silica particles by a standard nylon toothbrush [1].**

In studies concerning calcium carbonate particles with respect to relative dentine abrasion (RDA) testing a low rate was found [12]; other studies have shown the same conclusion and postulate that the addition of other particles, such as silica or aluminum trihydrate gives better cleaning power [50].

According to postgraduate work done at the University of Sheffield particle hardness and geometry are more important than particle size in determining scratch depth and frequency [2]. After testing a number of different particle sizes on perspex it was found there is no direct relationship between particle size and scratch frequency; instead shape, coefficient of friction and brittleness are thought to be leading contributors. For example, rod shaped calcium carbonate particles can be more susceptible to fracture due to their long shape. This fracture point may produce flatter/sharper edges for more effective stain removal. Early work has also shown that rods, due to this breaking down, can be more sensitive to human tissue whilst still severe to staining making it possible for it to be an 'intelligent cleaning agent' [3].

#### **1.3.4.1. Effect of Particle Size on Dental Tribology**

The size of particles with similar chemistry and morphology have been shown to have a significant effect on substrate erosion [51]. Wear will change from polishing in small nano to micron-sized particles to gouging in larger (millimeter) sized particles. Particles associated with severe wear in dental care are generally typically more than 5  $\mu\text{m}$  in size. This direct correlation of size and wear is thought to be caused by the strength of larger particles to resist breakdown, causing more material to be displaced per interaction [52].

This relationship between size and wear is not always seen, as smaller particles can be stronger than their larger counterparts and having smaller articles does mean and increase in particle numbers in a given space.

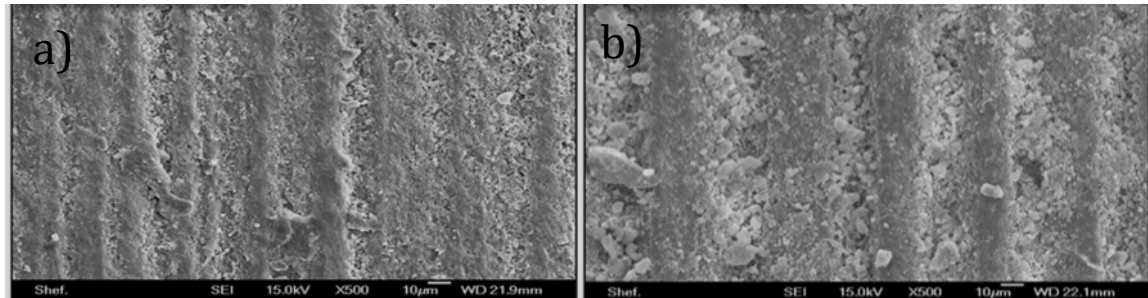
Ball-on-flat testing, similar to that done in this report, has shown in general larger particles produce fewer but larger wear features than the smaller particles [17]. But the larger particles do produce more wear in total [19].

#### **1.3.4.2. Effect of Loading on Dental Tribology**

Literature reports show that dentine wear by toothbrush/toothpaste increases with increasing load but decreases once the load is such that the filaments of the brush spread out [34].



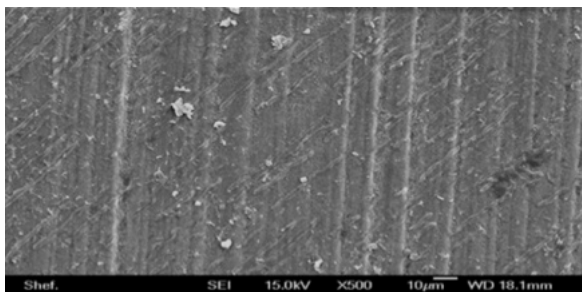
Some papers find that wear is independent of load though others find wear loss is influenced by load. Its effects seem to be very much connected to the type of particle used and its affinity to breakdown, though little work has been done to focus on the specific effects of shape and morphology on dentine wear [14, 17].



**Figure 20: Wear scar micrograph at a) low frequency (1.25Hz) and b) high frequency (5Hz)**

It is also observed that there is a significant difference in the morphology of wear scars on dentine at different loads and frequency. At low loads (around 2N) ploughing and delamination are present with a high frequency of shallow scratching [18, 35].

When load increases more severe delamination occurs and it is hypothesised that this is because at higher loads the particles act as a solid lubricant.



**Figure 21: Wear scar micrograph at high load (0.6N)**

#### **1.3.4.3. Effect of Co-efficient of Friction on Dental Tribology**

Wear also links directly to frictional properties of both the substrate and abrasive media. In wear studies dentine and enamel wear has been observed to increase with frequency and number of brush cycles but decrease in fluid. The extent of the effect of these factors on abrasivity is heavily dependent on the abrasive particle used and the composition of the toothpaste [15, 35].

Wear testing undertaken on dental material have shown that a lower co-efficient of friction and wear resistance are seen in the enamel

zone rather than dentin [49]. Wear mechanisms also vary between layers of the tooth due to the difference in hardness and frictional properties between these layers [32].

No work has been done linking calcium carbonate morphology and dental wear.

#### **1.3.4.4. Effect of Particle Hardness on Dental Tribology**

Particles with a hardness lower than that of the substrate they are abrading will cause less damage than that of a particle with a higher hardness.

The degree of hardness is significant as it will determine the plastic deformation of either the particle or surface. A particle with a significantly higher hardness than the substrate will penetrate the initial surface of the substrate to a greater degree. When a particle has a lower hardness to the surface it is more susceptible to both breakdown and deformation [52].

The hardness and properties of teeth is dependent on a person's age and health. Table 2 shows the average hardness, Young's modulus and Moh's hardness for a healthy adult (of age 18-35 years).

**Table 2: Averages properties of teeth for healthy adults [8, 21, 48]**

<b>Substrate</b>	<b>Average Hardness (GPa)</b>	<b>Young's Modulus (GPa)</b>	<b>Average Hardness (Moh)</b>
Dentine	0.6	18	3-4
Enamel	0.11	83	5
Stain/Surface pellicle	0.3	11	1 (can reach as high as 5 if left untreated)

#### **1.3.4.5. Effect of Particle Shape on Dental Tribology**

Previous preliminary work has shown the angularity of dental particles can have a significant effect on the rate of wear. This again is due to the plastic deformation of the substrate material (from dentine or perspex testing) [3].

Angular particles form rims or lips at the edge of the wear scar on the substrate surface whereas rounder particles tend to have more contacts required to generate wear due to less localised deformation caused [2].



### **1.3.5. Summary**

In oral care though it is desirable for a particle to be abrasive to provide efficient cleaning and removal of plaque and callus, it is also desirable for the abrasive particle to be sensitive to the dental substrate on which the plaque lies. More so, it is desirable for the particles to have an overall polishing effect to not only protect from further plaque build up (as a rougher tooth surface gives a better base for plaque formation) but also for aesthetic purposes.

The abrasive process involved in toothpaste is multifaceted and dependent of many variables such as loading, entrainment, and motivation. Therefore tribological testing must be done to assess and quantify how particles interact, whether they agglomerate, how aggressive in abrasive nature and observe more directly how they act dynamically with in-situ analysis. All of which is explored within this thesis.

### **1.4. PhD Objectives**

This work is sponsored by Unilever to develop knowledge and expertise for the impending addition of new particles and binders to the next generation of Unilever's toothpaste range. The primary aim of this project was to improve the understanding of how physical properties of the particles affect the abrasive properties of these particles and their effectiveness in toothpaste formulations.

The key aims were met by studying three different additions to toothpaste;

- Calcium carbonate particles of similar physical properties were studied to gauge their abrasivity and how variances in shape and agglomeration characteristics affect cleaning.
- Combining novel and bespoke nano-manipulation techniques with tribological testing to better gauge particles primary mode movement and motivation.
- Investigating particle interactions and observe how they make up a series of agglomerative collective particles.
- Investigating how the addition of citrus fibres affects abrasive cleaning and how this can be used to aid in the competitive toothpaste market.
- Gaining a better understanding of different binding polymers and how varying toothpaste formulations of silica based mixtures generates better cleaning efficacy and affects the abrasivity.

## **1.5. Thesis Layout**

Chapter 1 is a literature review useful for background information supporting later results within this project. Section 1.1 and its subsections give an overview of dental care, giving a history of toothpastes and an in-depth description of abrasive particles currently used. Section 1.2 and its subsections provide a review on the structure of dental materials and why the quality of this tissue is important in effective oral care. Section 1.3 and its subsections studies the tribology of toothpaste in other studies. This will be related to in further chapters to compare results found in this work. Chapter 1 also outlines the project objectives and thesis overview.

The materials and methods used commonly throughout this thesis are outlined in Chapter 2.

Chapter 3 introduces and characterises the calcium carbonate particles used throughout chapters 4-7. This chapter aims to familiarise the reader with the aesthetic and mechanical properties of these particles.

Chapter 4 uses linear reciprocation trials with a standard nylon toothbrush on perspex and copper substrates to determine the scratch characteristics of these calcium carbonate particles. This chapter finds scratch prevalence is not directly related to individual particle size.

Chapter 5 further demonstrates this using linear tribological testing. Substrates were then investigated under scanning electron microscope (SEM) to give a detailed analysis of particle behaviour under various operating conditions.

Chapter 6 utilises nano-manipulation technology, visualised under SEM, to determine the mechanistic and dynamic properties of each particle. A key finding within this chapter was to discern the predominant movement type for each particle and link this to previous scratch and wear trials within Chapters 4 and 5.

Chapter 7 explores the properties of these abrasive particles when dietary citrus fibres are added to toothpaste mixtures. Using the same tribological, reciprocating and nano-manipulation technology it was found these citrus fibres can have a positive effect on cleaning for certain calcium carbonate particles.

Chapter 8 investigates the suitability of new polymer binders in an already existing toothpaste brand, and if changing the formulation can better the whitening properties of the paste.

Conclusions, suggestions for future work and how this work impacted future Unilever toothpastes brands can be found in Chapter 9.

## **CHAPTER 2**

### **2. MATERIALS AND METHODS**

This chapter outlines the materials that have been investigated here as abrasives in oral care, and which methods were used to test and assess their abrasivity. The materials tested within this thesis were relevant to Unilever and as such provided by them.

This chapter also describes the procedures used to prepare and carry out work covered in Chapter 3-8. The methods outlined include preparing samples, linear wear testing, scratch testing, characterising particles and nano-manipulation testing. Many of these techniques have been developed throughout the course of the project.

#### **2.1. Materials - The Particles**

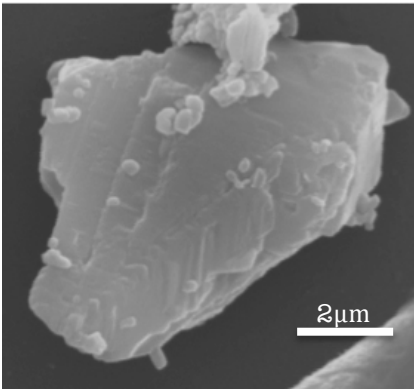
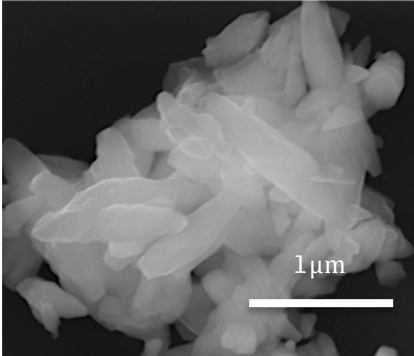
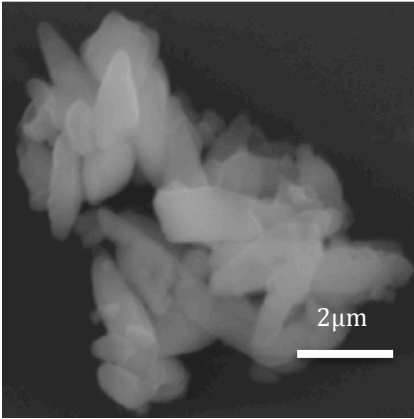
The suitability of particles which are required to act as gentle towards dental material but scouring towards plaque and pellicle is dependent on many factors including, shape, hardness and affinity to break down, to name but a few. Particles selected in this thesis are provided by Unilever (the sponsoring company of this study) and chosen due to their ease of manufacture, suitability for their brands, low production costs and biocompatibility.

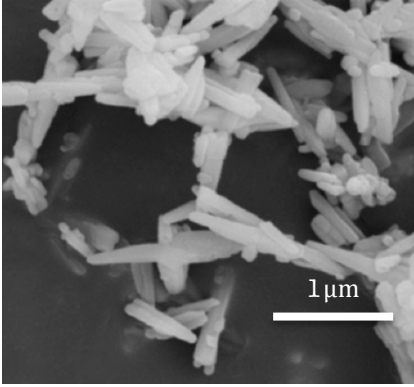
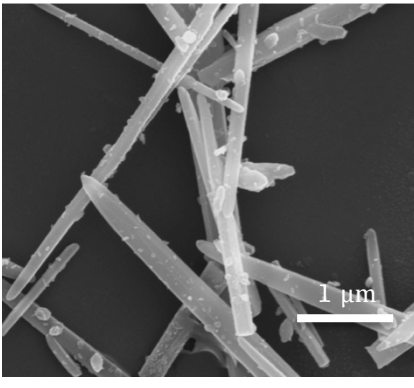
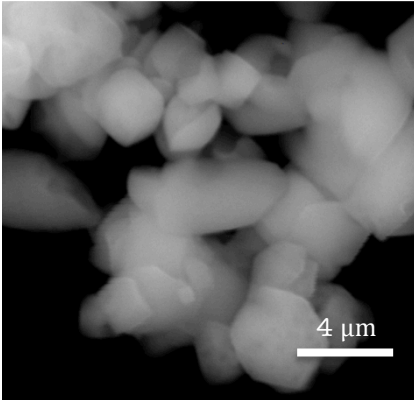
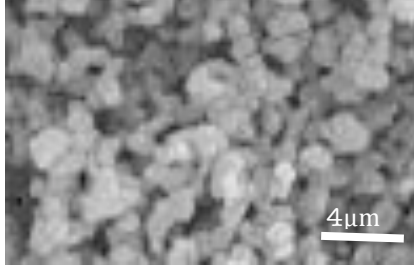
##### **2.1.1 Calcium Carbonates**

This study looks to further assess the abrasive behaviour and suitability of seven calcium carbonate particles of interest to Unilever (see Table 3), and to examine the effect on abrasive wear of these particles when citrus fibres are added. An assessment of how differing polymer binders in silica-based toothpaste formulations influences its effectiveness as an abrasive paste has also been carried out.

Table 3 outlines the calcium carbonate particles investigated in this thesis. All images shown in Table 3 were taken for this thesis, using the JEOL 6500F (shown in section 2.4.2, page 38). Particles were gold-coated for three minutes and all images were taken at 12.1mm WD (working distance) at 20kV. Each particle was imaged at a different magnification, at the most appropriate scale it was deemed to give a good indication of particle shape and size.

**Table 3: Overview of Calcium Carbonate particles used in this study.**

<b>Particle name</b>	<b>Obtained from</b>	<b>CaCO<sub>3</sub> structure and morphology</b>	<b>Image</b>	<b>Further information</b>
Omya 5AV	TOMPS [44]	Crushed calcite, Ground calcium carbonate (GCC)		A common abrasive in cleaning products. Has a large variance in size due to the milling process used to break it down.
S2E	Solvay Chemicals [45]	Calcite, Scalenohedral precipitated calcium carbonate (PCC)		PCC particle that has a ‘baguette’ shape, with a wider middle and tapering at the edges.
Strucal L	Speciality Minerals [46]	Calcite, Scalenohedral PCC		Similar in shape and structure to S2E particles but with a greater affinity to agglomerate.

Sturcal F	Speciality Minerals [55]	Aragonite, Arcicular PCC		Differs to many calcites occurring in an orthorhombic crystal structure.
Rods	Maruo Calcium	Aragonite, Arcircular needle PCC		These particles are created through a high heat precipitation process giving delicate particles with high aspect ratios.
Vicality Albafil	Minerals Tech [47]	Prismatic PCC		Albafil particles are polygonal in shape but the prismatic crystal structure of Albafil particles makes them appear rounded.
CalEsence 70	Minerals Tech [47]	Prismatic PCC		CalEssence particles are polygonal in shape and are the smallest PCC (0.7 μm) used in this study.

Although most particles were used in each trial, not all of the above were used every time, dependent on the relevant research aims for each experiment

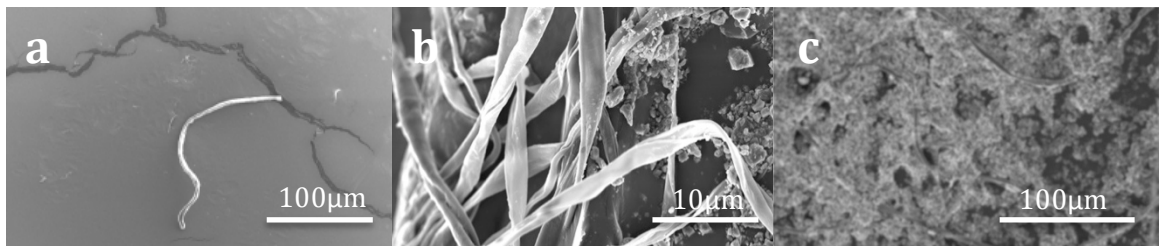
## 2.2. Citrus Fibres

The fibres used in this study are commercially available from Herba Foods Ltd. Sold as Herbacel AQ + type N [48]. The material exists as a fine fawn powder and is mixed with water at the desired concentration along with a preservative to inhibit microbial growth.

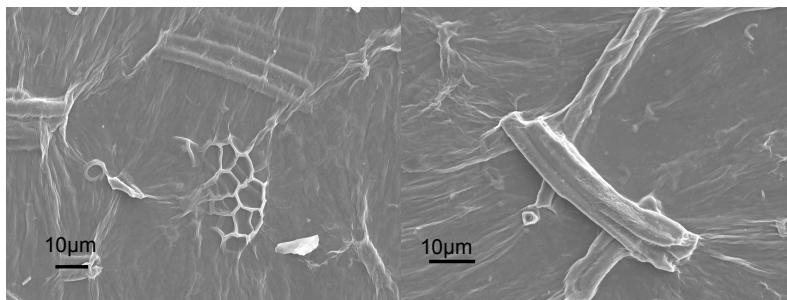
The citrus material is termed ‘fibres’ due to its dietary fibre composition, rather than its morphology. Whilst SEM has shown that many citrus fibres are indeed fibrous in nature (Figure 22) there are additional web-like or tube-like particles intermittently (seen in Figure 23) known as xylem vessels that are water transport channels also located in the peels of citrus fruits.

Obtained from the peel of harvested apples, limes and lemons, citrus fibres have a high water-binding capacity, an attribute favoured in toothpaste ingredients. They also provide a smooth texture in aqueous solutions (when compared to other cellulose-type fibres); hence their use in the food industry.

The particles do not dissolve in water but do have excellent swelling properties, making them ideal to thicken solutions.



**Figure 22: SEM images of dried citrus fibre solution a) Solo fibre b) Fibre ends c) Fibres amongst calcium carbonate particles.**



**Figure 23: SEM imaging of web-like and broken structures found within fibre paste.**

The citrus mixture is then subjected to mechanical shear (by milling) which helps to break down the powder (which essentially exists as plant cells). This process leaves the natural cell wall intact while removing natural sugars. Application of mechanical energy can help break down the cellulose rich components to expose microfibrils, which can then form a space-filling network of entangled high aspect ratio fibres. This manifests itself in the material becoming significantly more viscous.

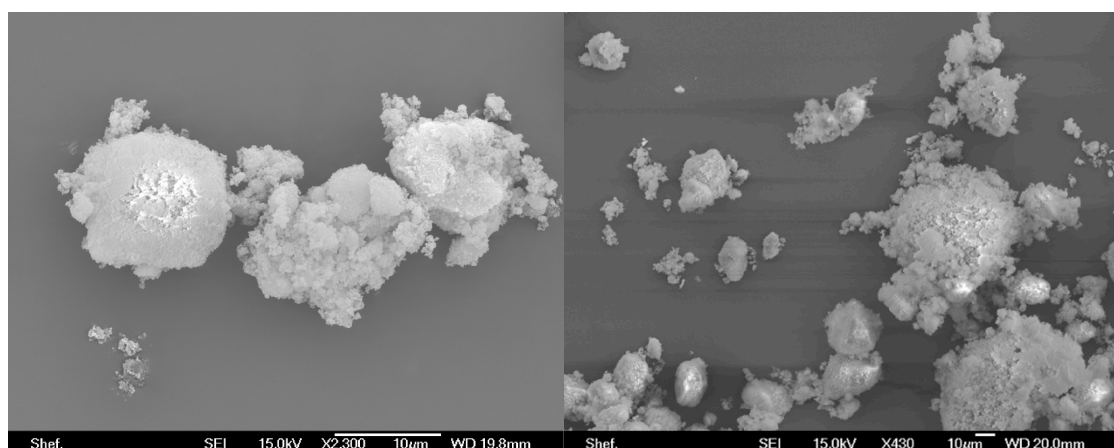
Fibres used in this study range between 50  $\mu\text{m}$  to 250  $\mu\text{m}$  in length with an average length size of 200  $\mu\text{m}$  (and modal width size of 1.6  $\mu\text{m}$  ). The morphology of these fibres are discussed further in Chapter 7. The fibres themselves are used in conjunction with different concentrations of the calcium carbonate particles described in Section 2.1.

## **2.3. Binders with Silica Particles**

### **2.3.1. Overview of Silica Particles Used**

The silica used in Chapter 8 within this thesis is Zeodent 113, provided from Huber Materials [49]. Zeodent 113 is a precipitated silica particle that is currently used in gel type toothpastes owned by the Unilever group.

Zeodent 113 is small in size individually but prone to form extremely strong agglomerations that are difficult to break down, effectively acting as one large particle. The modal cluster size for Zeodent 113 silica is around 20  $\mu\text{m}$ , but can range from 1-50  $\mu\text{m}$ . Individually it is a relatively small particle with an average particle diameter of 2  $\mu\text{m}$ .



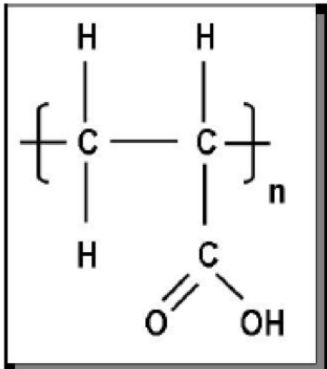
**Figure 24: SEM images of Zeodent 113**

### **2.3.2. Overview of Carbopol Binders**

In order for toothpaste to be of a suitable thickness (to be a squeezable paste that holds together during shear) a structurant or binder must be

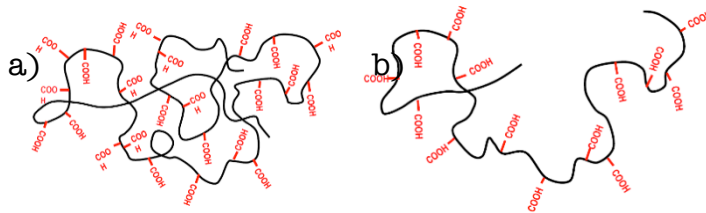


added along with the abrasive particles. For this study the structure of interest is a commercially available polymer called Carbopol from Lubrizol Plc. Carbopol [50] is a polyacrylic acid polymer.



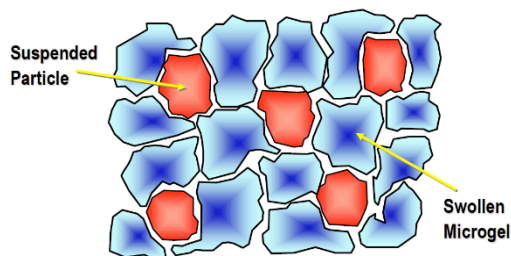
**Figure 25: Molecular formula of Carbopol [59]**

Carbopol polymers are very hydrophilic. This high affinity to water makes it an excellent thickening agent when hydrated the formulation thickens.



**Figure 26: a) Before hydration, the polyacrylic acid is tightly coiled b) After hydration, the polyacrylic acid begins uncoiling [59]**

When hydrated Carbopol thickens as it swells up easily. So when abrasive particles are added it separates ‘particle only’ zones and excludes abrasives from other zones.



**Figure 27: Suspension of particles in Carbopol polymer [59]**

Provided by Lubrizol, Carbopol is currently used as a thickening agent in ‘Zendium’ toothpaste. A newly acquired toothpaste brand by Unilever (formally Sara Lee). Lubrizol make a variety of different Carbopol based agents. Chapter 8 looks at not only differing the methodology of which

the original Carbopol is added to the toothpaste formulation but also replacing it with other Lubrizol products. This is gone into further detail in Chapter 8.

Table 4 highlights the acrylate based polymers used for formulations of interest to this study.

**Table 4: Overview of Carbopol pastes used in this study.**

<b>Brand name</b>	<b>Formulation information</b>	<b>Current uses</b>
C2985	Polyacrylic acid polymer	Zandium toothpaste
Ultrez 20	Alkyl Acrylate Crosspolymer	Body washes, skin gels
Ultrez 21	C10-30 Alkyl Acrylate Crosspolymer	Face lotions, shampoos
SLS Empicol and Carbomer2984	Confidential Unilever own-made polymer	
EasyGel	Confidential Unilever own-made polymer	
'BlackSheep'	Confidential Unilever own-made polymer	

A full breakdown of ingredients used in the pastes and preparations is outlined in Chapter 8 and Appendix A.

## **2.4. Methods**

### **2.4.1. Particle Sizing**

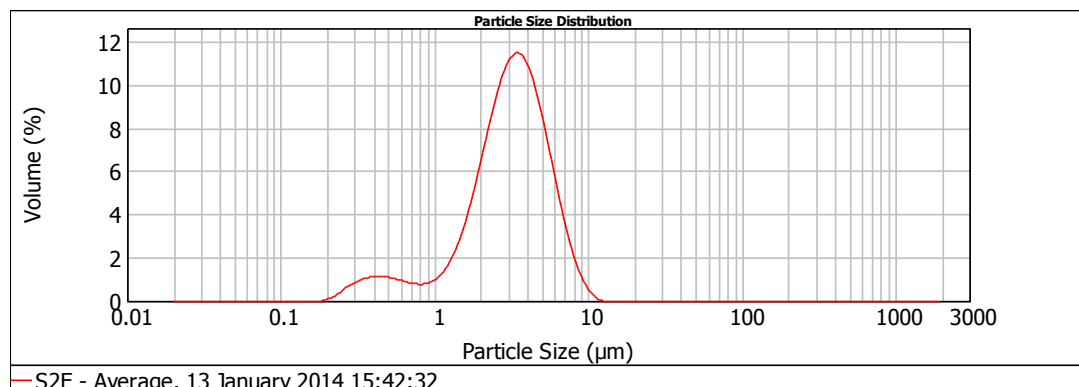
Particle size was determined using a combination of two methods. The first being laser diffraction technology (Figure 28). Laser diffraction technology scatters light from a focused laser beam and calculates mode

particle size based on the angular distribution of scatter of the light beam.



**Figure 28: Malvern Instruments Mastersizer 2000**

This provides accurate information about modal particle size in the particle suspension and produces a graph to give particle size distribution. Figure 29 gives a typical size distribution plot seen from this method.



**Figure 29: Size distribution plot for perlite particles.**

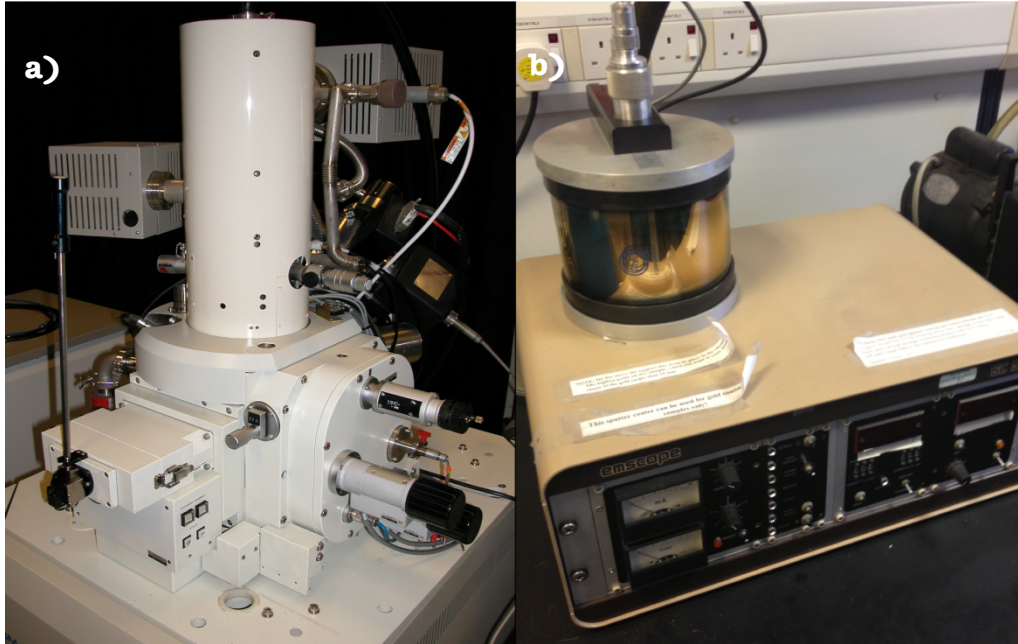
Particles were simply dispersed in water at a concentration of 0.5%. Though this information is highly accurate (to 0.02 µm) laser diffraction cannot discriminate against agglomerations therefore sizing from this method was done in conjunction with SEM imaging.

### **2.4.2. SEM Imaging**

A large portion of analysis within this thesis was done using scanning electron microscopy. Non-conductive particles and dentine (the main subjects of this thesis) are prone to high charging under the electrons and therefore were gold coated for 1 minute at 15mA current, using an Emscope SC-500 gold sputter coater (Figure 30). By introducing this

conductive nano-layer to the surface features of items could be seen clearer.

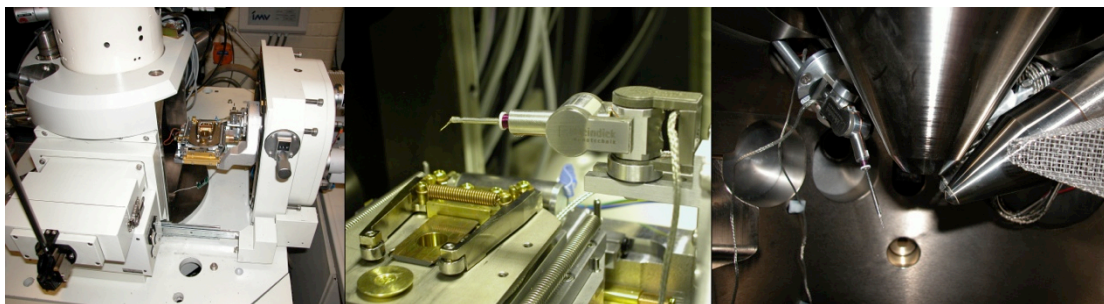
Particles were sprinkled onto an adhesive carbon tab and dental substrates hot mounted in conductive resin (Konduktomet), which also dehydrated the sample for SEM imaging . All images taken in this thesis were done using a JEOL JBM-6500F microscope.



**Figure 30: Images of a) JEOL JBM-6500F electron microscope and b) Emscope sputter coater.**

### **2.4.3. Nano-manipulation**

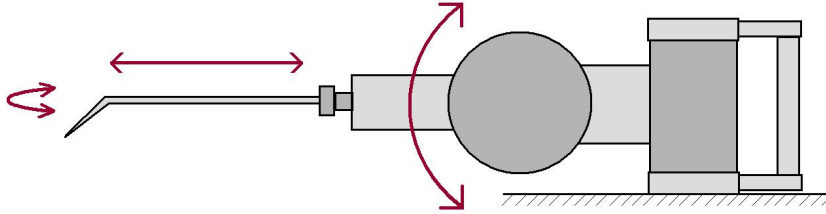
Within the JEOL-6500 pictured in Figure 30 there are two Kleindick MM3A manipulation probes (Figure 31).



**Figure 31: From left to right, JEOL-6500 SEM, Nano-manipulation probe, probes within SEM chamber.**

The probes have 3 dimensional freedom and are coordinated by user defined movements with a stable control system. This allows for instinctual and controlled movements. Fluid and sweeping motions are

allowed by a combination of the movements allowed, outlined in Figure 32.



**Figure 32: Diagram of nano-probe movements [2]**

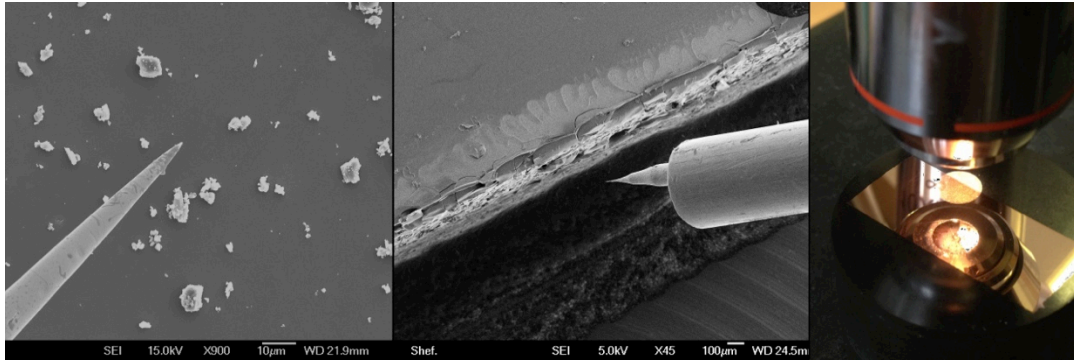
Both probes are controlled by two separate mechanical drives consisting of a piezoelectric slider and stator [51]. The contraction and expansion of the piezoelectric components can be varied according to the voltage applied. This allows both coarse and fine ( $<1 \mu\text{m}$ ) movements. Nickel chromium probes were used. These were prepared using electrochemical etching and attached at the front of the nano-probes.

Nanomanipulation of particle experiments were conducted on silicon, perspex or copper substrates. Perspex was used due to its similar mechanical properties (hardness of 3 Mohs) and nature to dentine, though it was impossible to image in SEM due to a large presence of charging. Instead it was mainly used as a comparative surface for the other two substrates to ensure they were representative of what was seen on perspex.

Silicon trials were often used to outline the mechanical behavior and movement of the particles on a flat, firm surface. Silicon is much harder than both dentine and the particles studied within this thesis, therefore it was not used to discern particle breakdown behavior.

Instead these mechanical trials were carried out on highly polished copper (to 0.5 micron - polished in the same way dentine samples in Section 2.2.4) Copper has a comparable hardness and resistance to deflection as soft dentine. This provided a good base on which to produce particle breakdown images as well as to study surface abrasive markings.





**Figure 33: Three substrate (left to right) SEM of particle on silicon, SEM of smooth perspex (as provided), polished copper.**

Particles were administered dry to each substrate due to the straining nature of SEM imaging in vacuum.

#### **2.4.4. Preparation Process for Dental Samples.**

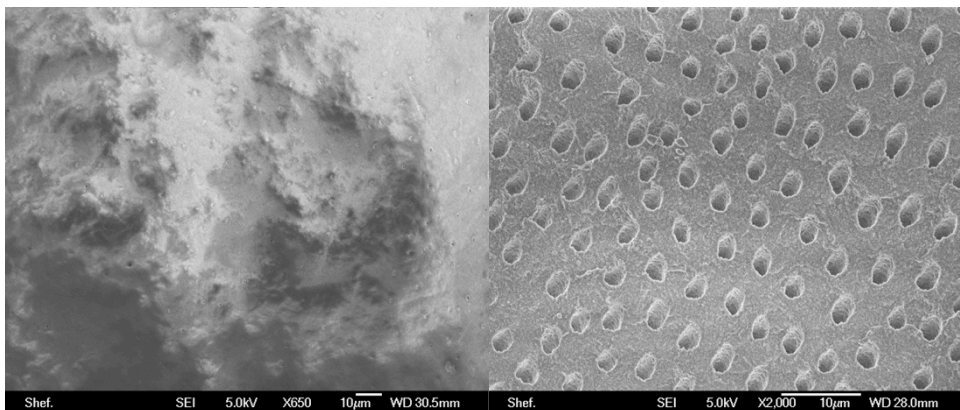
Much of the work done in this thesis was done on dental substrates. For this reason it was important to refine a process of preparing the samples to make it suitable for not only imaging but also for wear testing. The following methods were adopted for this work: -

- Samples were sourced from adult humans. All sources were removed by a dentist for cosmetic purposes and healthy when removed. No sources contained caries or disease. An example of the ethical permissions forms used and ethical approval, obtained on 1<sup>st</sup> June 2011 from the Mechanical Engineering Department of the University of Sheffield, can be seen in Appendix B.
  - The ethical approval for this project states Dr. Chris Rose was to obtain and store the samples and all samples used under the supervision of Prof. Rob Dwyer-Joyce. This complies with the legal responsibilities of all involved in this project, including the Human Tissue Act.
- Samples were stored in 10% neutral buffered formalin solution and sealed. All samples were then obtained within 2 weeks and prepared and tested/imaged within 24 hours.
- Teeth were sectioned mesio-distally (along the centre of the tooth) using a Wells 3241 180 µm diamond coated wire. The cutting process was water cooled to prevent drying of the sample.
- Samples were then mounted and staged within Konductomet mounting (20-3375-016) and wet ground to a coarseness of 120 microns, to remove any smear layers, on a Bueller Automet 250 (at settings touch force 20N, head speed 50 RPM and platen speed 240 RPM).

- Samples were then polished to 0.5 microns using diamond polishing slurry for 4 minutes at the same settings on the Automet. This process was then repeated again using a diamond polishing slurry of 0.25 micron.
- Samples were then ultrasonicated in distilled water for 5 minutes at 60Hz to remove any residual particles that may have entered the tubules and prevent a reformation of a smear layer.
- Samples were then ready to test upon or gold-coated for imaging.



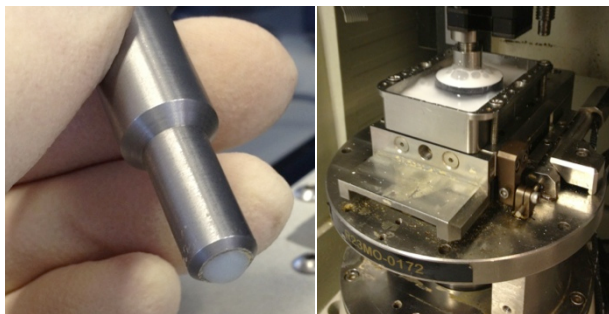
**Figure 34: Prepared tooth sample**



**Figure 35: Left, bisected tooth. Right, bisected tooth after the preparation method outlined above.**

#### **2.4.5. Dentine Wear Trials**

All dentine wear trials were conducted on a Bruker UMT 3 tribometer test rig in linear reciprocation mode. A nylon ball was used as the counterface. A ball was chosen over a toothbrush to give more control over the strokes and loading; and nylon ball was chosen, as it is a comparable material to the point contact made by nylon brush filaments.



**Figure 36: Ball holder for CETR trials and CETR set-up**

The CETR base reciprocated with a stroke length of 7.5mm under varying loads and frequencies. All frequencies and loads used within this study are comparable to that of the normal brushing speed and loading of the average person 18-65 years of age [9, 23].

#### **2.4.6. Profiling**

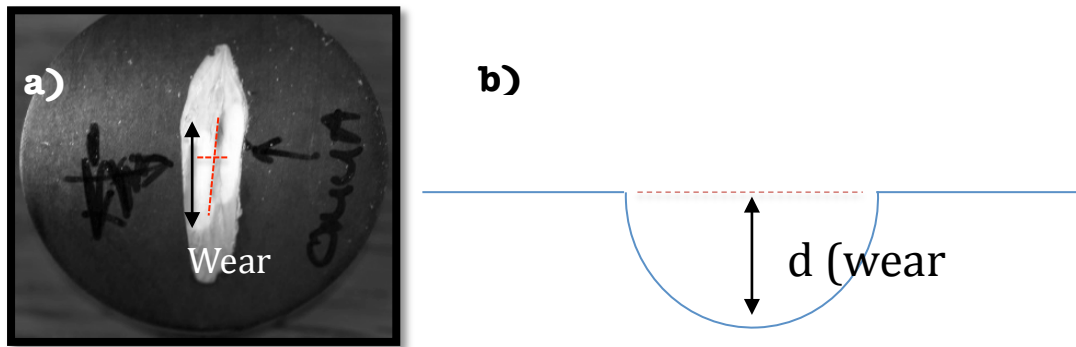
All wear profiles within this study were taken with a Detak profilometer, which is sensitive to 0.05 microns in depth.



**Figure 37: Veeco Detak 150 profilometer**

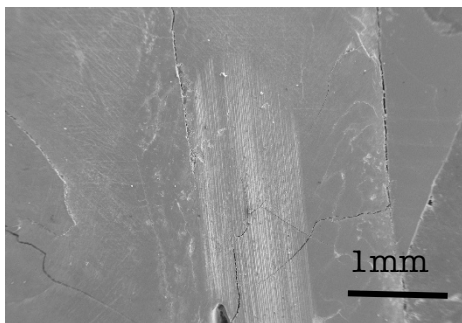
The overall maximum wear depth of the samples measured in the middle of the track, as annotated in Figure 38a.





**Figure 38** a) Image showing the position at which SEM images were taken in this thesis  
 b) schematic showing wear depth measurement of a wear scar.

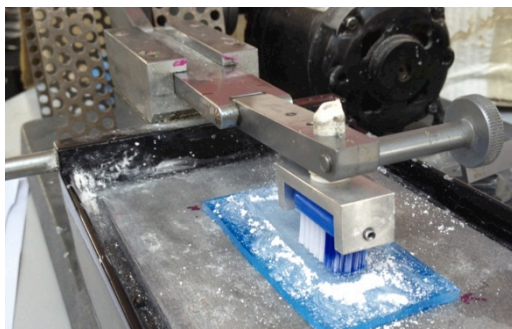
Representative SEM images of the wear tracks were taken from the central position of the wear scar at the lowest point. From these and additional SEM images, the scratch widths were determined.



**Figure 39:** SEM image of a typical wear scar after 30 minutes of testing.

### 2.4.7. Toothbrush Trials

Scratch trials were also conducted on perspex (of similar hardness to that of dentine) on a linear reciprocation rig.

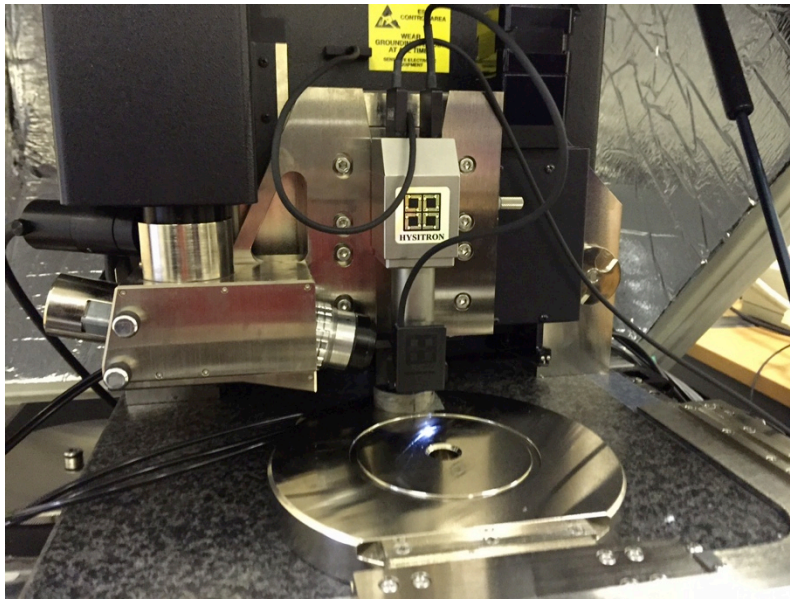


**Figure 40:** Linear reciprocation set-up; using perspex substrate and a Unilever standard brush head.

The toothbrush used was a flat-trim toothbrush with 8mm Nylon filaments (a standard Unilever brush). Each test was conducted for 3 minutes (typical brushing time) at a speed of 0.925m/s; stroke length 60mm to give the bristle enough room to fully go through each angle of the brushing cycle. The applied normal load could be varied and typically 3.92N (400g) was used as a standard.

#### **2.4.8. Atomic Force Microscopy (AFM)**

Scratched perspex samples were studied using a Veeco Dimension 3100 AFM. An AFM enables the mapping of surface topography of a wear region. AFMs use a small tip on a cantilever that moves along the surface to give an image of topography. All AFM conducted within this thesis were carried out with a Bruker OTESPA-R3 cantilever probe and tip, resonant frequency 300kHz and spring constant ( $k$ ) 26N/m. All AFM scans shown in this work were taken over 80  $\mu\text{m}$  squares located at the center, in the middle of the stroke length, of the scratch region.



**Figure 41: Veeco Dimension 3100 AFM.**

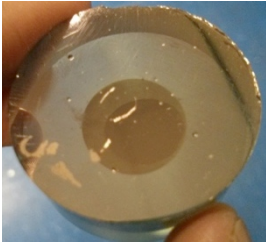
The AFM is able to provide detail of individual scratch depths, linear roughness and overall scan area roughness ( $R_a$ ).

#### **2.4.9. Hardness Testing**

In order to measure the hardness of micro particles the  $\text{CaCO}_3$  particles were dusted onto the surface of optically flat PMMA plate, and excess particles dusted off. A well was assembled around the particles stuck onto the PMMA and a soft resin (TAAB soft embedding resin (T029)) poured over the particles. This resin was cured in an oven at  $60^\circ\text{C}$  for 24 hours. The well was then removed and some particles were left embedded in the resin surface.

The samples were then mapped and indents performed both on the resin and on the particles, using a Hysitron 3000 indenter. Indentation was carried out using a peak force of  $50\mu\text{N}$ , 10 second loading, 10 second load hold and 10 second unloading. The unloading

was curve then analysed to give the hardness of the embedded particles.



**Figure 42: Sturcal F particles embedded in resin**

## **2.5. Summary**

This chapter has summarised the main materials explored in this project and how were characterised. The particles and methods described above are detailed further in the subsequent chapters of this thesis. In particular, further information about paste mixtures and particle dilution is provided in following chapters when necessary.

## CHAPTER 3

### CALCIUM CARBONATES AS ABRASIVES IN ORAL CARE

#### 3. Determining Particle Characteristics

Chapter 3 concentrates on the characterisation of the calcium carbonate particles used in this study; outlined in the Materials and Methods (Chapter 2). The particles were investigated for size, shape, fracture morphology, agglomeration properties and hardness.

##### 3.1. Particle Sizing

The calcium carbonate particles outlined in Section 4.1 were sized using laser diffraction; this was then confirmed using SEM images. The same particles were then brushed using the linear reciprocation rig, using both a 1:1 wt in distilled water dilution and dry.

The particles were also sized using laser diffraction (along with SEM) after 15 minutes of 60Hz ultra sonication, and after dry compaction between two optically smooth perspex plates with 300g of load spread over the top layer of perspex in the CETR tribometer, to guarantee all particles have been contained ensuring maximize breakdown of particles.

The modal diameter of the particles obtained from the tests are outlined in Table 5. Additional information regarding particle size scatter and ranges are included in Appendix C.

**Table 5: Particle sizing by laser diffraction, showing average modal particle diameter from 3 repeated tests and confirmed using 50 particle measurements from a minimum of 10 SEM micrographs.**

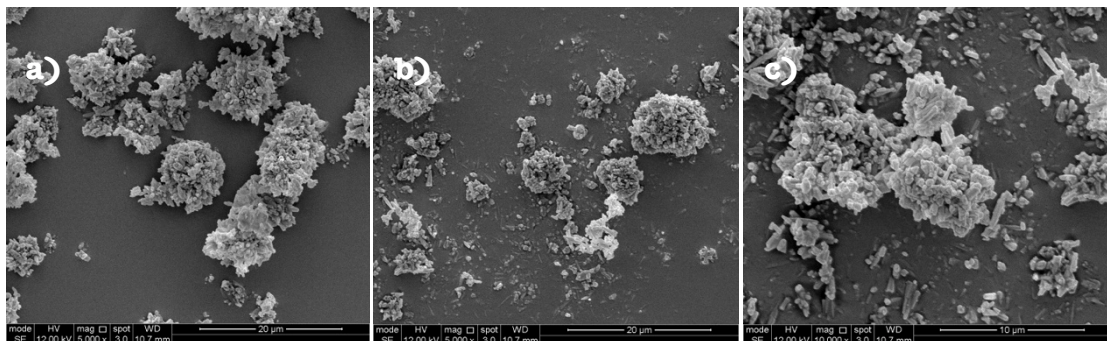
Particle Name	As received	After Ultra	Dry brushed	Fluid brushed	Dry Compaction
	Modal particle Diameter ( $\mu\text{m}$ )				
CalEssence 70	0.70	0.71	0.71	0.70	0.56
Sturcal F	1.60	7.12	1.55	1.30	1.02
S2E	3.45	3.65	2.05	2.02	1.95
Albafil	3.60	3.75	3.05	2.65	2.82
Rods	6.02	6.22	3.31	3.21	3.13
Sturcal L	6.73	12.51	6.56	7.20	6.63
Omya 5AV	7.85	10.64	6.54	6.64	6.13

### 3.1.1. Evolution of Particles

Each set of resultant particles obtained from the tests were imaged using SEM. If the particle was tested dry the particles were sprinkled onto a carbon tab and gold-coated. If the particles were tested wet the resultant solution was pipetted onto a carbon tab, this left to air-dry and then the sample was gold coated for imaging. This section outlines key finding from sizing testing.

CalEssence particles are extremely small and seem to exhibit no agglomeration properties, even when energy is added via ultra sonication. Dry compactions reduces the modal particle size marginally but particles do not breakdown via dry or fluid brushing; most likely as the particles themselves are too small to be captured or entrained by the nylon filaments [36].

Sturcal F particles individually are around  $1.6\ \mu\text{m}$  in length. It was seen when ultra sonic energy was applied to Sturcal F in solution larger agglomerations of particles were seen (around  $7.12\ \mu\text{m}$  in diameter). It should be noted that with all other testing though the modal particle size is given in Table 5 smaller peaks were seen between the  $5\text{--}8\ \mu\text{m}$  range, still suggesting strong agglomeration.

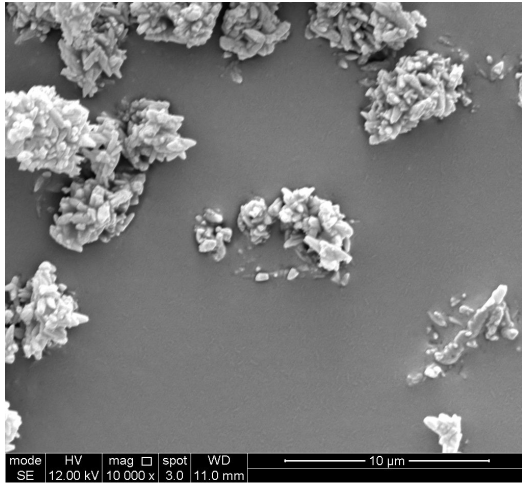


**Figure 43: Sturcal F particles imaged a) as received b) after fluid brushing c) after dry compaction**

Figure 43 shows a typical agglomeration within three scenarios. Each agglomeration is spherical with the tips of Sturcal F protruding outwards. Fracture of these particles can also be seen in Figure 43 parts a and b. Fracture is clean and usually at the tips of the particles creating smaller particles that scatter across the surface, explaining the modal particles size of around  $1.02\text{--}1.55\ \mu\text{m}$  after brushing and compaction testing.

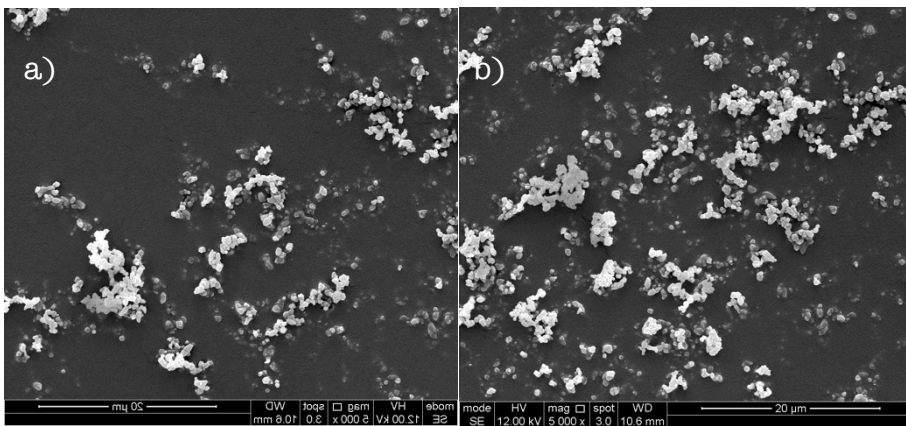
S2E exhibited little agglomeration across each scenario. Fracture across the scenarios was similar; clean fractures across the width of the particle normally within the middle section of the particle.





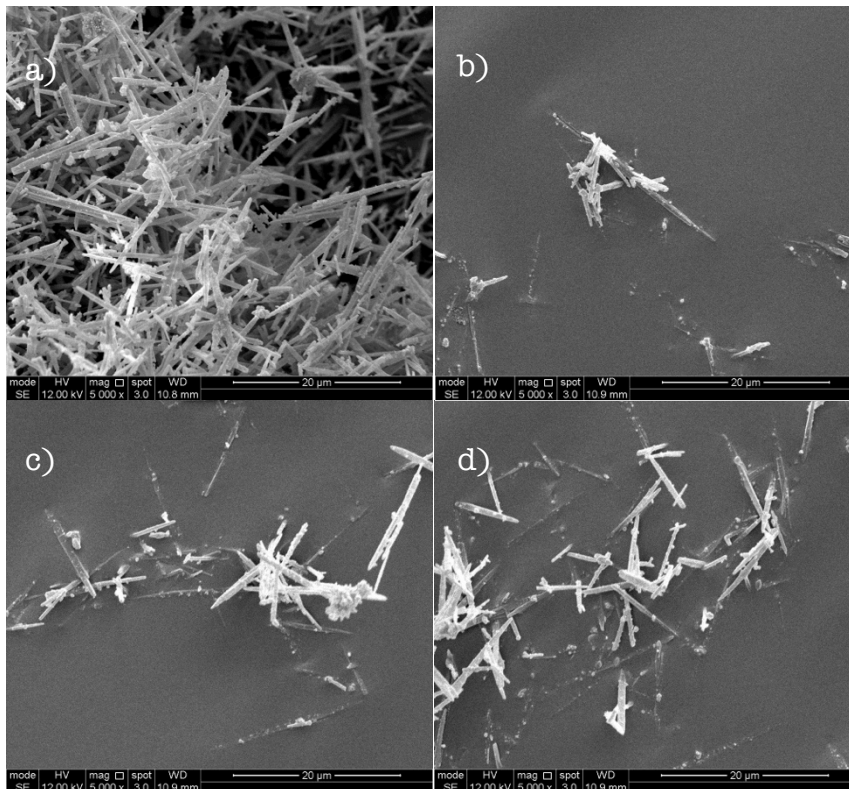
**Figure 44: S2E particles after dry brushing.**

Albafil exhibits similar behavior to S2E (no evidence of agglomeration) and has very little major breakdown so SEM images look similar across testing set-ups.



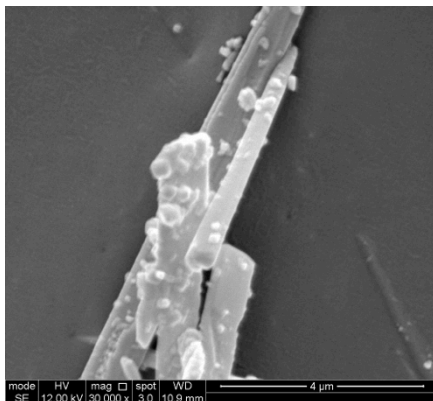
**Figure 45: Albafil particles imaged after a) dry brushing b) fluid brushing**

Rod particles were found to exhibit neat fracture at the tips (on both sides) at each scenario, as can be seen in Figure 46. The particles are loosely interwoven but did not forming adhesive agglomerations, rather just laying on top of one another.



**Figure 46: Rod particles imaged after a) ultra sonication b) dry brushing c) fluid brushing d) dry compaction.**

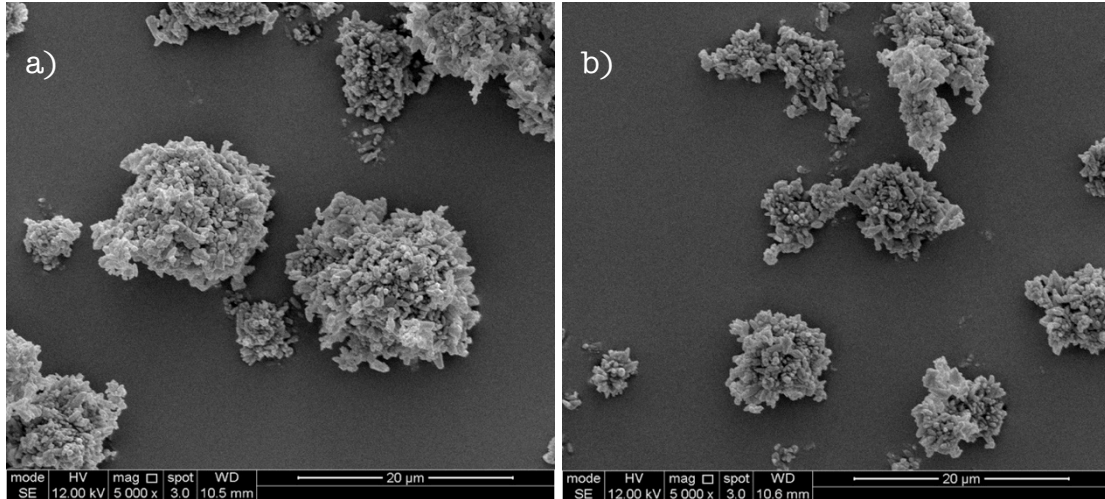
Fracture across each scenario can be seen to be neat across the width of the particle, as well as at the tips forming smaller ‘sub-particle’ that are just small triangle-like tip particles.



**Figure 47: Fracture across a Rod particle with smaller ‘tip sub particles’ laying across it.**

Sturcal L and Omya 5AV particles are resilient particles, both resisting large breakdowns from brushing or compaction.

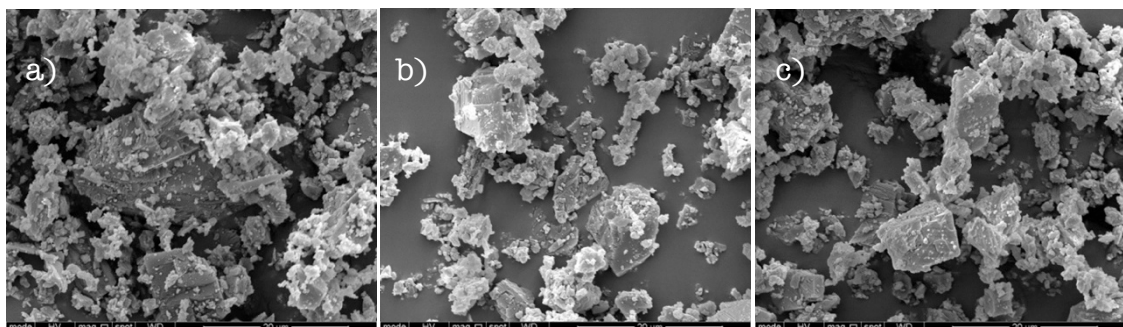
Sturcal L showed interesting agglomeration behavior, especially after ultra sonication. Like with Sturcal F though the modal particle diameter peak is shown in Table 5, small peaks were also seen between 10-25  $\mu\text{m}$  at every scenario.



**Figure 48: Sturcal L particles after a) ultra sonication b) fluid compaction.**

These large agglomerations can be seen in Figure 48. Large clusters can be seen with the tips and ends of the Sturcal L particles protruding outwards, creating spiky larger particles.

Omya 5AV particles are not PCC and instead crushed calcium carbonate. This means there is no regularity in shape or size across testing (both before and after).



**Figure 49: Omya 5AV particles imaged a) as received b) after fluid brushing c) after dry compaction**

This large variation in size and shape of particles makes it hard to generalise the breakdown behaviour of Omya 5AV at any stage of testing.

### **3.1.2. Discussion and Conclusions of Particle Sizing**

Particles were sized using laser diffraction technology. This obtains a modal particle size, assuming an error of  $\pm 0.05 \mu\text{m}$ . Since this cannot take into account agglomeration tendencies of the particles in water additional SEM analysis was undertaken. From basic SEM analysis



individual particle shape, size and overall geometry of any clusters can be observed directly.

From the SEM images in Section 4.1 (Table 3) it can be seen there is a good variation in the shape and particle geometry of calcium carbonate particles available. These different geometries (along with the different crystal structures) will lead to differences in particle breakdown and fracture. This in turn will directly lead to differences in abrasivity of these particles.

From the SEM images (Figure 43-50) it can also be seen there is more control in the uniformity, quality and integrity of particles made through a precipitation process rather than the grinding process of standard (Omya 5AV) particles used in toothpaste currently. Though this gives greater control over the properties of the particle produced it is notably a more costly process.

Particles are ordered in terms of size in Table 5, with CalEssence and Sturcal F being the smallest as received and Omya 5AV the largest. This project will also discern the importance of size with respect to abrasivity.

It can be seen the different shapes of the particles lead to a different breakdown mechanism of particles. For instant though Rods and Sturcal L are of similar length when received Rods have a greater tendency to breakdown due to their thin nature.



**Figure 50: SEM image showing clean fracture of rod particles from brushing testing.**

Prior to testing it was assumed that ultrasonication of the particles in solution would encourage particles to disperse and therefore reduce agglomeration effects. In actual fact this was not found at all. With a majority of particles (Sturcal F, Sturcal L and Omya 5AV) showing an inclination to agglomerate instead. The other particles, Rods, Albafil,

CalEssence 70 and S2E, didn't show a difference in modal particle size with ultrasonication, this with SEM confirmation suggest the particles do not agglomerate in solution, even with the extra ultrasound energy provided.

Sturcal L and F particles both form aggressive, spiky, strong agglomerations that will be more aggressive to surfaces than if the particles were acting individually. The tenacity of these, and all other particle agglomerates is further investigated in the following section.

### **3.2. Particle Agglomeration - Analysis by Particle Division**

#### **3.2.1. Experimental Procedure**

To further investigate these agglomerative particles without the aid of ultrasound energy, multiple divisions of particles between adhesive tape were studied to assess particle breakdown, tenacity and strength of agglomerations and how that varies particle to particle.

- Dry particles were scattered onto clear adhesive tape. Particles were distributed as evenly as possible and excess particles blown away by a discharge of compressed N<sub>2</sub> gas. This process was then repeated until there was a full and even coating of particles. At no point were the particles in contact with human hands, oils or moisture to ensure there was no contamination to the results.
- Particles were drawn apart using a clean secondary adhesive tape. Tape was folded, evenly and at a slow pace, back onto the primary adhesive tape and no pressure applied to minimize breakdown of particles.



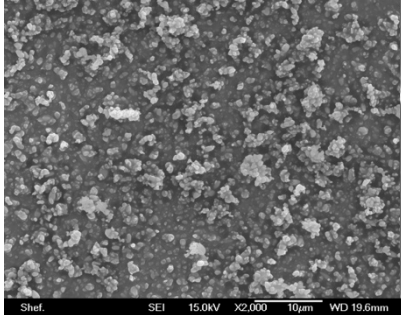
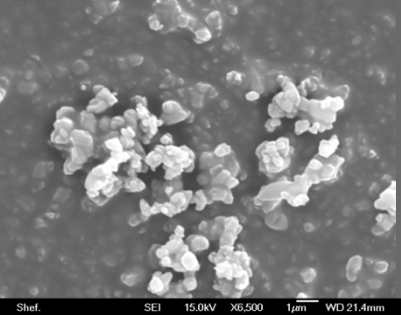
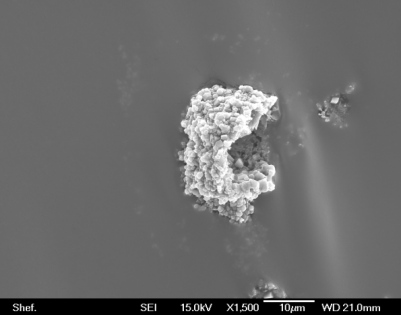
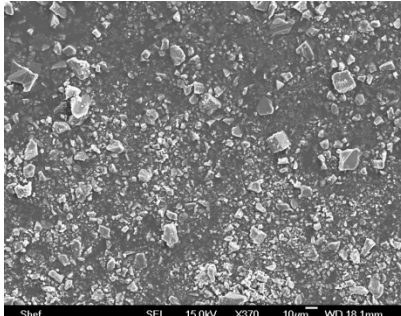
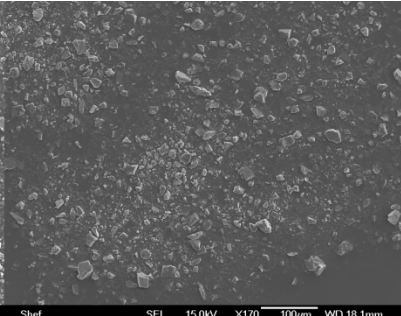
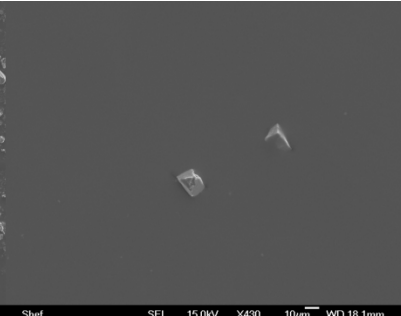
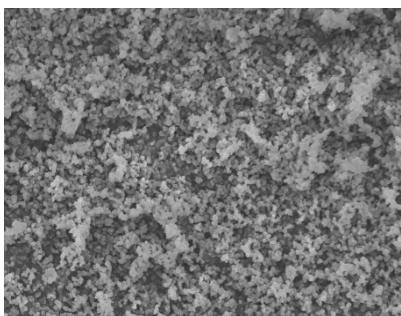
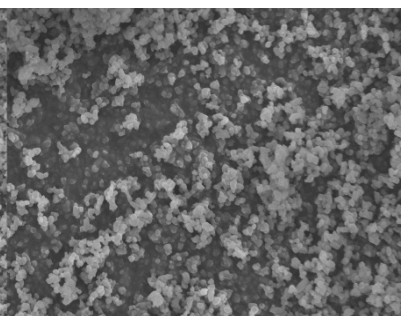
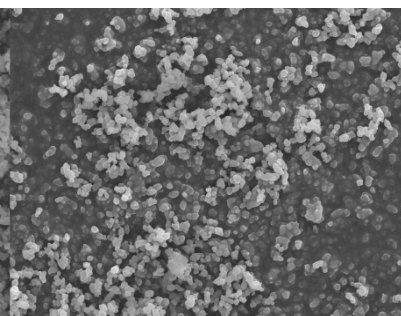
**Figure 5 1: Division of particles**

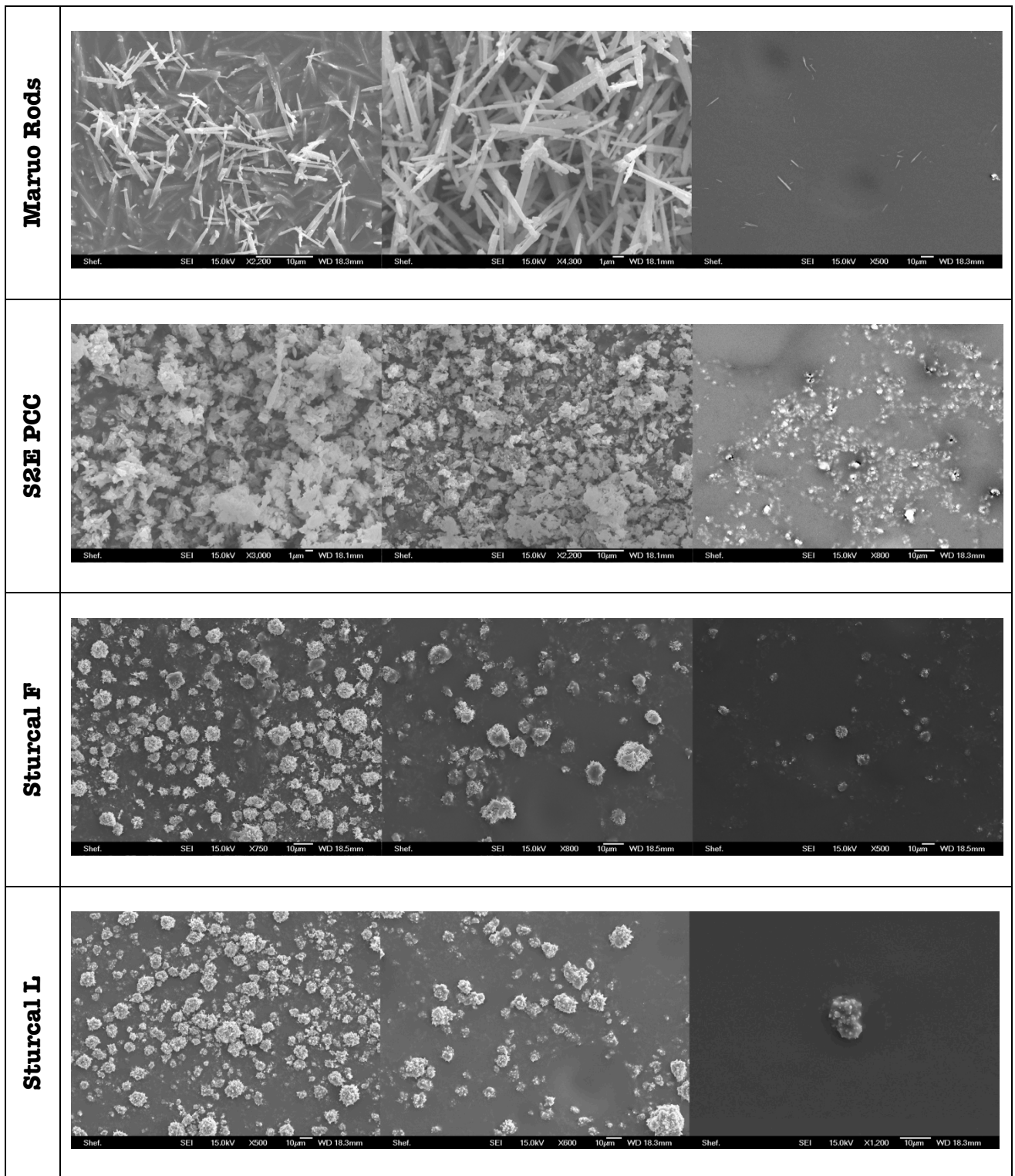
- This process was repeated for 1, 4 and 6 divisions.
- Particle divisions on were gold-coated and then studied using scanning electron microscope.

### 3.2.2. Results and Discussion

Table 6 compares SEM micrographs of remnant particle formations after 1, 4 and 6 separations between adhesive tape. Each image shown below is given at the best scale it was deemed to give a clear image of agglomeration number and shapes.

**Table 6: SEM images of the resultant particle formations after 1, 4 and 6 divisions**

	1 Division	4 Divisions	6 Divisions
CalEssence 70			
Omya 5AV			
Albafil			



CalEssence 70 is a prismatic particle that is very small in size. CalEssence 70 were very easily removed from the surface and showed small indications of particle gatherings on the tape (around 2 µm) but due to their random nature were not deemed strong agglomerations, even after 6 divisions.



Omya 5AV shows no obvious agglomerations between divisions. All the particles are large and remain independent of each other.

Similar in shape to Omya 5AV, Albalfil particles also show no obvious signs of agglomeration. Particles remain independent, though particle presence does decrease with each division. This behavior is likely to be due to the shape of Albalfil particles. Albalfil is a three dimensional polygon in geometry, giving a large surface contact area on the adhesive substrate making it more reluctant to leave the substrate surface, and Omya 5AV a more rounded version of this agglomeration shape.

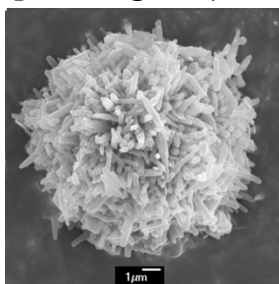
Initial particle scattering of Rods show that they are loosely interwoven but after divisions (especially after 6) it can be seen these interactions are extremely weak, and stronger bonding to the tape, and only a few scattered particles are left. This indicates particles are not held together rather they are geometrically inclined to interact and interweave but not pulled to stay together.

S2E particles exhibit some localised agglomeration scattered on the tape. Though these agglomerations are not steady in size or shape. Though the agglomerations do generally decrease in size throughout divisions (suggesting the larger agglomerations are easily removed from these foundations, see Figure 52) they have no defined structure or form.



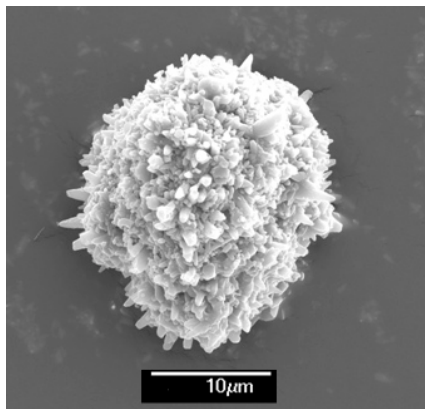
**Figure 52: Illustration showing how size decrease could be down to preferential removal of larger agglomerations**

Sturcal F shows very strong agglomerations. It was seen that these agglomerations do not pull apart easily (though the modal agglomeration size does progressively get smaller with the number of divisions). These agglomerations were found to be around 7  $\mu\text{m}$  in size, which is consistent with that found in earlier ultrasound testing. These agglomerations are spherical in nature with tips of the Sturcal F protruding and projecting outwards, rendering the overall structure quite angular, as can be seen in Figure 53.



**Figure 53: Typical Sturcal F agglomeration**

Sturcal L particles were seen to agglomerate in a similar fashion to that of Sturcal F; strong spherically arranged particles that do easily break apart, Figure 54.



**Figure 54: Typical Sturcal L agglomeration**

The modal agglomeration size was significantly larger with Sturcal L particles (around 15 µm in diameter).

### **3.2.3. on Agglomeration Trials**

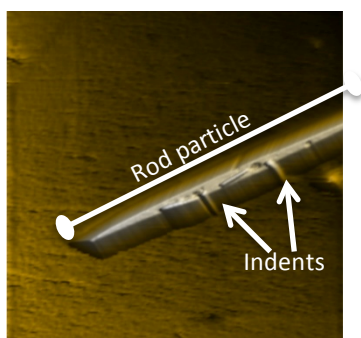
Omya 5AV and Rods had no affinity to agglomerate.

S2E particles do show a slight tendency to form agglomerations though there is no real interaction between agglomerations, agglomerations that were seen chaotic in nature and to uniform particle arrangement.

Sturcal F and Sturcal L particle show a high tendency to form spherical cluster agglomerates. It is hypothesized this affinity to agglomerate, and produce effectively larger particles, will show in later abrasion wear tests.

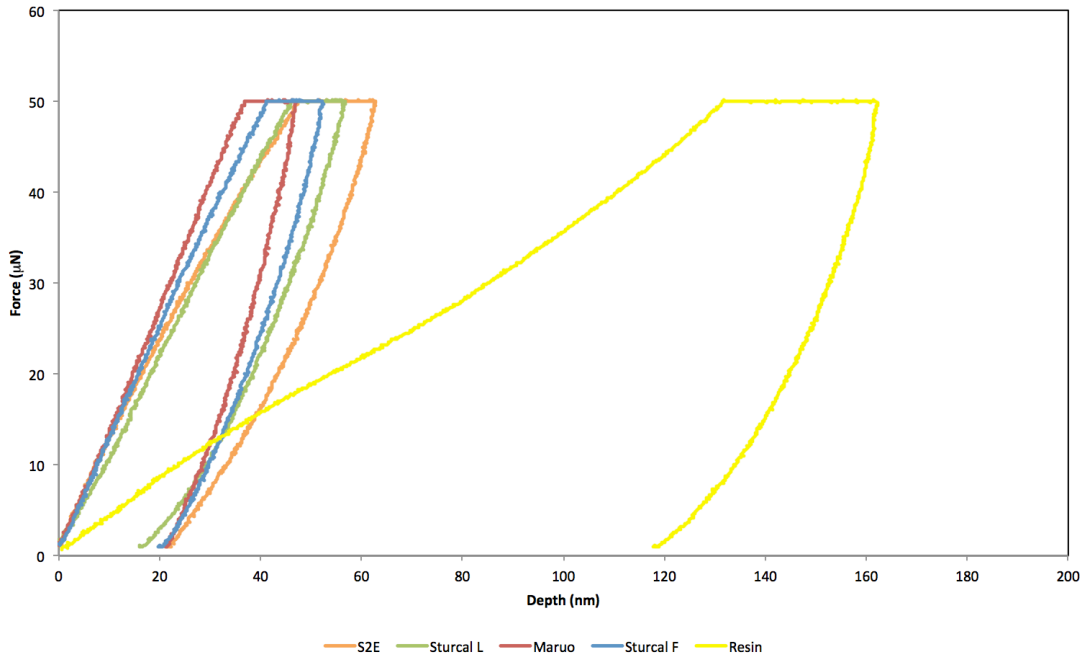
### **3.3. Hardness Characterisation Results**

Measurement of hardness of the CaCO<sub>3</sub> particles was undertaken via the nano-indentation method described in Section 4.2.9.



**Figure 55: AFM image of Mauro Rods particle after indentation**

Figure 56 shows the average of ten sets of results for each particle type. The hardness measured from this method can then be seen in Table 7. The depth of indentation on each particle was less than the particle width of each particle.



**Figure 56: Nano indentation of particles embedded in TAAB resin; curve of indentations. Each curve is the average of ten separate indentation curves.**

**Table 7: Hardness' of CaCO<sub>3</sub> particles, n=10**

Particle Name	Average Hardness Measured (GPa)	Standard deviation
Sturcal F	1.0	0.3
S2E	1.0	0.4
Rods	2.1	0.4
Sturcal L	1.0	0.3
Omya 5AV	1.0	0.3
Resin	0.2	0.05
Dentine [8, 9]	0.6	
Stain [8, 9]	0.3	

### **3.3.1. Hardness Characterisation Conclusions and Discussion**

It is clear from previous testing [2] that this information is only relative to the particles tested within this method, and the resin the particles are embedded in is having some effect.

From these numbers it shows only the Rods stand apart from the others. Which means differences in further wear testing undertaken in this project are due to morphology and shape of the particles rather than differences in intrinsic hardness.

Hardness testing of human teeth has shown that stain hardness is around 0.3 GPa and Dentine of around 0.6 GPa [8, 9]; though the methods used to generate this hardness data were different to that used in the above method. The resin is most likely to have an effect on hardness data within this experimental procedure and therefore particle hardness data in section 3.3 was primarily used to compare between particles themselves only. If all the hardness data compared directly, this testing has shown these micro-calcium carbonate particles are of a higher hardness than both dentine and staining, giving good reason to expect them to be abrasive to both surfaces.

### **3.4. Summary**

In this chapter the particle microstructure and mechanical properties of the calcium carbonate particles of interest to this study have been characterised.

Particle sizing has shown the calcium carbonate particles studied in this thesis vary in size from 1.60 to 7.85  $\mu\text{m}$ , with Sturcal F being the smallest and Omya 5AV being the largest. Particle brushing and compaction breakdown analysis has shown the Rods have the greatest affinity to breakdown, followed by S2E and Omya, Sturcal L and Sturcal F particles showed resistance to breakdown in both dry compaction and fluid breakdown.

Each particle was imaged via scanning electron microscopy. This visual characterisation highlighted the morphology differences between particles - particularly that between commonly used GCC and novel PCCs. The precipitated particles showed much more uniformity from particle to particle, in both shape and size. The nature of the milling process to produce GCC resulted in no natural shape bias, instead Omya 5AV was found to have a general large size and angular morphology of no set shape; unlike the precipitated particles. PCCs were all the same in terms of shape and had very little variance in size from particle to



particle. This uniformity did lead to a greater control in the fracture and breakdown size of the particles resulting from brushing and crushing. Improved uniformity does come at a cost, with PCCs being notably more expensive than GCCs, a factor important to the oral care industry.

When ultrasound energy was applied to the particles in solution Sturcal F and Sturcal L showed a great affinity to form agglomerations (both increasing in average particle diameter by 6  $\mu\text{m}$ ), whilst S2E particles and Rods did not. Omya 5AV average particle diameter did increase with ultrasound energy (by 2  $\mu\text{m}$ ) but not as dramatically as that shown with Sturcal L and Sturcal F.

Further agglomeration testing done by particle separation showed a similar pattern. Omya 5AV and CalEssence 70 was shown to have no to real agglomerations but Omya 5AV showed resilient large particles. S2E and Rods exhibited weak agglomerations with particles loosely connected to each other but easily drawn apart. Sturcal F and Sturcal L on the other hand showed strong agglomerations, spherical in shape with the ends of the particles themselves protruding outwards, with modal agglomeration size of the Sturcal L being significantly larger (15  $\mu\text{m}$  to Sturcal F's 7  $\mu\text{m}$ ). Again these results complied with the ultrasound agglomeration results shown in Section 3.1.

Particle hardness has been measured using nanoindentation on a TAAB resin base. This method has shown a range of hardnesses from 0.98 to 2.06 GPa (with the resin itself measuring at 0.21 GPa). This scatter gives reasonable validation of the method for it to be used as a comparison between the particles used in this section. Literature showed calcium carbonate to have an average hardness of 0.7 GPa [8] this indicates the TAAB resin has had an effect on the results in this section, showing these hardness results can only be used as a comparison scale for the particles in this study.

Generally particles have a measured hardness, using this method, of that close to 1 GPa. Showing it is only a difference in shape and morphology that defines these particles abrasivity. Only the Maruo Rods differing from this at 2.06 GPa. This is significantly higher than that of the other calcium carbonate particles.

The next 3 Chapters will further investigate the abrasive nature of these calcium carbonate particles. Chapter 4 will concentrate on the wear effects of these particles. Chapter 5 the wear substrate characteristics and Chapter 6 the particle movement and motivation.

## **CHAPTER 4**

### **SCRATCH ANALYSIS OF CALCIUM CARBONATE PARTICLES USING LINEAR RECIPROCATION**

Chapter 4 investigates the abrasivity of  $\text{CaCO}_3$  particles by evaluating the nature of scratches caused by calcium carbonate particles on different substrates and the different surface roughness and wear each particle produces. Scratch analysis on copper seen in this chapter is also implemented and continued in Chapter 6.

#### **4.1. Introduction**

The different morphology of different calcium carbonate particles is expected to affect their mobility on surfaces, and surface interactions leading to surface wear. Preliminary wear trials of the particles were conducted on perspex substrates using the linear reciprocating toothbrush rig. Tribological tests were conducted without water for 3 minutes.

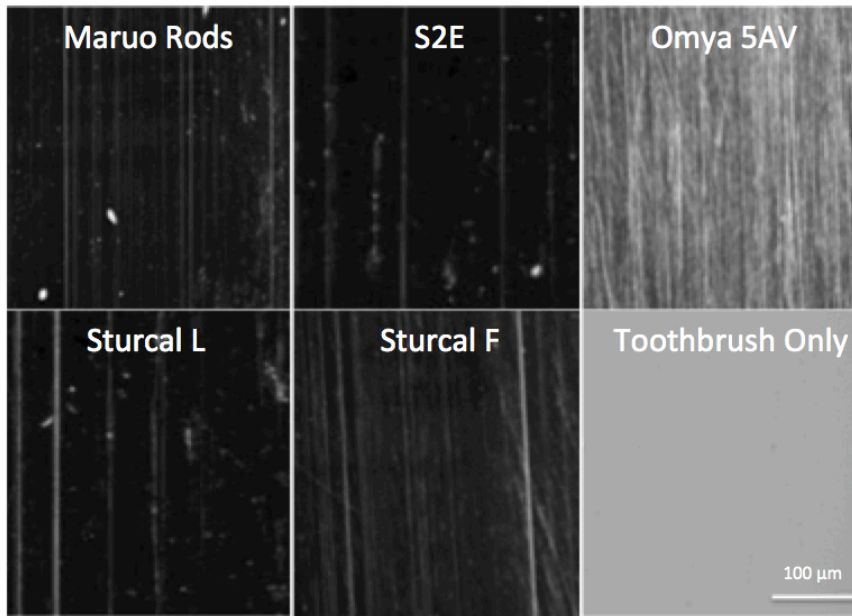
Scratch analysis was conducted post-trial using optical microscopy and AFM to map surface topography, to quantify scratch depths and surface roughness.

Secondary to this, the same rig was used to produce scratches from only one brush stroke (just forward) on a piece of highly polished copper. This was then studied under SEM.

#### **4.2. Experimental Results**

Figure 57 shows optical images of the scratch characteristics. Each image is taken at 10 x magnification in bright field mode using a Nikon Eclipse ME600 optical microscope. Figure 57 is purely an image to show the variety in scratch traits and frequency caused by each particle. This is further quantified in Figure 58, which shows AFM scans of the same Perspex scratch tests.

It is clear there is a lot of variance in not only the scratch frequency and severity but also in the residual scratches themselves.

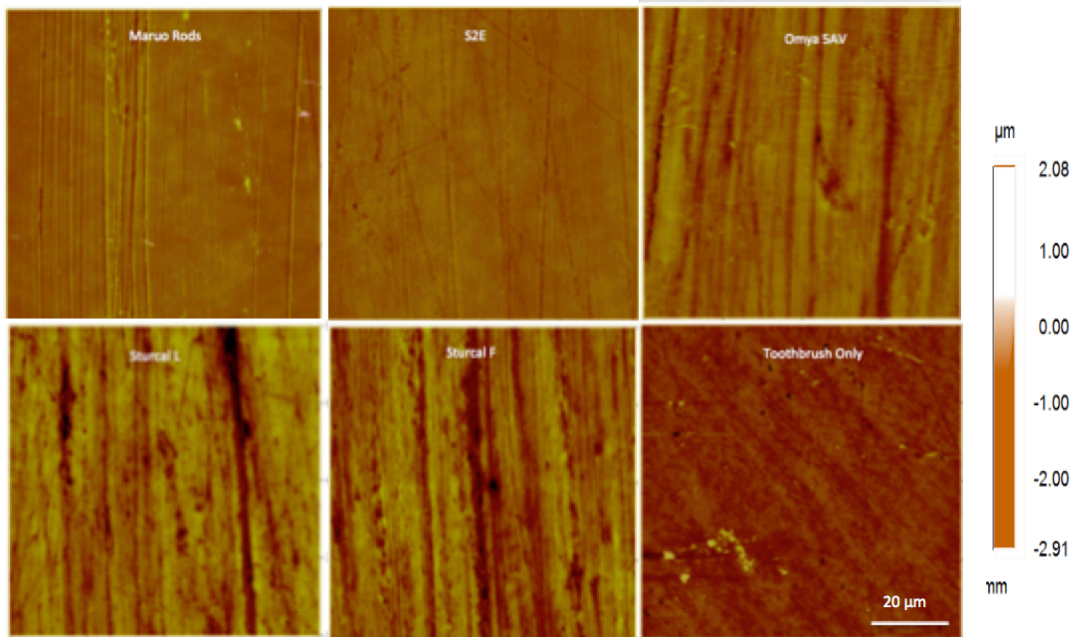


**Figure 57: Optical microscopy images of perspex scratch tests**

Maruo Rod and S2E particles have the lowest rate of deep residual scratches and therefore can be seen to be gentle and sensitive to the substrate. Omya 5AV, on the other hand, can be seen to be on the other end of the abrasivity scale. Omya residual scratches can be seen to be deeper and high in frequency, with no uniformity or clear scratch direction. Particles seem to have a high degree of freedom, even when captured by brush filaments, acting aggressively towards the substrate. This is a trait that would be useful in the removal of tartar build up, but will obviously come at a price for the dental substrate below. Both Sturcal L and Sturcal F do introduce some seemingly deep scratches and show a larger scratch frequency under the imaging conditions than that of the 'gentler' particles but lower than that of Omya 5AV. They have more uniformity and parallel scratches, suggesting good entrainment of the particles/their agglomerates within the toothbrush filaments.

Scratching trials with a dry toothbrush produces no notable scratches to the perspex surface (Figure 57).

To quantify the data surface height analysis by AFM analysis was done at the center of the perspex surfaces.



**Figure 58: AFM images of perspex scratch tests**

These AFM plots show depth of scratches by the darker shading, highlighting surface markings. It can be seen Omya 5AV, Sturcal L and Sturcal F have the deepest scratches, which was to be expected from the optical images previously.

Sturcal F showed the most chaotic and widespread surface topography, with a combination of deep and shallow residual scratches. Sturcal F particles were measured to be of average size 2 microns but the scratch sizes themselves are much wider than this suggesting strong particle agglomeration. This would also explain the wide variance in scratch widths found. Sturcal L showed widespread intermittent pock marking in the surface material. Suggesting a high rate of particle breakdown leading to smaller 'tip' particles digging into the surface.

Scratches from S2E and Rods look fairly shallow. Scratches from Rod particles look very neat and parallel.

The 2D surface maps in Figure 58 were obtained in conjunction with the linear height profile data, an example of which is shown in Figure 59.

The AFM scans also determined Ra across chosen scan lines. A summary of an average of ten AFM profile data plots, done at the centre of ten individual scratch trials, can be seen in

Table 8 (this data was collected perpendicular to reciprocation direction).

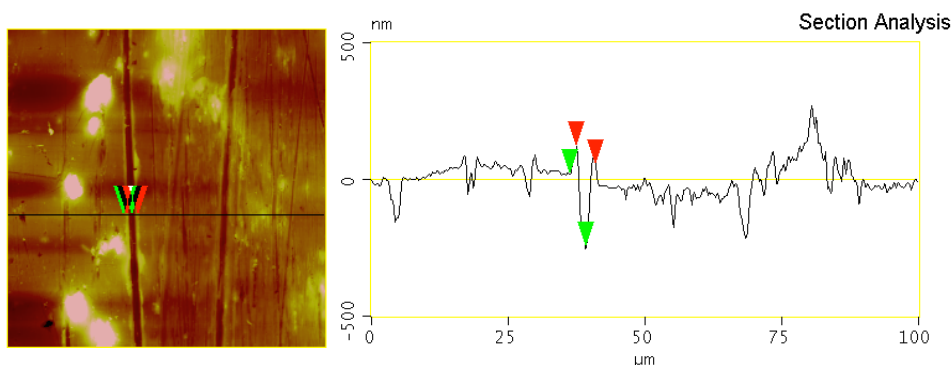
**Table 8: Data collected from AFM of perspex scratch trials. Average of ten trials.**

Particle	Average size (microns)	Average scratch frequency (/80 $\mu$ m)	Greatest Scratch Depth (nm)	Average scratch depth (nm)	Ra (nm)
Sturcal F	1.60	35	178	139	31
S2E	3.45	34	60	46	9
Rods	6.02	18	45	35	6
Sturcal L	6.73	33	118	36	24
Omya 5AV	7.85	22	241	225	40

It can be seen there is no clearly defined relationship between maximum scratch size, average scratch depth or even scratch frequency and particle size.

Omya 5AV produces the roughest finish post-brushing, which is highly undesirable from a consumers point of view (where a polished or smoother surface finish is more aesthetically pleasing).

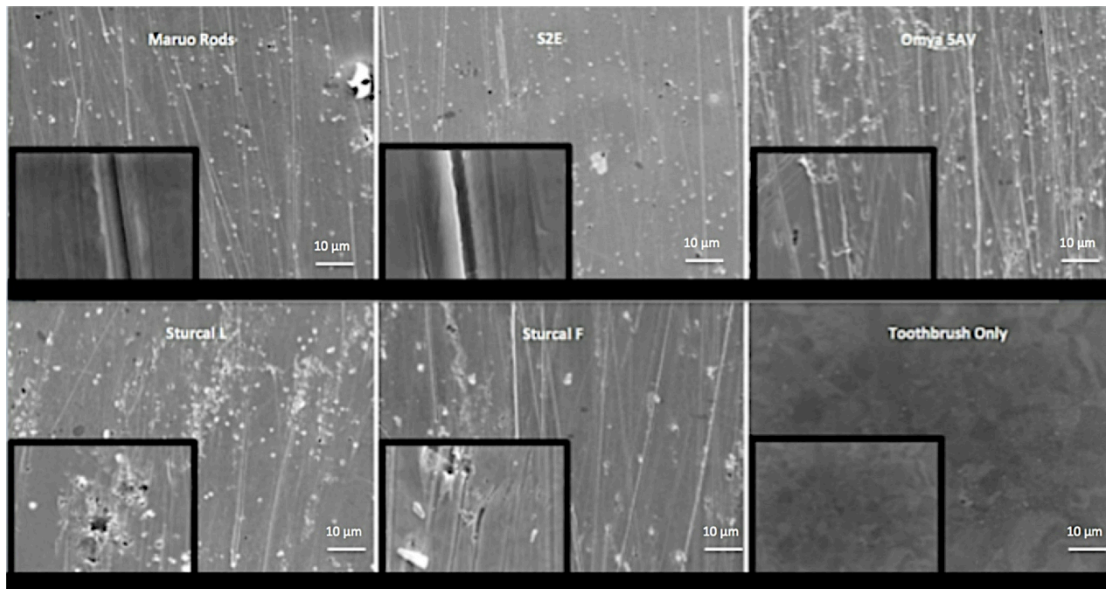
The most sympathetic particle was the Maruo Rods, with very shallow scratches, despite being of slightly larger size. Sturcal F, individually, is of a similar geometry to the Rod particles and smaller in size but instead Sturcal F produces much deeper scratches and a much rougher end surface. This could be due to, as discussed before, Sturcal F forms strong agglomerates and therefore are more readily entrained by toothbrush filaments. Whereas Rod particles are thin in length and mainly loose, so more prone to breakdown, making it harder for them to be captured by bristles.



**Figure 59. : Left: AFM image of S2E scratches. Right: Linear surface profile scan showing scratch depth and frequency.**

The scratch analysis suggests subtle differences shape and geometry to be more significant than particle size itself in how they move and how they themselves get captured by the brush. The particle movement and motivation is difficult to gauge from these AFM images.

To further investigate this one brush stroke was carried out using dry particles on a piece of highly polished copper. The resultant residual surface damage was then imaged by SEM, the resultant images of which can be seen in Figure 60.



**Figure 60: SEM images of brushed copper (higher magnification of individual scratch can be seen in bordered boxes).**

Microstructural analysis showed that Rod particles had generated extremely continuous scratches, which were more spherical in cross-section with raised, pronounced ridges. There was not a high prevalence of small scale scratching.

Scratches caused by S2E particles were extremely shallow, with a few deep scratches; showing particles can cause damage if entrained in a particular way.

Omya 5AV particles show evidence of high directional freedom of movement of the particles with a more variation in scratch depths and some gouging in large localised portions. The scratches frequently appear very intermittent showing evidence of very jagged scratches and irregular scratch lengths.

Sturcal L particles gouged the surface more than any other particle. The size and geometry of the gouges suggests individual particle penetration

which could suggest ploughing. The brushed copper showed more irregular surface damage than scratching.

Sturcal F testing showed a some considerably deep scratches with large penetration and gouging occurring at the end of these scratches. Suggesting the particle slides along until pushed to roll (most likely due to filament angle during the stroke) and subsequently penetrate into the surface of the copper.

These scratch trials were also used in conjunction with nanomanipulation trials in Chapter 6 to further analyse particle movement and motivation in-situ.

### **4.3. Conclusions**

This chapter has shown it is not the size of the particle that determines its abrasivity or ability to roughen a surface alone. The results in this chapter show there is also no clear relationship between size and abrasivity instead it is subtle variances in geometry that determines how a particle behaves, agglomerates and interacts with brush filaments and substrate.

From the results within this Chapter it can be seen that Omya 5AV generates the most roughening of substrate surfaces and produces the deepest scratches. However the largest particles were not always the most detrimental to a substrate surface. Sturcal F, the smallest particle in this study, exhibiting high roughening of surfaces, deep scratches and a large level of scratching and gouging. It is very likely this is due to strongly held together agglomerations and particle breakdown.

Chapter 5 continues to investigate surface roughness and wear depth by using dentine substrates.

## **CHAPTER 5**

### **HUMAN DENTINE WEAR BY CALCIUM CARBONATES**

Chapter 5 outlines investigations of the wear of polished human dentine with the calcium carbonate particles used in Chapter 4 using the linear reciprocating method summarised in Chapter 2 Section 2.4.5.

The abraded dentine samples were then characterised by SEM imaging and further analysed via profilometry for scratch and wear behaviour analysis.

#### **5.1. Wear Testing Using Reciprocating Tribometer Experimental Approach**

Nylon ball-on-tooth linear reciprocating wear trials were conducted with particles in fully saturated solution. This solution was constantly replenished at the contact zone. Each test was carried out for 30 minutes under the following condition; 0.3N load at 1.25Hz frequency, 0.3N load at 2.5Hz frequency, 0.3N load at 5Hz frequency, 0.45N load at 2.5Hz frequency and 0.6N load at 2.5Hz frequency. A final test was then carried out at 0.3N load at 2.5Hz frequency with the suspended particle solution with 10% wt particle and 10g added SCMC (Sodium Carboxymethyl cellulose) and glycerol binding agent to give a paste consistent with that of a typical toothpaste.

#### **5.2. Results**

The maximum depth of the resultant dentine wear scars for each scenario with each particle is shown in Table 9 below. Each test was repeated 3 times, each wear test result was within  $\pm 2 \mu\text{m}$  of each other. Table 9 shows the average of these tests.

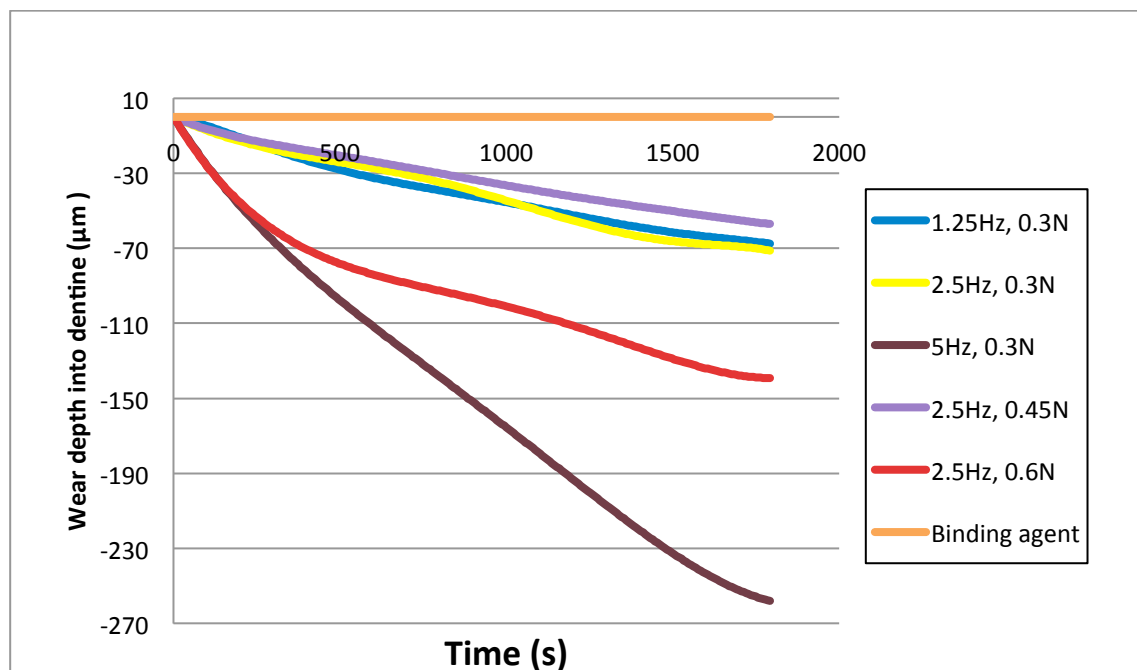


**Table 9: Dentinal wear depth after 30 minutes (n=3 each trail had a scatter of  $\pm 2 \mu\text{m}$ ).**

Frequency/L	Overall wear profile depth, d ( $\mu\text{m}$ )					
	Omya	S2E	Sturcal	Sturcal F	Rods	Albafil
<b>1.25Hz, 0.3N</b>	48.1	12.2	48.6	22.6	54.2	69.7
<b>2.5Hz, 0.3N</b>	82.2	40.9	128.8	84.2	46.9	72.6
<b>5Hz, 0.3N</b>	224.4	169.2	124.8	333.6	44.3	259.8
<b>2.5Hz, 0.45N</b>	52.5	103.9	201.3	49.6	58.8	52.3
<b>2.5Hz, 0.6N</b>	73.1	26.1	79.8	55.6	25.4	140.9
<b>Binding</b>	5.3	1.5	9.0	2.3	8.2	7.8

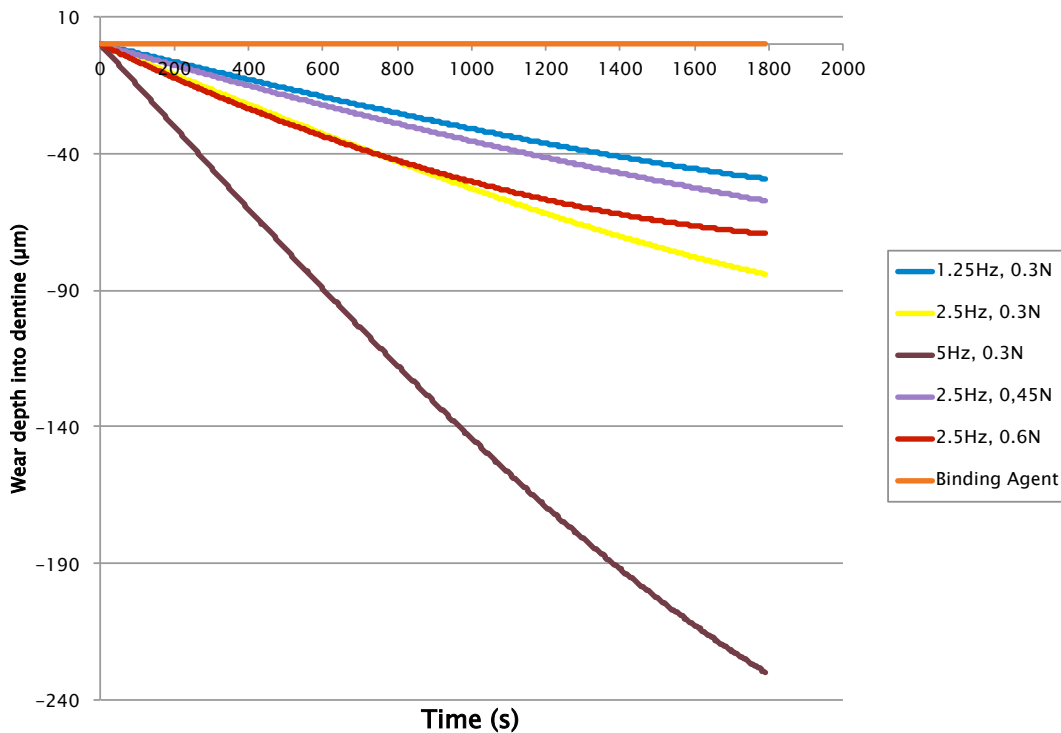
### 5.2.1. Wear Depth Comparisons Through Scenarios

The following graphs show the position of the nylon ball during testing, measures in-situ by the Bruker UMT 3 CETR displacement sensor. The position of the ball was set to zero prior to the start of each test scenario. The nylon ball position gives a good indication of the rate of wear/material removal during testing throughout the different scenarios.



**Figure 61: Change in vertical ball position for dentine abrasion by Albafil particles at each scenario (average trend line, n=3)**

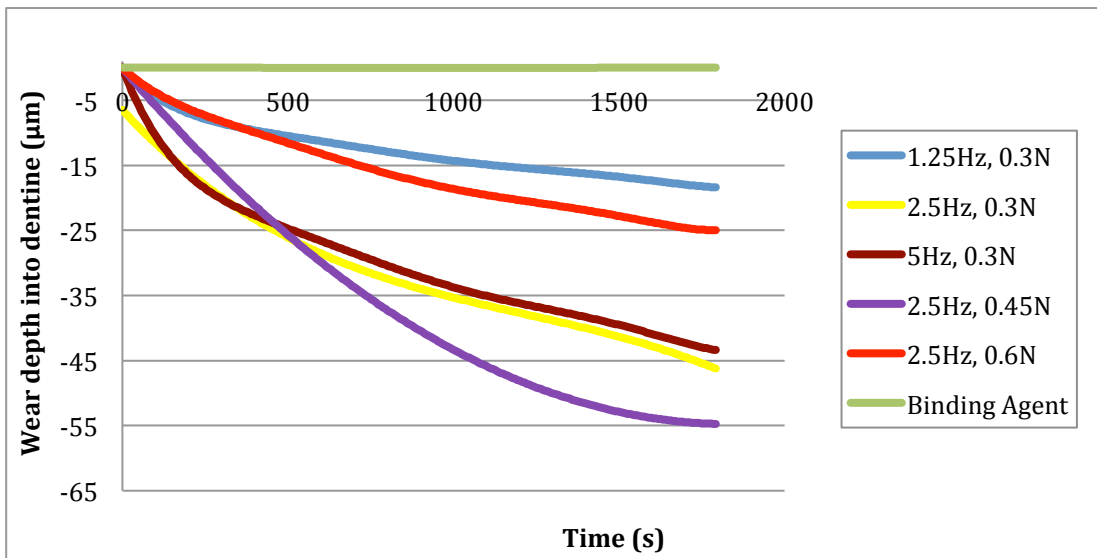
It is clear with higher frequencies the rate of material removal is higher for Albafil. Wear also rapidly increases for the higher load (0.6N). At lower loads and frequencies the wear rate and end wear depth is comparable. The addition of SCMC binding agent to the paste significantly lowers wear, useful for daily toothpastes.



**Figure 62: Change in vertical ball position for dentine abrasion by Omya 5AV particles at each scenario (average trend line, n=3).**

Figure 62 shows the change in nylon ball position during each wear test using Omya 5AV particles. The medium load and frequency produce more overall wear. It can be seen an increase in loading does not produce a systematic change in the resultant wear depth instead an increase in speed had the most dramatic effect on material removal (this fits with earlier testing, in Chapter 3) showing that Omya 5AV particles are large in size and not prone to easy breakdown, still being significantly strong at higher loads. It can also be seen the introduction of a binding agent reduces scratch prevalence and overall wear dramatically.

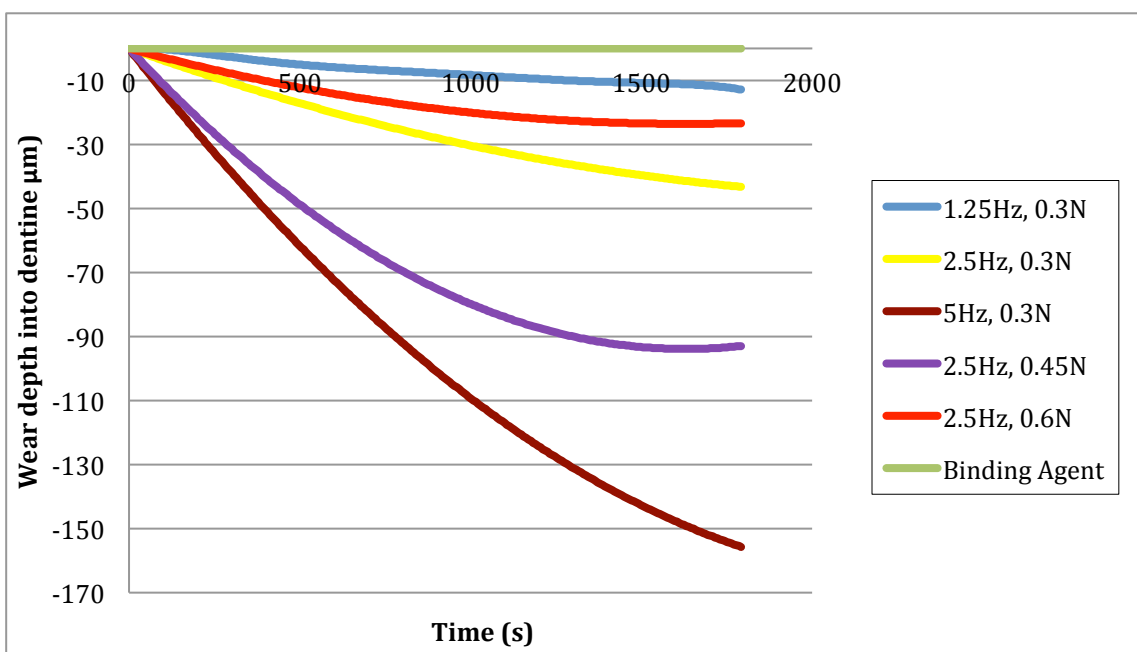
The nylon ball position during wear testing with Rod particles can be seen in Figure 63.



**Figure 63: Change in vertical ball position for dentine abrasion by Rod particles at each scenario (average trend line, n=3).**

Firstly for Rod particles it should be noted that even the highest overall wear depth (58.5 µm at 2.5Hz, 0.45N) is very low compared to the previous two graphs (both above 200 µm), so scatter seen in Figure 63 is much smaller than it appears. In terms of trends the opposite can be seen for Rod particles, an increase in load (0.45N to 0.6N) shows a decrease in wear depth, this suggests a high rate of particle breakdown. Thus the largest decrease in wear rate is seen with increasing load to 0.6N, increasing overall particle breakdown. Increasing frequency does initially increase wear rate (1.25Hz to 2.5Hz) but significantly increasing frequency (from 2.5Hz to 5Hz) does not have an effect on wear.

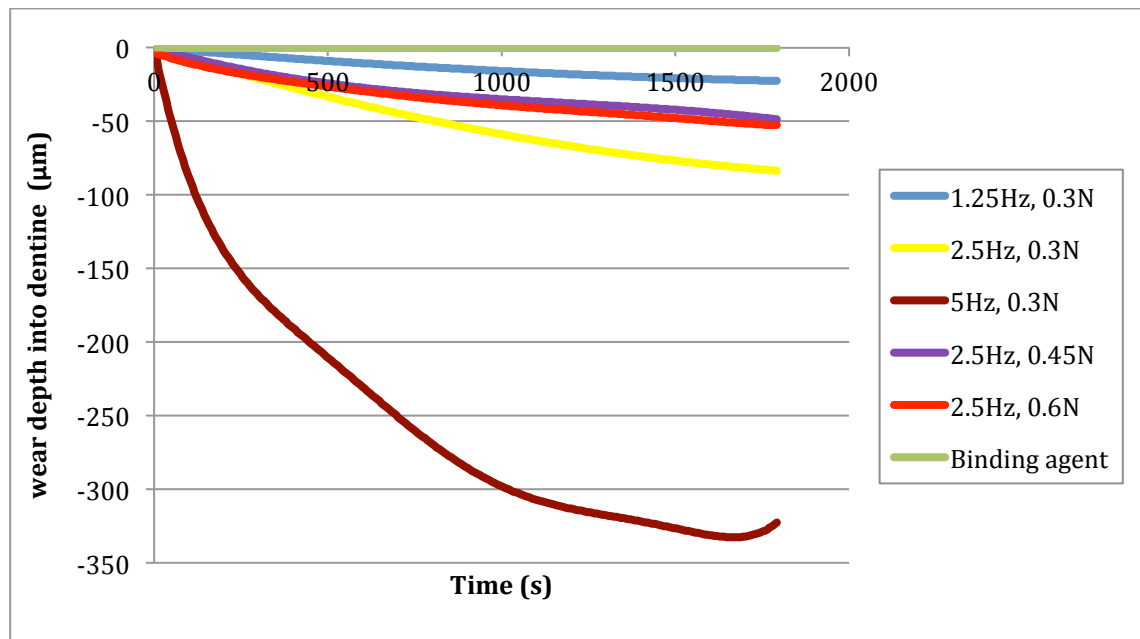
Figure 64, shows the resultant ball penetration into dentine during wear by S2E particles for each testing scenario.



**Figure 64: Change in vertical ball position for dentine abrasion by S2E particles at each scenario (average trend line, n=3).**

Substrate penetration with S2E particles was highest at highest frequency (5Hz, 0.3N). The measure wear depth at 2.5Hz, 0.45N was 3 times higher than 2.5 Hz, 0.6N suggesting a very high rate particle breakdown. Again the introduction of binding agent significantly reduced scratch prevalence.

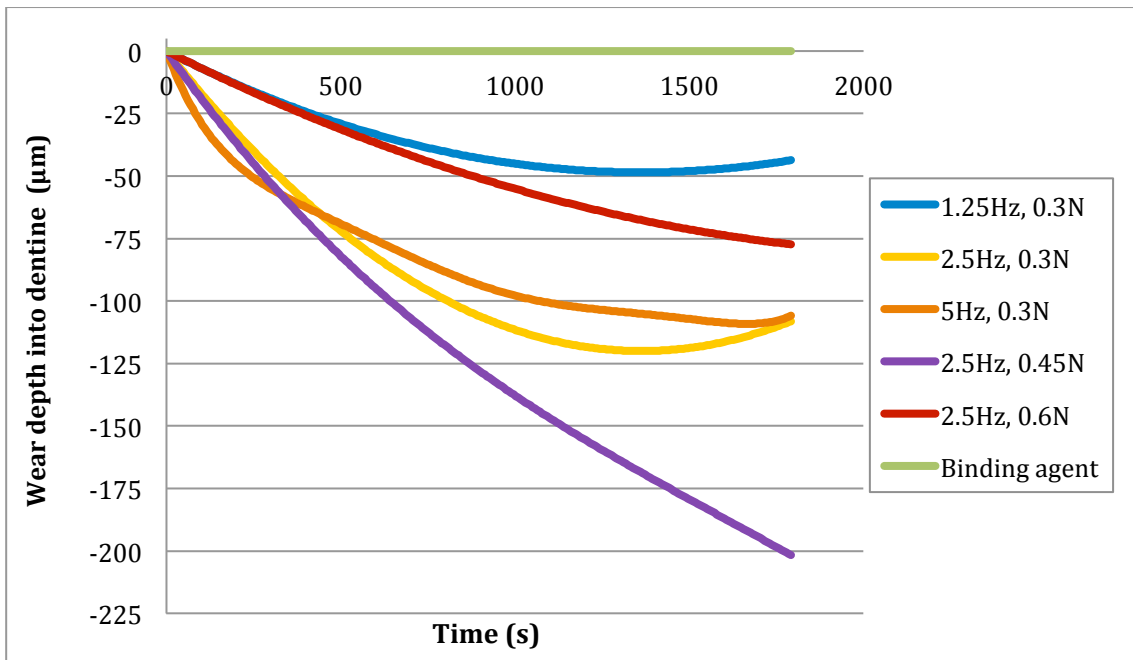
Figure 65, shows the change in nylon ball position during testing scenarios of Sturcal F particles.



**Figure 65: Change in vertical ball position for dentine abrasion by Sturcal F particles at each scenario (average trend line, n=3).**

Like with S2E particles and Omya 5AV particles the highest speed (5Hz at 0.3N load) has the most notable effect on substrate penetration. It is shown to be significantly larger in contrast to all other scenarios, especially early on in the trial. Increasing in loading did not have much effect on wear rate (increasing marginally from 0.3N to 0.45N but not increasing at all when 0.6N was used at 2.5Hz); suggesting a consistency regularity in particle behaviour at higher loading.

This can be seen in contrast with Sturcal L, the graph of which can be seen below in Figure 66. Which in Chapter 3 was shown to agglomerate similarly to Sturcal F particles but forming larger clusters. Although aggressive behavior can be seen with both with Sturcal L there seems to be no apparent relationship between ball penetration and load or frequency, as the largest ball penetration is seen at medium load and frequency (2.5Hz and 0.45N).



**Figure 66: Change in vertical ball position for dentine abrasion by Sturcal L particles at each scenario (average trend line, n=3).**

As with all particles it can be seen that with the addition of a binding agent the end ball position for the trail is again significantly low. This shows in ‘real-life’ toothpaste formulation the abrasives will be held in suspension and whilst material removal will take place it will be relatively low daily – as needed for a commercial brand.

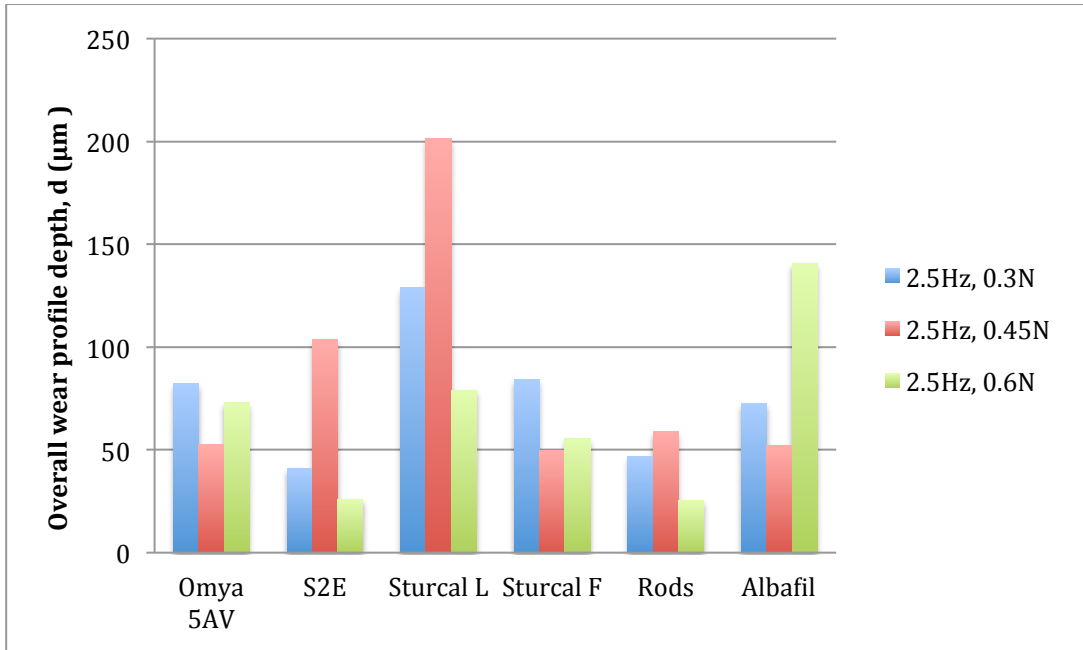
Using water only under the same testing scenarios on dentine showed no wear. These markings can be seen in the SEM imaging (Figure 70).

The nylon ball for each test was viewed under an optical microscope after each scenario. Wear on the ball itself was minimal and negligible.

### 5.2.2. Overall Particles Comparison

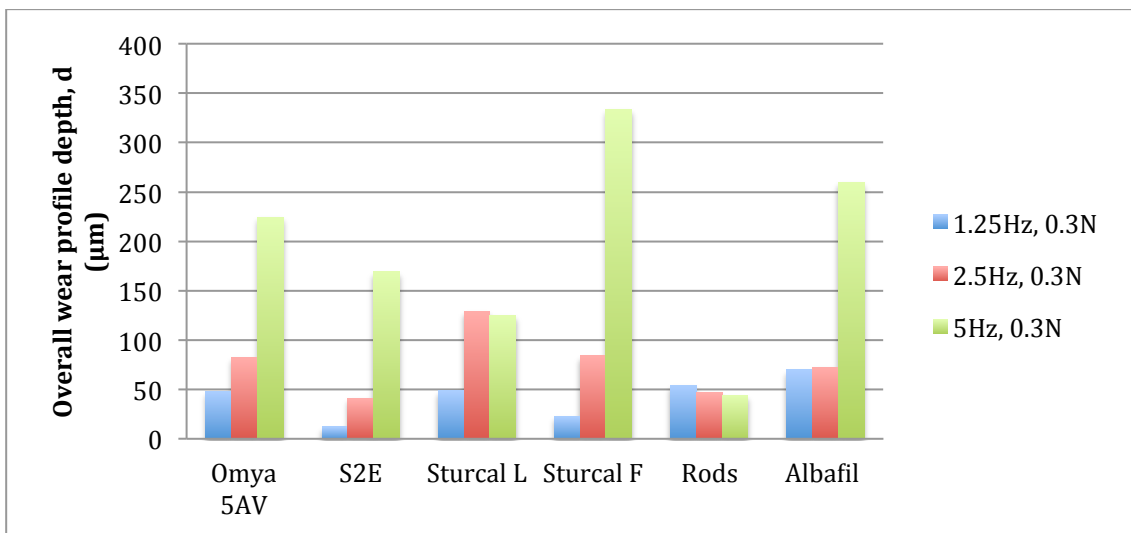
The six particles investigated have distinct morphologies and chemistries, so it is pertinent to compare their behaviour under identical testing conditions. Figure 67 and Figure 68 plot overall charts of the test results shown in Section 7.2 for each particle with increasing frequency (Figure 68) and increasing load (Figure 67).

It can be seen in general that the most abrasive particles are Omya 5AV, Sturcal L, Sturcal F and Albafil (with S2E and Rods gentler on dentine relatively).



**Figure 67: Effect on increasing load on each particle (n=3).**

In general no real systematic pattern that can be seen with increasing load to wear depth. The most notable increase in wear depth with loading is seen with Sturcal L at 0.45N, which was much higher than seen at 0.3N or 0.6N with the same particle; S2E and Rod particles showed the same trend. Omya 5AV and Sturcal F showed a decrease between 0.3N to 0.45N and then a slight increase going from 0.45N to 0.6N though not gaining as high an overall wear depth as seen with 0.3N with each particle.



**Figure 68: Effect of increasing frequency on each particle (n=3)**

Increasing frequency (1.25Hz to Hz) shows a clear pattern of increasing material removal. Increasing frequency increased the path length of the dentine all on the tooth, with each area being subjected to increased

number of strokes. However in each case it is not a linear pattern of wear related to rubbing distance frequency i.e. doubling frequency each time does not simply double wear caused. This suggests a change in particle movement as frequency changes, for example from rolling to sliding or vice versa. This pattern is discussed more in Chapter 6.

### 5.2.3. Effect of Frequency

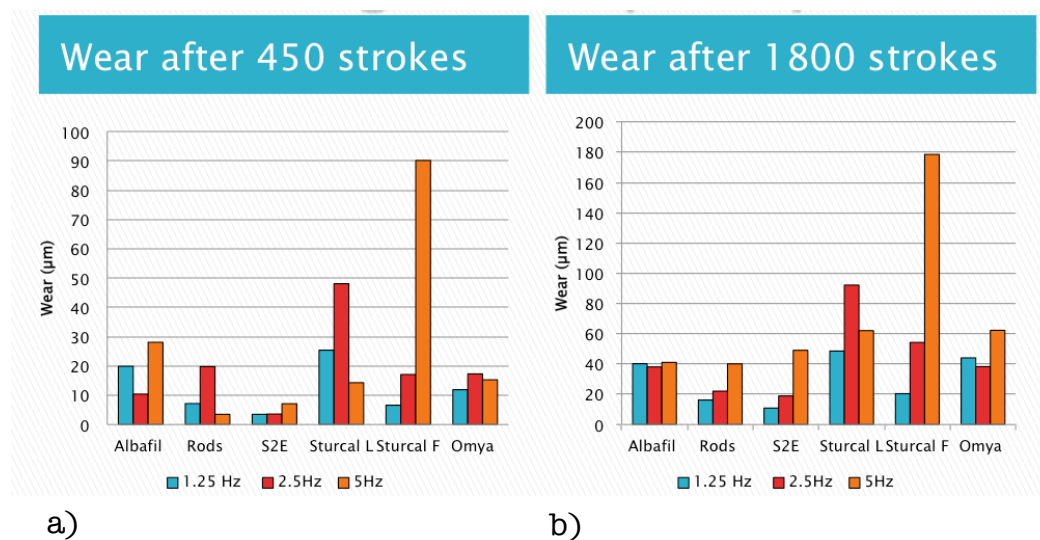


Figure 69 a) Wear after 450 strokes and b) Wear after 1800 strokes for each test scenario. (1 cycle is 2 strokes)

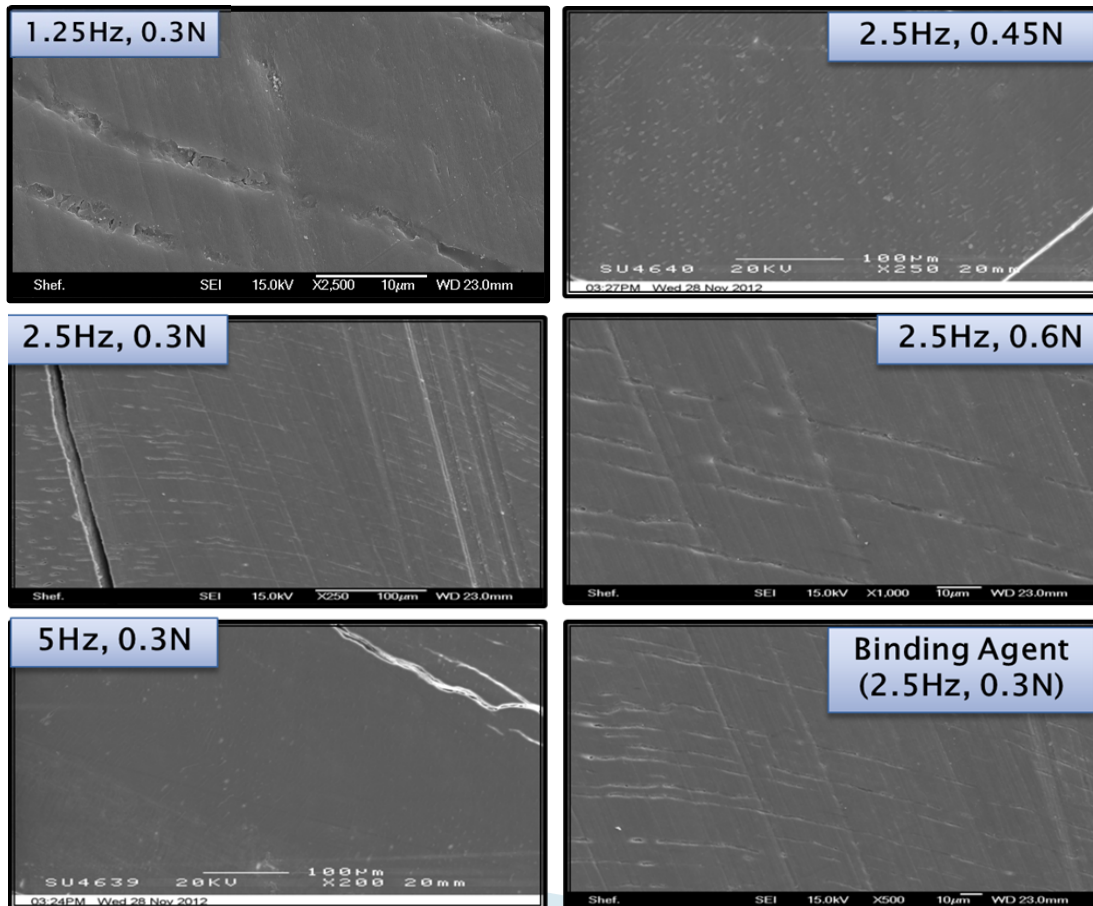
Figure 69, investigates the link of material loss with the number of strokes (as at the end of 30 minutes a test done at 1.25Hz will have undergone 2250 strokes which for a test at 5Hz will occur at 450 seconds). Figure 69 shows that after the same number of passes there is a significant difference in material loss for different frequencies, meaning that it is not just the additional strokes that led to increased wear at higher frequency testing. This demonstrates that there is something intrinsically different about particle behaviour at different speeds.

### 5.2.4. Imaging of Dentine Damage

To further investigate the mechanisms of dentine wear by different particles each tooth wear scar was investigated under SEM. Before testing each tooth was sectioned and polished to 0.25 microns, clear dentine tubules can be seen and no discernable scratches (Section 4.2.4, Figure 35). Figure 70 shows SEM images of dentine samples abraded with only water (no particles). It is evident there is little to no wear at each frequency and loading. Mild scratching that can be seen is very shallow and in the direction of movement of the nylon ball. These

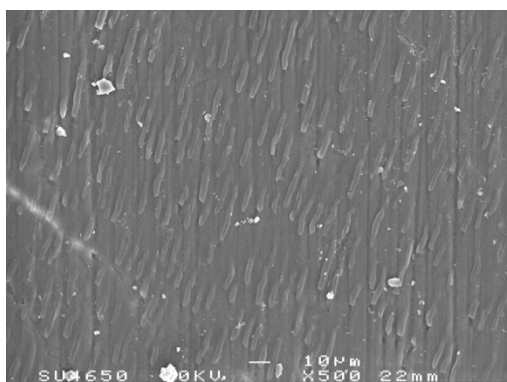


scratches are extremely infrequent and likely the result of third body abrasion from macroscopic loose dental material. This compared to the SEM images seen of the wear tests done with particles is extremely low in residual scratching and so it can be safely said all scratches seen in testing with particles are caused by the only the particles themselves and not the nylon ball.



**Figure 70: SEM images of dentine abraded by a nylon ball with water lubricant and six testing conditions**

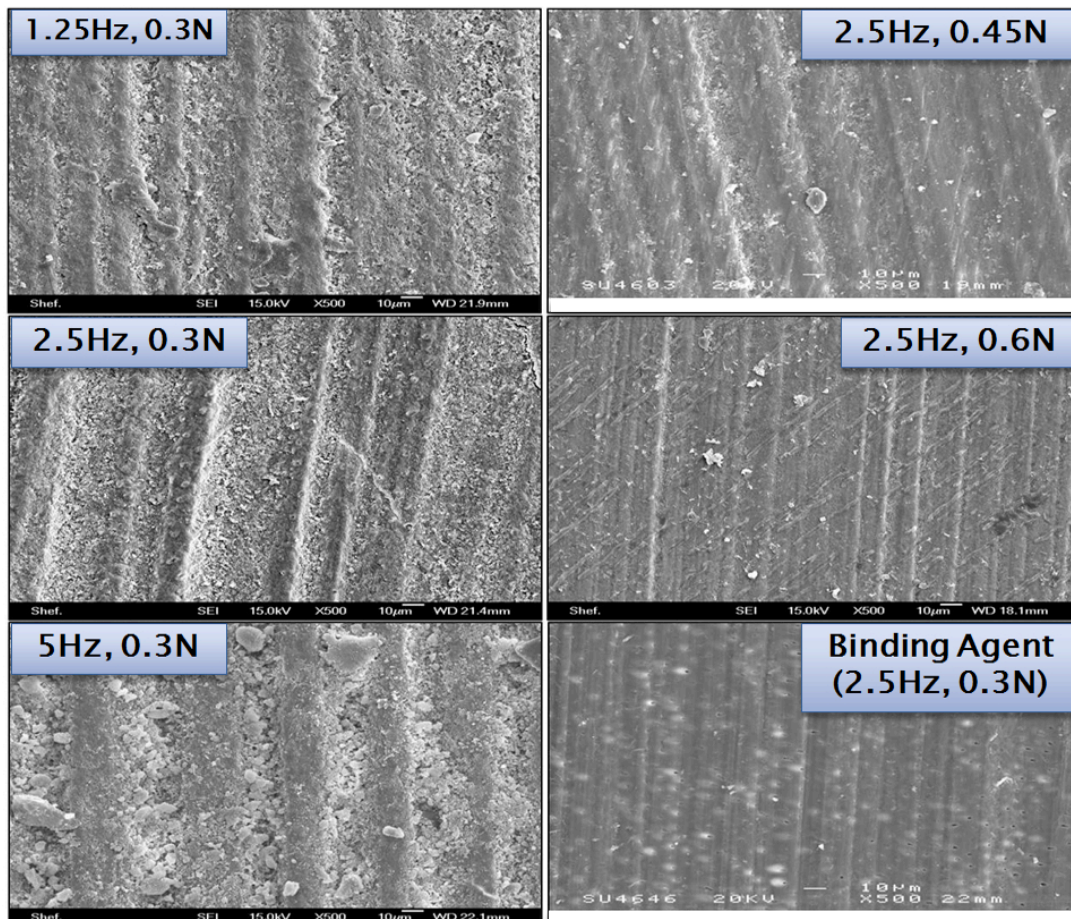
Figure 71 shows dentine abraded with 10g SCMC binding agent only in water (no particles). Again no wear track or scar was formed but a smear layer was formed on the outermost layer across the rubbing region.



**Figure 71: SEM image of dentine abraded by nylon ball with 10g SCMC only with water lubricant at 2.5Hz, 0.3N.**

The central portions of wear track shown in the SEM images were also analysed using profilometry to determine the scratch morphology. A summary of the profilometry data is detailed in Section 5.2.5.

Figure 72, shows the SEM grid for dentine samples tested with Omya 5AV particles.



**Figure 72: SEM images of dentine abraded by a nylon ball and Omya 5AV solution at six testing conditions**

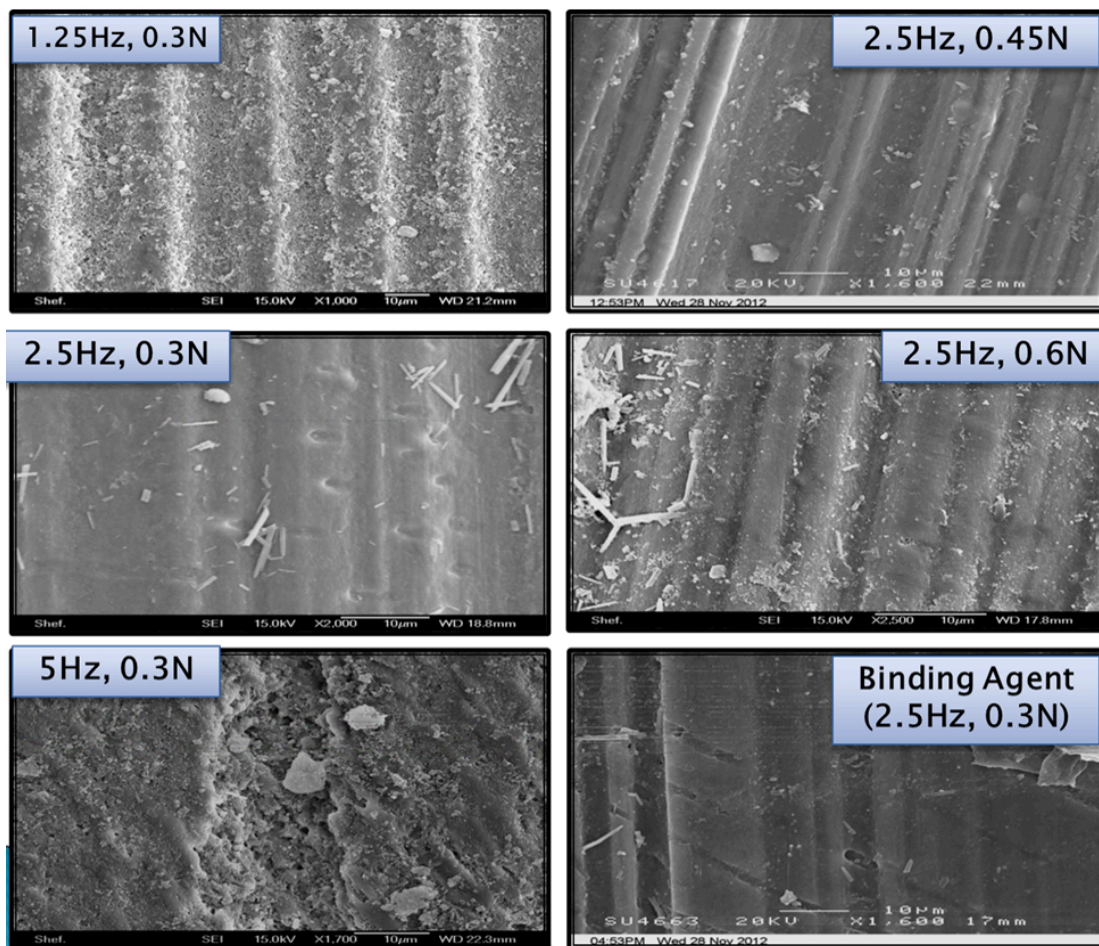
Dentine surfaces exhibit significant residual surface damage after wear using Omya particles. Scratch tracks within the wear scar can be seen to be significantly wider than the Omya particle themselves, indicating tracking of the particles. Wear tracking occurs when particles are caught in an initial scratch or groove formed on the smooth substrate surface resulting in the increase of the scratch depth and width throughout each pass [39]. This entrainment of particles causes wear tracks resembling scratches that are larger in size than the abrasive particle itself.

Omya is generally an aggressive particle with dentine surfaces in every wear scenario showing increased surface degradation and macroscopic galling (and no smoothing or polishing effects on scratch surfaces). Increasing frequency also increases the aggregation of Omya 5AV



particles, in both individual scratch widths and overall wear scar depth; this can be seen in the 5Hz, 0.3N images of Figure 72. Scratches introduced with the presence of binding agent are relatively shallow despite Omya being a large particle.

Figure 73 shows SEM images of dentine tested with Rod particles under each testing condition after 30 minutes.

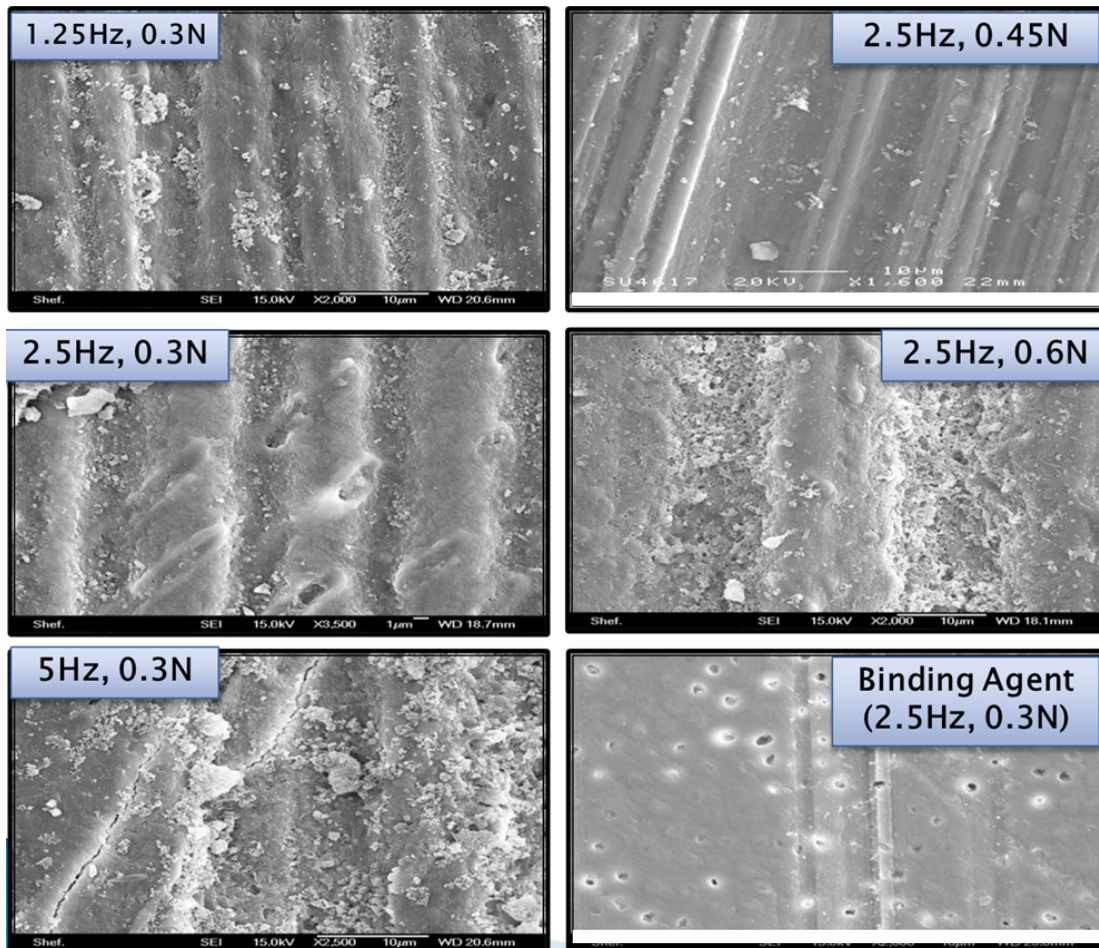


**Figure 73: SEM images of dentine abraded by a nylon ball and Rod particle solution at six testing conditions**

In comparison rod particles are fairly gentle in nature, with a mixture of mainly shallow scratches and some infrequent deep scratches. This behaviour is most likely due to their flat shape and the ease to which they fracture. This can be seen in the SEM images provided (Figure 73), where increasing load (and therefore breakdown) does not lead to significantly greater material removal or surface degradation but rather deeper and neater scratches. Increasing speed (particularly from 1.25Hz to 2.5Hz) significantly reduces scratch widths and frequency leading to deep infrequent scratches. Though the widest scratches are seen at the lowest speed indicating a high degree of particle tracking. The

introduction of binding agent has a certain polishing effect as scratches produced are neater and the inter-scratch regions clearly much smoother.

The SEM images shown in Figure 74 illustrate dentine surfaces after abrasive testing with S2E particles.



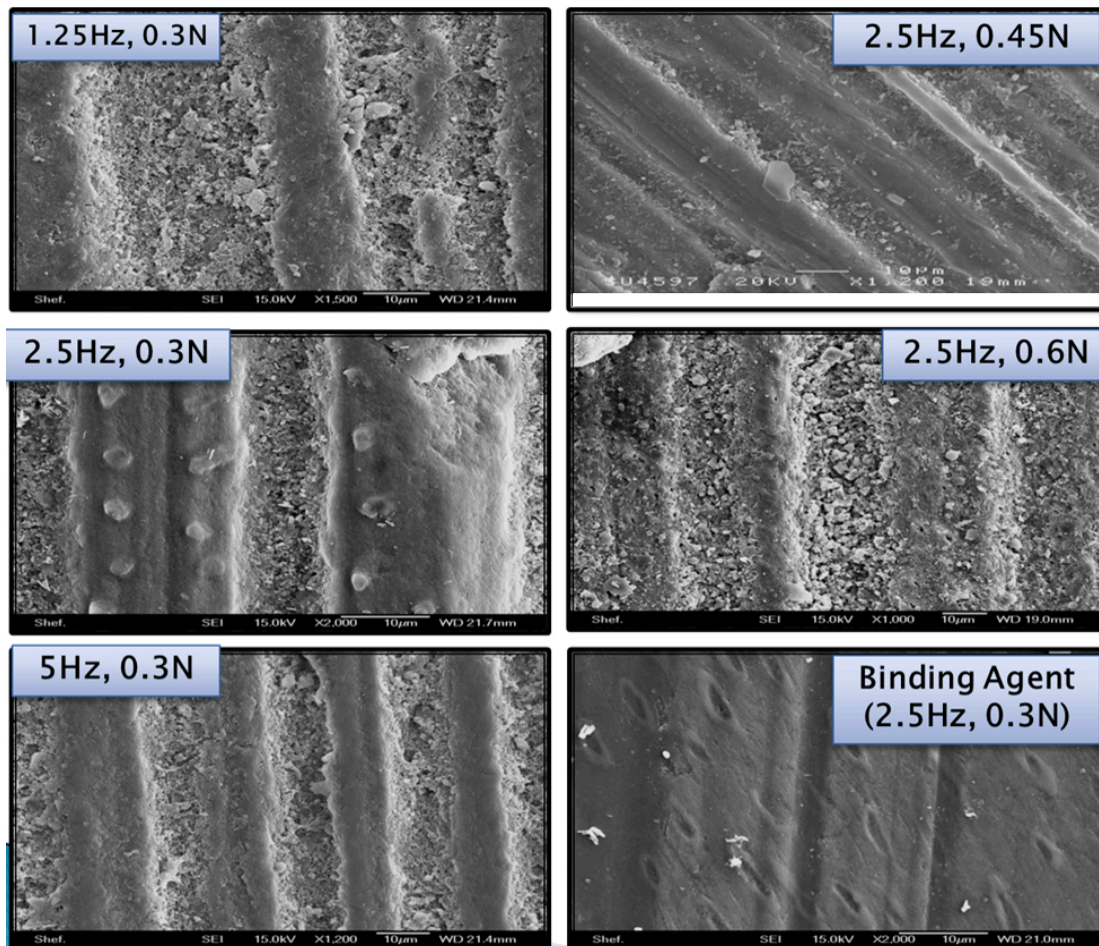
**Figure 74: SEM images of dentine abraded by a nylon ball and S2E solution at six testing conditions**

Increasing frequency of reciprocating wear testing of dentine with S2E particles increases scratch uniformity, continuity and neatness, suggesting improved security of particle entrainment. Higher loads (0.6N) created much larger individual scratches and caused surface roughness; though individual scratches at 0.45N were found to be much neater. Overall S2E particles had the lowest peak scratch widths and thus acted well as gentle abrasive; the images seen in Figure 74 were taken at a much higher magnification to that of other SEM grids seen in this chapter, to give a clearer view of results discussed in this section, but also illustrating how sympathetic S2E particles were to the dentinal surface comparatively to the other calcium carbonate particles. Testing



at 2.5Hz, 0.3N showed a slight formation of a smear layer, seen at the edges of the tubules. This formation exposes the edges of the tubules to the surface. The introduction of a binding agent dramatically reduced residual scratch frequency and depth.

Figure 75 shows SEM images of the scratches in dentine observed after 30 minutes of testing at various loads and speeds with Sturcal F particles.

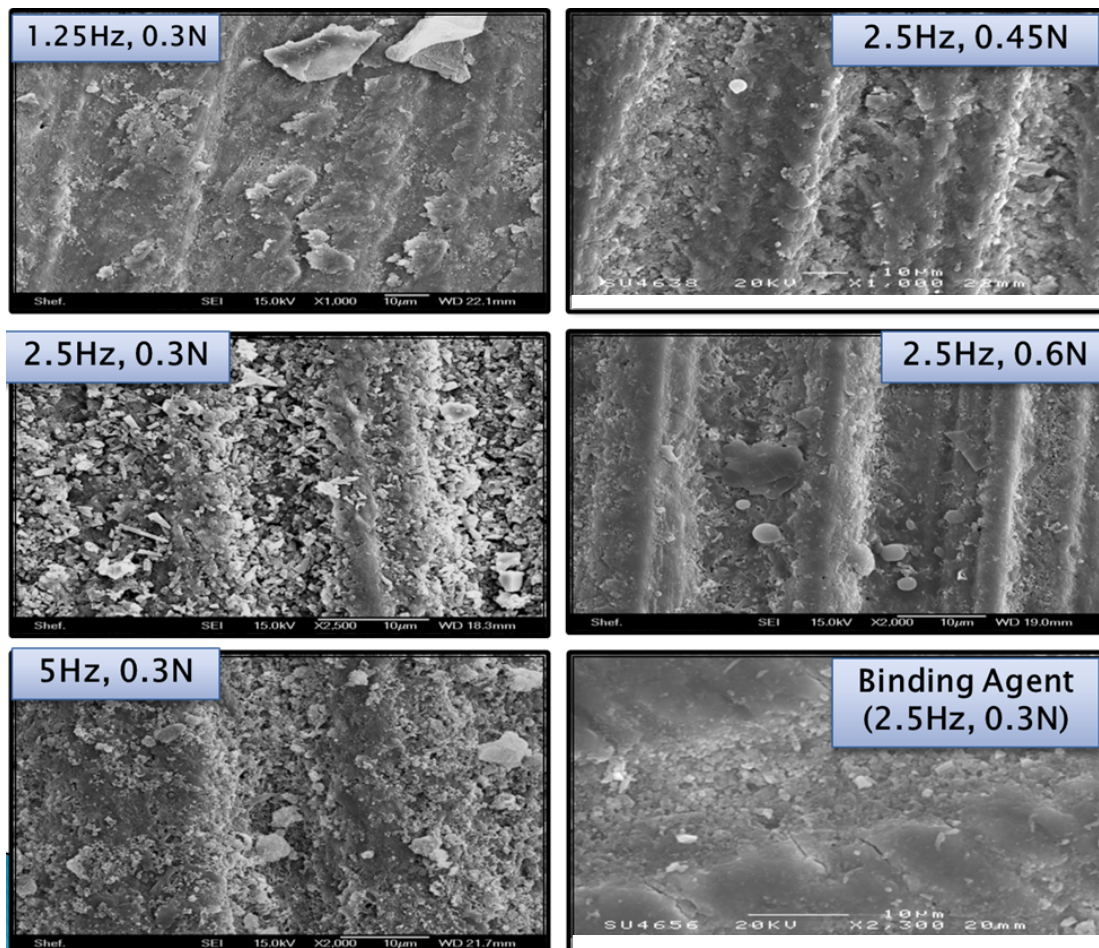


**Figure 75: SEM images of dentine abraded by a nylon ball and Sturcal F solution at six testing conditions**

Sturcal F particles produced extremely deep scratches in dentine with a significant presence of particle fragments within scratches and the dentine in-between the scratches relatively smoothed. Chapter 5 showed that Sturcal F particles form strong spherical agglomerations with protruding tips these may be the cause of the large amount of particles left. Increasing load dramatically decreased regularity and consistency of scratches with significant debris across the surface. Again the highest frequency (5Hz at 0.3N) had the most significant effect on final overall wear depth and had the most notable increase from all the testing. Of all the  $\text{CaCO}_3$  particles investigated in this thesis Sturcal F showed the

lowest scratch frequency (though still very deep) with the introduction of binding agent.

Figure 76 shows the representative SEM images of dentine wear testing done with Sturcal L particles.



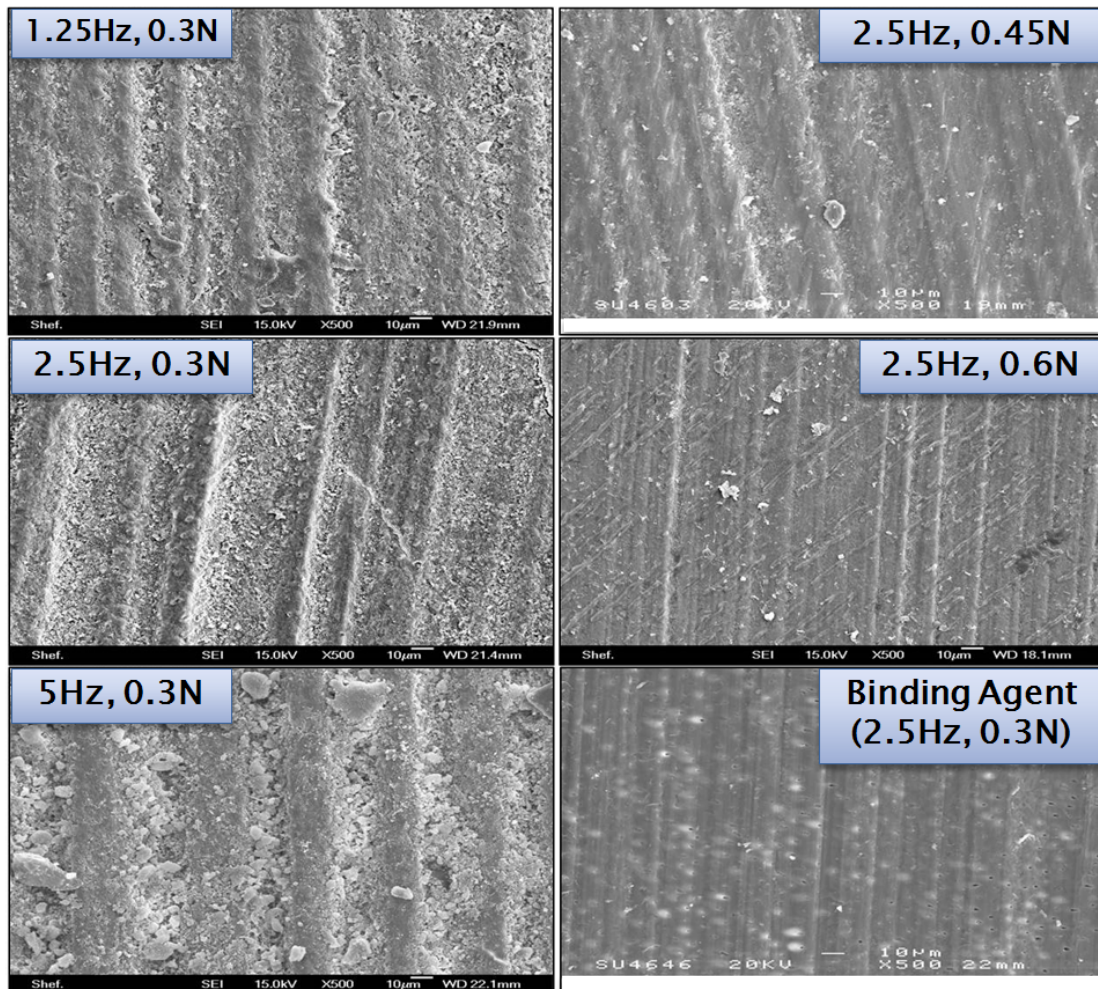
**Figure 76: SEM images of dentine abraded by a nylon ball and Sturcal L solution at six testing conditions**

Mostly throughout the test scenarios individual wear widths are similar. Lower speed, 1.25Hz, 0.3N, trials created dramatically raised scratch boundaries with Sturcal L, as there is an increase in particle breakdown with increasing speed. Higher load trials show more aggressive material removal within scratch tracks. The largest ball penetration is seen at medium load (0.45N) showing there is no apparent relationship between ball penetration and load.

Figure 77 shows the SEM images obtained from dentine tested with Albalfil particles. Scratch widths from this testing increase dramatically with an increase in frequency. The increase of loading led to the development of irregular non-uniform scratches suggesting a mechanistic variation when load is varied most likely to the freedom of



Albafil to rotate in the contact region, as load increases rotation of particles and movement increases.



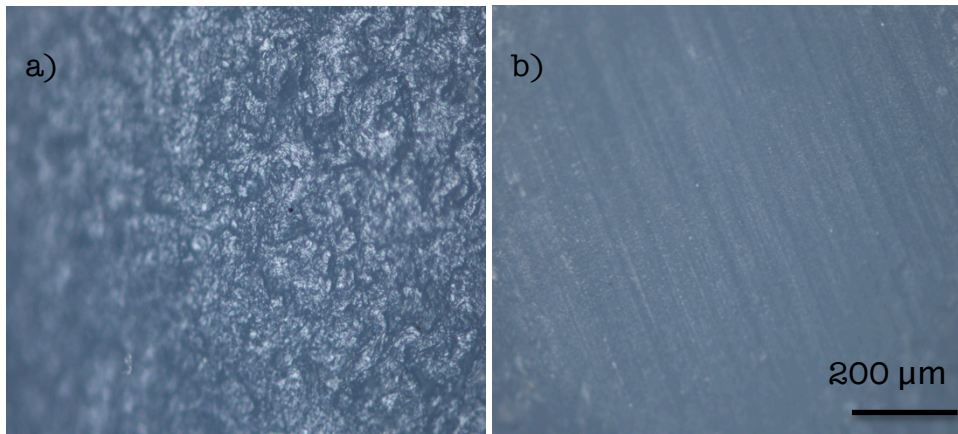
**Figure 77: SEM images of dentine abraded by a nylon ball and Albafil solution at six testing conditions**

#### **5.2.4.1. Discussion and Conclusion of Imaging of Dentine Damage**

Ball-on-flat testing, similar to that done in this report, has shown in general larger particles produce fewer, larger wear features than that of smaller particles [40], but the larger particles do not always produce more wear in total [52]. Here we see similar behaviour.

Instead of particle size being the determining parameter for dentine wear, here it is observed that particle breakdown plays a more meaningful part. From observations of residual wear seen in the SEM images particles with a higher affinity to break down (S2E and Rod particles) act the gentlest on dental material. Whereas particles that either agglomerate highly or do not breakdown as readily (Omya 5AV and Sturcal L) cause the most damage and wear.

The nylon ball was imaged after each test performed in the chapter. Each ball showed no particle adhesion onto the nylon surface, rather just linear wear scars in the direction of motion. A lack of adhesion shows the ball had point contact and acted similarly to a nylon brush (rather than a pad surface dragging the same particles across the substrate surface).



**Figure 78: Nylon ball a) unused (before testing) b) used (post testing with Omya 5AV at 2.5Hz, 0.3N)**

Each tooth in this thesis was sectioned mesio-distally isolating palatal, lingual and buccal faces. The testing was done on the central plane of the dentine section of the tooth surface, where tubules are parallel to wear direction. This regulates the capture effect of the dentine tubules for each particle and mimics the orientation seen at the tooth surface of exposed dentine near the gum line. Each wear face was also polished to 0.25 micron ensuring a regular tooth roughness at the beginning of each test.

Any debris visible in this or other sections are primarily residual after washing process and should not be seen to imply particle tenacity post testing. It is also possible that debris is mixed with worn dentine. Contributing to particle density and increasing wear as the wear scar increases over time.

#### **5.2.5. Profilometry of Scratches.**

To investigate further the residual wear resulting from abrasion of testing profilometry was done across 100  $\mu\text{m}$  at the bottom centre of dentine wear track, to determine scratch widths and roughness, the results are shown in Table 10:

**Table 10: Profilometry across the residual scratch tracks from linear reciprocation trials (n=3).**

Particle	Scenario	Particle size	Minimum observed scratch width (µm)	Maximum observed scratch width (µm)	Average scratch width (µm)	Overall wear profile depth (µm)
Omya 5AV	1.25Hz, 0.3N		11.7	30.46	21.7	48.1
	2.5Hz, 0.3N	7 µm	2.16	44.62	5.45	82.12
	5Hz, 0.3N		4.72	28.7	15.18	224.4
	2.5Hz, 0.45N		4.08	13.74	8.32	52.51
	2.5Hz, 0.6N		1.74	5.84	2.27	73.1
	Binding agent (2.5Hz, 0.3N)		0.58	6.7	2.5	65.3
Rods	1.25Hz, 0.3N		15.77	30.45	20.3	54.2
	2.5Hz, 0.3N	6 x 0.5 µm	0.47	10.77	2.88	46.98
	5Hz, 0.3N		3.13	17.29	7.86	117.3
	2.5Hz, 0.45N		5.32	22.58	10.81	210.8
	2.5Hz, 0.6N		0.92	6.78	2.78	25.4
	Binding agent (2.5Hz, 0.3N)		0.89	9.47	1.62	8.23
	Mixtures [Rods+Omya] (2.5Hz, 0.3N)		3.45	13.45	10.5	170.9
S2E	1.25Hz, 0.3N		2.18	7.67	3.3	12.27
	2.5Hz, 0.3N	3.18 µm	2.54	3.51	3.1	30.86
	5Hz, 0.3N		4.63	21.29	9.44	169.2
	2.5Hz, 0.45N		1.88	3.78	2.33	103.9
	2.5Hz, 0.6N		2.44	24.12	18.49	26.1
	Binding agent (2.5Hz, 0.3N)		0.76	3.34	1.68	1.45
	Mixtures [S2E+Omya] (2.5Hz, 0.3N)		3.73	11.82	5.03	79.5
Sturcal F	1.25Hz, 0.3N		8.73	26.7	9.19	22.6
	2.5Hz, 0.3N	1.3 µm	1.54	27.81	10.52	84.19
	5Hz, 0.3N		7.54	41.95	17.95	233.6
	2.5Hz, 0.45N		2.91	13	7.89	49.6
	2.5Hz, 0.6N		5.55	36.22	21.31	55.58
	Binding agent (2.5Hz, 0.3N)		1.92	4.23	2.95	2.29
	Mixtures [S.F+Omya] (2.5Hz, 0.3N)		13.4	24.5	15.6	120.8
Sturcal L	1.25Hz, 0.3N		0.38	14.58	12.15	18.6
	2.5Hz, 0.3N	7 µm	7.83	28.81	16.88	128.76
	5Hz, 0.3N		6.61	26.19	15.88	44.8
	2.5Hz, 0.45N		10.02	28.22	18.88	49.6
	2.5Hz, 0.6N		1.48	15.92	7.88	83.3
	Binding agent (2.5Hz, 0.3N)		14.61	26.63	17.46	109
	Mixtures [S.L+Omya] (2.5Hz, 0.3N)			23.4	10.8	101.8
Albafil	1.25Hz, 0.3N		0.45	13.45	12.45	69.7
	2.5Hz, 0.3N	3.6 µm	6.78	28.9	11.34	72.6
	5Hz, 0.3N		6.56	5.67	6.78	259.8
	2.5Hz, 0.45N		11.9	5.66	4.32	52.3
	2.5Hz, 0.6N		2.3	3.45	2.11	140.9
	Binding agent (2.5Hz, 0.3N)		12.45	3.45	11.34	7.8
	Mixtures [Albafil+Omya] (2.5Hz, 0.3N)		10.9	12.3	7.8	83.4
Water (no particle)	1.25Hz, 0.3N		~	~	~	~
	2.5Hz, 0.3N		~	~	~	~
	5Hz, 0.3N (run 1)		~	~	~	~
	5Hz, 0.3N (run 2)		~	~	~	~
	2.5Hz, 0.45N		~	~	~	~
	2.5Hz, 0.6N		~	~	~	~
	Binding agent (2.5Hz, 0.3N)		~	~	~	~

In oral care it is not only important to abrade plaque material whilst minimising damage to dental material but also to produce a smooth not rough surface after brushing in order to give both a polishing effect to teeth and also a pleasant tactile aftermath to the tooth surface.

These scratch depths correspond with the agglomeration results seen in Chapter 3. Larger particles (Omya 5AV) and particles that form strong agglomerations (Sturcal F and Sturcal L) form the deepest scratches. Rods and S2E are the most sympathetic to the dentine substrate; this was expected as it was seen in the SEM images from this chapter and perspex scratch testing done in Chapter 4.

The following graphs, 79-83 compare resultant dentine roughness after testing with different particles compared to overall wear for the different testing regimes. Each graph is ordered to show increasing overall dentine wear.

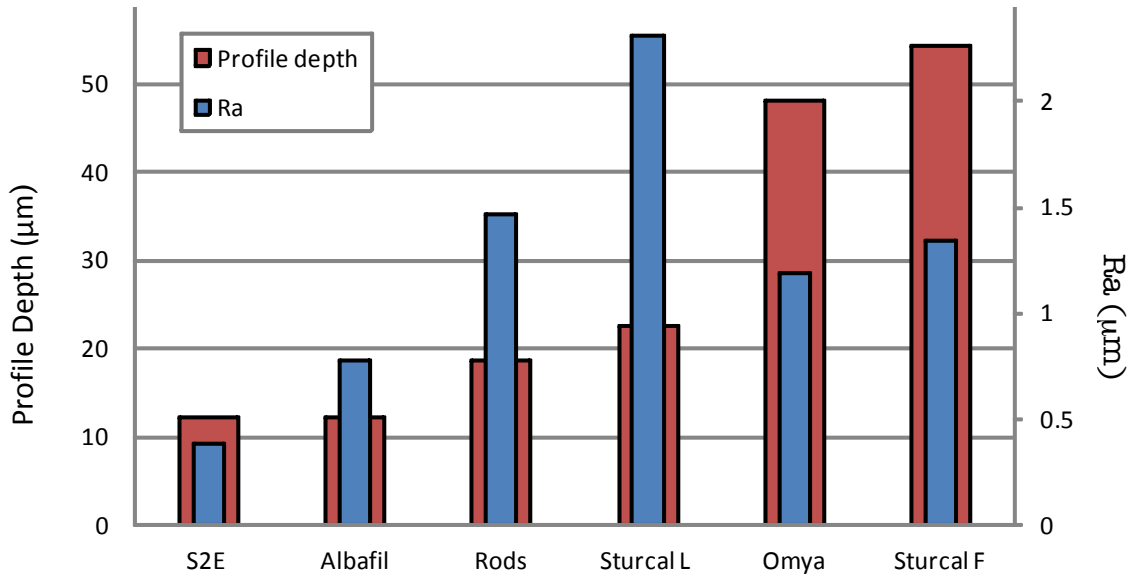


Figure 79: Resultant dentine wear and roughness at 1.25Hz, 0.3N

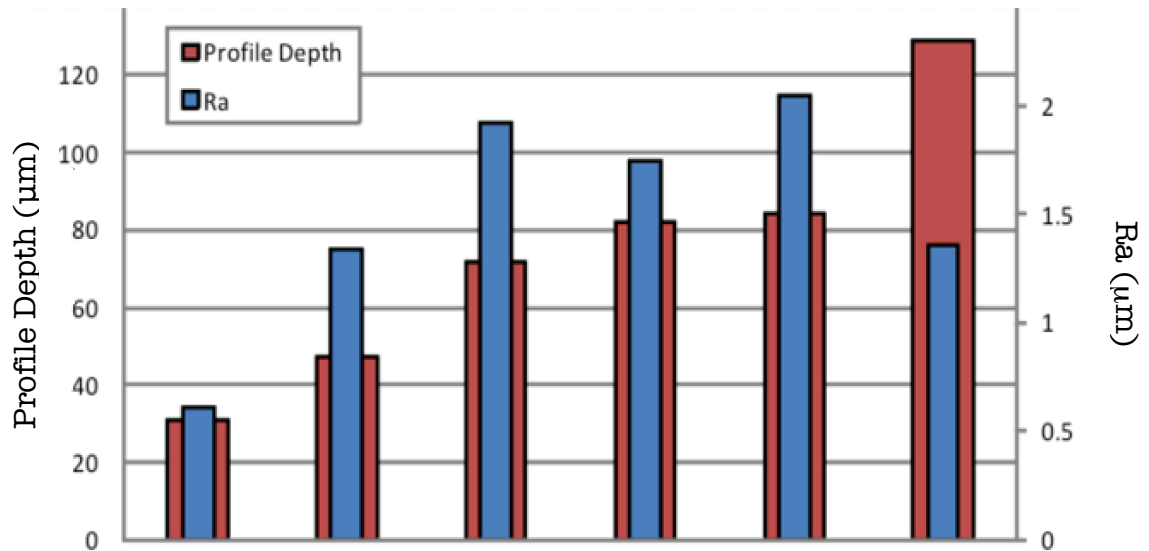


Figure 80: Resultant dentine wear and roughness at 2.5Hz, 0.3N

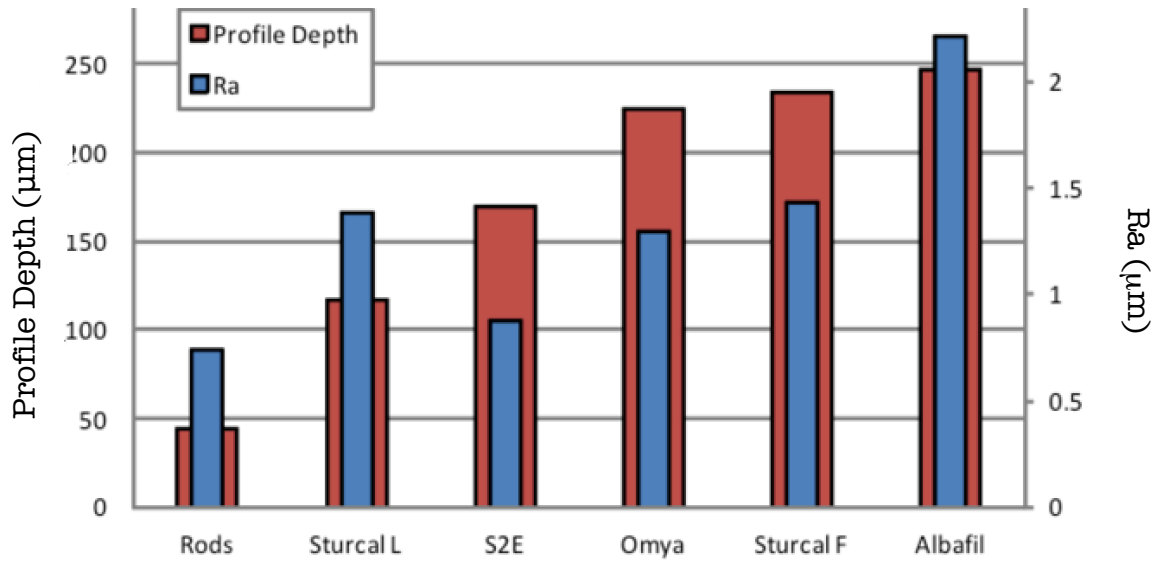


Figure 81: Resultant dentine wear and roughness at 5Hz, 0.3N

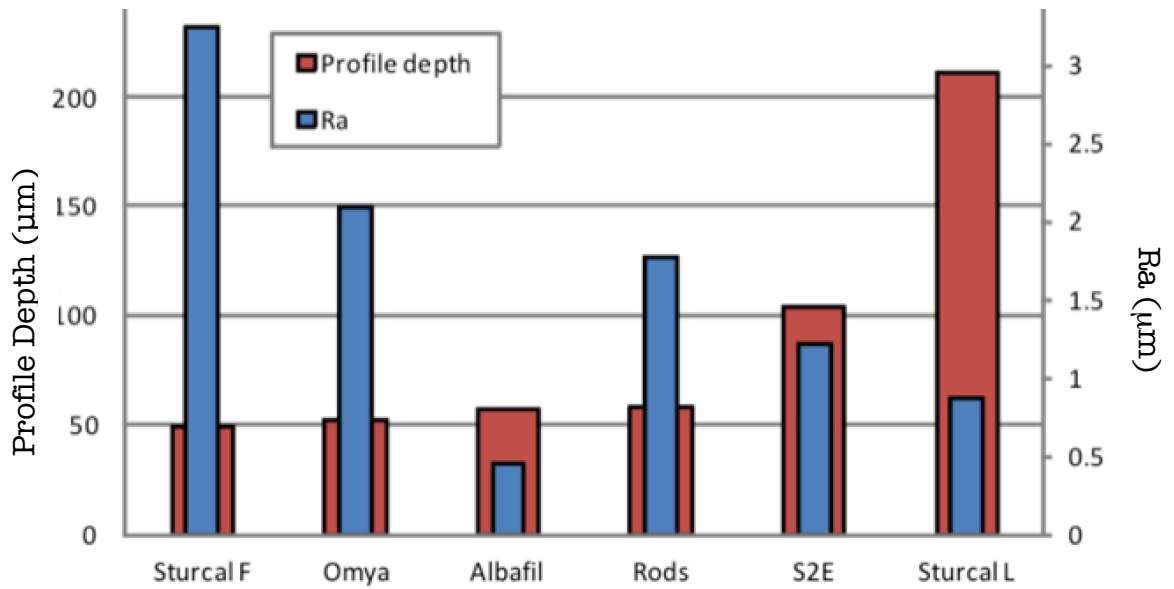
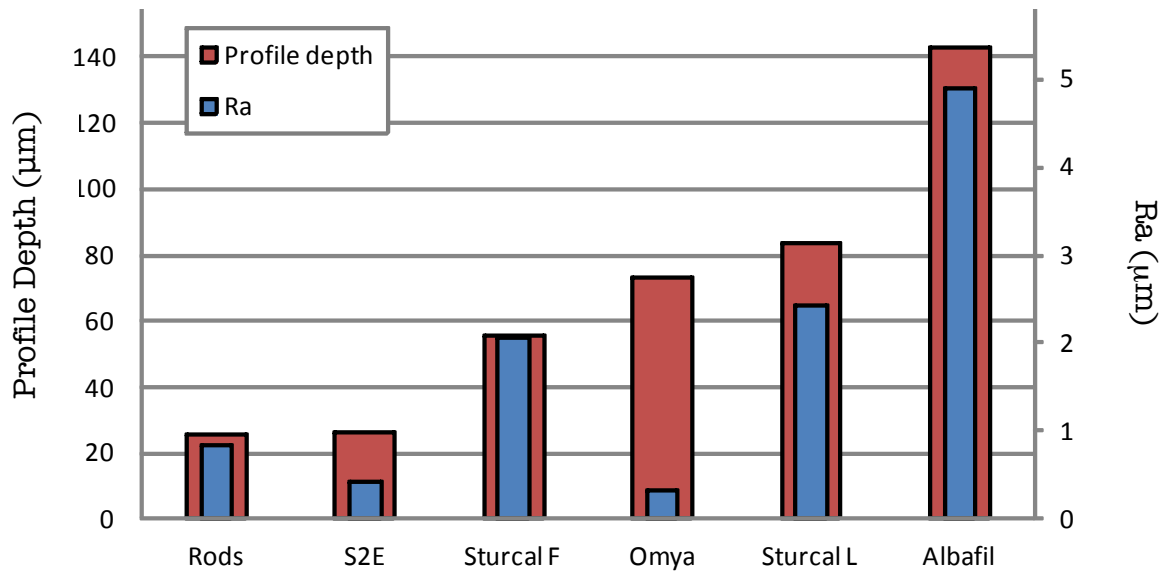


Figure 82: Resultant dentine wear and roughness at 2.5Hz, 0.45N





**Figure 83: Resultant dentine wear and roughness at 2.5Hz, 0.6N**

From these results it can be concluded most particles have a direct correlation between maximum profile depth and residual roughness at the centre. Though there are a few cases that do not follow this general behaviour, such as Omya at 2.5Hz, 0.6N or Sturcal L at 2.5Hz, 0.45. With these particles it is most likely particle breakdown and shape changes lead to the variation in deeper scratches (Figure 72 and Figure 76), leading to a change in overall roughness.

These results also correspond with the maximum scratch depths and average scratch depths seen in Table 10.

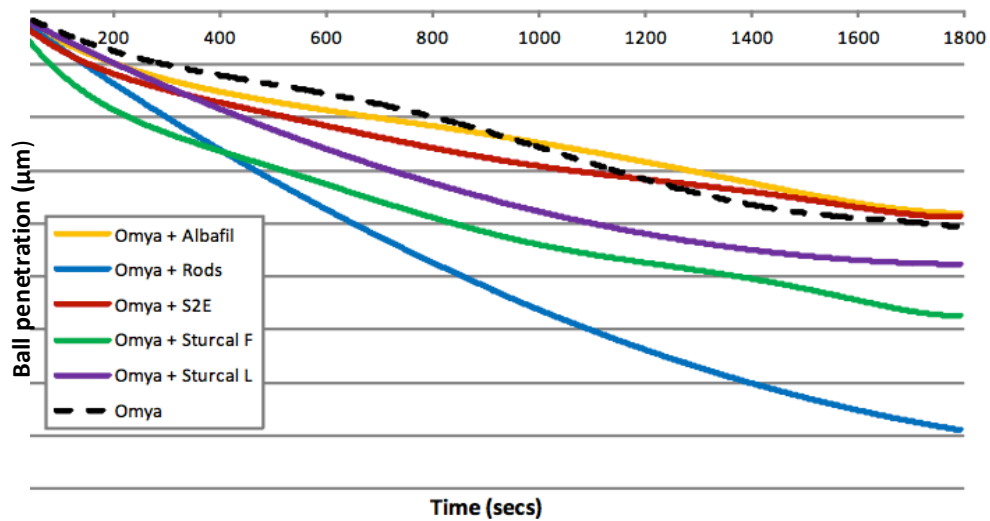
### **5.2.6. Particle Mixtures**

Commercial toothpaste usually contain more than one abrasive. A combination of two particles of differing shapes and sizes can have a synergistic effect direct from behaviour obtained when particles are used in isolation.

Here Omya 5AV was selected as the base in all mixtures investigated, as it is the ‘standard’ commonly used particle in Signal Unilever toothpaste and oral care products due to its cost-effective price, ease of manufacture and accessibility. A mixture of two fully saturated solutions (Omya 5AV in solution and the testing particle in saturated solution) was made with a 1-1 ratio of the two types of particles.



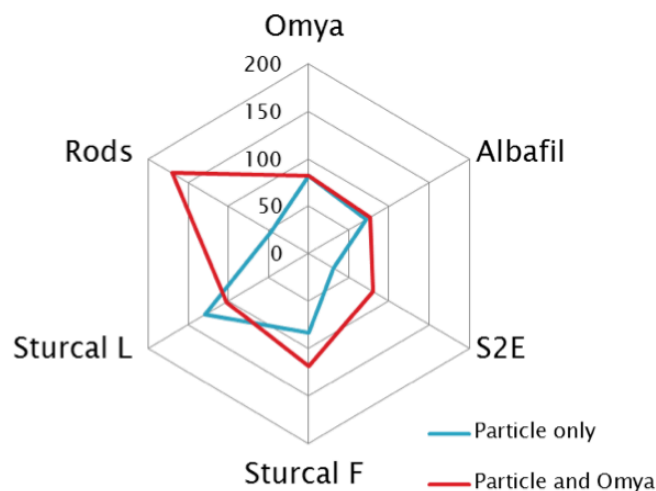
Trials on particle mixtures were run at 0.3N, 2.5Hz for 30 minutes. Figure 84 shows the wear depth achieved by each mixture during the trial.



**Figure 84: Wear depth over time for particle mixtures with Omya 5AV (2.5Hz, 0.3N). Average trend line, n=3.**

For Omya itself reducing its concentration and mixing with particles can lead to an increase in surface penetration. An increase in wear can particularly be seen when mixed with Sturcal L, Sturcal F and Rod particles. The biggest increase can be seen with the addition of Rod particles (almost doubling the wear rate).

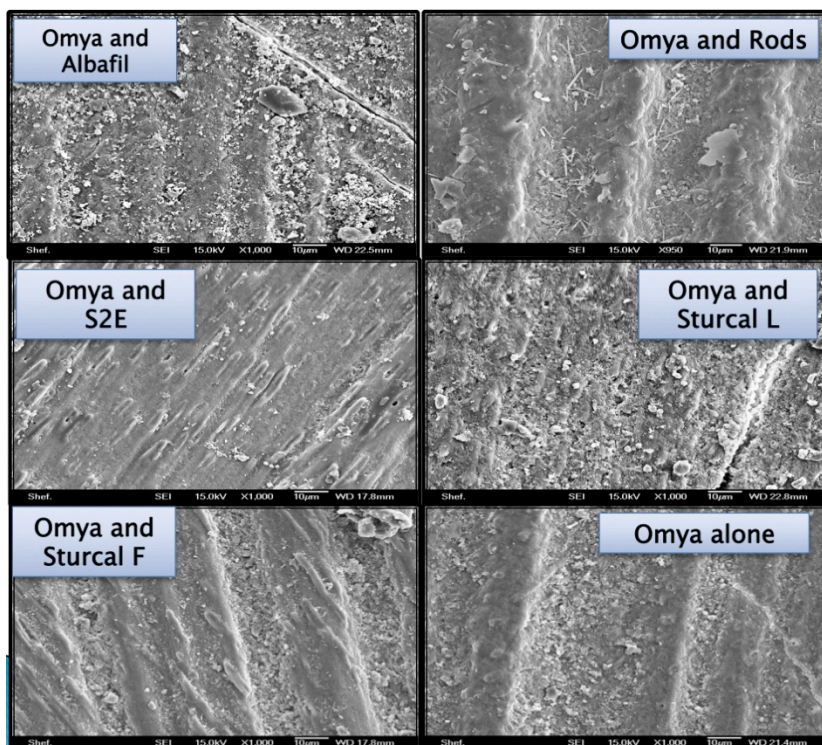
Figure 83 compares the profile depth for 30 minutes at 2.5Hz, 0.3N, when the particles themselves are only used and the particles in mixtures.



**Figure 85: Comparison of wear depths of particles mixed with Omya 5AV and particles themselves.**

Under this testing scenario (without mixtures), the order of abrasivity was S2E, Rods, Albafil, Omya 5AV, Sturcal F, Sturcal L (Figure 85). In this scenario it can be seen that mixing the particles with Omya has led to an increase in wear over pure Sturcal F, S2E and Rod particles. Profile depths for Albafil particles are similar both individually and as mixtures (Figure 84 and Figure 85). Since Albafil particles are similar to in shape to Omya particles it is thought there are no additional effects as the particle shall be motivated similarly. Rod and S2E particles again show a significant increase in wear. A reduction in wear is seen for Sturcal L particles to halfway between components. The increase in wear for S2E is comparable to that of Omya 5AV particles alone but for Rods and Strucal F there is a significant increase, beyond the individual components for both particles. A reduction in aggressiveness is most likely due to the lowered presence of Sturcal L particles, that were most abrasive than Omya 5AV when used independently.

Figure 86 shows the SEM images obtained from the worn dentine from this testing.

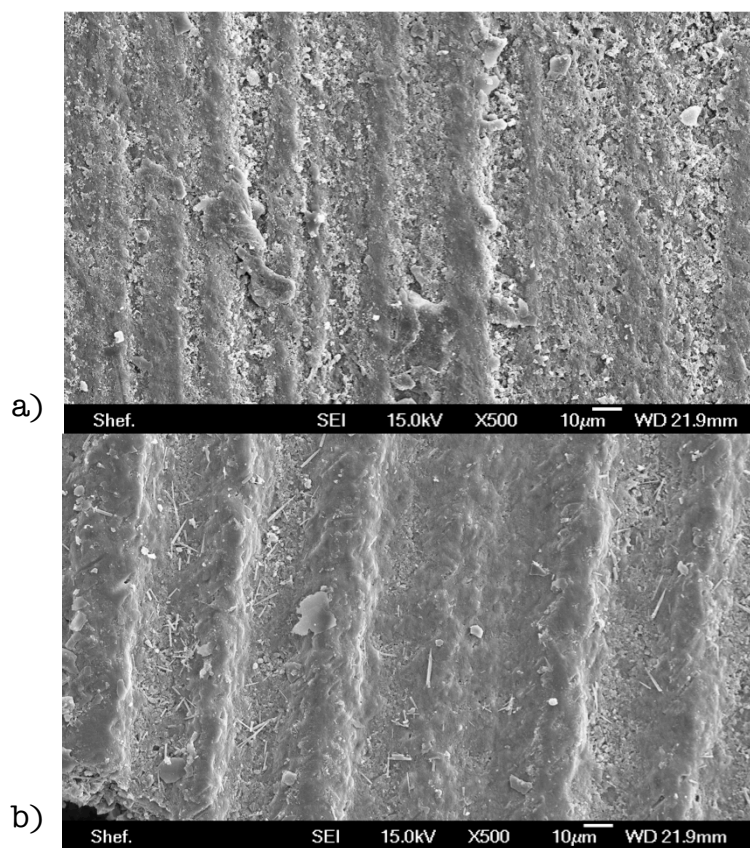


**Figure 86: SEM grid of wear testing by calcium carbonate particles mixed with Omya 5AV particles**

SEM show that wear is distinctly different with the varying mixtures. SEM analysis for Albafil, Sturcal L and Sturcal F showed no major differences between that and the particles alone. S2E and Rod particles both exhibit polishing behaviour when in a mixture with Omya. The most dramatic effect was with the introduction of Rod particles. Above it can

be seen mixing Rod particles with Omya 5AV particles leads to increased wear overall but from the SEM images above a notable that the surface finish after abrasion with Omya 5AV and Rod particles produces a smoother more polished end surface than that just worn with Omya 5AV particles. This polishing effect of the Rod particles has been confirmed in scratch analysis testing within this thesis. This effect can be seen in more detail in Figure 87 below.

Though wear tracks are still seen the scratch edges or ‘scratch shoulders’ of the wear tracks are less raised and pronounced. Resulting in a smoother finish within and around the wear scars.



**Figure 87: a) Dentine worn with Omya 5AV only and b) Dentine worn with Omya 5AV and Rod particle mixture**

It should be noted that these synergistic changes in wear performance for mixtures can be useful (as noted for Rod particles above) but also in other cases (such as mixtures of Omya 5AV with Sturcal L particles or Albalfil particles) a reduction in wear can be seen or even no discernable change in performance at all. PCC particles can be costly to include in toothpaste mixture where ground calcium carbonate is normally used. These costs can be off-set or minimised using a mixture if PCCs and GCC, depending on the properties the toothpaste desires.

### 5.3. Conclusions

Several observations can be made from investigations within this Chapter.

The most aggressive particles in terms of scratching are not always the largest particles. Subtle changes in geometry, shape and particle integrity play a larger role in defining the abrasivity of particles.

Secondly it can be seen that particle abrasive behavior is also dependent on the speed and load it is subjected to. These conditions will affect a particles and cluster breakdown and behavior affecting its cleaning properties. This has been seen in work done on silica particles for household cleaning products [5, 21].

Speed has a greater effect on wear than load; and this is not simply due to the additional strokes taken per trial at higher frequencies but rather it affects the way the particles are entrained.

It is notable that the addition of binding agents into an abrasive paste in useful in controlling abrasivity of the particles and maintaining control between strain removal and remaining gentle to dental material. The SCMC binding agent mimics the rheology, viscosity and flow of a toothpaste. Sturcal L was the only particle that had a high magnitude of scratch depth on dentine with the binding agent added suggesting it is not suitable for commercial toothpastes.

Some particles are more prone to tracking behaviour (Omya 5AV decreases with load, Rods only at low speed, Sturcal F consistently), which shall increase the depth of resultant scratches in the wear scar.

Previous work done on testing oral abrasive particles has shown micro-scratching from abrasive pastes does commonly occur in parallel lines (as seen in this chapter) and tracking a prevalent feature [53]. S2E had the greatest variation in scratch characteristics between the various testing scenarios. Sturcal F showed the most increase in surface degradation and roughness with load whilst Sturcal L had the most aggressive material removal, especially when at high load; most likely due to their agglomerative natures.

In some cases, a mixture of particles lead to the synergistic change in wear characteristics and particle abrasive behavior. Mixing Omya 5AV with Sturcal L particles lead to a reduction in wear whereas mixing with Rod particle lead to the highest increase in wear. This mixture (or Rod and Omya 5AV particles) also showed promising polishing effects.

Trials without particle (only water) produced no noticeable wear demonstrating the wear observed with particle testing is the effect of the particles themselves.

The next Chapter investigates the particle movement behaviour of each of these particles using in-situ nanomanipulation technology.

## **CHAPTER 6**

### **Particle Nano-manipulation**

Investigations of the wear of dentine by calcium carbonate particles have demonstrated that dentinal wear depends on the type of particle used. To quantify this further Chapter 6 investigates the motivation, movement and behavior of each calcium carbonate particle in-situ using nano-manipulation technology on silicon, perspex and copper substrates.

#### **6.1. Background Information**

As explained in previous chapters it is not always the biggest particle that yields the largest wear, even when particles have the same mechanical properties otherwise. Instead subtle differences in shape and agglomerations can have a great effect on the particles mechanisms of movement, determining dynamic properties and inter-particle relationships. Chapters 4 and 5 hypothesised on particle movement traits via surface markings. But due to a lack of control of variables it is sometimes difficult to discern exactly how an individual abrasive particle has acted. This Chapter used the nano-manipulation techniques outlined in section 2.2.3. and SEM imaging to directly motivate abrasive calcium carbonate particles on a silicon substrate (as silicon provides a firm, flat, low friction surface on which to motivate the particles) to observe their dynamic behaviour, movement mechanisms and agglomeration tendencies. Particle breakdown and agglomeration breakdown was also characterised on a copper substrate (due to its similar hardness to dentine) under direct loading.

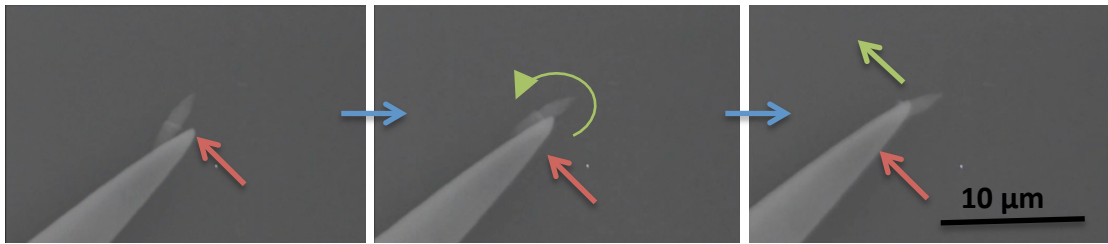
Copper scratch tests SEM images seen in this chapter are the same as those from Chapter 4.

#### **6.2. Results**

Particles were sprinkled onto the substrate surface (either copper or silicon) and motivated using the nano-probes outlined in Chapter 4. Particles were moved left to right on silicon substrate to determine the particles main mechanism of movement and loaded on top of on the copper substrate to determine particle and particle agglomerates breakdown.



### 6.2.1. Motion of S2E



**Figure 88: Progressive screenshots of SEM nano-manipulation trials of S2E particles; the red arrow indicates the direction of movement of the nano-probe and the green arrow indicates the movement of the particle.**

Figure 88 shows screenshots of video analysis of S2E on the silicon substrate with the red arrow showing the direction of movement of the probe. A series of videos taken like that in Figure 88 shows S2E primarily will roll onto its longest flattest side and then exhibit only sliding behaviour along that face. This is represented more clearly in a schematic within Figure 89.

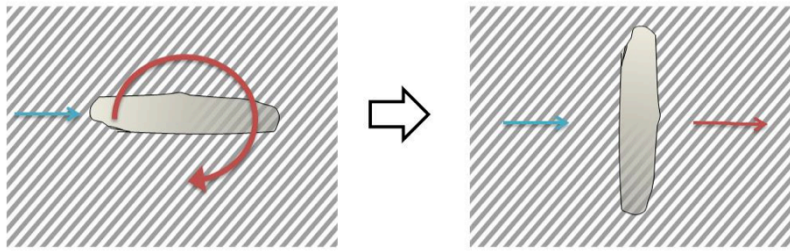


**Figure 89: Simulated images of mechanism seen in particle nano-manipulation trials of S2E**

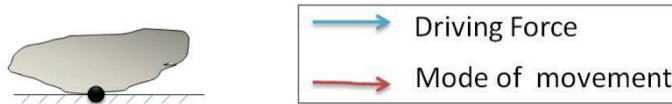
Figure 89 shows a schematic of the movement seen in nanomanipulation trials, made on Blender software program. No equations or mechanical characteristics were inputted into Blender, rather it is just a video graphic showing movement seen in various nano-manipulations trials. This schematic was created for each particle.

Figure 89, derived from a combination of videos like that seen in Figure 88, shows the schematic of the mechanism of movement involved with S2E particles upon a polished silicon substrate. On silicon, S2E particles exhibit mainly sliding motion with only intermittent rolling when trying to find a comfortable face to slide along.

Plan view:



Side view:

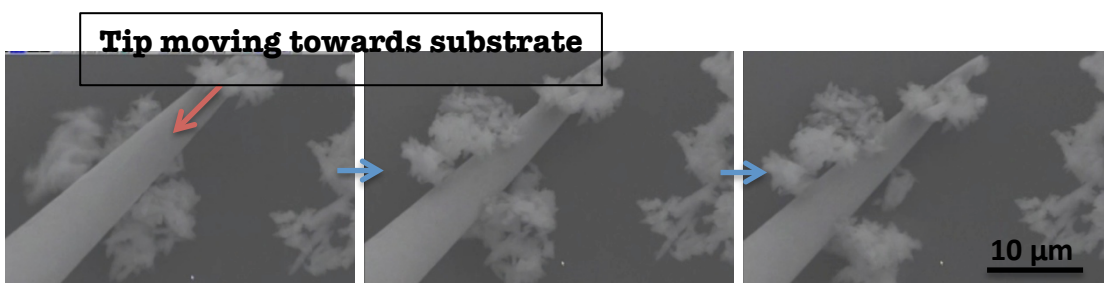


**Figure 90: Diagram of most common mechanism of movement seen in S2E nano-manipulation trials.**

S2E particles are relatively smooth and regular in shape. SEM analysis shows that S2E particles are oblong or ‘lozenge’ in shape with symmetrical tapered edges and thicker middle. This thicker middle gives it a preferred point contact at the middle of the particle; at which it readily slides across on. This primary sliding movement, found from video images of nanomanipulation trails, with S2Es readiness to rotate along the same face, reduces the likelihood of gouging into a substrate surface when moving. These tapered edge also makes it likely to escape contact from loading from above by toothbrush bristles and therefore are more resistant to breakdown.

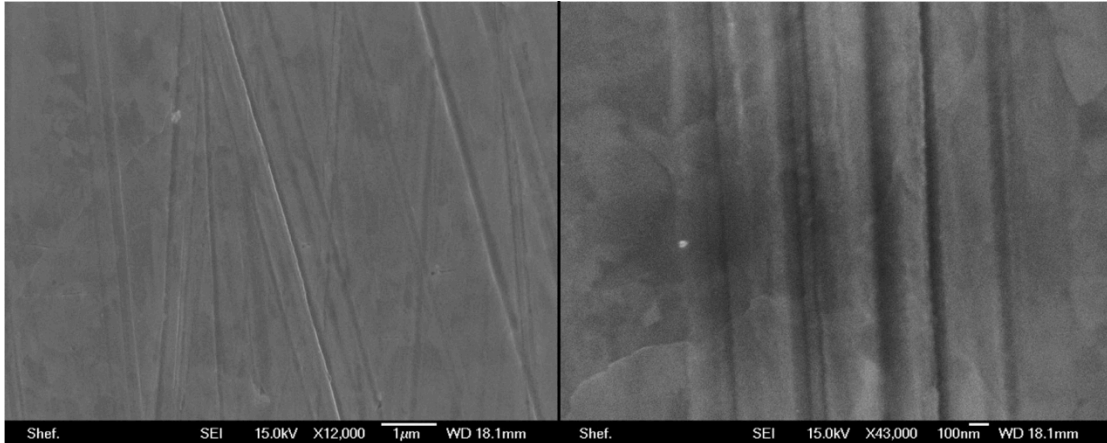
Figure 91 shows the S2E particles being loaded by the nano-probe on a copper substrate.

Particle agglomerations of S2E particles (seen in Figure 91) are clear but with no clear arrangement and are easily broken apart by the application of light loading and passive strokes of the probe.



**Figure 91: Progressive SEM images of SEM agglomerations being loaded and easily broken apart.**

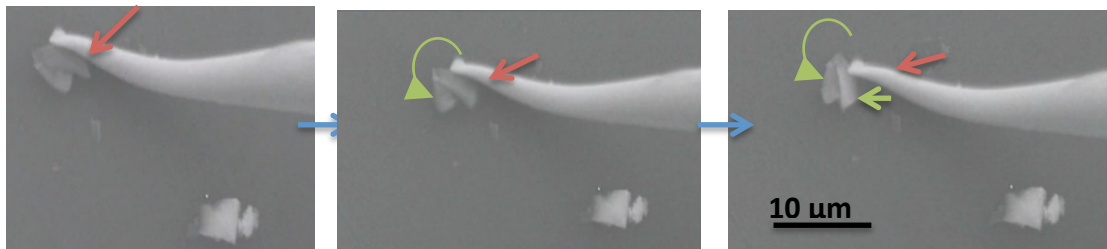
Surface markings from polished copper brushed with S2E particles (Figure 92) agrees with this. S2E is indeed sympathetic to the substrate. There is little to no intermittent gouging on the surface and the scratches seen continuous in nature. The width and depth of the scratches were also seen to be small (and the scratches themselves very neat), showing particles do not readily refashion their position, from their large flat side, once motivated.



**Figure 92: SEM imaging of surface scratches on copper substrate brushed with S2E particles (particles brushed downwards).**

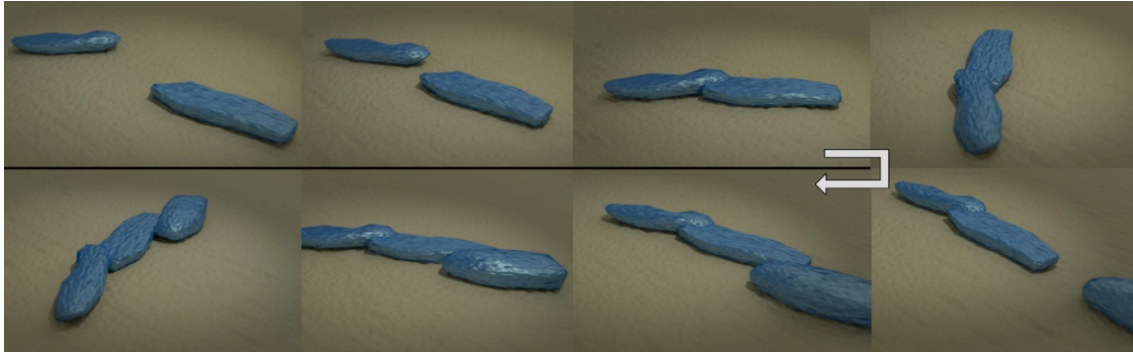
### 6.2.2. Motion of Sturcal L

Sturcal L is similar in shape and structure to S2E particles (both are scalenohedral calcium carbonates) but Sturcal L has a greater affinity to agglomerate.



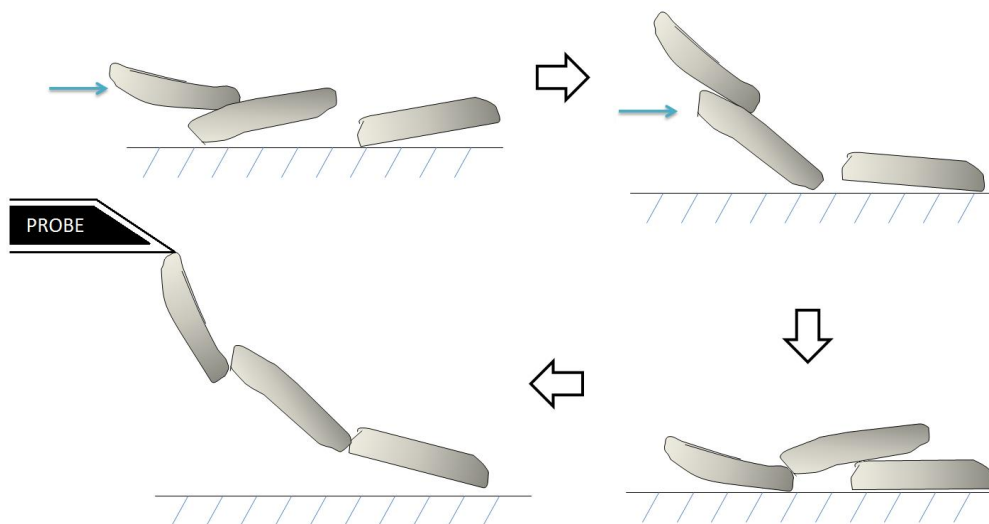
**Figure 93: Progressive screenshots of SEM nano-manipulation trials of Sturcal L particles**

All nano-manipulation trials conducted with Sturcal L showed Sturcal L particles individually had no primary mode of movement, rather the most striking observation was how readily Sturcal L would attract other particles. This is shown in the schematic within Figure 94.



**Figure 94: Simulated images of mechanism seen in particle nano-manipulation trials of Sturcal L particles**

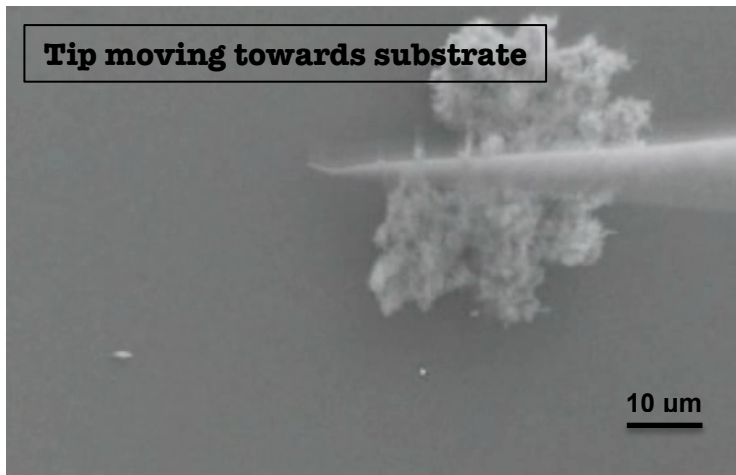
Sturcal L displayed no consistent dynamic behavior or distinct movement behavior during nanomanipulation trials. It was seen to roll and slide on silicon substrate, favouring no particular orientation. Instead it was noted that particles were strongly attracted to one another even when the area of contact between particles was small.



**Figure 95: Diagram of most common mechanism of movement seen in Sturcal L nano-manipulation trials**

Loading Sturcal L on both perspex and silicon substrates (like that imaged in Figure 96) showed little in-situ particle breakdown due to the strong nature and shape of Sturcal L. Sturcal L particles when acting in isolation were fairly sympathetic to the copper substrate surface it was testing on. However most particles were not found in seclusion, instead Sturcal L particles form strong agglomerations (as discussed in Chapter 3) which changed their mechanical behavior.

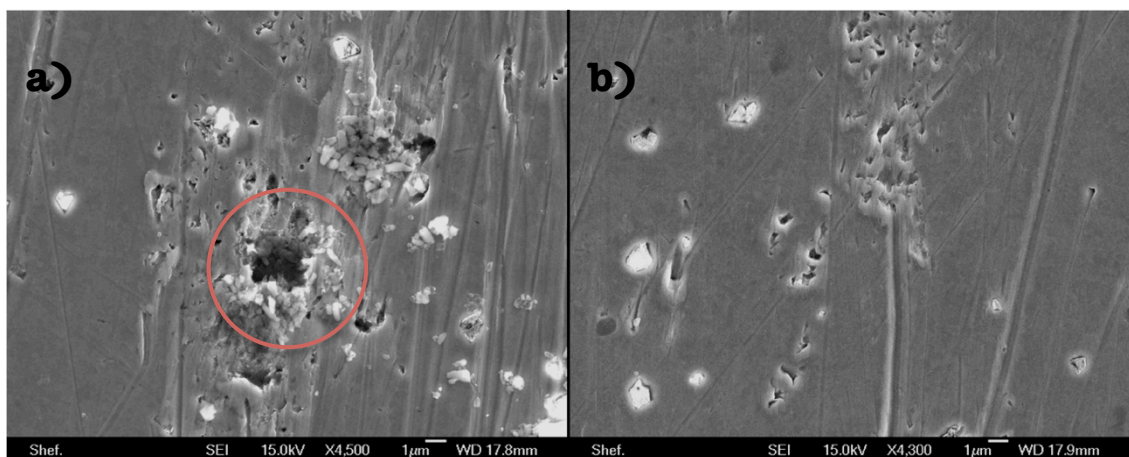




**Figure 96: Agglomeration of Sturcal L particles resisting breakdown.**

Many agglomerations, like those seen in Figure 96 were seen during trials, with the average agglomeration size seen to be around 15 μm in diameter. Agglomerations themselves had a large degree of rotational freedom and were easily engaged by the nanoprobe and manipulated. No individual particles would breakoff from the agglomerate even when the packet of particles was motivated and displaced, highlighting the strength of the agglomerations themselves. Agglomerates themselves were fairly dense and compact with particles arranged to be pointing outwards rather than being a chaotic mass of particles.

The size and strength of these agglomerates, with the tips of particles projecting out, caused notable gouging to copper substrates (see Figure 97).



**Figure 97: SEM image of polished copper brushed downwards with Sturcal L (particles brushed downwards).**

Figure 97 highlights the small scale scratching generated by individual particles as well as more macroscopic galling with material removal from Sturcal L agglomerates (circled in Figure 97). Surface indentations from projected tips can also be seen and gouging of the substrate surface can

be seen from agglomerations rolling along the surface as they are entrained by the brush filaments. This highlights just how abrasive Sturcal L can be to dentinal substrate materials due to its ability to form strong and sturdy agglomerations despite its relatively small individual particle size.

### 6.2.3. Motion of Sturcal F

Sturcal F particles are small (average 1.6  $\mu\text{m}$  in length) aragonite PCC particles. They have an orthorhombic crystal structure and taper at one end.

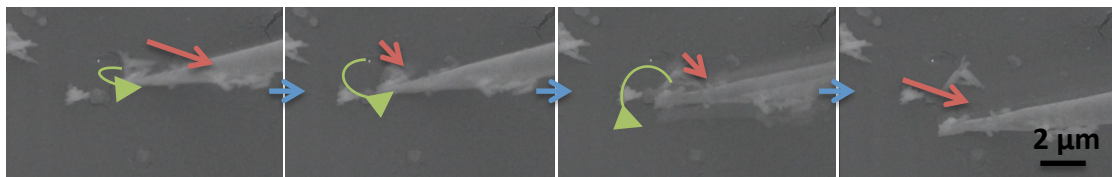


Figure 98: Progressive screenshots of SEM nano-manipulation trials of Sturcal F particles

The videos for Sturcal F shows the tapered edges of Sturcal F causes it to tumble and encourages rolling behaviour for the particle. This is outlined evidently in Figure 99.

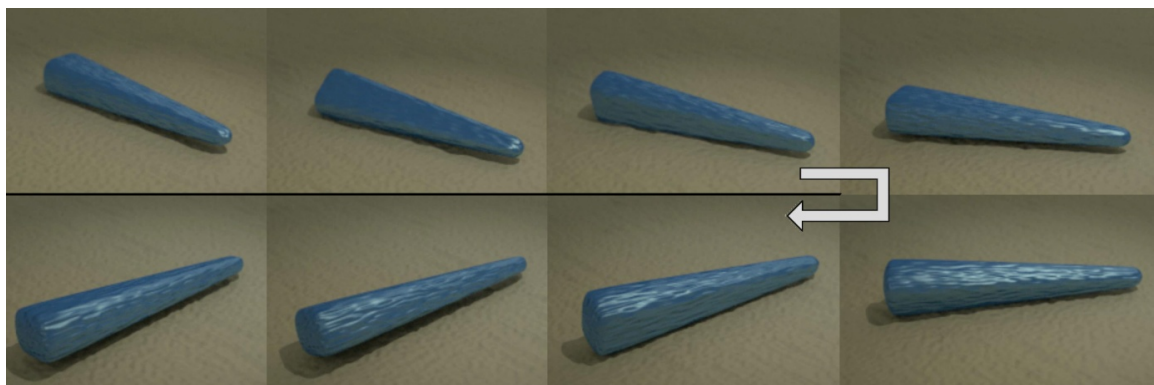
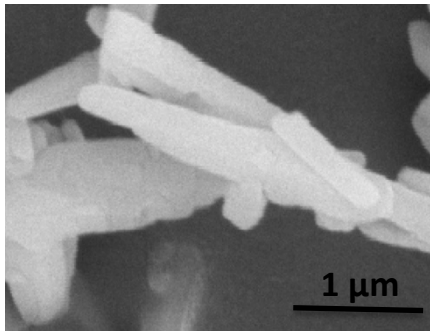


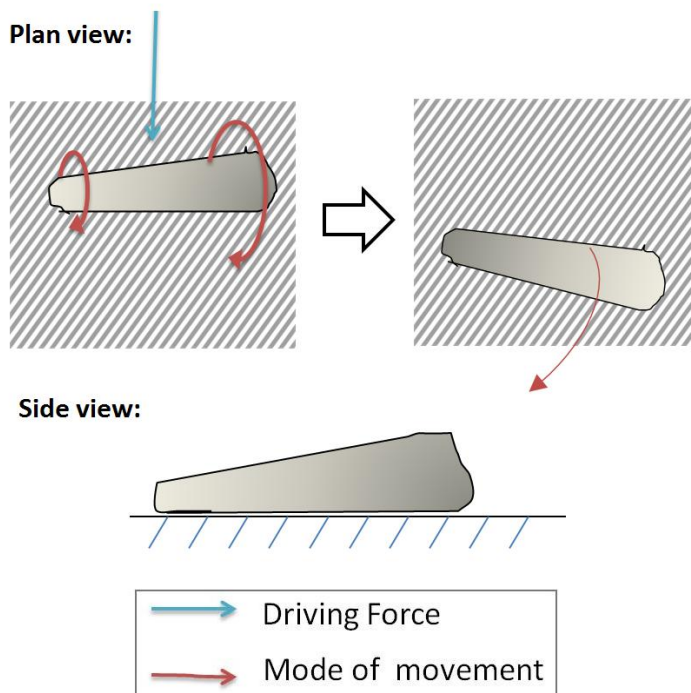
Figure 99: Simulated images of mechanism seen in particle nano-manipulation trials of Sturcal F particles

Sturcal F is an aragonite  $\text{CaCO}_3$  particle like the Rod particles. Both particles can be closely compared due to their flat long edge surface, but there are subtle differences. Sturcal F particles have one edge that tapers, giving it an overall wedge shape, and it is shorter than rod particles. As a result it is more stub like and less fragile than Rods. These small differences in shape give the two particles two completely different ways of interacting with surfaces.



**Figure 100: SEM image highlighting flat sides and tapered edges seen in Sturcal F particles**

Sturcal F showed no tendency to slide despite its flat side edge, unlike the rod particles that are further discussed in Section 6.2.5. Instead the wedge like shape favours rolling (as can be seen in more detail in the diagram in Figure 101 below).



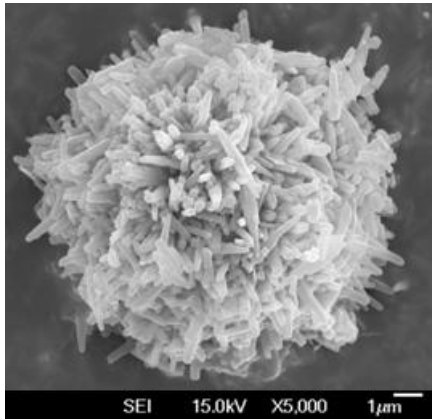
**Figure 101: Diagram of most common mechanism of movement in Sturcal F nano-manipulation trials**

The unsymmetrical shape of the edges of the Sturcal F particle causes it to tumble and move in a progressing arc along the substrate surface.

Attempts to fracture Sturcal F on a perspex surface showed Sturcal F to be much stronger than Rods particles, though breakdown was achievable. The particles would fracture relatively smoothly just like Rod particles.



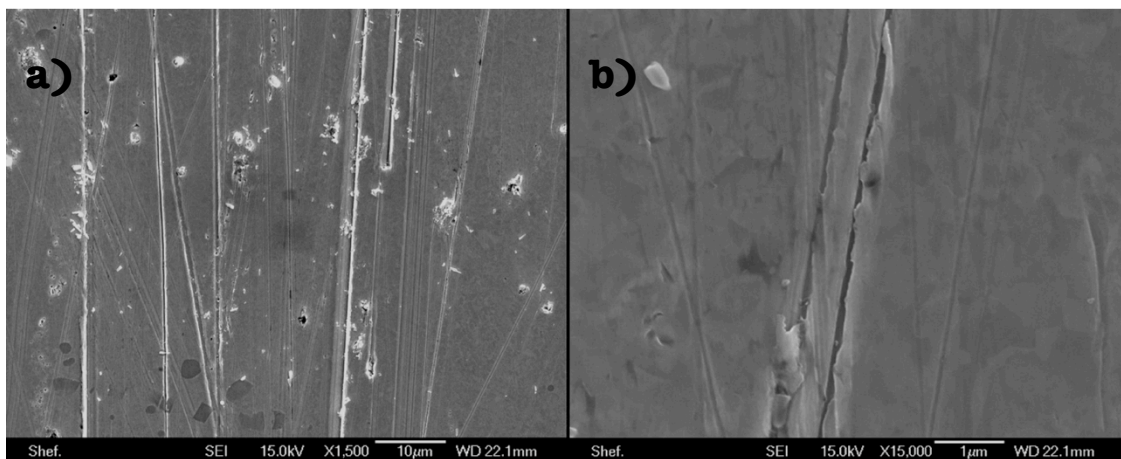
Sturcal F formed agglomerations much like Sturcal L (though much smaller in size - on average around 7-10  $\mu\text{m}$  in diameter). These agglomerations were less ordered than that seen with Sturcal L (Figure 96 and 102).



**Figure 102: SEM image of a typical Sturcal F agglomeration.**

These contrasting agglomerates were found to be much more easily broken apart using the probes. The agglomerates of Sturcal F did show a high degree of directional freedom, not dissimilar to Sturcal L particles, most likely due to similar spherical nature.

The copper scratch testing showed many individual scratch marks along with intermittent gouging and pock marking, from rolling agglomerations (Figure 103).



**Figure 103: SEM imaging of Sturcal F copper scratch trials (particles brushed downwards).**

The copper trials show immediately a reduction in macroscopic galling and surface damage, as compared to that seen with Sturcal L, most likely due to the reduction of the strength and the different arrangement of the agglomerations formed with Sturcal F.

Higher magnification SEM images of the scratches (an example of which can be seen in Figure 103b) reveals the scratches and markings to be less smooth than marking caused by other particles. Suggesting particles are less likely to remain in a steady position and instead small discrete rotations and rolling of the particle, due to its tapered edges, are responsible for its jagged scratches.

#### 6.2.4. Motion of Omya 5AV

Omya 5AV is the only GCC used in this study. It is commonly used as an abrasive in oral care products but has a large variety of shape and size due to the crushing process used to break it down.

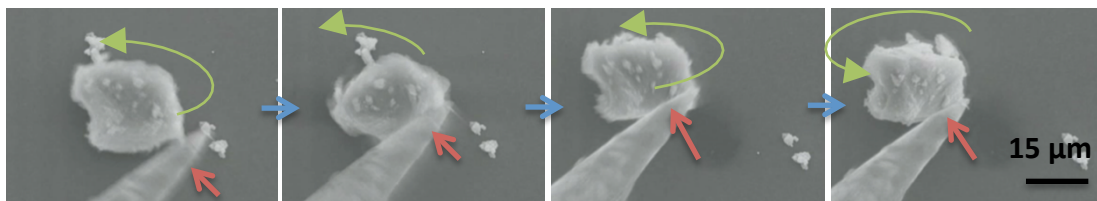


Figure 104: Progressive screenshots of SEM nano-manipulation trials of Omya 5AV particles

The random sizing and shaping of Omya 5AV meant Omya has multi-directional freedom of movement. Omya is extremely angular due to the milling process of its manufacture. These angular sides cause a high degree of rolling behaviour and little to no sliding motions.

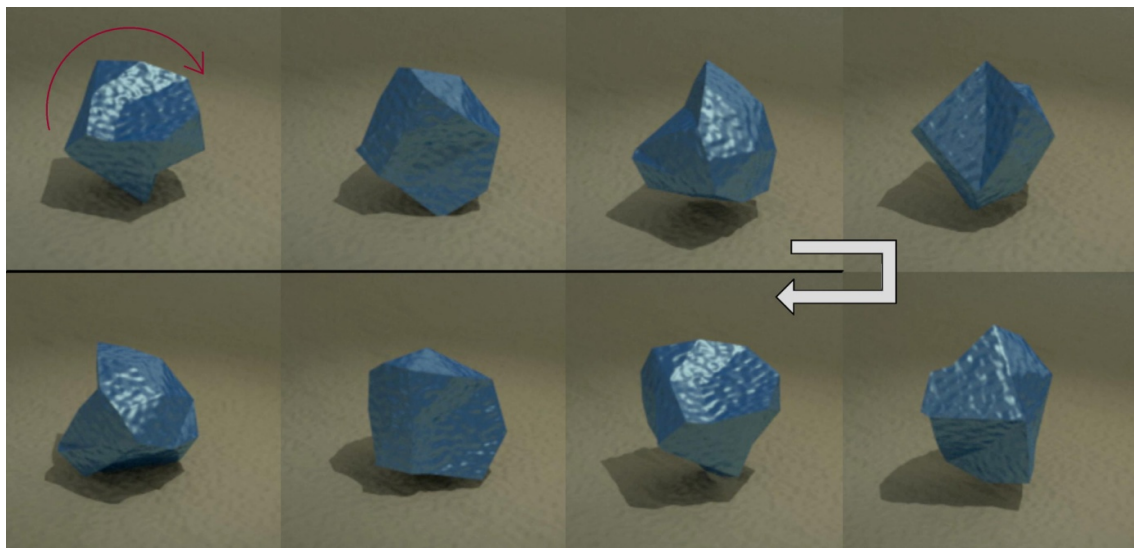
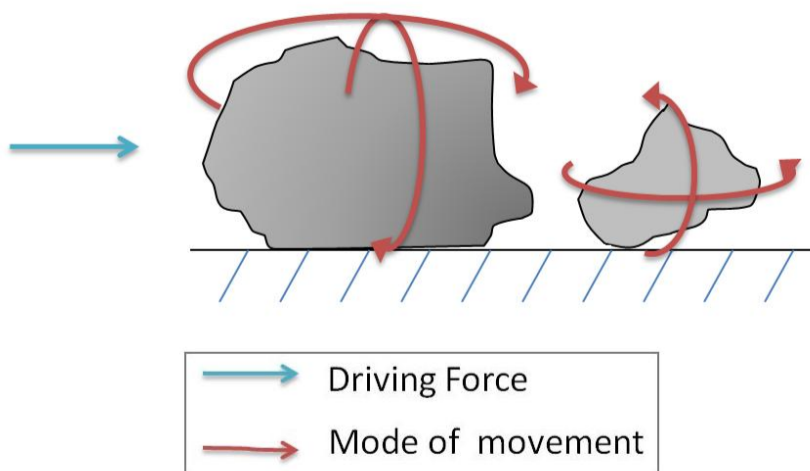


Figure 105: Simulated images of mechanism seen in particle nano-manipulation trials of Omya 5AV particles

The morphology variance in Omya 5AV particles gives for a variability of available movements and freedom for the particles. Nano-manipulation trials on silicon (Figure 104) show the particles are free in their movements, when motivated particles will tumble along its edges and

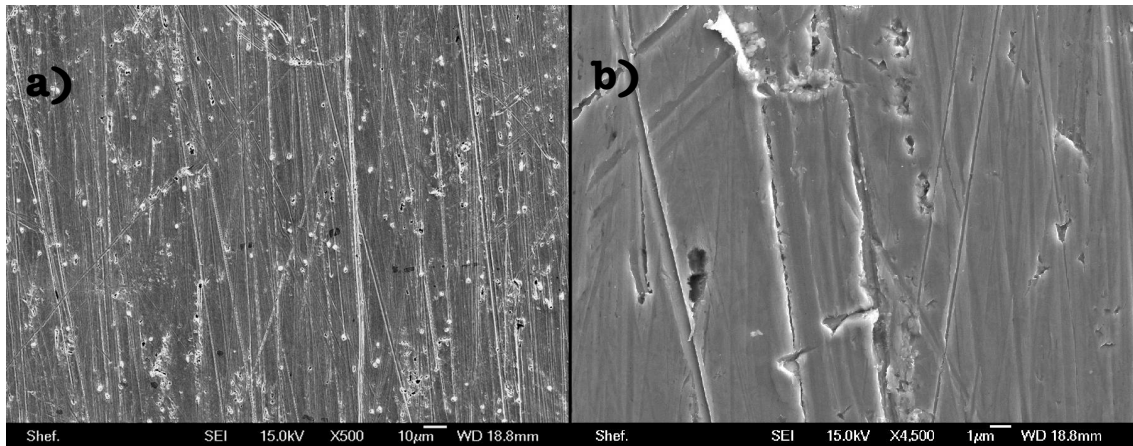
asperities, and also show an affinity to slide if on a comfortable and large particle surface/edge. Mostly it was difficult for Omya 5AV particles to begin sliding due to its angular projections; instead it would dig into the substrate at edges making rolling its primary behaviour (as seen in Figure 105 schematic).

Omya particles have little to no interaction with each other, instead operating in isolation. Any instances of close particles were easily moved apart with the nanomanipulator, and there was no inter-particle adhesion observed.



**Figure 106: Diagram of most common mechanism of movement seen in Omya 5AV nano-manipulation trials**

Direct normal loading of the particles was difficult due to their angular nature and the substrates flat surface; Omya 5AV would roll along its edges instead of fracturing when loaded. As a result particle breakdown was infrequent. Some particles did show partial fracture lines or cracks and loading of these particles did cause a breakdown of the particle.

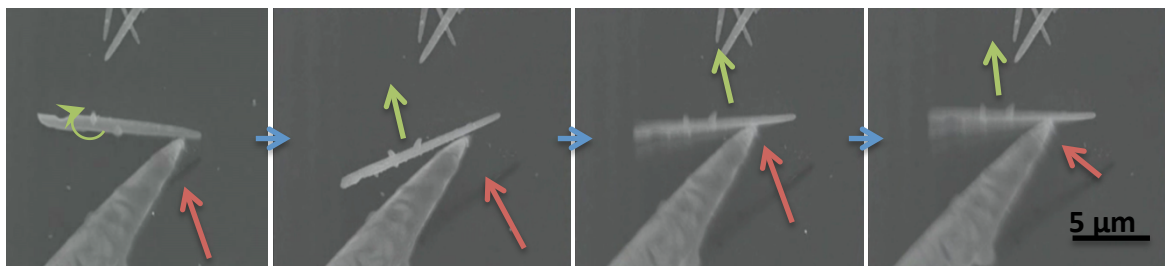


**Figure 107: SEM imaging of copper scratch trials conducted with Omya 5AV particles (particles brushed downwards).**

Figure 107 shows the damage Omya 5AV caused to a copper substrate during scratch trials. There is a significant amount of surface damage and the highest scratch frequency rate from all types of particles tested. Scratch depth and directionality varied greatly. Deep gouging and high substrate material removal indicated large-scale surface damage. Scratch wall edges are uneven in nature suggesting a high tendency for the Omya 5AV particles to roll along and shows the turbulent movement of entrained particles.

### 6.2.5. Motion of Rods

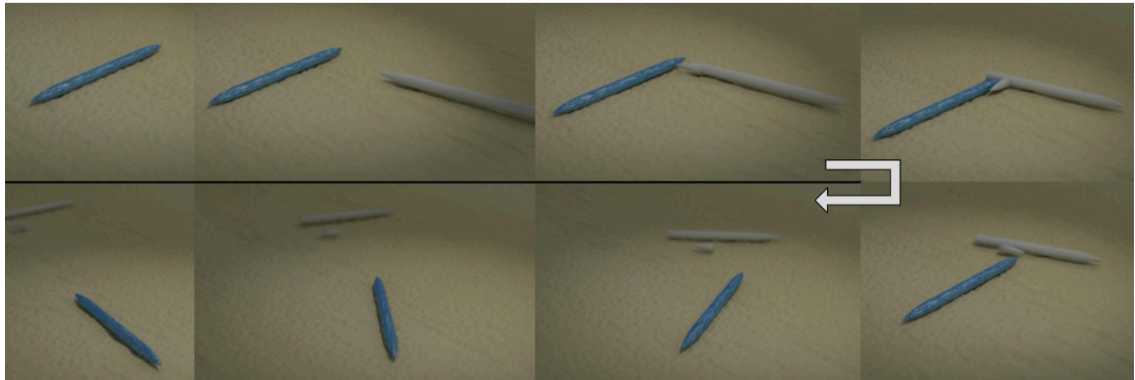
Rod particles are another aragonite particle (like Sturcal F). Unlike Sturcal F Rods have a high aspect ratio, and are extremely thin making them delicate in nature.



**Figure 108: Progressive screenshots of SEM nano-manipulation trials of Rod particles**

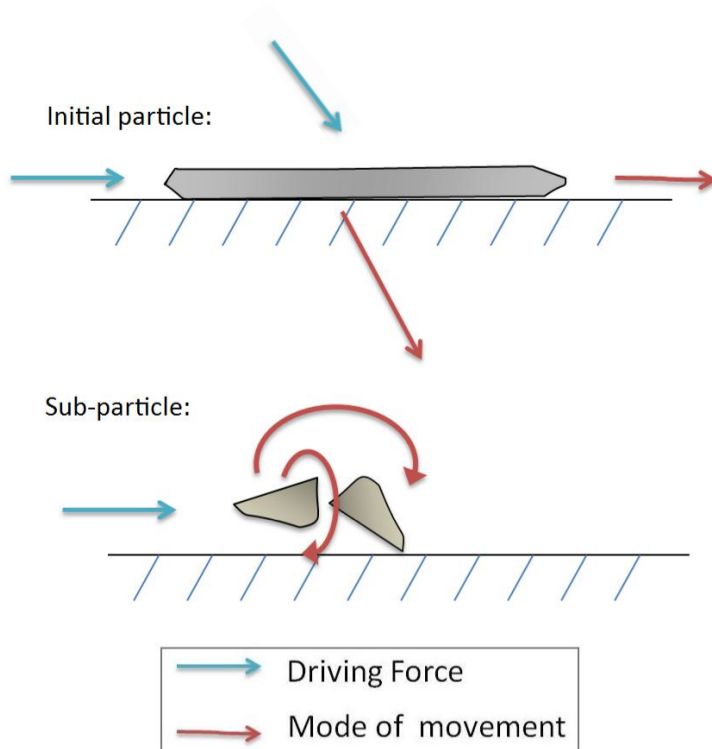
Rods when sprinkled dry onto the polished silicon substrate were always found lying flat on their longest and largest face. They slide along this face when motivated by the nano-probe.





**Figure 109: Simulated images of mechanism seen in particle nano-manipulation trials of Rod particles**

Nano-manipulation of Rod particles show they prefer to slide along their long flat side and are difficult to encourage to roll. When coming in contact with another particle Rods would again slide along in contact but will not adhere to the contacting particle. Instead this particle was easy to shake off and leave once the direction of motion was changed.

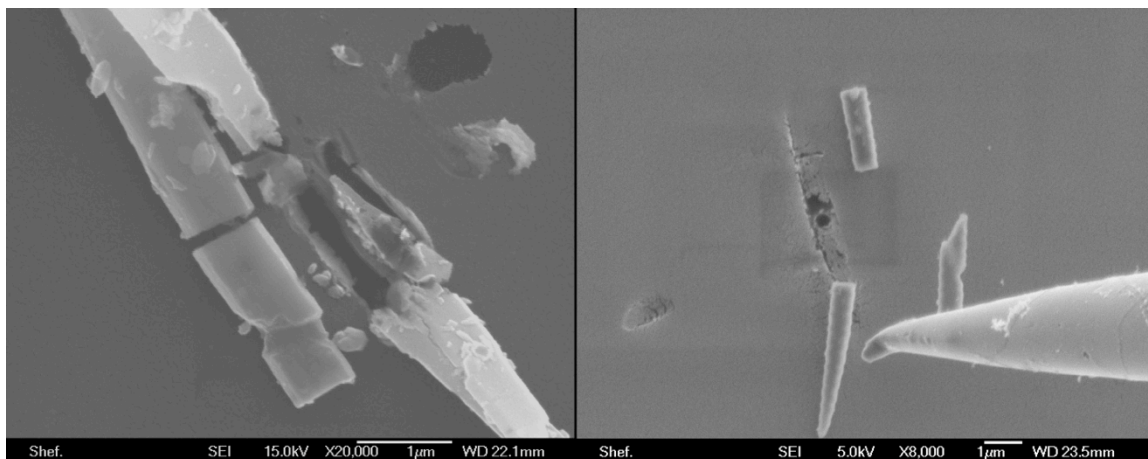


**Figure 110: Diagram of most common mechanism of movement seen in rod nano-manipulation trials**

The cross section of Rods shows they have a long upper and lower flat surface that lie parallel to the substrate surface with tapered symmetrical edges.

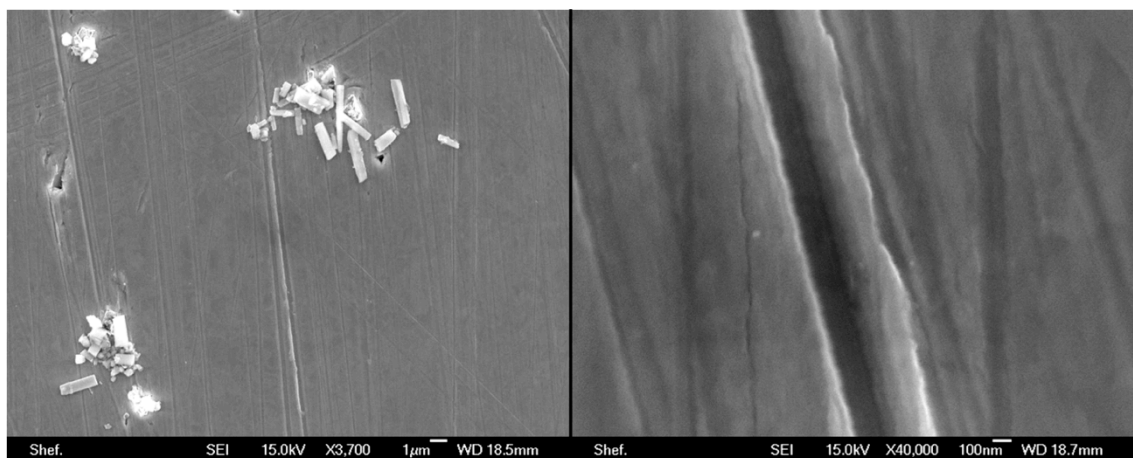
Particles do not form agglomerates but the long thin style of these particles does lend itself to form loose woven lattices (seen in Chapter 3 - Figure 46) that were again easily torn apart using the nano-probes.

Rod particles on a perspex surface were easily fractured when loaded from above by the nano-probes. Fractures were clean and neat. Rod particles are fairly delicate and easily broken. The softer nature of perspex (more similar to dentine than silicon - seen in Figure 111) allowed for more deflection and rotation of the rods whilst under loading. This led to increased surface marking at the fracture point.



**Figure 111: SEM image of fractured rod particles upon Silicon (left) and Perspex (right)**

This fracture often led to secondary sub-particles of the tips of the Rod particles. These smaller tip particles exhibit different behaviour to the larger parent particle, demonstrating mainly rolling behavior and are the main cause of damage on the copper trials conducted, though damage caused is still mild.



**Figure 112: Copper scratch trials conducted with rod particles (particles brushed downwards).**



Figure 112 shows the gentle nature of the Rod particles. Scratch frequency on copper substrates was the lowest of all particles, and the depth of these scratches relatively shallow. Scratches themselves are very smooth with a smooth contoured profile; suggesting particles find a comfortable orientation to remain during a brush stroke; normally on the largest flat side. Deep surface gouging can be seen in isolation from the sub-particle tips caused by particle fracture.

### 6.2.6. Motion of Albafil

Albafil particles are polygonal in shape with a prismatic crystal structure.

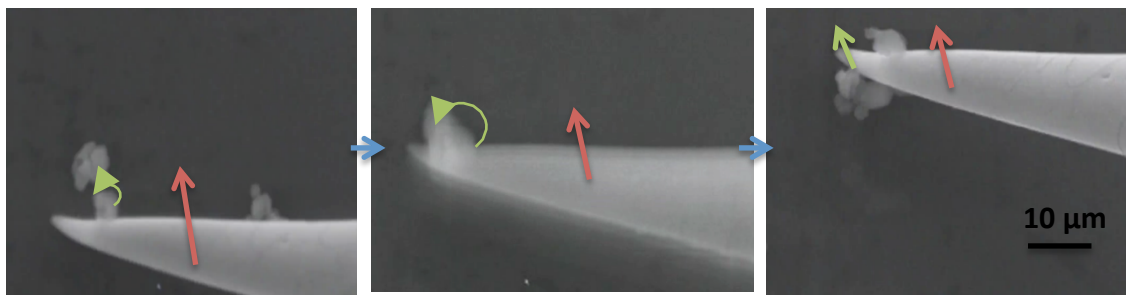


Figure 113: Progressive SEM screenshots of nano-manipulation with Albafil particles

Albafil is an angular particle, like Omya 5AV, and, like Omya, they would tumble and roll due to these edges. But Albafil particles have one primary large face. Once it was on this face it would rest on it and exhibit sliding motion.

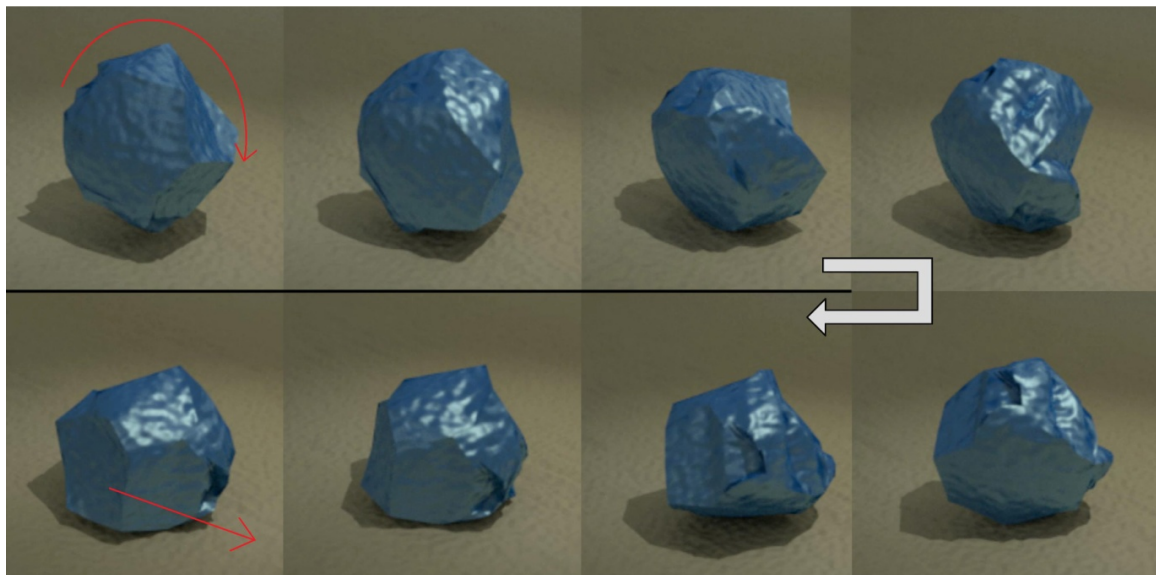
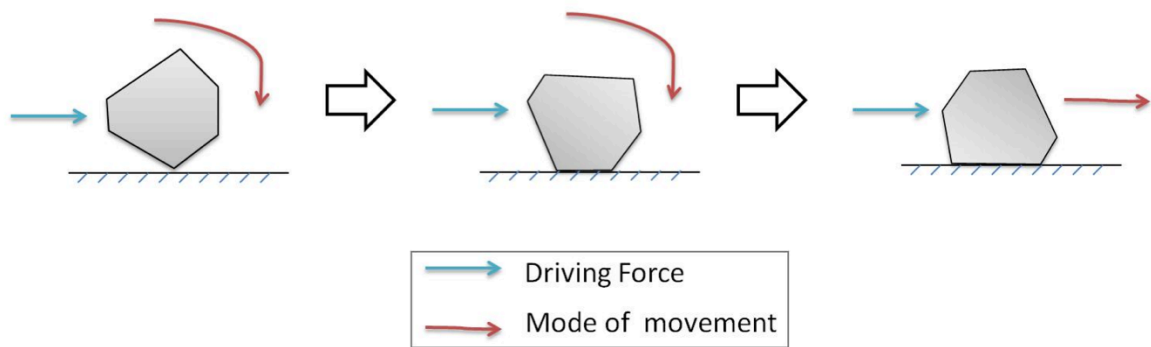


Figure 114: Simulated images of mechanism seen in particle nano-manipulation trials with Albafil particles

Albafil particles are polyhedral in geometry with a variance in the number of faces present in each particle. Each Albafil particle has a

single face, or to parallel faces, that are notably larger than the other faces.

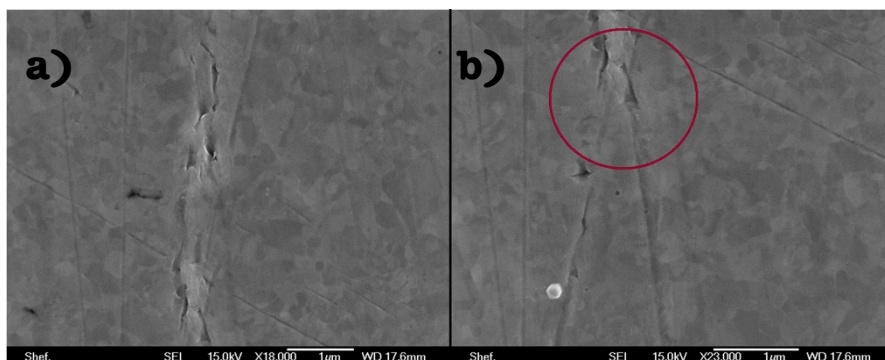
Albafil particles are small in size however the large surface area of the flattest size on which it chooses to rest on does form a large net particle surface-substrate contact area.



**Figure 115: Diagram of most common mechanism of movement seen in Albafil manipulation trials**

Manipulation trials showed particle movement would initiate with rolling along its smaller edges until resting on its aforementioned largest planar face whereupon it would it would slide along. It was noted it was difficult to encourage the particle to initiate rolling again once lain on its largest face. This was observed on both silicon and Perspex substrates.

Evidence of rolling behaviour was seen in the copper scratch trials. Figure 112 shows discrete markings of where the Albafil particles were rolling (red circle) along its angular sides, leading to intermittent jagged surface markings. Thereafter smoother scratch marks can be seen where the entrained Albafil particle started sliding.



**Figure 116: Copper scratch trials with Albafil particles (particles brushed downwards).**

When loaded on from above with the nano-probes Albafil showed a strong resilience to breakdown or fracture. Though particles do remain in close

contact with neighbouring particles they do not form strong agglomerations. Gathered particles will separate easily.

### **6.3. Discussion**

From the in-situ nano-manipulation of particles conducted within this chapter it can be seen that varying the size and shape of a particle dramatically affects the predominant way it moves and how it interacts with other similar particles. This change leads to dramatically different dynamic characteristics influencing the particles abrasivity. The two predominant mechanisms of movement of dry particles observed in-situ were rolling or sliding. Wet copper scratch trials showed surface markings from rolling particles were more damaging than those caused by sliding particles.

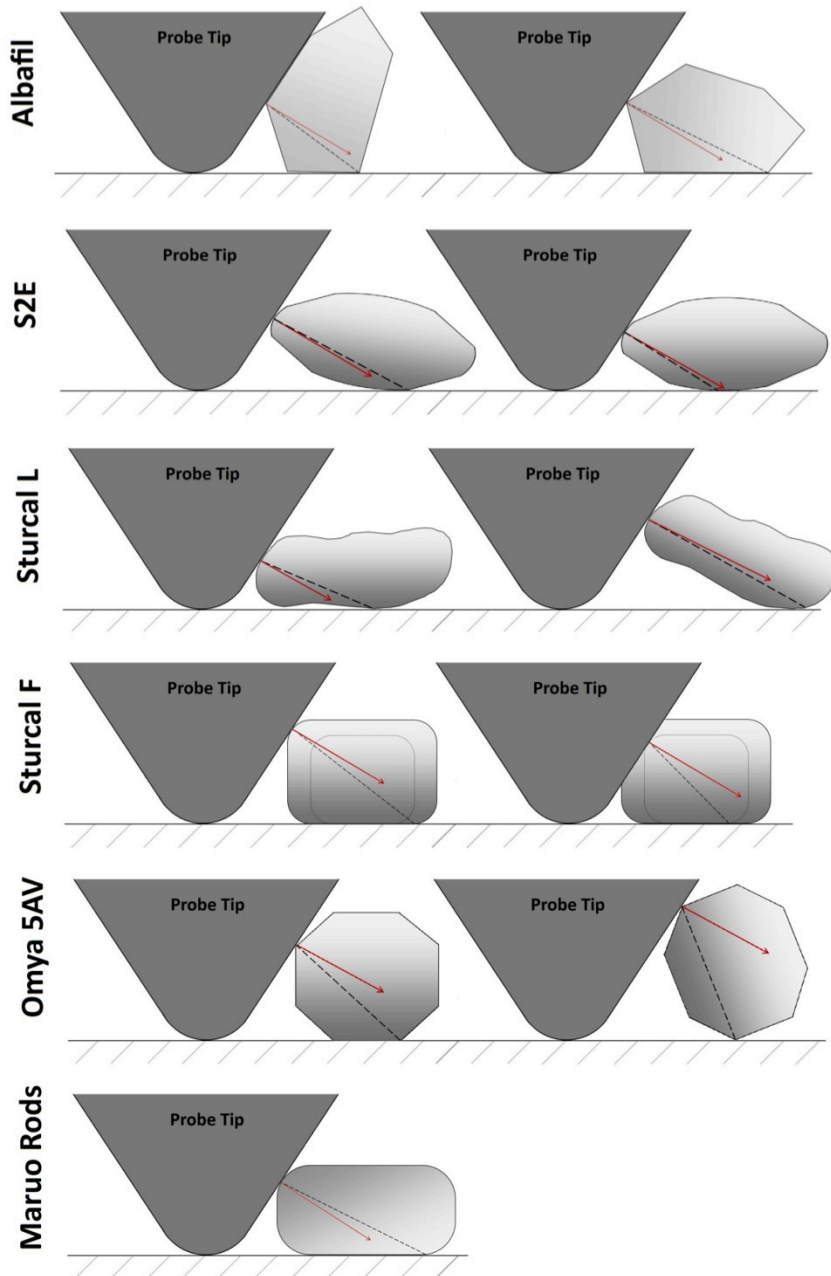
Analysis conducted within this research suggests that particles with multifaceted edges and polyhedral particles are more likely to encounter a hinged environment that shall produce torque making the particle roll upon its multiple faces. This system is unstable and further progression of movement of the particle will only encounter more torque and therefore additional rotation in the direction of motivation. From this research it was also seen in order for a particle to slide it must have sufficient contact with the substrate surface and be on edge at which the sliding force exceeds that of the rolling force, the likelihood of this and the surface area on which it is in contact with will determine whether the sliding motion is maintainable for this particle.

All movements within this chapter are further collaborated and consistent with in previous Unilever work [2].

Previous research has shown in order to sustain a rolling motion is only feasible if the substrate criterions (friction and roughness) and particle corrugation is high enough to overcome its adhesion. This will allow the particle to engage in a rotation, this will create torque leading a rolling motion in a direction perpendicular to motivation [54-56]. Figure 117 shows a free body schematic of probe-particle interactions. The dashed line connects the point of contact between the probe and the pivot point of the particle that is in contact with the substrate below. The red arrow shows the normal force applied by the probe tip onto the particle. Through extensive manipulation trials it was found that if the force exerted by the tip is located above the dashed pivot line there is torque making the particle more likely to roll. If the force is exerted below or equal to the dashed line then the particle will most likely favour sliding.

Figure 117 summarises the typical behavior of particles under the two loading conditions.

There are many factors that determine the movement of a particle, friction, shape, size, loading and area of contact. Friction acting between a particle and the substrate increases with increasing contact area, which again will vary depending of particle shape and size and what face the particle is resting on. In addition to this though every care was taken within each trial to move the nano-probe steadily and at the same rate and speed each time, there will invariably be variations in loading. So it should be noted Figure 117 is a simplification of what was seen in videos, made only to illustrate particle movements of specific faces when dry and manipulated with the nanomanipulator.



**Figure 117: Simplified illustrations showing particle-probe interaction.**

Omya 5AV is produced via a grinding process this means that its shape varies from particles to particle. This being said Omya 5AV rarely has any flat surfaces, again due to its manufacturing process, and therefore unlikely to slide due to it not being able to find a flat surface to slide along. Close inspection of copper scratch trials confirm this and showed evidence of the particles rolling when in contact and entrained.

Albafil is a multi faceted particle, like Omya 5AV, but with significantly reduced scratch frequency and general damage. This is most likely due to the fact Albafil is a precipitated calcium carbonate and therefore there is

more control on the shape and size of these particles. Also largely its sides are flat, therefore a rolling motion is only seen on the shorter sides and a sliding motion favoured once the particle is resting on its most comfortable predominate largest flat side.

Rod particles had the largest flat surfaces and were consistent in shape and size due to their precipitation manufacturing process. Falling freely on the flat surfaces Rod particle don't roll and instead remain in contact with the substrate on the flats the space and slide along. This is shown in Figure 117 with only one free body diagram, as there was no other particle orientation. This was apparent in copper scratch trials as Rod particles exhibited the lowest scratch prevalence and surface damage compared with all particles. Rod and Sturcal F particles were prone to producing sub-particles by losing tips doing fracture that caused intermittent pock marking during scratch trials.

S2E particles displayed point contact on the substrate surface this meant they exhibited slight rotational behaviour but the primary movement was that of sliding. This showed in scratch trials where markings were fairly gentle to the substrate service.



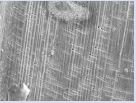


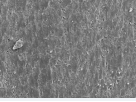
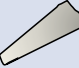
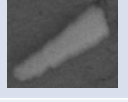
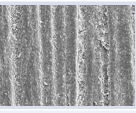

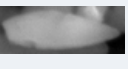
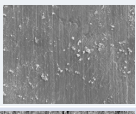
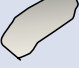
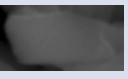
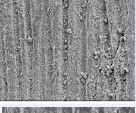

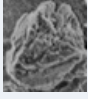
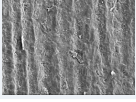
Sturcal L and F have smoother and flatter geometries, as they are PCC's. In general this should mean that they are more sensitive to the substrate surface when acting in isolation. However due to the agglomerations formed with these particles significance of this damage was seen more with Sturcal L then F due to the strong nature and larger size of the agglomerations found. Damage caused by the strong agglomerations can be reduced with the addition of surfactant or a binding agent but further research would need to be done in order to confirm this.

#### **6.4. Conclusions**

A summary of the observations for Chapter 6, for the calcium carbonates studied in this thesis are shown in Table 11.



**Table 11: Summary of observations with calcium carbonate particles**

Particle	Shape	Image	Size (µm)	Predominant movement	Likelihood of fracture	Affinity to agglomerate	Dental wear (x500)	Wear depth (µm)	Additional Observations
Albafil			3.6	Rolling then sliding	Low	Low		230	High speed encourages rolling
Rods			6 x 0.5	Slide	High (tips)	Medium		275	Fractured tips roll
Sturcal F			1.3	Roll about axis	Low	High		300	Very strong agglomerations
S2E			3.2	Slide	Medium	Medium		361	Rotate and slide
Sturcal L			7	Roll about axis	Low	High		804	Very strong agglomerations
Omya			7	Roll	Low	Low		819	High directional freedom

Real-time evaluation of the dynamic motion behavior of six calcium carbonate particle types using SEM and nano-manipulation technology was carried out in the chapter. This was done on three substrate; Silicon, perspex and copper. Silicon and perspex were used to determine movement behavior of the particles and copper to determine scratch behaviour.

For the same testing environment subtle differences in particle geometry and shape have had a significant effect on the mechanism adopted for movement. It was found that particles more prone to a sliding mechanism than rolling mechanism were more sensitive to the substrate surface. With particles preferring rolling demonstrate higher scratch frequency and scratch depth during testing.

The most significant substrate damage was introduced in particle with a high tendency to form strong agglomerates. Particles with the strongest agglomerates demonstrated significant surface damage, which would not be expected looking at the particles individual geometry.

In general from this chapter it can be concluded that PCC particles that do not have a high tendency to agglomerate are statistically less likely to roll then slide and therefore more sensitive to the dental substrate surfaces, whilst still capable of providing effective cleaning, than ground

calcium carbonate that is currently used and therefore has an advantage.

## **Chapter 7.**

### **Introducing Natural Citrus Fibres to Toothpaste Formulations to Aid in Abrasive Cleaning.**

Chapter 7 investigates the effect of adding natural citrus fibres to the calcium carbonate solutions used in Chapters 5 and 6. It was found in Chapters 5 and 6 that precipitated calcium carbonated demonstrate an advantage in tooth cleaning solutions over the currently used ground calcium carbonate (Omya 5AV). This work aims to further the effectiveness of these PCC particles with the addition of citrus fibre; with the aim of reducing the amount (and therefore cost) of specialised abrasive particles within toothpastes formulations.

#### **7.1. Overview of Fibres and Usefulness in Toothpastes.**

The toothpaste industry is a highly competitive market with a few main competitors. These firms actively develop new products promoting gentle cleaning, tooth whitening, sensitivity and stain removal.

The variety of toothpastes available in the market has made it vital for oral care manufacturers to make their toothpaste economically competitive. Promoting a brand that is either competitively priced or slightly undercuts the competition in price can build brand loyalty. There are many costs in the marketing of toothpaste that are common to all firms, such as production, advertising, storage and transportation. Pricing strategies have to be considered and the cost of production heavily evaluated before a new brand name is marketed [57, 58].

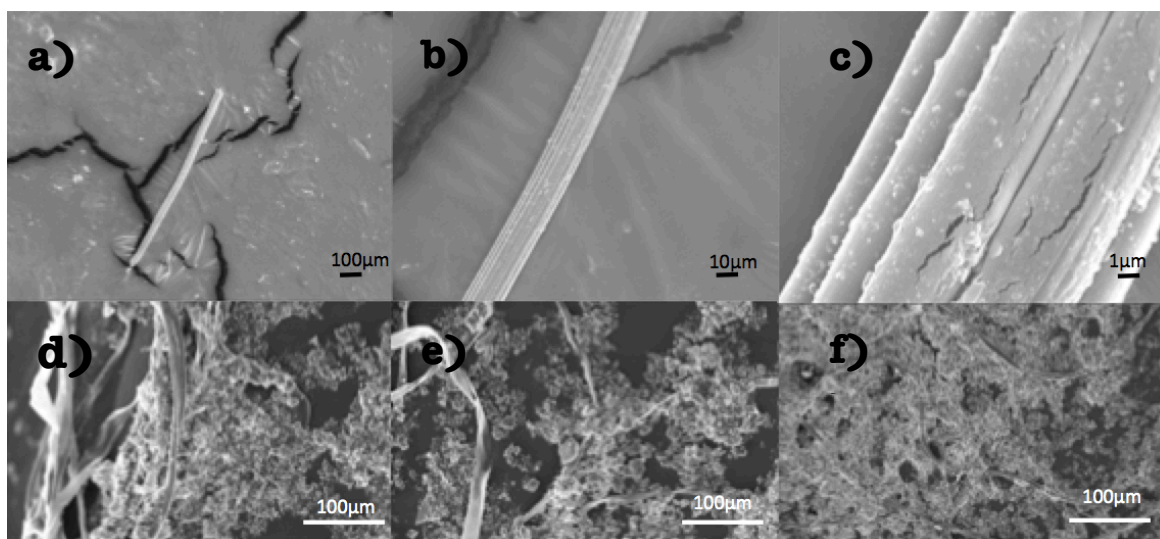
One way to reduce the cost of production in toothpaste is to include citrus fibre by-products from the fruit juice industry into oral care to improve cleaning; this is a new formulation and therefore there is no previous testing of citrus fibres within cleaning.

##### **7.1.2. Citrus Fibre Characterisation**

Citrus crops are the most abundant in the world and the peel (almost a quarter of the fruit mass) contains natural fibres, which have already been utilised in a few industries [68], such as an organic thickening agents in low fat mayonnaise to stabilise oil droplets [68, 69].

The full origins of the fibres provided for this study are given in further detail in Chapter 4 Section 4.2. Briefly, they are derived from the peel of citrus fruits, in this case apples, and obtained from Herbacel Ltd. SEM images of typical citrus fibres can be seen in Figure 118.

SEM images within this chapter are of solutions ultra-sonicated, dropped onto a carbon stub and air-dried. It can be seen there is little interaction with other fibres or abrasive particles.



**Figure 118: SEM images of citrus fibres alone (above), with Omya 5AV (below)**

## **7.2. Dentinal Wear Testing with Citrus Fibres**

Wear of polished human dentine by CETR linear reciprocation trials using a nylon ball and a range of particle and citrus fibre pastes were used in this chapter.

Initially dentine wear testing was done only with Omya 5AV particles and added citrus fibres (Experiment A) at various loads (0.75N, 1.5N, 3N) and frequencies (2.5Hz, 5Hz, 10.7Hz) in order to assess the effect of the addition of citrus fibres, if any. The paste formulations used are as follows:-

- 0.25% wt fibres only
- 1% wt fibres only
- 10% wt Omya particles only
- 0.25% wt fibres with 10%wt Omya particles
- 1% wt fibres and 10% wt particles

Pastes were mixed with distilled water only and particles continually replenished in the contact zone.

The same pastes were also brushed for 10 seconds with a linear reciprocating brush rig onto optically smooth copper for individual scratch analysis.

Once it was seen that the fibres do have a tribological effect, linear reciprocation trials were then conducted with 1.5N at 10.7Hz with pastes containing five other calcium carbonates. These being CalEssence 70, S2E, rods, Sturcal L and Sturcal F (Experiment B). Each particle was mixed into three different solutions:-

- 10% wt particle only
- 0.25% wt fibres and 10% particles
- 1% wt fibres and 10% wt particles

These same particles were also then mixed in pastes with 1% wt citrus fibres and varying particle content (Experiment C):-

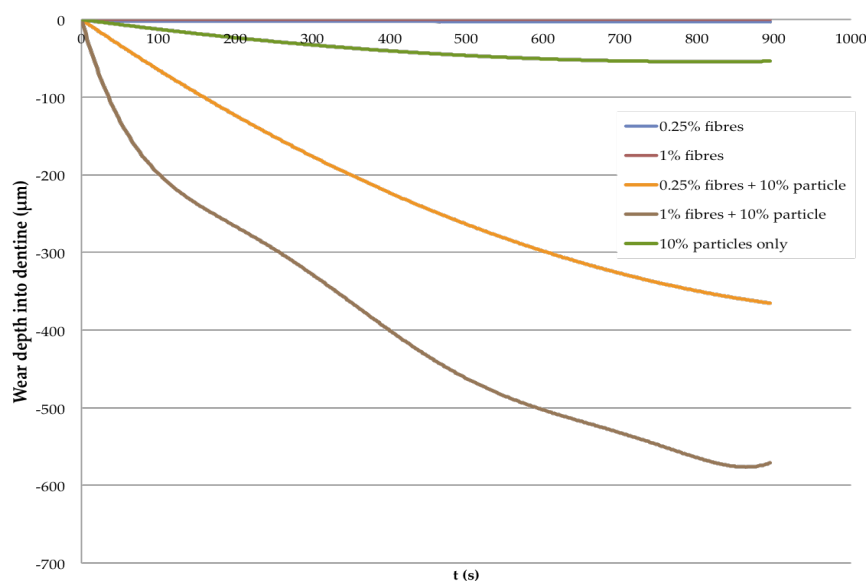
- 1% wt citrus fibres and 5% particles
- 1% wt citrus fibres and 10% particles (from Experiment B)
- 1% wt citrus fibres and 20% particles

Further in-situ visualisation was undertaken via nanomanipulation of a 1% wt fibres paste with 10% wt Omya 5AV particles inside SEM.

## 7.3. Results

### 7.3.1. Experiment A

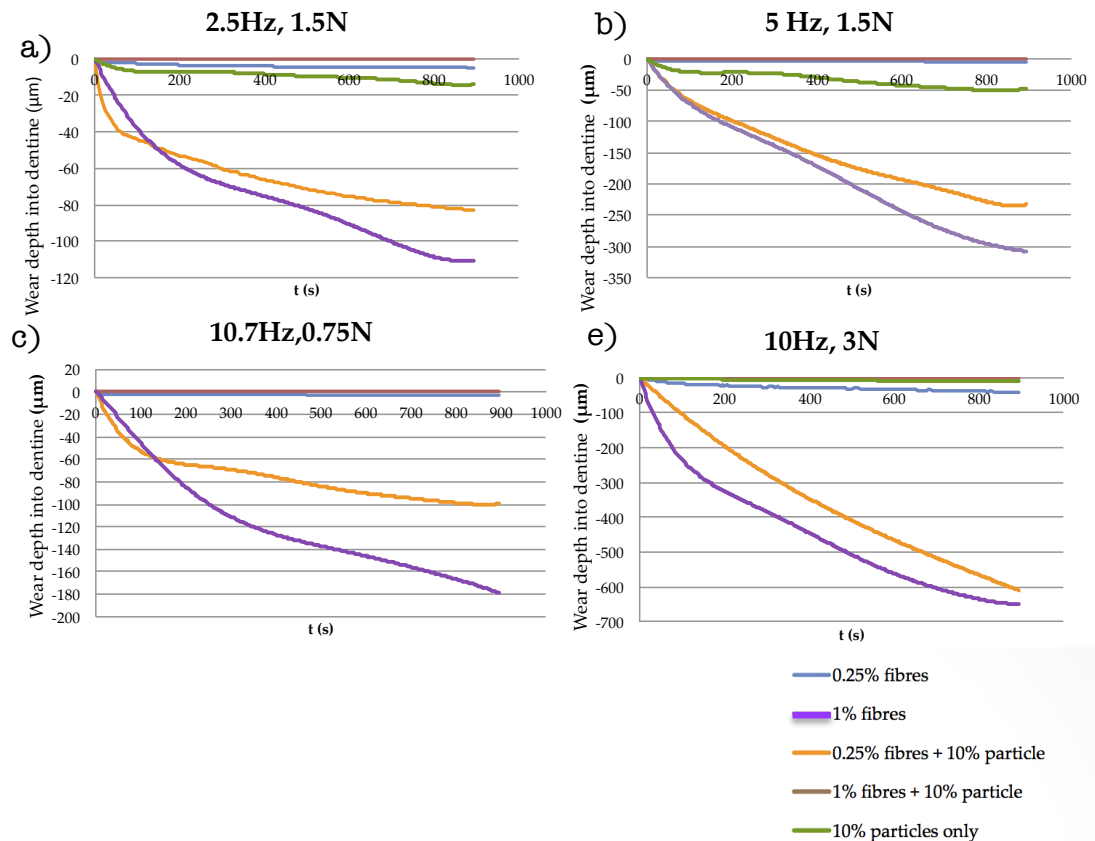
Figure 119 shows the progressive wear of the dentine substrate with the 3 Omya mixtures (two with added citrus fibres) and pastes with only fibres added. Abrasive testing with citrus fibres and no added particles resulted in no dentine wear. Each wear test was undertaken 3 times and had a scatter of  $\pm 2 \mu\text{m}$ .



**Figure 119: Graph showing dentine wear for Omya 5AV and fibre pastes tested at 10.7Hz, 1.5N (n=3).**

Figure 120 shows that the addition of fibres to Omya particle pastes resulted in a dramatic increase in wear. An increase in the concentration of fibres also resulted in an increase in abrasive power.

The same trend was seen irrespective of frequency and load conditions settings (see Figure 120) used for experimentation. Each time the addition of 1% fibres caused around 1.5 times more wear than the addition of 0.25% fibres.

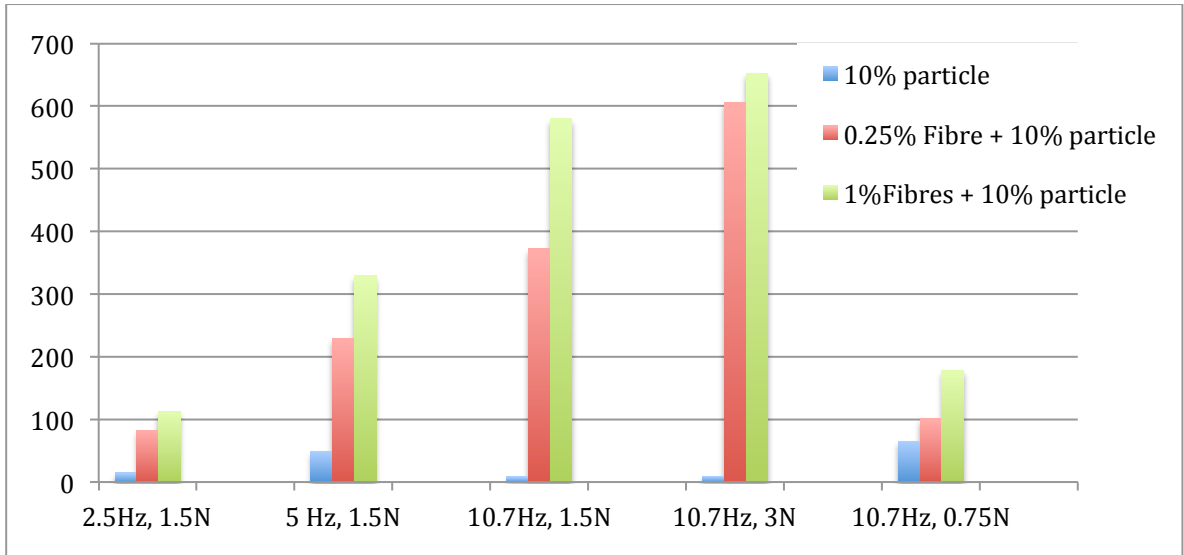


**Figure 120: Overall results of Experiment A. Each paste was tested three time for 15 minutes at a) 2.5Hz, 1.5N b) 5Hz, 1.5N c) 10.7Hz, 0.75N, e) 10.7Hz, 3N.**

This effect of an increase in wear with the addition of additional fibres is consistent throughout scenarios as the particle used has not been changed, but to a different degree for each scenario as particle behavior and the way in which it is entrained will change with different frequency and loads.

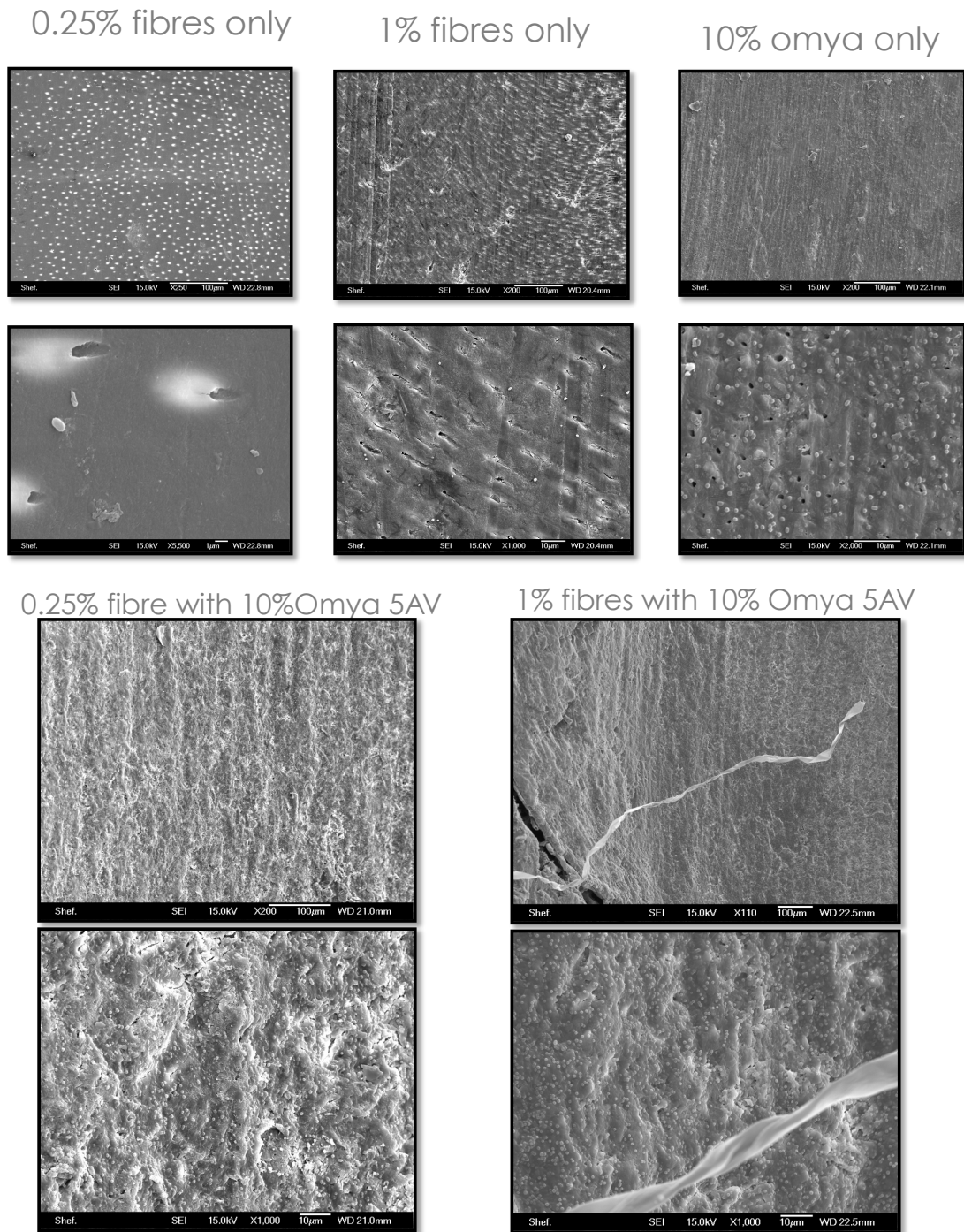
An increase in frequency shows a clearer increase in wear whereas in increase in load is more erratic though does still show an increase in loading increases the effect of wear with citrus fibres.





**Figure 121: Summary of the average maximum dentine wear depth in 15 minutes, results obtained from Experiment A (n=3).**

After the reciprocating wear testing, the worn dentine was imaged using SEM imaging technology. The resultant images of the worn dentine can be seen in Figure 122.

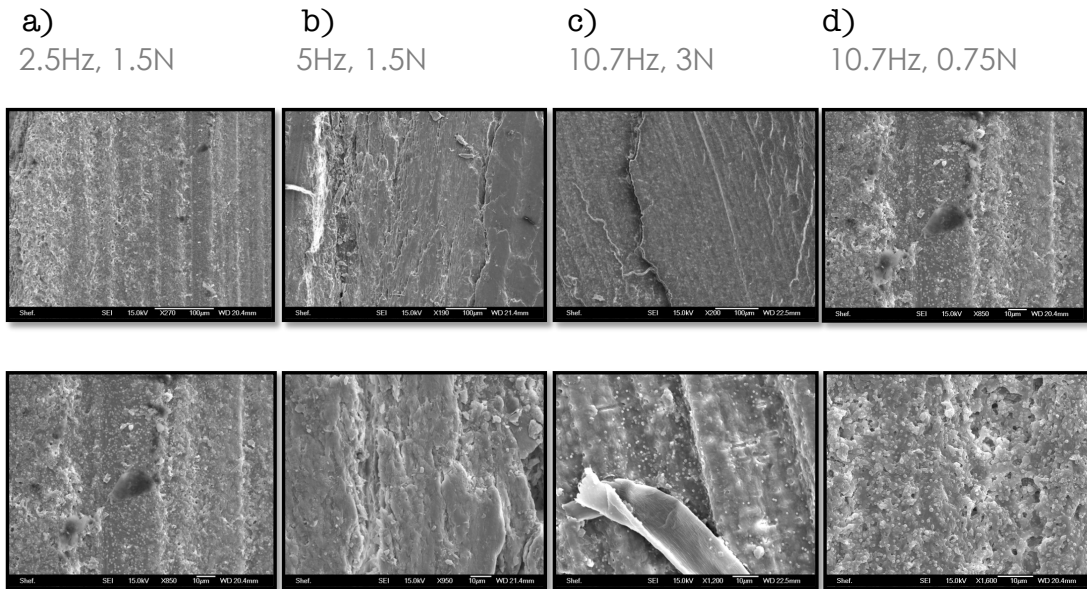


**Figure 122: SEM of dentine wear in Experiment A. Each tooth was imaged after 15 minutes of wear at 10.7Hz, 1.5N using pastes containing a) 0.25% fibres only b) 1% fibres only c) 10% Omya only d) 0.25% fibre with 10% Omya particles e) 1% fibres with 10% Omya 5AV particles.**

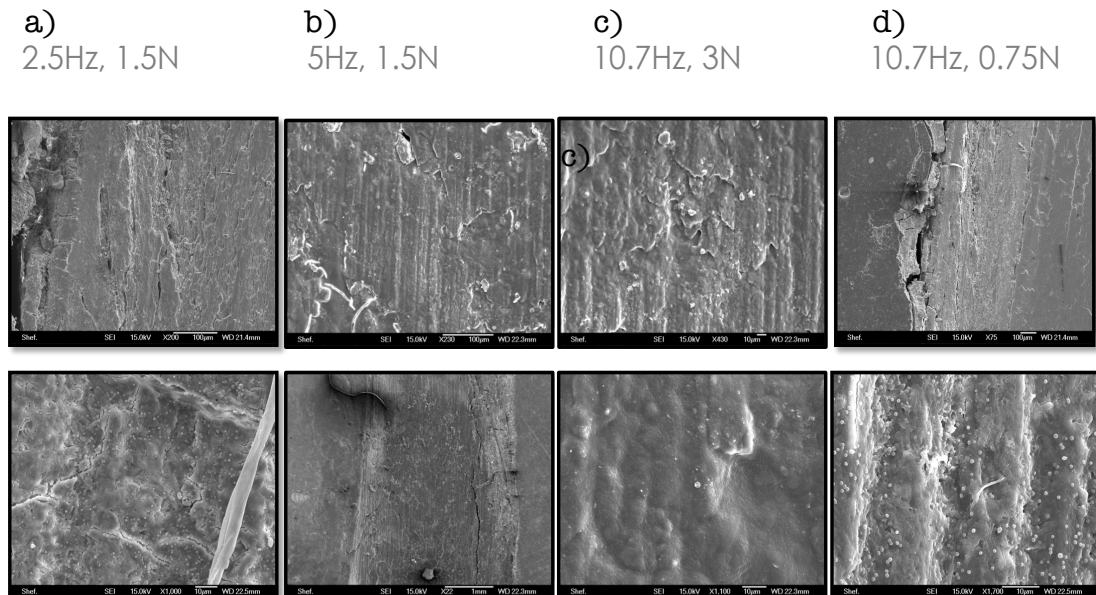
The SEM images shown in Figure 122 show that wear is intrinsically different for pastes including both Omya 5AV and citrus fibres. The most notable effect was these wear trials using citrus fibres appear to have a smoother surface finish, showing little to no evidence of tracking like that of the trials of particles only in water (Chapter 5 - Figure 72). This

suggests the particles are being encouraged to move around by the presence of fibres rather than being entrained and getting caught in scratches.

For other frequencies and loads the following was seen with 10% particles and 0.25% fibres (Figure 123) or 1% fibres (Figure 124):-



**Figure 123: SEM of dentine wear with 0.25% fibres and 10% Omya 5AV particles at a) 2.5Hz, 1.5N, b) 5Hz, 1.5N, c) 10.7Hz, 3N d) 10.7Hz, 0.75N.**



**Figure 124: SEM of dentine with 1% citrus fibres and 10% Omya 5AV particles at a) 2.5Hz, 1.5N, b) 5Hz, 1.5N, c) 10.7Hz, 3N d) 10.7Hz, 0.75N.**

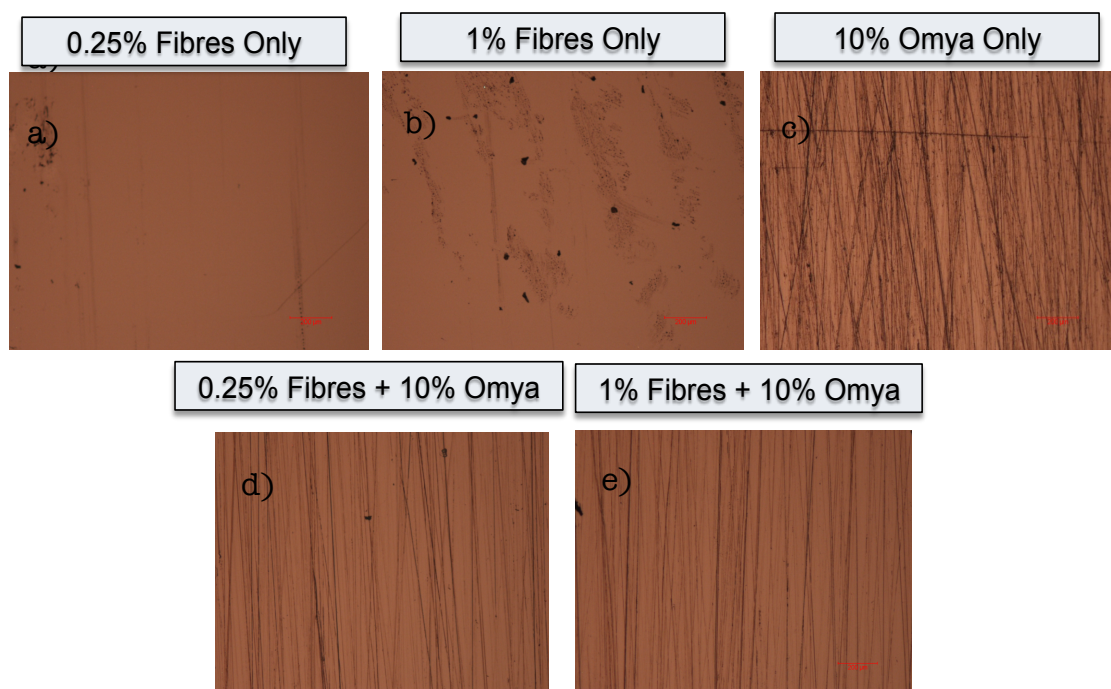
There is not much difference seen in surface morphology between the different scenarios, just the amount of material removed. It appears the



addition of fibres entrain the particles differently at the ball/dentine interface. It appears the fibres enable particles to act together and in multiple directions to 'sweep' away material.

It was of interest to further explore this proposed mechanism in detail. The pastes used above were brushed on optically smooth copper for 10 seconds under a load of 1.5N. Each test was repeated 3 times and the figures below are representative of surface detailing seen along all tests scratch tracks.

Figure 125 below shows the optical images taken of scratch surface markings on copper.



**Figure 125: Optical microscopy images of copper brushed with a) 0.25% fibres only b) 1% fibres only c) 10% Omya only d) 0.25% fibre with 10% Omya particles e) 1% fibres with 10% Omya 5AV particles and a toothbrush after 10 seconds under a load of 1.5N.**

Again, wear surface markings are smoother using citrus fibres, rather than just particles alone. This suggests the substrate is removed in neater, as seen in SEM images of Figure 122, 124 and 125 suggesting the fibres encourage particles to move around in a more controlled manner and cause post-scratch smoothing.

AFM analysis of the centre of the wear tracks is shown in Table 12.

**Table 12: AFM of copper brushed with pastes from Experiment A (n=1)**

Paste	Condition	Ra (nm)	Deepest Groove
1% fibres and 10% Omya particle	2.5Hz, 1.5N	16	62
	5Hz, 1.5N	19	65
	10.7Hz, 1.5N	21	85
	10.7Hz, 3N	16	151
	10.7Hz, 0.75N	18	117
0.25% fibres and 10% Omya particle	2.5Hz, 1.5N	31	92
	5Hz, 1.5N	23	68
	10.7Hz, 1.5N	26	91
	10.7Hz, 3N	29	167
	10.7Hz, 0.75N	28	100
10% Omya particle only	2.5Hz, 1.5N	32	186
	5Hz, 1.5N	33	162
	10.7Hz, 1.5N	33	162
	10.7Hz, 3N	24	63
	10.7Hz, 0.75N	32	156
1% fibres only	2.5Hz, 1.5N	3	-
	5Hz, 1.5N	1	-
	10.7Hz, 1.5N	3	-
	10.7Hz, 3N	3	-
	10.7Hz, 0.75N	1	-
0.25% fibres only	2.5Hz, 1.5N	2	-
	5Hz, 1.5N	2	-
	10.7Hz, 1.5N	4	-
	10.7Hz, 3N	2	-
	10.7Hz, 0.75N	1	-

AFM analysis shows the deepest groove seen is diminished with the addition of fibres, along with a decrease in end surface roughness, when compared to that of using particles without the addition of fibres. The AFM confirms that the addition of citrus fibres results in a smoothing effect of the wear surface despite the increase in wear depth.

Using just fibres in a paste gives no wear and no difference in surface roughness.

### 7.3.1.1. Effect of Frequency

As previously seen increasing stroke frequency had a significant effect on wear. The wear effect of the citrus fibres increases overall with each increase in frequency, regardless of the number of strokes passed and percentage of fibres introduced.

Figure 126 shows the dentine wear for 450 and 1800 completed strokes as a function of stroke frequency.

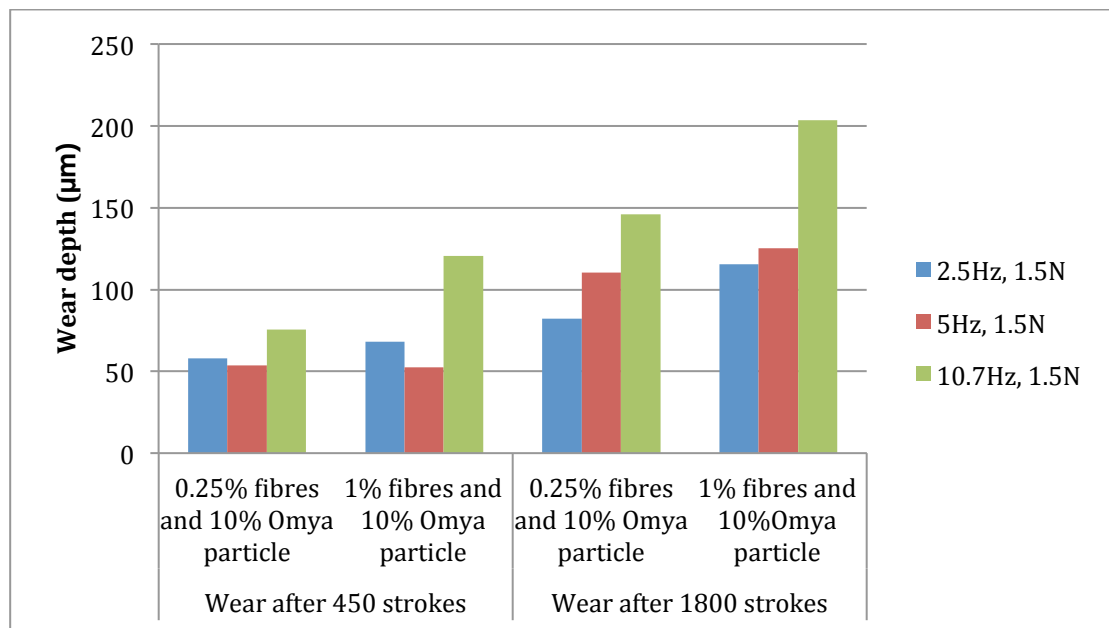
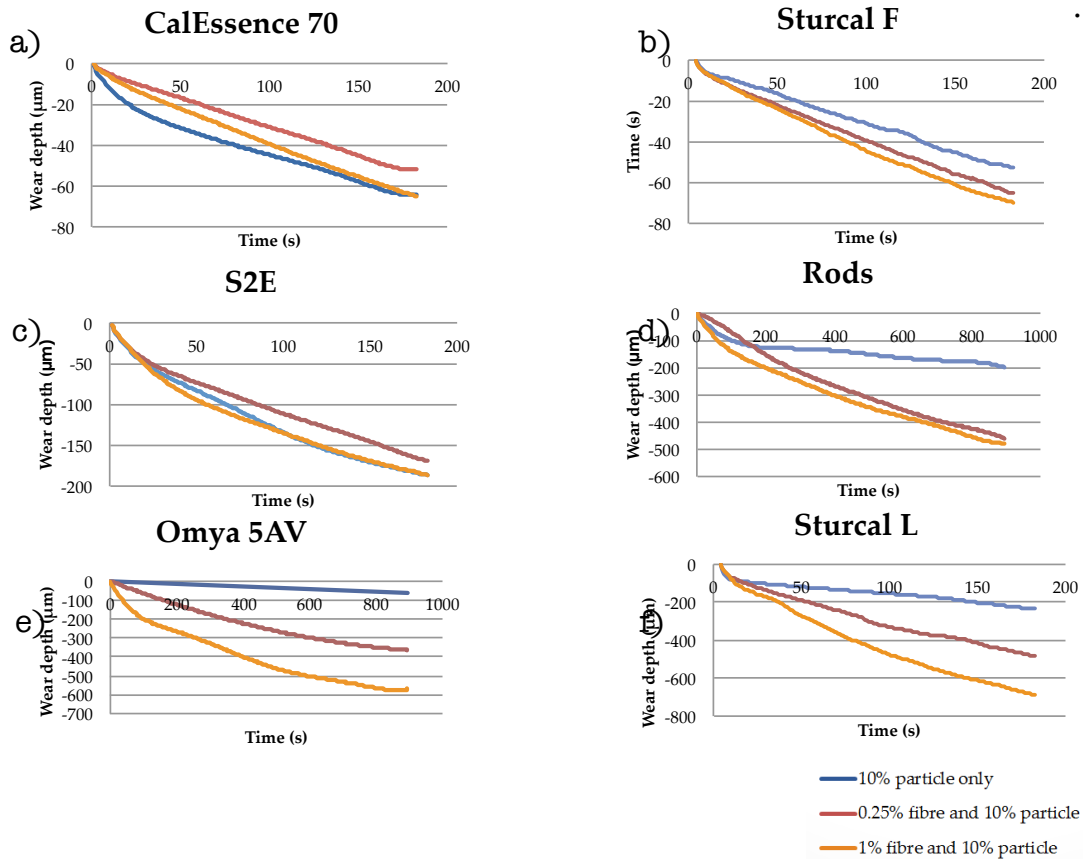


Figure 126: Wear at 450 and 1800 strokes for each scenario of Experiment A.



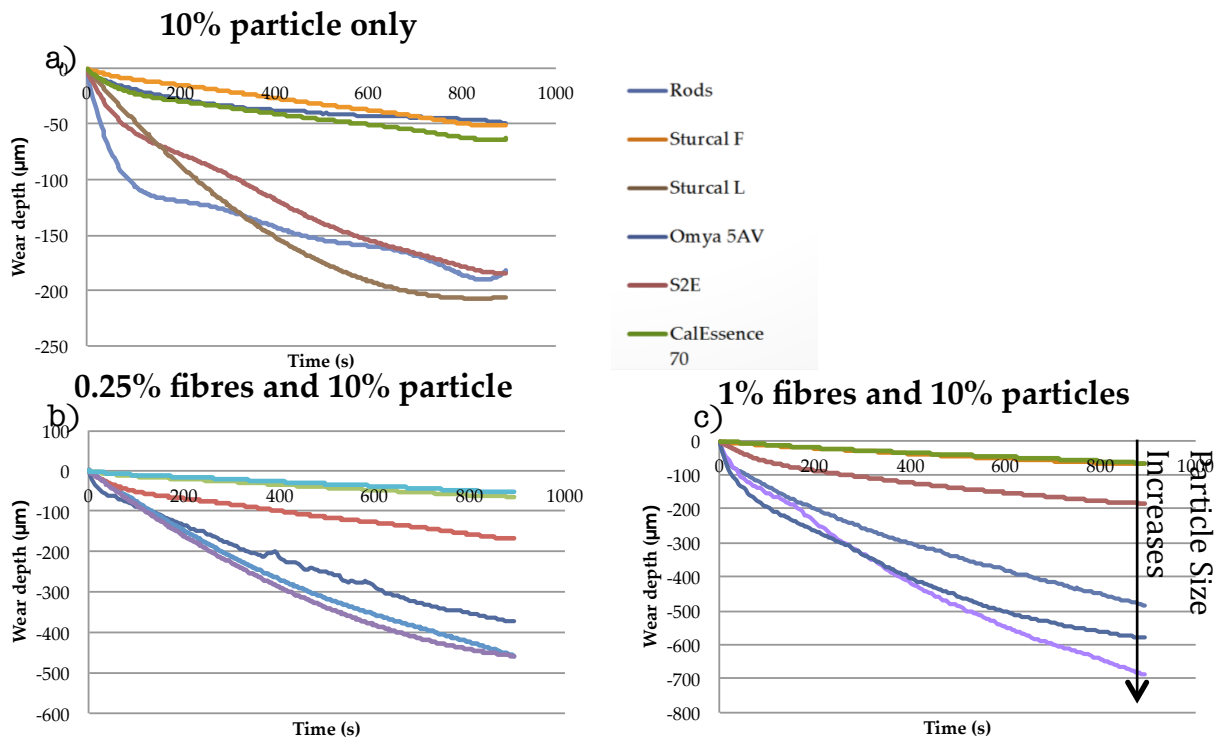
### 7.3.2. Experiment B

The effectiveness of citrus fibre addition on wear modification was investigated for different calcium carbonate particles. PCC's CalEssence 70, S2E, rods, Sturcal L and Sturcal F were wear tested at 10.7 Hz with 1.5 N load. The results of which can be seen in Figure 128.



**Figure 127: Overview of dentine wear depths seen with Experiment B using a) CalEssence70 b) Sturcal F c) S2R d) Rods e) Omya 5AV f) Sturcal L. The above figures show average trend lines for three tests, where overall test scatter was  $\pm 2 \mu\text{m}$ .**

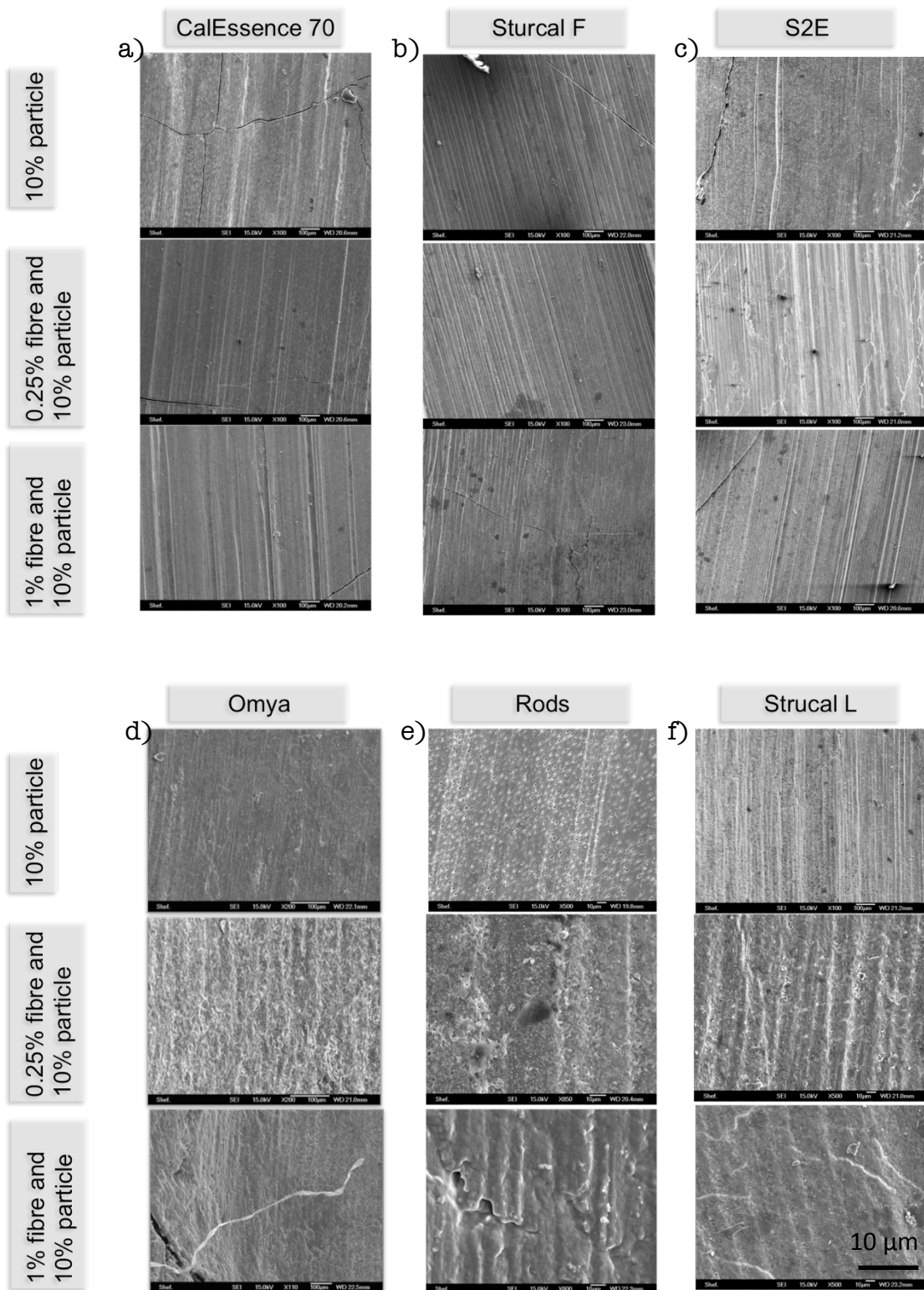
Experiment B showed the addition of citrus fibres did not have the same effect on all particles. Figure 127 a-c shows the wear rate of trials involving the smaller three particles are unchanged in wear with the addition of fibres whereas Figure d-f (trials involving particles larger than 6 microns) show a significant increase in wear. It should also be noted that the fibres did not effect the abrasivity of those particles they did have an influence on at the same rate.



**Figure 128: Summary of Experiment B by solution a) 10% Omya 5AV particle only, b) 0.25% fibres and 10% wt Omya 5AV particle and c) 1% fibres and 10% Omya 5AV particles. The above figures show average trend lines for three tests, where overall test scatter was  $\pm 2 \mu\text{m}$ .**

Figure 128 shows that without the addition of citrus fibres the magnitude of wear each particle produces is independent of size (with Omya 5AV -  $7.85 \mu\text{m}$  - particle producing low wear and S2E -  $3.45 \mu\text{m}$  - particles relatively higher wear). But it can be seen with the addition of fibres the order of wear directly correlates with the size of each particle.

This pattern of abrasivity and wear behaviour of the calcium carbonate particles changing for the largest three particles with the addition of fibres was also seen within the SEM images of the dentine.



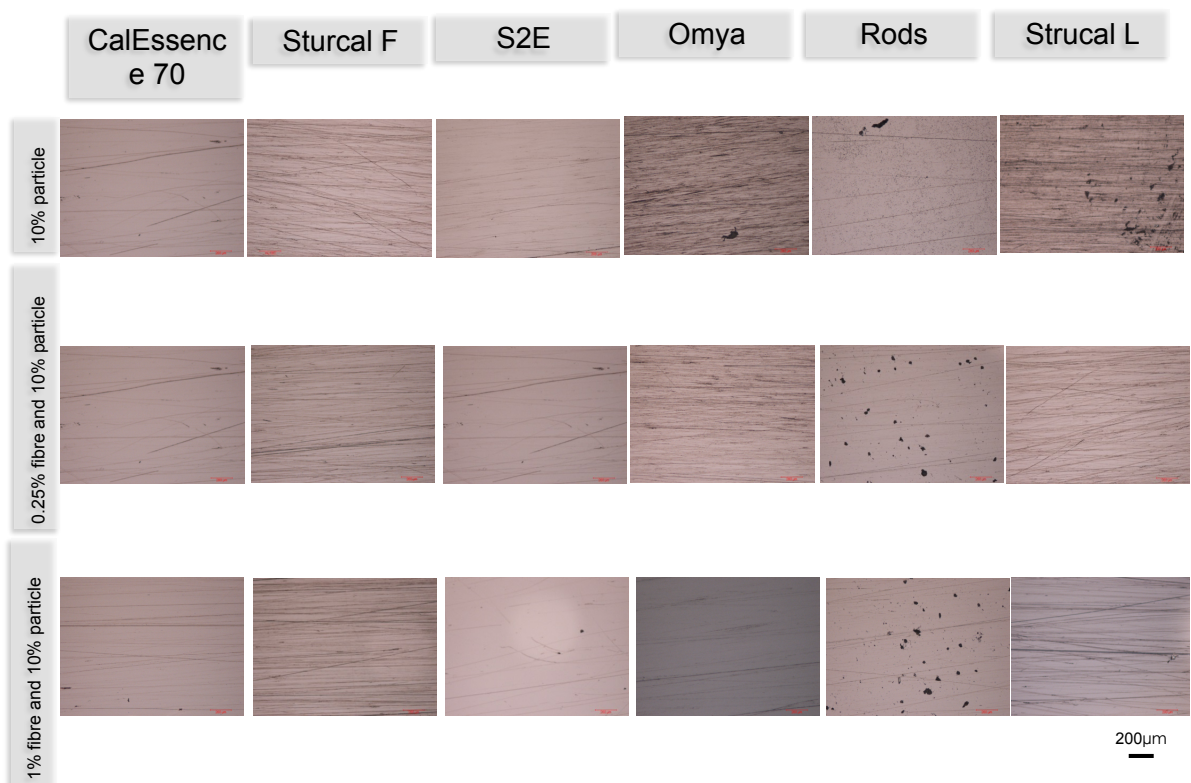
**Figure 129: SEM images of the dentine substrate tested in Experiment B after testing under 10.7Hz, 1.5N for 15 minutes with various pastes.**

It was seen the smaller particles are less influenced by the addition of the citrus fibres, most likely due to their smaller size leading to less entrainment by the large fibres. These testing results did not seem to be affected by average particle breakdown/agglomeration size. The addition

of fibres must discourage the formation of such agglomerates or break them down during mechanical shear of the solution.

The nature of surface degradation seen in Figure 129 also seems different. The smaller particles produce more macroscopic galling and tracking lines than the larger particles when citrus fibres are involved. This, again, suggests the larger particles are encouraged to move around by the fibres as they ‘sweep’ away material rather than moving in repetitive lines following the nylon ball direction.

Figure 130 below shows the results of the copper scratch test done with these pastes.



**Figure 130: Optical images of scratched copper from Experiment B. Each test was repeated 3 times and the images above are a good representation of what was seen along each test scratch track.**

The smaller particles (CalEssence 70, Sturcal F and S2E) have similar copper scratch frequencies regardless of fibre presence. The larger particles, do exhibit a change in behavior with the addition of citrus fibres. The Omya 5AV and Sturcal L particles show neater more uni-directional scratches when in pastes including fibre whereas the imaged residual scratch frequency can be seen to decrease for the same case with Rod particles but with more putting marks, indicating further particle breakdown in these scenarios for the Rod particles.

These samples were then analysed by AFM for roughness and groove sizes to quantify whether the same polishing effect was still seen. The results of this can be seen in Table 13.

**Table 13: AFM analysis of scratched copper trials shown in Figure 130 within Experiment B (n=1).**

Particle	Modal particle size ( $\mu\text{m}$ )	10% particle only		0.25% fibres and 10% particle		1% fibres and 10% particle		Difference in Ra between pastes with no fibres and 1% fibres (%)
		Ra	Deepest Groove	Ra	Deepest Groove	Ra	Deepest Groove	
		Average (nm)						
		Ra	Deepest Groove	Ra	Deepest Groove	Ra	Deepest Groove	
CalEssence 70	0.70	9.	>1	8	1	9	1	0
Sturcal F	1.60	13	8	17	2	13	8	2
S2E	3.45	6	3	7	4	6	6	0
Omya 5AV	6.02	33	162	26	91	21	84	-36
Rods	6.73	43	52	30	19	28	19	-53
Sturcal L	7.85	28	61	12	42	10	35	-171

Worn copper surface roughness values show a decrease when citrus fibres are added in the pastes with the larger particles with the largest particles (Omya 5AV, Sturcal L and Rods) more affected. This indicates surfaces are smoother than if brushed with pastes containing particles only, supporting the theory the particles are more inclined to move around, removing the substrate in layers rather than directional notches, as seen in SEM images. This again shows that added citrus fibers generate a resultant smoother surface giving a polishing effect.



### 7.3.3. Experiment C

All 6 Calcium carbonate particles were put in new mixtures with 1% fibres and varying particle content (5%, 10% and 20%) to see if the density of particles have any effect.

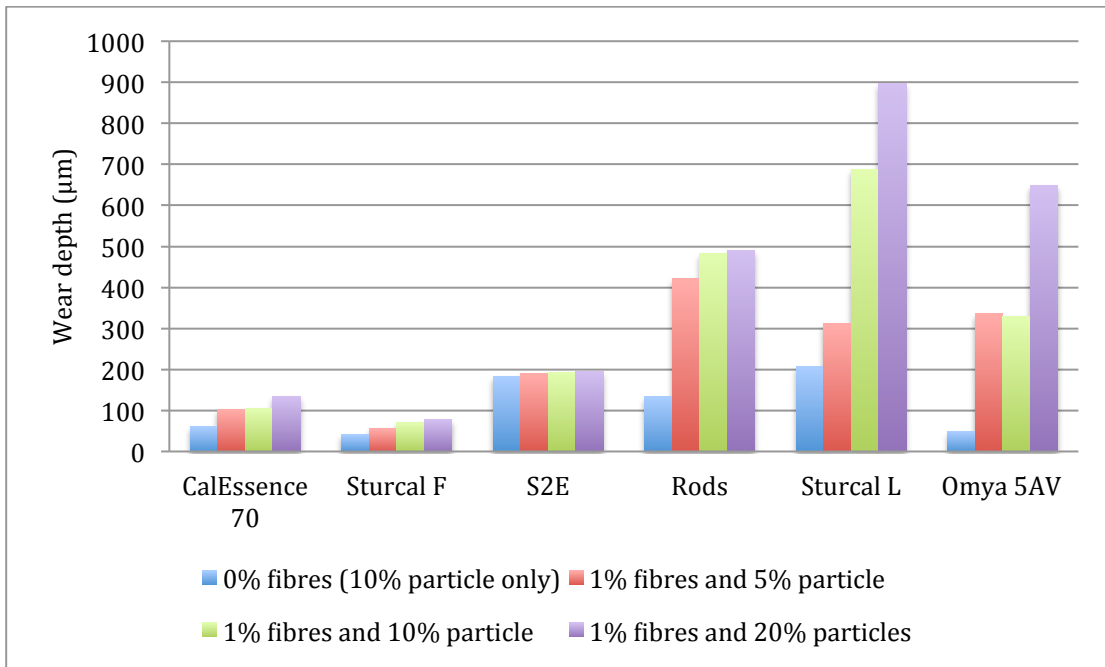


Figure 131: Average wear depths from Experiment C, varying particle content (n=3).

In general Experiment C has shown what has been shown in many other papers (and discussed further in Section 9.4 below) [62, 70], that an increase in particle concentration increases wear in third body abrasion. Though to the degree at which this increase occurs is dependent on more than just particle size.

Under the test conditions used, dentine wear with CalEssence 70, Sturcal F and S2E particles does not increase dramatically with the addition of fibres or the addition of additional particles.

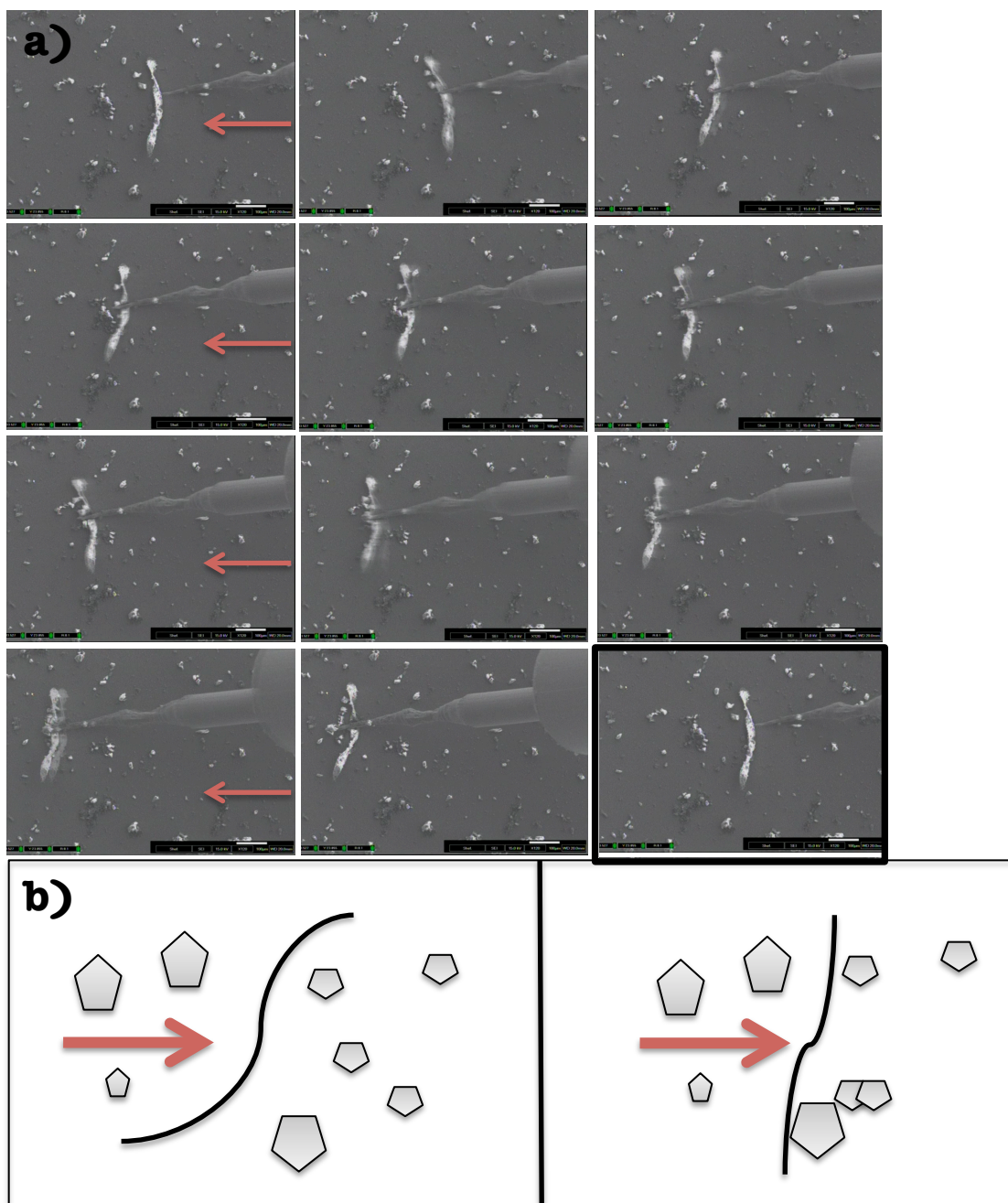
Rod particles exhibit a major increase in dentine wear with the addition of fibres, even with only 5% particles present. But doubling or quadrupling the particle concentration thereafter does not have as great an effect, indicating the fibres can only entrain a small maximum number of rod particles at any given time most likely due to the flat nature of the rod particles and their weak inter-particle weaving.

A more dramatic increase is seen with Sturcal L and Omya particles suggesting better interaction and entrainment between the particles and fibres at a higher concentration of particles.



### 7.3.4. Nano-manipulation

To clarify the mechanism of fibre-particle interaction nano-manipulation techniques were utilised to visualise this mechanism.



**Figure 132: a) SEM screen shots of citrus fibres entrapping and dragging Omya 5AV particles across Silicon substrate b) Simplified schematic of movement mechanism seen.**

Various trials show citrus fibres moving across the substrate in the direction pushed, entrapping and dragging along Omya 5AV particles in the same direction, as shown in Figure 132. Not all particles in the path moved due to the 3D shape and nature of the fibre.

Particles caught in fibres were restricted in rotational movement about their own axis, choosing instead to slide along the side originally entrapped in.

Once entrapped particles would freely slide along the axis of the citrus fibre changing position (illustrated in Figure 132a) but not rolling away nor altering point of contact to the substrate surface.

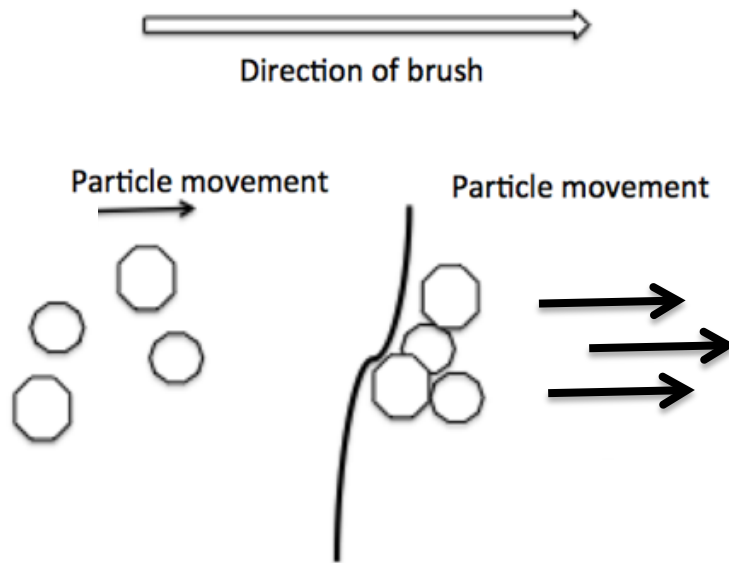
#### **7.4. Discussion**

In general the effectiveness of an oral care composition to remove plaque or staining can be improved by the incorporation of additional abrasive powders [71]. However, this can have a detrimental effect onto the tooth surface, causing additional wear and damage, as well as increasing the cost of abrasives added, particularly if PCC's are used. It has been found that the cleaning efficacy of toothpaste comprising of calcium carbonate abrasives can be enhanced by the addition of citrus fibres.

Experiments undertaken with citrus fibres show that for the calcium carbonates only particles greater than 6 microns were affected by the fibre addition. The original aim of this chapter, to save cost on abrasive particles, would apply. It seems there is a direct relationship between particle size and effective capture between the fibres, and in turn wear rate/cleaning ability.

Obviously the higher dentine wear rate seen with 20% particles, 1% fibre is not desirable in an oral care capacity. And instead a smaller concentration of particles would be more suitable. It also means a combination of smaller abrasive particles can be used in conjunction with these larger particles as they are unaffected by the addition of fibres.

Early SEM imaging indicates that the particles do not actively adhere to the citrus fibres (Figure 118). Since the particles are loose, and not attached to the fibres themselves, it seems the fibres will cause free abrasive polishing, rather than track lines. The fibres will mechanically push or sweep around the particles. The particles themselves will be free to orient themselves differently during each pass, enabling varying surface contact. It is most likely the fibres are caught in the brush and pushing the particles along, enabling better entrainment [59, 60].



**Figure 133: Simple schematic of particle movement, seen in SEM nano-manipulation**

This extra mechanical stimulus inhibits the formation of directional grooves (Figure 132) and widens the effective point contact area of the particles, as the 100-200  $\mu\text{m}$  ribbon-like citrus fibres are dragged across the surface.

This multi-directional wear passing is desirable in oral care as getting a smoother surface is perceived as a polishing effect, with less scratches seen and felt on the surface on dentinal material.

The modification of surface abrasion by changing the mode of particle motion has been seen in previous work where encouragement of sliding of particles along a substrate rather than rolling was observed to cause micro-cutting and rather than deep indentations in the wear surface [68].

Theorised particle motion and entrapment by citrus fibres, further exemplified in Figure 118, was confirmed using nano-manipulation technology.

The second major advantage of the citrus fibres is the clear demonstration of smoothing of the wear surface. This work has already been taken further and a patent for “Oral Care Compositions” covering the used of dietary fibres within oral care containing various calcium carbonate abrasive particles has been filed by Unilever Plc [71].

## **7.5. Conclusions**

This chapter has shown the addition of citrus fibres to abrasive particle formulations for oral care is demonstrated to modify the wear of human dentine. For particles larger than 6µm increasing citrus fibre concentration increases dentinal abrasivity, indicating particle entrapment at the substrate surface. Dentinal wear for smaller particles (less than 6 microns) was unaffected by the inclusion of citrus fibres, showing a lack of particle entrapment. The loading of toothpastes can be therefore potentially reduced by the addition of fibres.

Surfaces worn by mixtures including the fibres appear smoother, with less tracking than similar pastes without fibres, and wear testing on polished copper substrates demonstrates roughness values were indeed lower with added fibres than those without, showing a polishing effect. This is highly desirable for toothpastes as it will produce a tactile and aesthetically pleasing end result on the tooth surface for consumers.

It is therefore concluded for this chapter that the addition of citrus fibres, a waste product of the food industry, to toothpaste formulations with optimal particle size can reduce the need for abrasive particles in oral care products, with the added bonus of reducing surface roughness.

Chapter 8 investigates the effect of different binders in pastes containing Zeodent 113 silica particles (used within the Zendium toothpaste brand).

## CHAPTER 8

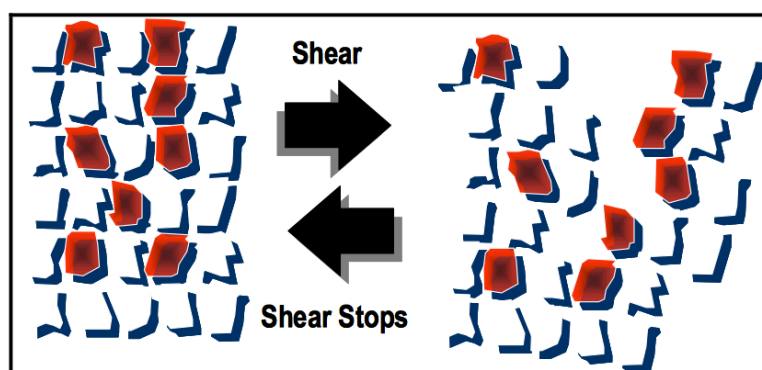
### SILICA AND CARBOPOL PASTES

Chapter 8 explores the impact differing polymer binders and thickening agents can have on particle agglomeration and inter-particle bonding within already formulated and currently used toothpaste mixtures.

The microstructures of the silica and Carbopol pastes are first evaluated by optical imaging, and this effect of changing the polymer binder is then further characterised via SEM imaging, agglomeration and particle sizing, dentine wear testing and scratch testing. These investigations have the overall aim of ascertaining the suitability of specific polymer structurants as binders, and their effectiveness in bettering a dentifrice formulation.

#### 8.1. Background

Carbopol is a cross-linked polyacrylate polymer that has found a wide range of usage due to its excellent thickening properties. It is highly useful in toothpastes as a binder where it gives high gloss, a smooth texture, good particle suspension, negligible toxicity and excellent viscosity stability [50]. As well as this, Carbopol polymers have a shear-thinning effect on formulations so pastes could exhibit high apparent viscosity whilst flowing freely under little pressure; making it ideal for tube or pressure packed products such as cosmetics or toothpaste [59, 72].



**Figure 134: Viscoelastic behaviour of Carbopol. When squeezed (applied shear force) the structure flows like a liquid but recovers quickly once shear is removed [59] .**

Carbopol can also impart these desirable characteristics at low concentrations, under 0.2%, whereas comparable thickening agents, (such as Xanthan gum and silica thickeners) require a concentration of around 0.85% making it cost-effective for the market.

Carbopol also has the benefit of bio-adhesion which enhances the bioavailability of active ingredients, such as fluoride in oral care (also outlines in Section 4.3.2.) [1, 73].

These properties make Carbopol binders highly advantageous for toothpastes from both an aesthetic and practical perspective.

Lubrizon Carbopol is currently used in many commercially available products from a range of companies including; Gleem, Crest, Simply White, Rembrandt, Oral-B and Zendium.

This research is done primarily for the optimisation of Zendium toothpaste (a Unilever owned brand). Zendium uses hydrated silica Zeodent 113 (Chapter 2, Section 2.3.1) as its principal abrasive. Calcium carbonate abrasives are not compatible with the Carbopol thickening agent as it forms coagulates leading to an unpleasant end texture. Silica Zeodent 113 abrasives have been found to be the correct size and shape for Carbopol to provide an acceptable viscosity and yield value when it is suspended with it in a mixture, forming an effective abrasive cleaner of the dental surfaces.

## **8.2. Formulation Information**

A range of pastes were used to observe and evaluate the effects of Carbopol thickeners in a toothpaste mixture. A brief breakdown of the pastes used can be seen below, a full breakdown of ingredients used is listed in Appendix A. Further information about the commercial use and rheology of the Carbopol gels is detailed in Chapter 2 Section 2.3.2.

- BZ1 - No Carbopol added. Only Xanthan gum is used as a thickener.
- BZ2 - No structurants (Carbopol or Xanthan gum)
- BZ3 - Carbopol 2984 and Xanthan gum added.
- BZ4 - No Xanthan gum, only Carbopol 2984 used.
- JZ1 - An in house remake of BZ4.
- JZ2 - Carbopol 2984 added earlier than in the making of JZ1 - methods outlined below - otherwise same mixtures.
- JZ3 - Carbopol Ultrez 20 used. Same method as JZ1
- JZ4 - Carbopol Ultrez 21 used. Same method as JZ1.
- JZ5 - Carbopol 2984 added at high shear along with other ingredients in paste. Otherwise same as JZ1.
- JZ26 - Cross-linked polymer 'Black Sheep' used. Same method as JZ1.



- JZ33 - Cross-linked polymer 'SLS Empicol and Carbomer2984' used. Same method as JZ1.
- JZ36 - Cross-linked polymer 'EasyGel DO' used. Same method as JZ1.
- JZ7 - Remake of BZ2. No structurants added (Carbopol or Xanthan gum).
- JZ8 - No base silica structurant, No structurants added (Carbopol or Xanthan gum).
- JZ9 - No abrasive silica added. Carbopol 2984 used.

Xanthan gum is commonly used in toothpaste formulations to encourage thickening in emulsions and pastes. Only pastes JZ1, JZ2 and JZ3 include this for initial testing to compare pastes of similar thickness with and without Carbopol. In all pastes (apart from JZ8) Zeodent 165 is also included as a structurant. Zeodent 165 is a standard clear thickener, making it useful in gel type toothpaste formulations. It is not intended as an abrasive silica and is removed from JZ8, which is tested for abrasivity to ensure this.

The list of numbered ingredients for each paste can be seen in Appendix A. BZ1 to BZ4. JZ1, JZ3, JZ4, JZ26, JZ33, JZ36, JZ7, JZ8 and JZ9 are manufactured using the following method:-

1. The major ingredients (12-21) were mixed for 5 minutes to allow all ingredients to dissolve.
2. Glycerol and Sorbitol (22+23) were added and mixed for a further 5 minutes.
3. The thickening silica (3) was added over the top and mixed for a further 5 minutes.
4. The abrasive silica (1) was added over the top and mixed for a further 5 minutes.
5. The steretah surfactant (12) was melted in a glass jar and whilst hot, added over the top and mixed for a further 5 minutes.
6. Finally the thickening Carbopol surfactant (6, 7, 8, 9, 10 or 11) or xanthan gum (5) was added over the top and mixed for a further 5 minutes.

JZ2 was manufactured using the following method

1. The major ingredients (11-19) and thickening Carbopol (5, 6, 7, 8 or 9) were mixed for 5 minutes to allow all ingredients to dissolve.
2. Steps 2-5 of method above were then carried out in the same fashion. Step 6 was not needed.

JZ5 was manufactured using the following method:-

1. The major ingredients (11-19) and were mixed for 5 minutes to allow all ingredients to dissolve.
2. Glycerol and Sorbitol (20+21) were mixed with thickening Carbopol (5, 6, 7, 8 or 9) added and mixed for a further 5 minutes.
3. Steps 3-5 of typical method above (for JZ1) were then carried out in the same fashion. Step 6 was not needed.

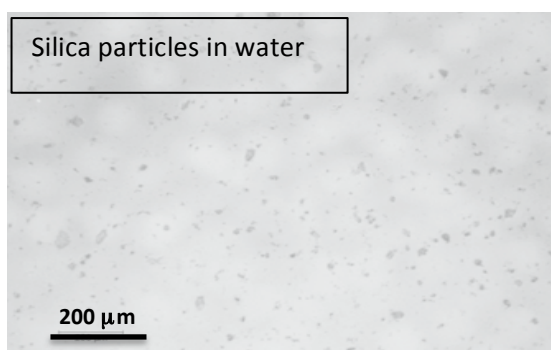
### 8.3.1. Optical Imaging of Pastes

To evaluate the microstructure of the fluid pastes, 10 $\mu$ l of diluted pastes (1:2 in water) was pipetted onto a glass slide and a further glass slide placed on top (care was taken to place slide with no pressure).



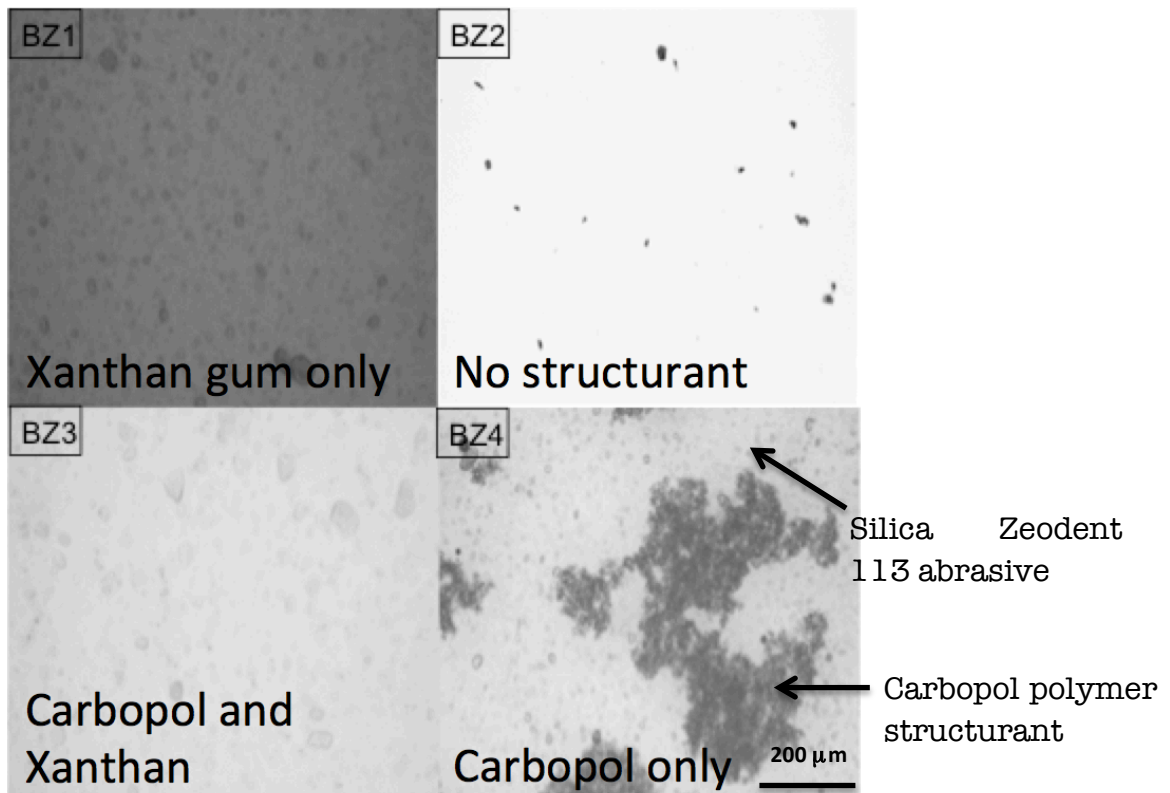
**Figure 135: Schematic of slide set-up to image fluid paste**

Each paste was then imaged from above optically, in transmission mode. All images below are taken at x10 magnification.



**Figure 136: Optical image of silica Zeodent 113 abrasives diluted in water**

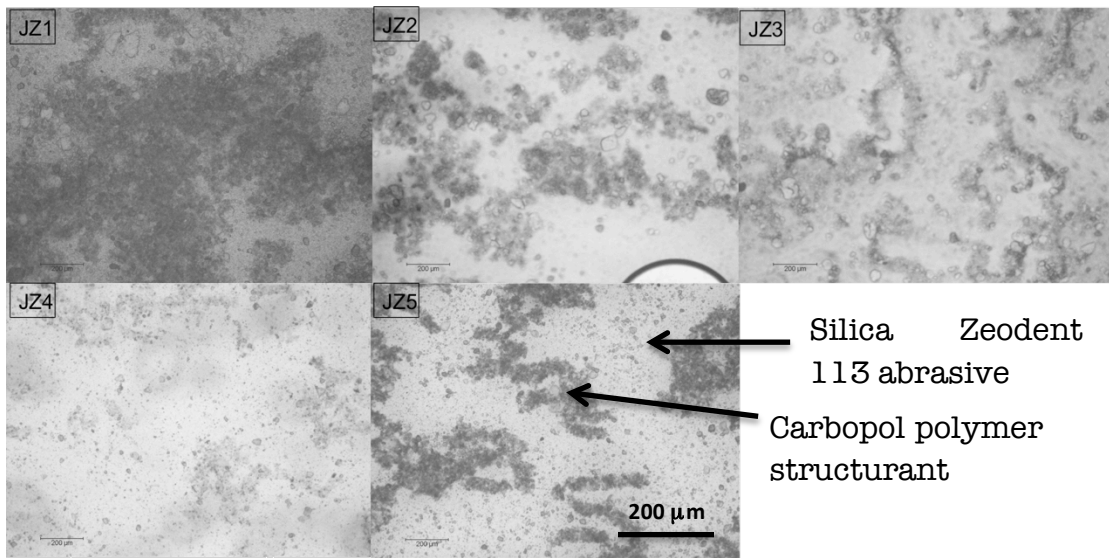
Figure 136 shows an image of 10%wt silica Zeodent 113 abrasive in just distilled water. Zeodent particles can be seen as small dark shapes. A distribution of particle clusters are visible with each particle being smaller than 10  $\mu$ m. This was used as a comparative to analyse the rest of the pastes.



**Figure 137: Optical Image grid of BZ1-4**

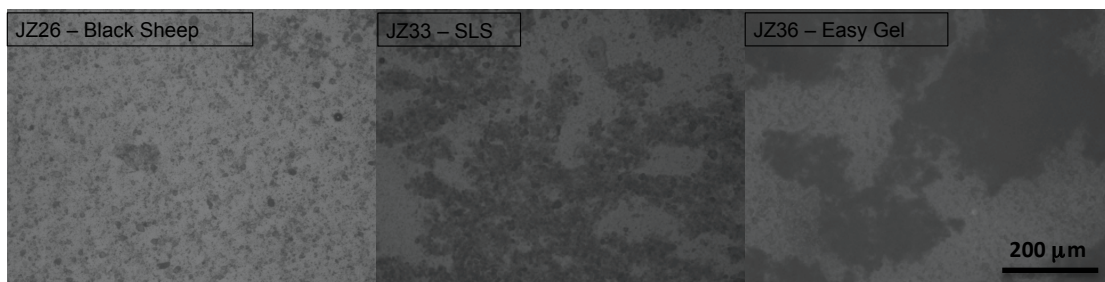
Formulation BZ2 does not contain Carbopol or Xanthan structurants and looks visually similar to what is seen in Figure 136. BZ1 has only Xanthan gum as its main structurant, though does not look dissimilar to BZ2, except from the addition of slightly larger dark spots that are small particle clusters. BZ4 is the most visually different of all four pastes in Figure 137. The additional dark spots seen in clusters are hydrated Carbopol 2984 added to the mixture. This added polymer expands when hydrated taking up space within the solution and therefore the areas where abrasives are found shall be more concentrated. The same is not seen with BZ3 though Carbopol is an ingredient. It is believed either the Xanthan gum, that is also contained within the paste, inhibits the Carbopol hydrating and therefore swelling and taking up space, as seen with BZ4 or the addition of Xanthan may soften the Carbopol further, changing rheology of the mixture.

Figure 138 shows similar optical images for JZ1-5 microstructures.



**Figure 138: Optical images of JZ1-**

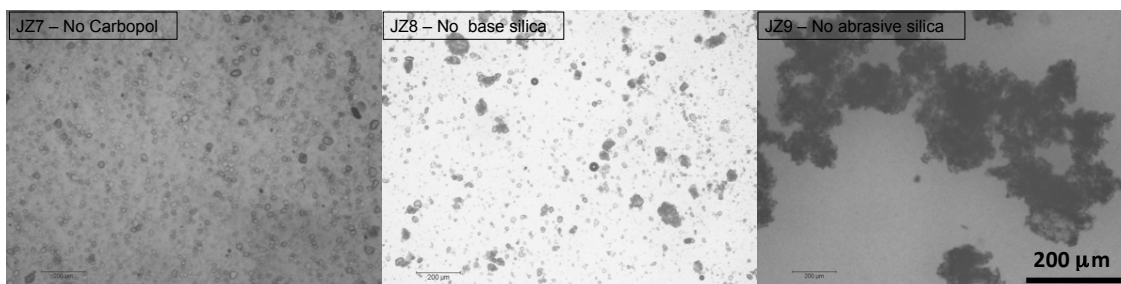
Each paste from JZ1-5 contained a Carbopol polymer binder variant. JZ1, JZ2 and JZ5 each contain Carbopol 2984 all added in the same concentration just at differing stages of the method. This clearly has an effect on the hydration of the Carbopol. Adding early or later at a higher shear (JZ2 and JZ5 respectively) decreases hydration seen, filling up less space over the slide. JZ3 - made with Ultrez 20 Carbopol - exhibits some hydration but the polymers seem to only fill up small thin zones along the slide. JZ4 uses Ultrez 21, which does not exhibit the same swelling as the others. The Carbopol can be seen in light grey patches across the slide but not in clear defined areas as seen with JZ1-3 and JZ5.



**Figure 139: Optical images of JZ26, JZ33 and JZ36**

Each of the pastes seen in Figure 139 are made with Unilever own polymers. Using Black Sheep (JZ26) the paste shows no polymer traces and shows no trace of particle binding at all and looks very similar to BZ1, where Xantham gum was used as the main structurant. JZ33 (SLS Empicol and Carbomer2984 polymer) shows grainy agglomerations are formed, shown in the optical image with large dark areas filling up the

slide. Easy Gel polymer paste (JZ36) also has large distinct areas in the optical microscope indicating it could perform similarly to commonly commercially used Carbopol 2984, as seen in JZ1.



**Figure 140: Optical images of JZ7-9**

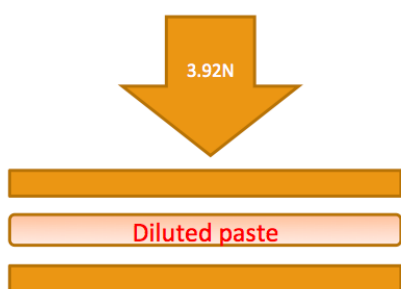
JZ27 has no Carbopol structurant within the solution and look similar to Figure 136, which is as expected. JZ8 has no base silica structurant and looks again similar to Figure 136 with the present of abrasive silica clearly seen. JZ9 has no abrasive silica and clear spaces can be seen in between the Carbopol dark spots.

### **8.3.2. SEM Imaging of Brushed Pastes**

Each paste was diluted 2:1 in water, the typical dilution of toothpastes in research to mimic conditions within the mouth.

This solution was brushed with the linear reciprocating toothbrush rig for 3 minutes under a force of 3.92N onto a Perspex substrate.

A second set of particles were diluted and crushed with a force of 3.92N between two Perspex plates.

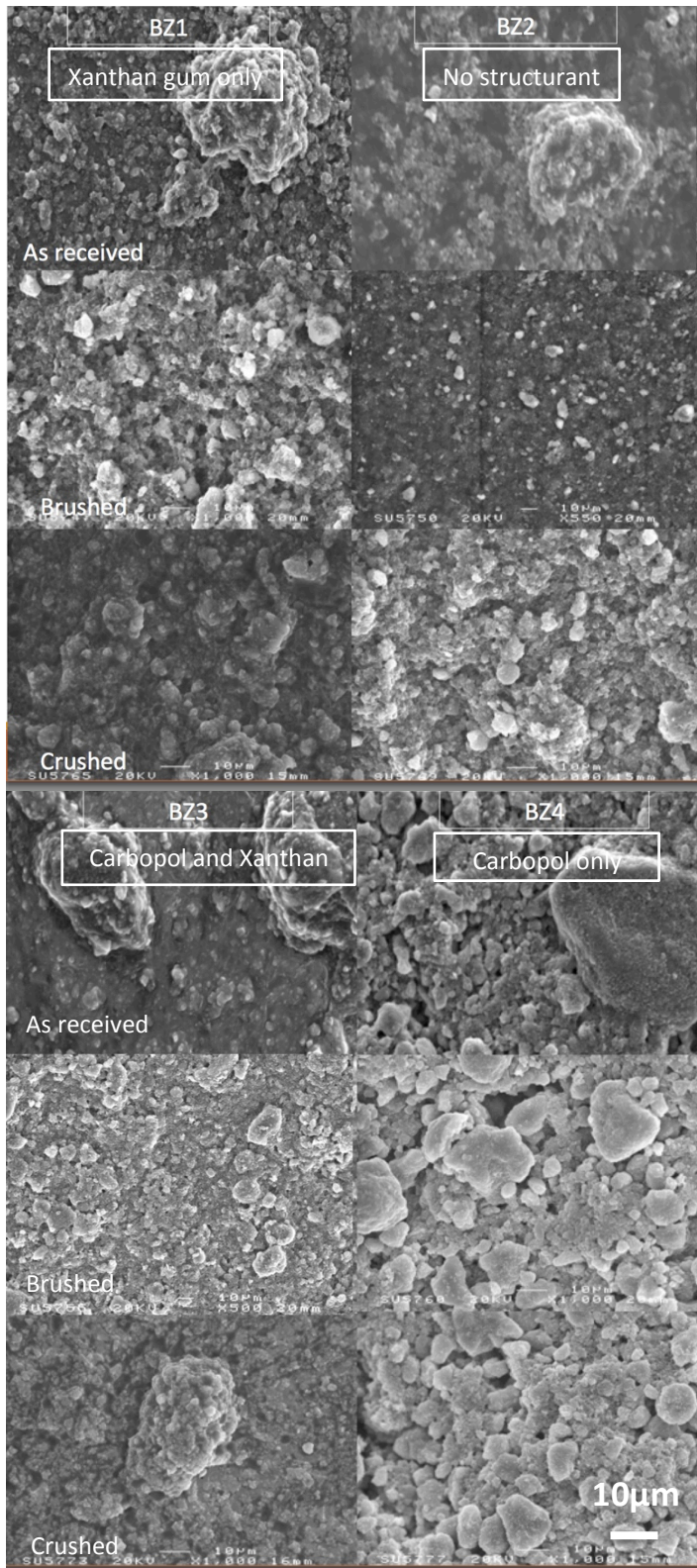


**Figure 141: Schematic of crushing particles method**

The resultant solutions were then pipetted onto a carbon stub, left to air dry, gold coated and imaged with SEM. The average particle size was also characterised using laser diffraction.

Figure 142 shows the resultant SEM images of particles from trials conducted with BZ1-4.





**Figure 142: SEM images of BZ1-4.**

BZ1 has Xanthan gum acting as its main structurant. Due to this it is essentially a suspension of particles in a thin paste. Particles are loosely clumped together. There is little difference in composition between the brushed and crushed particles. The removal of this gum structurant does

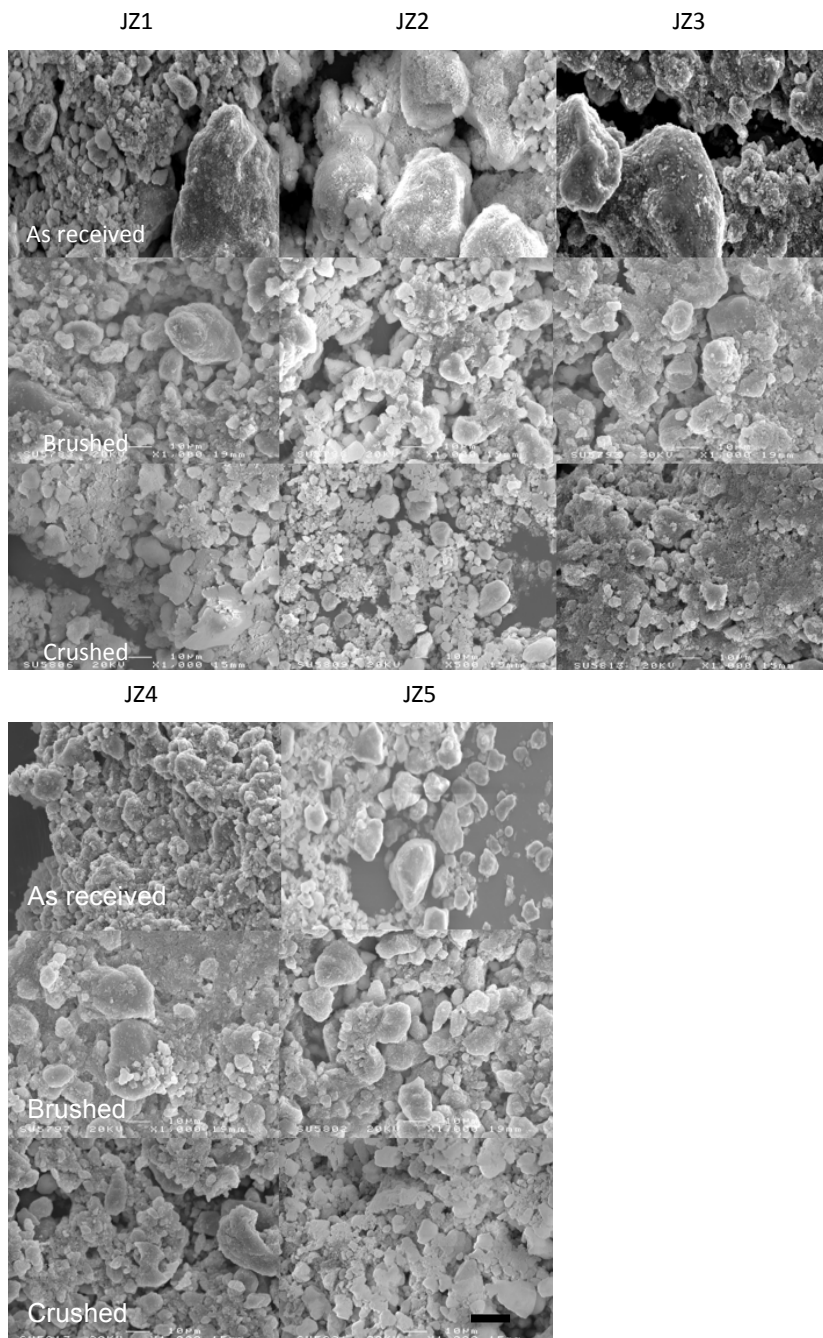


not make for much difference in the particle scatter, for any scenario, as can be seen with the imaging of for BZ2.

The Carbopol paste begins to bind the abrasive silica together, Figure 142 shows a higher degree of agglomeration for BZ3 pastes than BZ 1 or 2 as received. Though these agglomerations look less smooth, most likely to the effect of the added Xanthan gum. These agglomerations can also be seen, though smaller, after crushing.

BZ4 contains only Carbopol as its surfactant (there is no Xanthan gum). BZ4 shows much larger agglomerations than any of the previous pastes. There are discrete and clear agglomerates that are well bound together – looking more like dried and cracked held-together pastes than loosely held pastes, as seen in BZ1-3. Even after brushing and crushing trials the agglomerations are comparatively large, though there does seem to be a larger agglomerate breakdown when the paste is crushed (explained further in Table 14).

Figure 143 shows the SEM grid pre and post trials using JZ1-5.



**Figure 143: SEM images of JZ1-5**

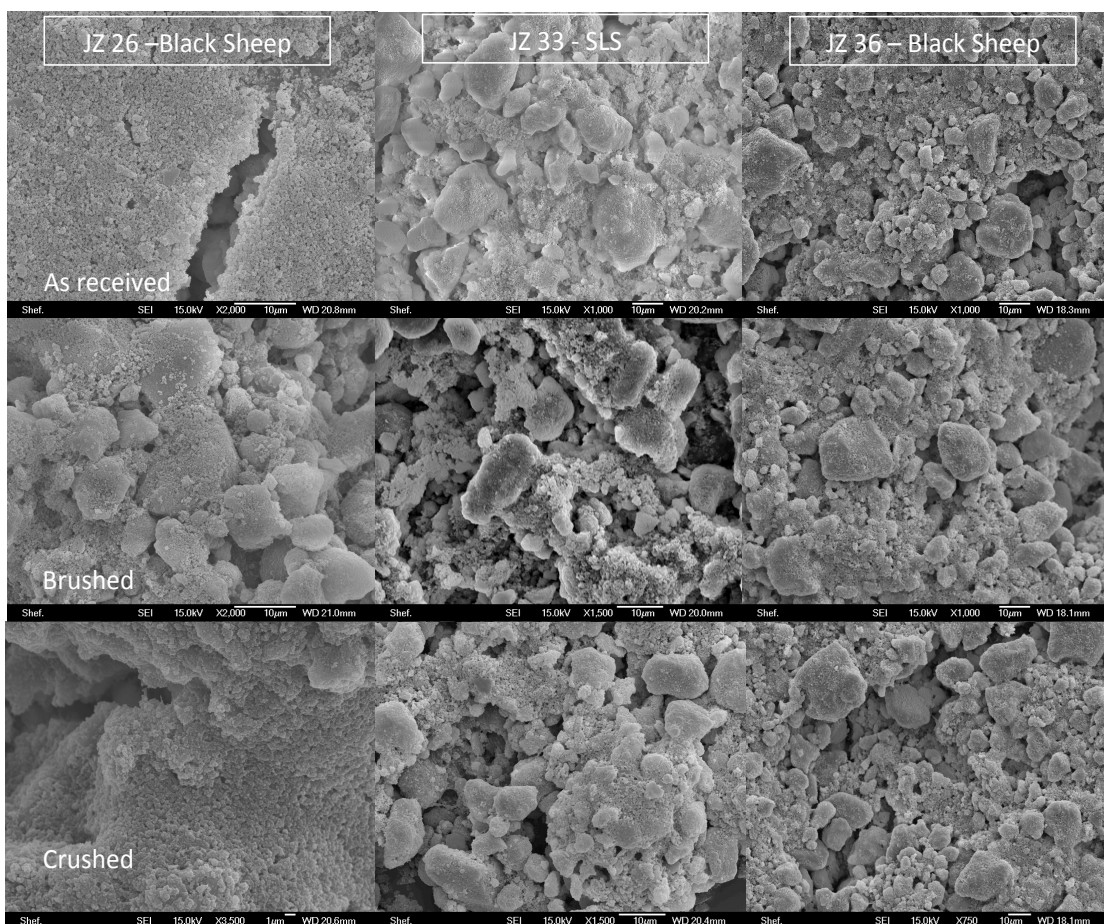
JZ1 is the same paste as BZ4, seen in Figure 142 the only difference being the technician in charge of manufacture. No difference can be seen from the BZ4 trials. Agglomerations are still clear and held together well after brushing and crushing.

JZ2 is the same paste as JZ1 but the Carbopol was added earlier in the methodology. Particle agglomerations with JZ2 seem larger in size than seen with JZ1 but appear more grainy when held together, though they seem to hold together well under brushing.

JZ3 was made with Carbopol Ultrez 20 polymer. This polymer does not appear to hold together agglomerations well under both brushing and crushing trials, where large volumes of individual particles and smaller crushed agglomerations were seen. As received agglomerations were still relatively large in size (around 10 microns).

JZ4 was made with Carbopol Ultez 21 polymer. In general the microstructure of this paste was visually close to JZ3, with fewer clumps seen after both brushing and crushing.

JZ5 contains the same constituents as JZ1 except the Carbopol 2984 was added at high shear. Agglomerations seen with this paste have more broken off edges, though they are of similar size to that seen with JZ3 and JZ4 (shown further in Table 14).



**Figure 144: SEM images of trials with JZ26, JZ33 and JZ 36**

JZ26, JZ33 and JZ36 were made using undisclosed Unilever manufactured polymers.

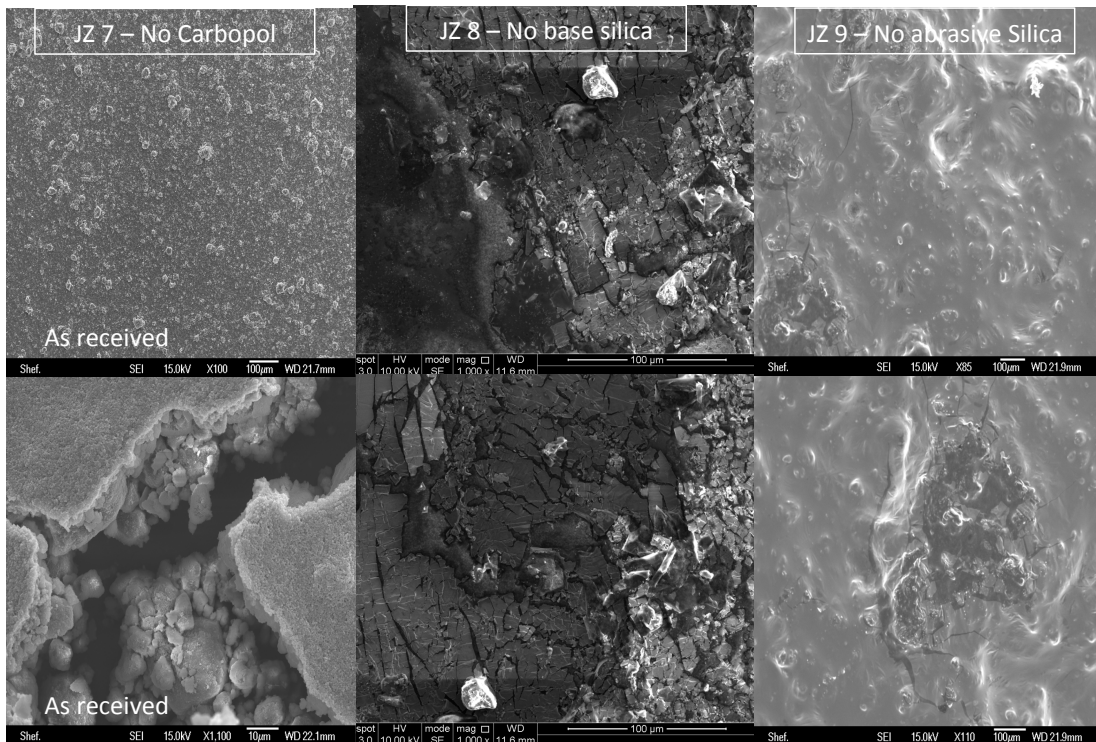
JZ26 appears to be a significantly weak binder, showing no major agglomerations as received. Brushing and crushing this paste does



appear to cause particle clumping together, most likely due to the movement at slight shear from the trials.

JZ33 contains grainy agglomerations. Agglomerations as received look fairly large, but when sized in laser diffraction (results in Table 14) are slightly smaller (though still larger than JZ26), this indicates these agglomerations are loosely held together and break apart easily.

JZ36, made with Unilever manufactured 'Easy Gel', shows distinct larger and clearer agglomerations during all phases. Sizing data reflects this.



**Figure 145: SEM images of JZ7-9. No processing.**

JZ7 is a remake of BZ2 with no Xanthan or Carbopol structurants. Results are very similar. A few agglomerative chunks can be seen but essentially all particles are loose and not strongly agglomerated.

JZ8 contains no base silica Zeodent 165 structurant, and proves the images shown above in Figure 142-146 are that of the abrasive silica and not other ingredients present in all the pastes. Very little is seen overall other than cracking of dried paste on the carbon tab.

JZ9 was also imaged for the same reasons, this paste contains silica Zeodent 165 structurant but no abrasive silica. This shows no particles are present and very little overall to image, again showing all SEM micrographs above are that of the abrasive silica in the pastes.

### 8.3.3. Particle Sizing

Table 14 shows the summary of particle agglomeration sizing done for the trials shown in SEM evaluation. The sizes quoted below are averages over 50 particles and checked with laser diffraction.

**Table 14: Summary of particle sizing, average over 50 particles.**

Formulation name	As received ( $\mu\text{m}$ )	Brushed ( $\mu\text{m}$ )	Crushed ( $\mu\text{m}$ )
BZ1	3.6	2.5	2.6
BZ2	3.0	3.0	2.8
BZ3	5.2	3.1	3.6
BZ4	15.0	12.6	10.7
JZ1	13.7	10.5	12.3
JZ2	16.0	14.6	12.0
JZ3	10.2	7.6	5.4
JZ4	10.2	7.5	5.0
JZ5	10.0	10.0	7.0
JZ26 - Black Sheep	5.5	5.2	4.9
JZ33 – SLS Empicol	6.0	5.9	3.4
JZ36 - Easy Gel	8.2	8.3	7.8
JZ7	3.2	3.2	2.4

From this table and the SEM evaluation it can be seen a lack of Carbopol seems to leave the particles loose and able to act individually. Whereas agglomerations formed with Carbopol binder/structurant forms strong ‘chunks’ of particles that are bound together.

The overall strength and composition of these ‘chunks’ varies with changing both the type of Carbopol used and the method in which they are added to the toothpaste mixture.

Pastes made with Carbopol 2984 showed overall the largest agglomerations (at an average agglomeration size of 16µm as received, breaking down to 12µm when crushed). Commercially available Carbopol Ultrez 20 and Carbopol Ultrez 21 both showed agglomerations of 10 µm in diameter, however these agglomerations broke down when crushed to around half their original size. Unilever made Black Sheep, SLS Empicol and Easy Gel did not create many agglomerations as large as those found with any commercial paste. The Black Sheep polymer did not seem to form any clumping or agglomeration, showing sizing results similar to that of a paste containing traditional Xanthan gum, however it did show a high resistance to particle breakdown thereafter. SLS Empicol gel generates similar sized but stronger agglomerations. Easy Gel had the largest and strongest agglomerations overall from the Unilever made polymers, having agglomerations of around 8µm at each scenario (Figure 144).

Even slight variations in the Carbomer polymer used, like that seen between JZ1 and JZ3, in Figure 158, where agglomerations for JZ3 are more grainy and less compact than those seen with JZ1, have a significant effect on overall breakdown and consequently the effective abrasivity of the product. This was tested further with abrasive testing.

#### 8.3.4. Perspex Scratch Testing

Initial testing was done on perspex with a standard Unilever toothbrush for 3 minutes. Each paste was diluted 2 to 1 with distilled water.

Optical imaging of the center of the perspex brushed with pastes BZ1-4 can be seen below in Figure 146.

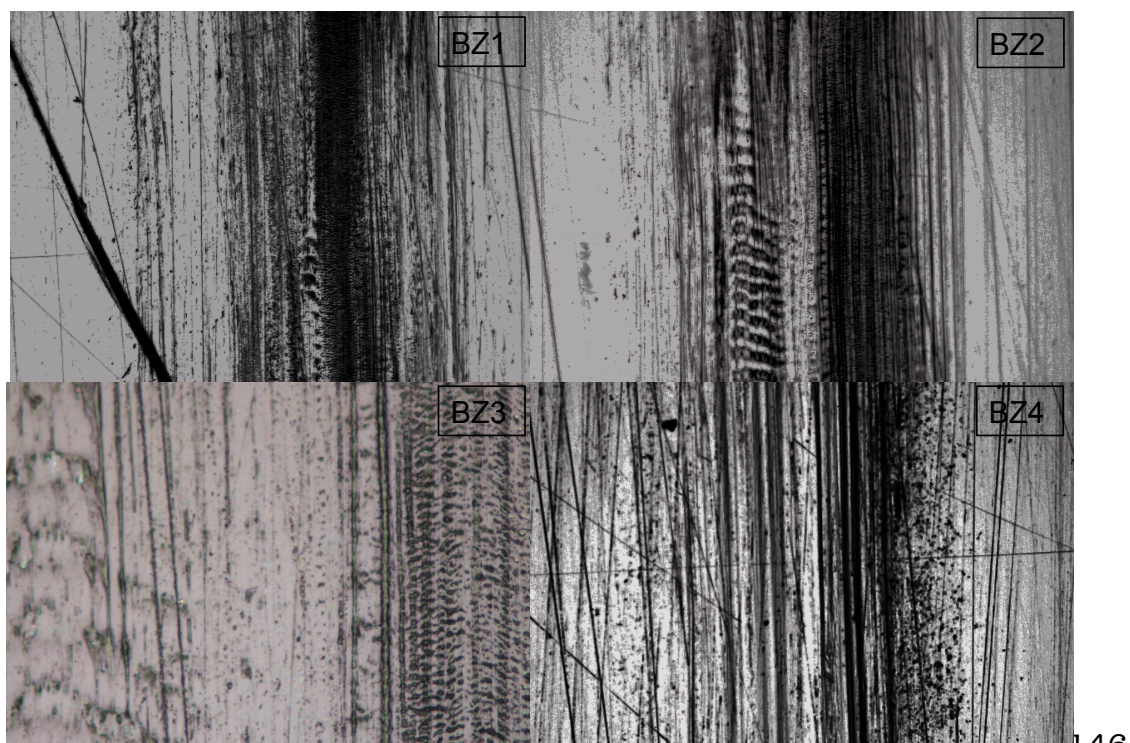


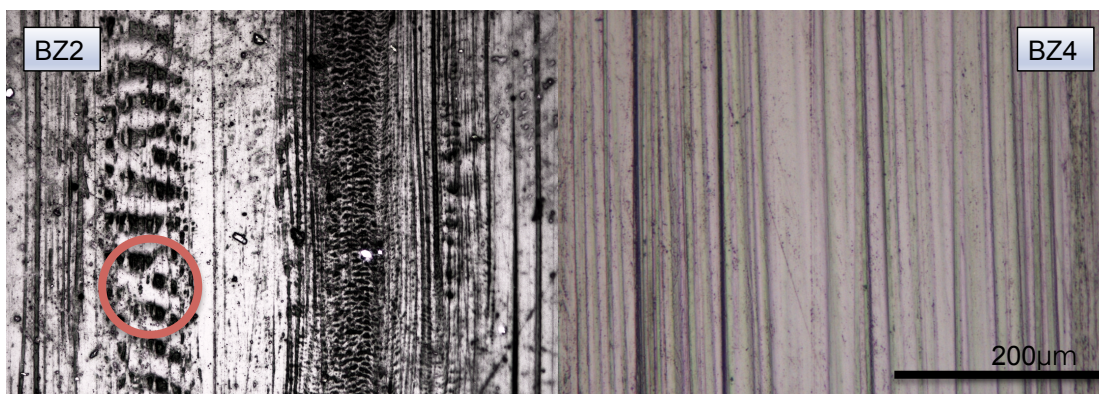
Figure 146: Perspex testing of BZ1-4

100 µm

146



BZ1-3 have similar streaking wear patterns along the direction of the brush unlike BZ4. This can be seen in further detail in Figure 145.



**Figure 147: Comparison of testing with BZ2 and BZ4**

Figure 147 shows the difference in wear patterns exhibited by BZ2 (no structurants) and BZ4 (that has Carbopol 2984 as its main structurant). In BZ4, surface scratches are continuous along the direction of scratch motion. However, it seems agglomerations in mixtures BZ1-3 are encouraged to a roll along the surface causing intermittent markings (circled in red in Figure 147).

AFM analysis of the surface topography of the perspex wear tracks from BZ1-4 showed the following:-

**Table 15: AFM analysis of BZ1-4 perspex scratch tests (n=1)**

	BZ1	BZ2	BZ3	BZ4
Ra (µm)	0.9	0.5	0.7	2
Deepest Groove (µm)	3.6	2.1	3.6	7.1

From Table 15 it can be seen with the addition of Carbopol residual wear surfaces are rougher and the grooves found deeper.

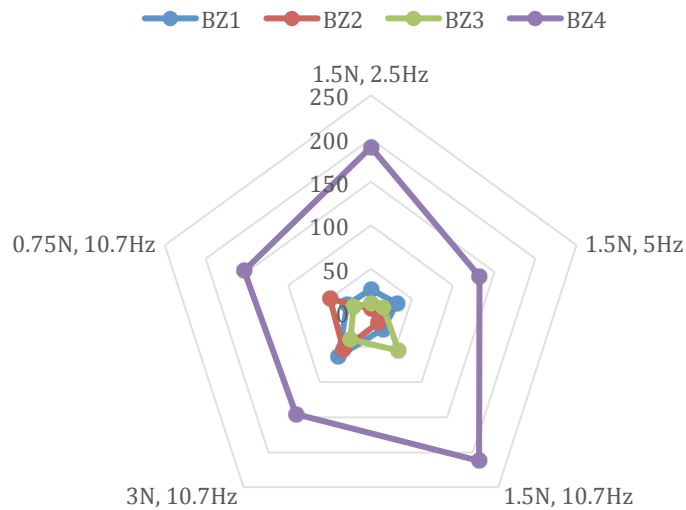
To evaluate their effectiveness in toothpastes, this is further compared to wear depth and surface analysis of worn dentine, with all pastes, in the following section.

### **8.3.5. Dentine Wear Testing**

Initially trials were conducted with only BZ1-4 to determine the effect Carbopol polymers have on the abrasivity of a toothpaste, if any at all.

CETR linear reciprocation trials were carried out using a nylon ball and polished human dentine as the substrate. Each trial was conducted for 15 minutes, with a 6.1mm diameter nylon ball, at a stroke length of 7.5mm. Dentine wear using differing loads (0.75N, 1.5N and 3N) and differing frequencies (2.5Hz, 5Hz and 10.7Hz) were compared.

In Figure 148 the overall maximum wear depths of each trial can be seen.



**Figure 148: Overall dentine wear results of trials conducted with BZ1-4. Average over 3 trials.**

From this experimentation it was observed that the Carbopol 2984 had an increasingly noteworthy effect on the abrasivity of a traditional toothpaste mixture (that only uses Xanthan gum as its structurant – BZ1). BZ4 (where Carbopol 2984 is used as the primary structurant, with no added Xanthan gum) has the overall largest dentine wear regardless of load or frequency.

BZ3 pastes also contained the same volume of Carbopol within the mixture as BZ4. It was seen in Section 8.3.2 - Figure 142 that the Xanthan gum also contained in the paste inhibits the Carbopols hydration and therefore effecting the overall mixtures abrasivity.

To investigate the role of Carbopol further, reciprocating wear trials were then conducted with all pastes outlined in Chapter 8, Section 8.2. Each trial was conducted for 15 minutes under 1.5N at 10.7Hz frequency.

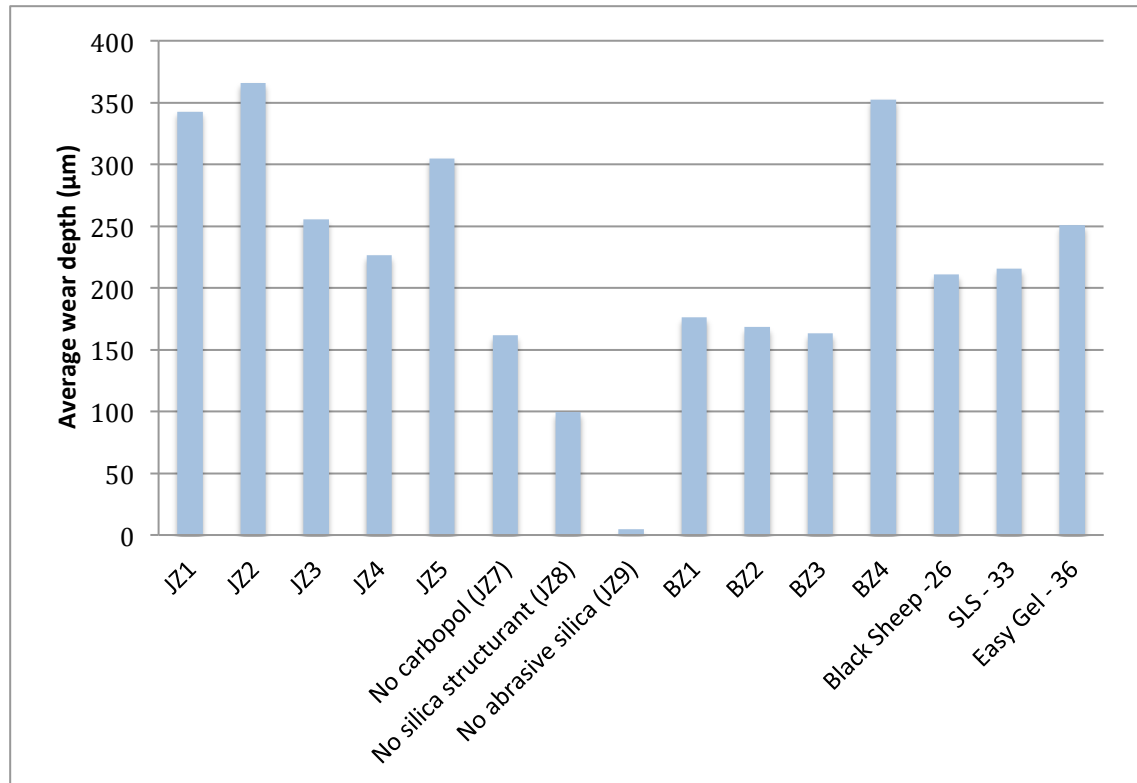


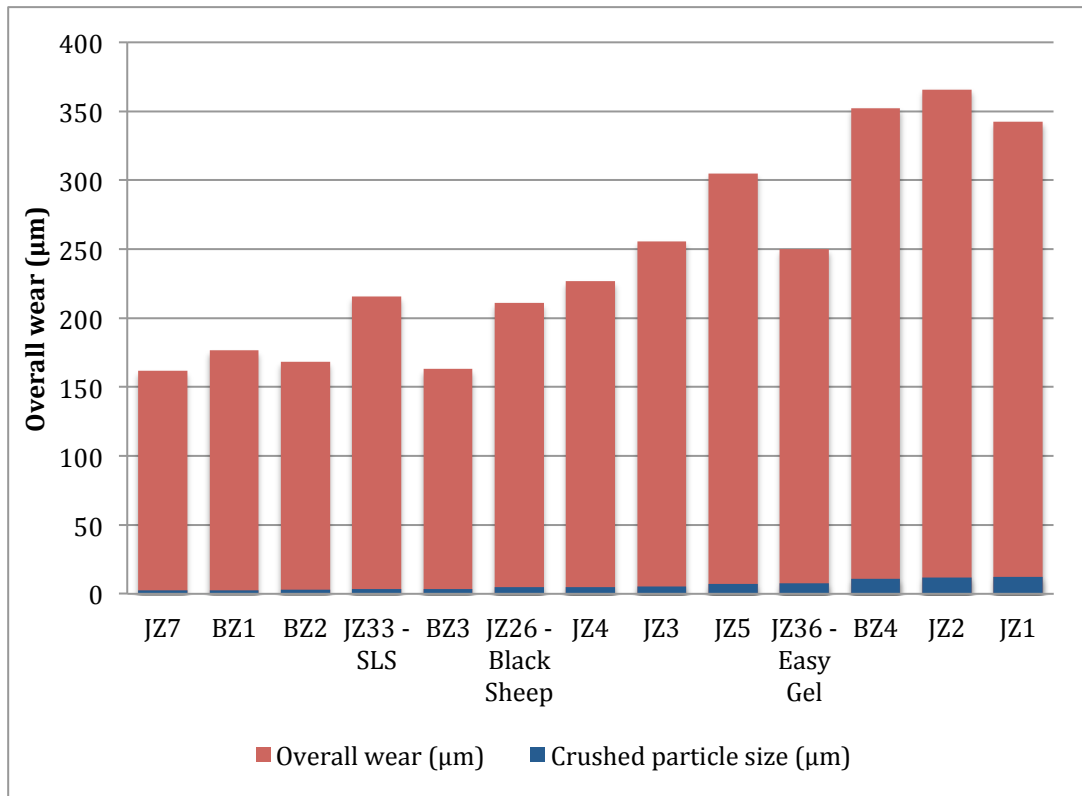
Figure 149: Graph showing average wear test results for abrasive silica based pastes (n=3).

The final depth of the dentine wear scar can be seen below in Figure 149.

Minimal wear was found when paste without abrasive silica was used (JZ9). The small wear track that is observed is most likely from the other constituents within the paste.

Pastes with no Carbopol at all (JZ8, BZ1 and BZ2) produced significantly less wear than similar pastes with Carbopol polymer structurants added into the mixture.

In general the dentine wear caused by pastes with Carbopol polymers in the mixture fits in almost perfectly with what is seen in the agglomeration sizing data from section 8.3.3. The pastes with the largest agglomeration clumps post-brushing and crushing (JZ1 and JZ2 had agglomerations around 12µm post-crushing) produces the most dentine wear. The particles are in order of crushed particle size in Figure 150 and wear rate can clearly be seen to be increasing.



**Figure 150: Overall wear of trials in order of crushed particle size**

Overall pastes with Carbopol 2984 performed best, giving the highest cleaning rate regardless of method of paste manufacture. It can be seen that the traditional methodology (JZ1/BZ4) or adding the Carbopol 2984 early (JZ2) produces the highest overall wear. Adding the Carbopol 2984 later in the manufacture process under shear (JZ5) did affect the wear the paste can produce slightly, and this was seen in the SEM and sizing data where agglomerations were grainy and did not hold together as well as the other Carbopol 2984 pastes under loading.

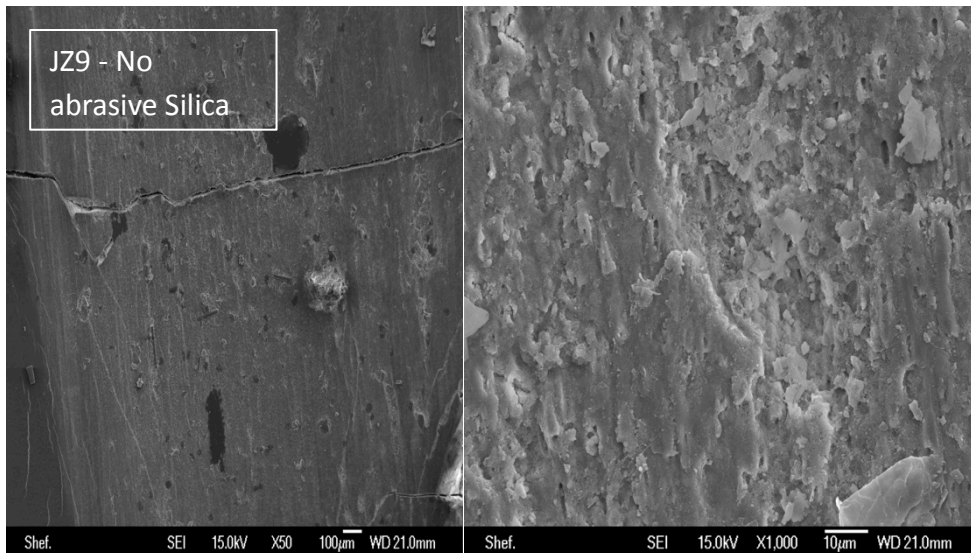
Using Ultrez 20 or Ultrez 21 Carbopol (JZ3 or JZ4) has no advantage over Carbopol 2984 as it does not perform better in wear and is still sourced from an outside commercial company to Unilever Plc.

Unilever polymers (Black Sheep - JZ26 and SLS Empicol - JZ33) performed similarly in wear tests, and though caused more wear than existing formulations without Carbopol they did not out perform any pastes with commercially available Carbopol. From the three Unilever polymers EasyGel caused the highest wear though again was unlike that of any of the obtainable polymers on the market.



### 8.3.6. SEM Analysis of Dentine Wear Tracks

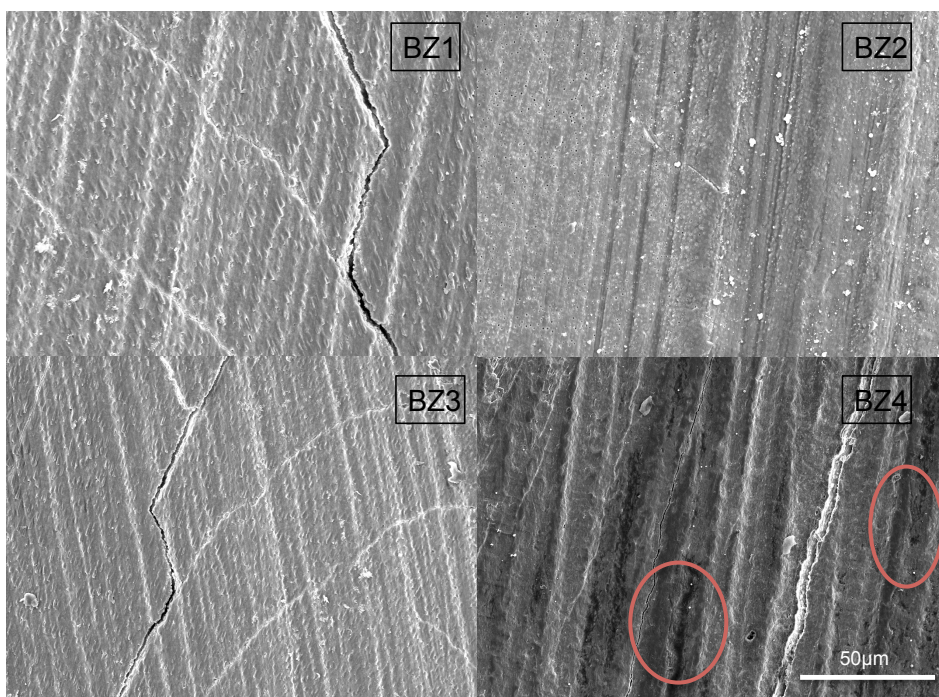
The center of each dentine wear scar was imaged with SEM. Figure 151 shows the resultant wear with no abrasive silica added to the formulation.



**Figure 151: Wear scar produced by JZ9**

Wear without the abrasive Zeodent 113 silica was minimal and the resultant marks left show no wear tracking marks, rather just surface damage to the polished dentine surface from the nylon ball and other constituents of the paste.

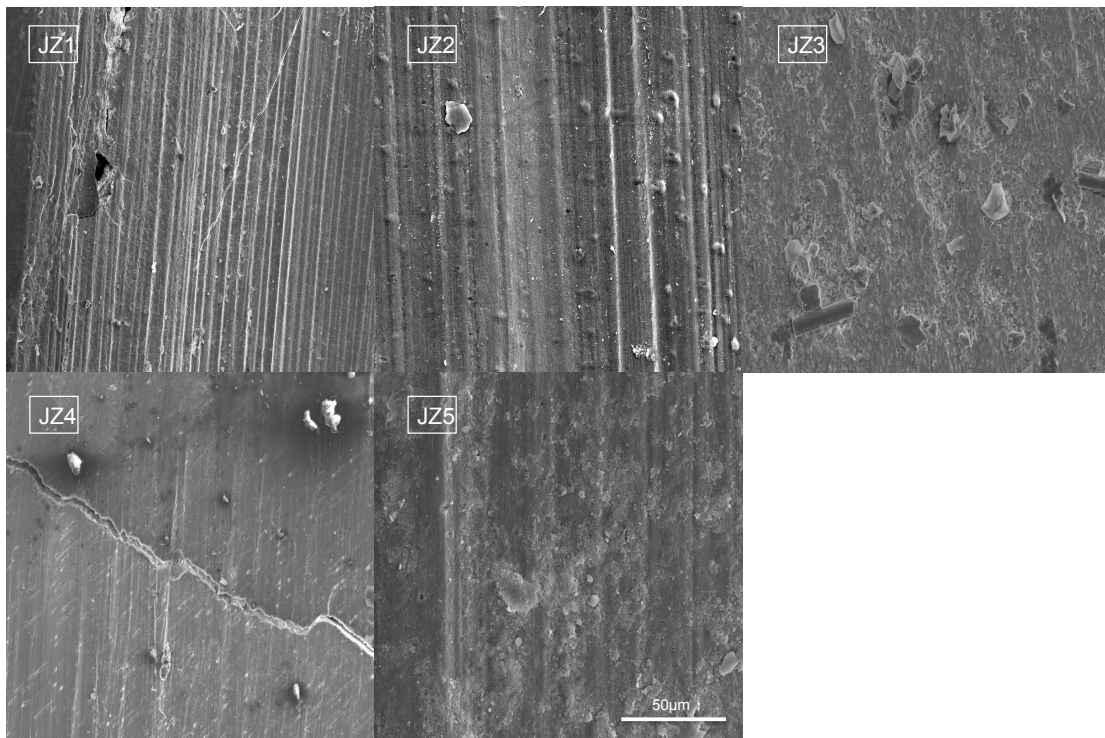
Figure 152 shows the surface morphology of resultant wear scars of trials conducted with BZ1-4.



**Figure 152: SEM images of dentine wear scars produced by BZ1-4**



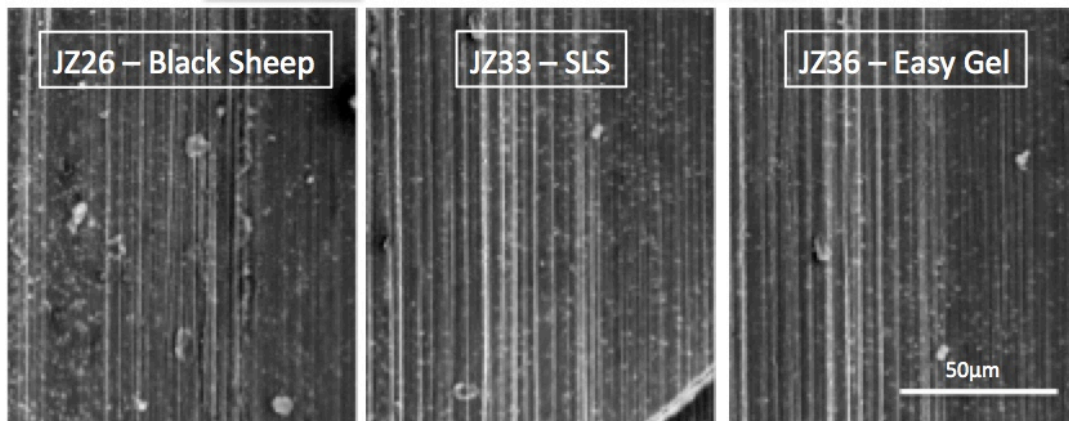
Wear caused by formulas BZ1-3 have less distinct wear tracks than those produced by BZ4 which have increased macroscopic damage in the form of pitted surface markings (circled in red), potentially the result of projections of rolling masses of particles. Contrastingly in trials with BZ4, which has a much higher overall wear depth, the scratches are more striated and controlled suggesting particles aren't encourage to move around individually; rather the Carbopol binder in the mixture keeps them in place and holds agglomerations together, which is supported by earlier SEM data.



**Figure 153: SEM images of wear scars produced by JZ1-4**

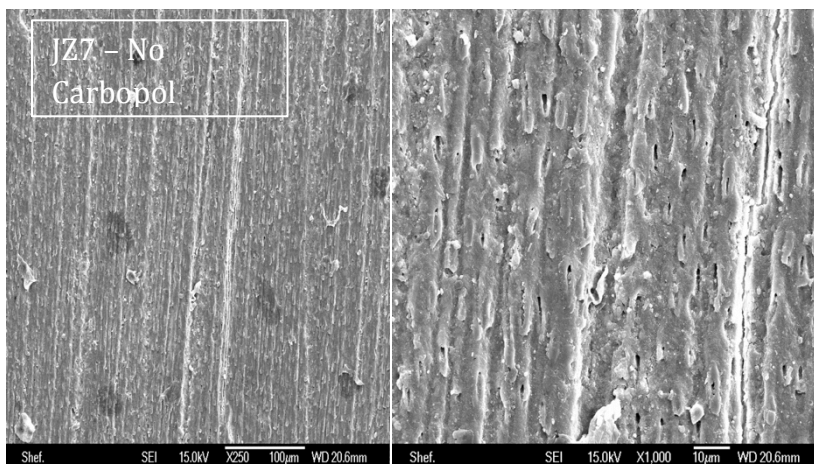
Pastes JZ1 and JZ2 with the highest wear rates, both encourage tracking wear marks on dentine, with JZ1 producing the deepest wear scar overall.

Pastes JZ3 - JZ5 made less distinct wear makings, indicating particles were acting more individually (most likely due to a strong breakdown in agglomerations) than as clear agglomerations that are held in place.



**Figure 154: SEM grid of wear scars produced by JZ26, JZ33 and JZ36**

Wear scratches within wear scars of all three pastes using Unilever in-house made polymers were extremely neat and uniform all the way along the track (Figure 154). Easy Gel (JZ36) produced the widest seen wear scratches within the scar itself, as well having the deepest overall wear depth from all three.

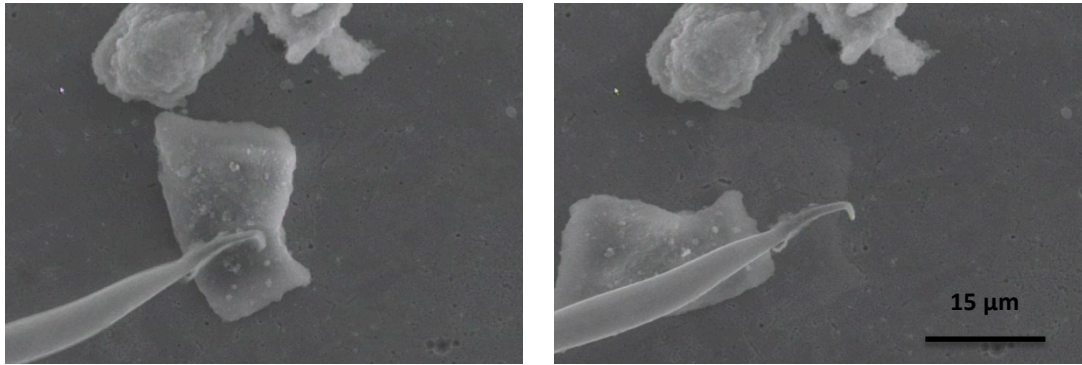


**Figure 155: SEM wear scars produced by JZ7**

Figure 155 shows dentine wear from pastes with no Carbopol structurant within the formulation (JZ7). A lack of polymer within the mixture results in no binder for the particles within the pastes, changing the rheology of the paste itself and allowing the particles to move more freely and gouge and pit into the surface, as can be seen in Figure 155.

### **8.3.7. Nanomanipulation Trials**

Figure 156 shows a screen shot of a nano-manipulation trial conducted on dried JZ4 agglomerations. Small amounts of the JZ4 paste was spread onto silicon substrate and left to dry. Only this paste was tested for the purposes of this thesis.



**Figure 156: Screenshots of nano-manipulation trial of JZ1**

Agglomerations were loaded from above, by pressing with a NiCr tip, to examine agglomeration break up properties. Trials were conducted numerous times, and in each case agglomerates did not break up instead loading would encourage the particles to recoil off the silicon substrate surface.

Trials were then conducted on a thicker dried layer of paste, as seen in the SEM images of Section 10.3.2. the paste underneath would provide a softer surface on which to load onto the agglomeration to prevent bouncing off the harder substrate surface, as seen with previous trials.



**Figure 157: Probing into JZ4 paste**

Loading onto a dried paste layer showed the flexibility of the paste. Loading into the agglomerations causes a clean break. The agglomerates do not break off into individual particles readily, rather the Carbopol binds the particles together well enough to keep them intact into to separate agglomerations even after loading, showing evidence they will entrain well into toothbrush bristle as agglomerates rather than break apart when subject to loading from the bushing process.



## **8.4. Discussion**

Carbopol is currently used as a binder in various commercially available toothpastes. Research in this thesis was done on varying this binder in pastes containing Silica Zeodent 113 as an abrasive, to aid in the research and development of Zendium toothpaste.

The effect of changing polymer binders on abrasivity investigated within this chapter differs from conventional methodologies, which are primarily a study of the stability rheology changes of the overall paste and its overall sedimentation change. This work primarily focuses on the imaging of the interactions of the abrasive particles themselves and its agglomerates and linking the observed particle behavior to abrasive performance.

Each paste made within this study has been deemed of a suitable rheology, viscosity and thickness to be commercially used as toothpaste in a traditional squeezable tube. They have also been tested to be of a suitable RDA (between 60-100 dependent on paste used, a full table of which can be seen in Appendix D).

### **8.4.1. Discussion of Imaging and Microstructure**

Mixtures containing any polymer-based structurant/binder invariably showed dark clusters of areas where the polymer in the paste gathered. Film thickness underneath the microscopic slides based on a 1.8 x 1.8 cm coverslip with 10 $\mu$ l of fluid was determined as an approximate film thickness of around 30 microns. This is larger than any of the constituents of the paste - the largest of which being 15 $\mu$ m diameter agglomerations of individual abrasives silica particles. This means optical images taken within this Chapter have the possibility of imaging overlapping of particles/polymers within the film between the microscopic slides.

BZ1, BZ2 and JZ7 and JZ8 contained no Carbopol or Unilever own polymer within the mixture. Optically imaging, these showed a clear lack of the dark cloudy patches seen on all other pastes when imaged; giving evidence for this being the polymer taking up space within the fluid.

JZ9 had no abrasive silica within the mixture but Carbopol 2984 was included. Carbopol 2984 can clearly be seen as dark spots with the rest of the slide remaining clear (Figure 140); giving evidence that the abrasive silica, Zeodent 113, are the more separated and smaller darker spots around the slide in other pastes.

### **8.4.2. Discussion of Composition and Processing**

BZ1 is a copy of Unilever current brand Prodent that uses a silica abrasive Zeodent 113 in a Xanthan based paste. BZ4/JZ1 were copies of formulations found in Zendium and Gleem toothpastes (currently found on market) and are of a similar make-up in ingredients to other brands, including Oral B and Crest. Testing on this paste is used as a 'base' result on what is necessary to achieve for a good marketable paste and how other formulations compare.

JZ2 and JZ5 have the same formulations as JZ1 but were manufactured with slightly different methodologies. In paste JZ2 the Carbopol was added early with all other ingredients in the mixture. This caused a slight increase in wear and cleaning along with an increase in RDA (to 100.8), rendering it unsuitable for gentle whitening. The method in which Carbopol was added to JZ5 meant additional shear for the polymer paste. This additional shear thins the polymer. This additional shear changes the viscosity and rheology of the end product causing a decrease in overall wear the product causes. This decrease in wear makes paste JZ5 less effective in cleaning and whitening than JZ1, so the method of which JZ1 was manufactured was deemed the most effectual.

### **8.4.3. Discussion on Key Wear and Link to Microstructure**

JZ3 and JZ4 were manufactured in the same way as JZ1 but with different commercially available polymers, Carbopol Ultrez 20 and Carbopol Ultrez 21. Both exhibited a decrease in wear for testing in this thesis whilst not having a significantly lower RDA to give it any advantage for Unilever to pursue with any further testing. JZ26 (Black Sheep), JZ33 (SLS Empicol) and JZ36 (Easy Gel) were all produced with Unilever made polymers. These pastes have the added advantages of being patentable, unique to Unilever and cheaper to produce in-house. All three pastes have similar RDAs (70-78) with JZ36 giving the most significant wear from all three pastes and in effect giving the most cleaning affects on teeth stains. Though this paste still performs poorer than commercially available JZ1 so will not be used in future products, rather further resources will be used to better polymer mixtures now a main sustainable method has been adopted (that of JZ1).

Pastes with no abrasive silica involved caused minimal wear, as expected.

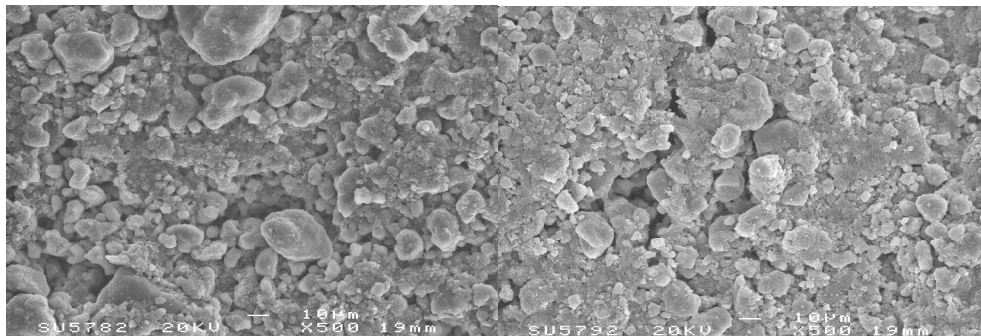


## 8.5. Conclusions

Experiments were undertaken to analyse and understand the effect of different polymer structurants as effective binders for silica based abrasive toothpastes.

There is a clear difference between pastes that contain polymer structurants and Carbopol polymers and those without. Pastes with only traditional Xanthan gum as its main structurant did not perform as well as those with only polymer binders in the mixture. The addition of both Carbopol 2984 and Xanthan gum inhibited the performance and effect of the Carbopol polymer on the abrasivity of the paste. Pastes with polymer Carbopol binders added affected the rheology of the end paste. The shear-thinning properties of the Carbopol 2984 allowed more neat and discrete scratches on brushing scratch trials done on Perspex substrates.

Overall the efficacy of abrasion of the pastes was directly related to the agglomeration sizes of silica abrasives found after brushing, crushing or mechanical shear of the paste. The larger the end agglomerates or the better they resisted breakdown the more the paste would wear into a polished dentine surface on linear wear testing. From this it was seen pastes JZ1 or BZ4 had the largest agglomerates (both as received and after brushing and crushing) so produced the most dentine wear in testing, which relates to the greatest cleaning efficacy for the paste.



**Figure 158: Typical agglomerations for JZ1 (left) and JZ3 (right)**

In general, pastes with Carbopol in them contained shear-thinning properties, resulting in more neat discrete scratches. Carbopol was also found to encourage agglomerates within the paste due to its hydration properties. Optical imaging showed Carbopol caused phase separation with regions of abrasive-only areas in the paste, resulting in increased wear on polished dentine surfaces.

Again, pastes with no abrasive silica and just binder caused minimal wear.

## CHAPTER 9

### Conclusions

The aim of this project was to fully characterise, understand and observe the wear behaviour of oral care formulations containing abrasive particles of interest to Unilever Plc, in order to develop the next generation of their toothpaste range. Geometric properties of the particles were analysed and this related to how the particles scratched dental and testing substrates. In-depth individual chapter conclusions can be seen within the thesis text. The following points were found to be the main concluding points of this work:-

- The calcium carbonate particles within this thesis were between 0.7-7.85 micron in modal size.
- Initial linear wear testing showed that size was not the only determining factor in a particles ability to abrade the substrate surface. It was found smaller particles (such as Sturcal F at 1.60  $\mu\text{m}$ ) can be as abrasive to dentine as larger particles (such as Omya 5AV at 7.85  $\mu\text{m}$ ). Instead it was seen that factors such as geometry, angularity and agglomerative properties more important.
- In-situ visualisation of the dynamic motion of the six calcium carbonate particles found particles with an affinity to roll rather than slide the more abrasive to the substrate surface, demonstrating high scratch frequency and scratch depths in wear testing.
- Rod particles had the highest tendency to slide due to its flat facets. Omya 5AV, the standard GCC currently used in Signal toothpaste, was the most abrasive to dentine due to its angular and random nature, favouring only a rolling mechanism.
- This evaluation of the movement of the particles both individually and in agglomerations highlights the importance of multiple particle properties, rather than the original assumption that only an increase in size would lead to an increase in wear or cleaning.
- Chapter 7 highlights how the addition of citrus fibres in available toothpaste formulations can easily modify the cleaning efficacy. It was found that particles larger than 6  $\mu\text{m}$  are entrained by the investigated citrus fibres, increasing their overall dentinal abrasivity.
- Surfaces worn by mixtures that contained citrus fibres and particles larger than 6  $\mu\text{m}$  were less rough than surfaces worn by the same paste without fibres. This end polishing effect than is highly desirable and marketable in oral care, due to the pleasing aesthetic results.
- Nano-manipulation trials found particles did not adhere to the citrus fibre surface. Rather, the fibres would sweep particles across the

substrate when motivated (by nylon brush bristles). Causing particles to sweep across the surface, rather than be individually entrained by brush bristles. It is this change in entrainment that leads to the smooth end result in wear caused by pastes including the citrus fibres.

- Citrus fibres are a waste product in the food industry and currently used as a thickening agent in certain food products and therefore are easily obtainable to Unilever Plc at low cost. The addition of these fibres in toothpaste can reduce the need for high concentrations of abrasive particles in oral care products and therefore reduce the cost of adding more costly PCCs to existing pastes.
- Clear differences were seen between pastes that contained Carbopol as a binder, when compared to other pastes. Pastes with only Xanthan gum used as a binder did not perform as well in abrasive testing as those that contained Carbopol polymer in them.
- Overall pastes with Carbopol in them contained shear-thinning properties, resulting in more neat discrete scratches. Carbopol was also found to encourage agglomerates within the paste due to its hydration properties. Optical imaging showed Carbopol caused phase separation with regions of abrasive-only areas in the paste, resulting in increased wear on polished dentine surfaces.
- It was also found that Carbopol 2984 (that used in the Zendium paste) was the most effective binder. It was found that the paste which produced the most wear, and therefore the most aggressive whitening, was that already used to produce Zendium toothpaste.

### **9.1. Industrial Applications and Future Recommendations**

Currently Unilever Plc. are actively pursuing development of, or continuing research into, the following:

- Rod PCC particles shall be added to commercial Signal toothpaste in late 2016. Rod particles have been found to be a gentle whitening calcium carbonate when used in conjunction with Omya 5AV (that is already in Signal toothpaste).
- In addition to this a patent has been filed on the tubule blocking properties and dental hypersensitivity findings of Rod particles. Rods have been found to be effective in infiltrating and remaining within exposed dentine tubules lumens, properties that Omya 5AV does not possess. The primary mechanism of this seems to be due to the gentle nature and easy fracture of Rod particles. Fractured tip particles seem to occlude tubules and remain in location effectively [2].
- Citrus fibres are still used as a thickening agent but no further testing is currently planned to use it as an aid in oral care.

- Carbomer2984 is still used in Zeodent and Gleem toothpaste. Further research is going into this and other silica based pastes for the next generation of whitening toothpastes within the Unilever range.

The following suggestions for future research and recommendations for future products are based on the results found within this project:

- PCC have a clear advantage over currently used GCCs. PCCs offer more constrained and uniform geometries of particles, making abrasive properties easier to control. PCC also have pre-determined shape and therefore can be made to be less likely to roll.
- To optimise the PCC used, a revision of currently available micro-calcium carbonate particles would be necessary (and probable with changes in pressure and temperature during the manufacturing process). An ideal abrasive particle, from the work in this thesis, would be flat on both the upper and lower face, like that of the Rod particle to encourage sliding and contact with the substrate surface. Increasing the width of the particle would lower the aspect ratio of the particle giving the particles more strength and making them more resistant to fracture. A resistance to breakdown would increase the cleaning life of a single particle, leading to a reduction in the concentration of particles needed in the toothpaste. Limiting the fracture would also limit the number of tip particles broken off during brushing. The angular tip particles were most likely to roll during testing and caused higher surface pitting and damage. With this in mind it would also help to decrease the tapering tips, another outcome of increasing the width of the particle. However, though these changes would lead to a better oral abrasive it would counteract the dentinal tubule blocking properties found in Rod particles that are increasingly beneficial to Unilever, for both marketing unique selling point purposes and forming a multi-functional oral cleaning paste.
- Further testing into citrus fibres and its beneficial side effects within abrasive cleaning would be highly recommended. In not only in oral care, but also in how this small change in formulation would affect household cleaning products, where a high polishing effect is high priority (for surface and counter cleaning). This work has demonstrated this for applications with a toothbrush but further testing would be needed with cloth and scouring pads.
- Research into different rheologies of binders for silica-based toothpastes is ongoing within Unilever. This research will likely lead to the next generation of toothpaste within the Zendium brand.

## References

1. Organisation, W.H. *Oral Health*. 2015 [cited 2015 23/03/2015]; Available from: [http://www.who.int/topics/oral\\_health/en/](http://www.who.int/topics/oral_health/en/).
2. Rose, C., *Investigating the efficacy of novel abrasive particles in oral hygiene.*, in *Department of Mechanical Engineering*. 2015, University of Sheffield.
3. Wilkins, E.M., *Clinical practice of the dental hygienist* Vol. 11. 2012: Lippincott Williams & Wilkins.
4. Darby M L, W.M.M., *Dental Hygiene Theory and Practice*. 2010.
5. Lewis, R.S.C.B., R. S. Dwyer-Joyce, *Particle motion and stain removal during simulated abrasive tooth cleaning*. *Wear*, 2007. **263**(1-6): p. 188-197.
6. Berkovitz, B.K.B., G. R. Holland. B. J. Moxham., *Oral anatomy, histology and embryology*. . 2009: Mosby.
7. Tegethoff, F.J.R., E. Kroker, *Calcium carbonate : from the Cretaceous period into the 21st century*. 2001, Birkhauser: Basel.
8. Joiner, A., *Whitening toothpastes: A review of the literature*. *Journal of Dentistry*, 2010. **38**, **Supplement 2**(0): p. e17-e24.
9. Minerals, S. *A Range of Abrasivities*. 2015 [cited 2015 11th March ]; Available from: <http://www.mineralstech.com/Pages/SMI/Toothpaste.aspx>.
10. J. .L. Knowlton, S.E.M.P., *Handbook of Cosmetic Science & Technology*. 2013: Elsevier.
11. Reynolds, A.P., *Contents of toothpaste - safety implications*. *Australian prescriber* 1994. **17**: p. 49-51.
12. MacDonald, E., A. North, B. Maggio, F. Sufi, S. Mason, C. Moore, M. Addy, N.X. West, *Clinical study investigating abrasive effects of three toothpastes and water in an in situ model*. *Journal of Dentistry*, 2010. **38**(6): p. 509-516.
13. Sharif, N., E. MacDonald, J. Hughes, R. G. Newcombe, M. Addy, *The chemical stain removal properties pf 'whitening' toothpaste products: studies in vitro 2000. 188(11)*. *British Dental Journal.*, 200. **188**(11).
14. West, N.X., et al., *In situ randomised trial investigating abrasive effects of two desensitising toothpastes on dentine with acidic challenge prior to brushing*. *Journal of Dentistry*, 2012. **40**(1): p. 77-85.



15. Grabenstetter Rj Fau - Broge, R.W., et al., *The measurement of the abrasion of human teeth by dentifrice abrasives: a test utilizing radioactive teeth.* (0022-0345 (Print)).
16. Dörfer, C.E., *Abrasivity of Dentifrices from a Clinical Perspective.* The Journal of Clinical Dentistry, 2010. **21**: p. Supplement.
17. Itthagaran, A., N. M. King, Y. M. Cheung, *The effect of nano-hydroxyapatite toothpaste on artificial enamel carious lesion progression: an in-vitro pH-cycling study.* Hong Kong dental journal, 2002. **7**(2): p. 61-66.
18. Hefferren, J. and N. Li, *Dentifrice Abrasives: Heroes or Villains? A Peer-Reviewed Publication.* RDH, 2005. **25**(12): p. S3-S9.
19. BIOREPAIR. *Biorepair: the enamel repairer.* 2011; Available from: [http://www.biorepair.co.uk/wp-content/uploads/2009/05/BioRepair\\_Brochure.pdf](http://www.biorepair.co.uk/wp-content/uploads/2009/05/BioRepair_Brochure.pdf).
20. Joiner, A., et al., *A novel optical approach to achieving tooth whitening.* Journal of Dentistry, 2008. **36**, **Supplement 1**(0): p. 8-14.
21. Ashcroft, A.T., et al., *Evaluation of a new silica whitening toothpaste containing blue covarine on the colour of anterior restoration materials in vitro.* Journal of Dentistry, 2008. **36**, **Supplement 1**(0): p. 26-31.
22. Mathenson, J.R., T. F. Cox, N. Baylor, A. Joiner, R. Patil, V. Karad, V. Ketkar, N. S. Bijlani, *Effect of toothpaste with natural calcium carbonate/perlite on extrinsic tooth stain.* International dental journal, 2010. **54**(5): p. 321-325.
23. Group, Y.M. *Tooth Anatomy* 2011 [cited 2011 11/11]; Available from: <http://www.yalemedicalgroup.org/stw/Page.asp?PageID=STW026281>.
24. Dictionary, M. *Periodontium.* 2007 [cited 2015 26th March 2015]; Available from: <http://medical-dictionary.thefreedictionary.com/periodontium>.
25. Moore, W.J., *Biology of the Periodontium.* Journal of Anatomy, 1970. **106**(Pt 3): p. 579-580.
26. Ho, S.P., et al., *The tooth attachment mechanism defined by structure, chemical composition and mechanical properties of collagen fibers in the periodontium.* Biomaterials, 2007. **28**(35): p. 5238-5245.

27. Costa Da Almada, G.R., G. F. Molina, C. A. Meschiari, F. Barbosa de Sousa, R. F. Gerlach. , *Analysis of enamel microbiopsies in shed primary teeth by Scanning Electron Microscopy (SEM) and Polarizing Microscopy (PM)*. Science of the Total Environment, 2009. **407**(1): p. 5169-5175.
28. CHANDRA, *Textbook of Dental and Oral Anatomy Physiology and Occlusion*. 2004: . Jaypee Brothers Publishers.
29. DEPARTMENT OF CONSERVATIVE DENISTRY AND ENDODONTICS. KVGDC, S. *Types of Dentine* [cited 2015 25th March ]; Available from: <http://image.slidesharecdn.com/dentin-150125010616-conversion-gate02/95/dentin-46-638.jpg?cb=1422169650>.
30. J .H. Kinney, S.J.M., and G.W. Marshall, *THE MECHANICAL PROPERTIES OF HUMAN DENTIN: A CRITICAL REVIEW AND RE-EVALUATION OF THE DENTAL LITERATURE*. Critical Reviews in Oral Biology & Medicine, 2003. **14**: p. 13-29.
31. Thompson, V.P. and N.R.F.A. Silva, *1 - Structure and properties of enamel and dentin*, in *Non-Metallic Biomaterials for Tooth Repair and Replacement*, P. Vallittu, Editor. 2013, Woodhead Publishing. p. 3-19.
32. Zheng, J., et al., *Effect of water content on the nanomechanical properties and microtribological behaviour of human tooth enamel*. Wear, 2013. **301**(1-2): p. 316-323.
33. Lewis, R., R.S. Dwyer-Joyce, and M.J. Pickles, *Interaction between toothbrushes and toothpaste abrasive particles in simulated tooth cleaning*. Wear, 2004. **257**(3-4): p. 368-376.
34. Addy, M., S. Goodfield, and A. Harrison, *The use of acrylic to compare the abrasivitant stain removal properties of toothpastes*. Clinical Materials, 1991. **7**(3): p. 219-225.
35. Joiner, A., *14 - Colorimetric evaluation of tooth colour*, in *Colour Measurement*, M.L. Gulrajani, Editor. 2010, Woodhead Publishing. p. 343-e1.
36. Porter, A.E., R. K. Nalla, A. Minor, J. R. Jincheck, C. Kisielowski, V. Radmilovic, J. H. Kinney, A. P. Tomsia, R. O. Ritchie, *A transmission electron microscopy study of mineralization in age-induced transparent dentin*. Biomaterials, 2005. **26**(36): p. 7650-7660.
37. MJR, I.A.I.N., *The density and branching of dentinal tubules in human teeth*. Archives of Oral Biology, 1996. **41**(5): p. 410-412.

38. Carvalho, R.M., M. Yoshiyama, P. D. Brewer, D. H. Pashley, *Dimensional changes of demineralized human dentine during preparation for scanning electron microscopy*. Archives of Oral Biology, 1996. **41**(4): p. 379-386.
39. Frank, R.M., *Ultrastructure of human dentine 40 years ago - progress and perspectives*. Archives of Oral Biology, 1999. **44**(2): p. 979-984.
40. Nore, J.E., R. J. Feigal, J. B. Dennison, C. A. Edwards, *Dentine bonding: SEM comparison of the dentin surface in primary and permanent teeth*. Pediatric Dentistry, 1997. **19**(4): p. 246-252.
41. Koester, K.J., J. W. Ager III, R. O. Ritchie, *The effect of aging on crack-growth resistance and toughening mechanisms in human dentine*. Biomaterials, 2008. **29**(10): p. 1318-1328.
42. Wong, Y.X.Y., *Morphological/chemical imaging of demineralized dentin layer in its natural, wet state*. Dental Materials, 2010. **26**(5): p. 433-442.
43. Hoshi, K., S. Ejiri, W. Probst, V. Seybold, T. Kamino, T. Yaguchi, N. Yamahira, H. Ozawa, *Observation of human dentine by focused ion beam and energy-filtering transmission electron microscopy*. Journal of Microscopy, 2001. **20**(1): p. 44-49.
44. TOMPS. *Omya 5AV*. [cited 2015 29th March ]; Available from: <http://www.tomps.com/calcium-carbonate-omya-bl-og-p-76.html>.
45. Chemicals, S. *S2E*. [cited 2015 29th March ]; Available from: <http://www.solvaychemicals.com/EN/products/pcc/FineUncoatedPCC.aspx>.
46. Minerals, S. *Sturcal PCC*. [cited 2015 29th March ]; Available from: <http://www.mineralstech.com/Pages/SMI/Personal-Care.aspx>.
47. MineralTech. *CalEssence 70 PCC*. 2013 [cited 2015 19th April]; Available from: <http://www.mineralstech.com/Documents/MTI/MSDS%26TechnicalDataSheets/Adams/AdamsSPCCProducts/CalEssence70.pdf>.
48. HerbaFoods. *Dietary Fibres*. [cited 2015 29th March ]; Available from: [http://www.herbafood.de/fileadmin/user\\_upload/Veroeffentlichungen/Functional\\_Properties\\_Herbacel\\_AQ\\_Plus\\_Fruit\\_Fibres.pdf](http://www.herbafood.de/fileadmin/user_upload/Veroeffentlichungen/Functional_Properties_Herbacel_AQ_Plus_Fruit_Fibres.pdf)  
<http://www.herbafood.de/en/products/dietary-fibres/herbacel-aq-plus/index.htm>.

49. Materials, H. *Zeodent 113*. [cited 2015 29th March]; Available from: <http://www.hubermaterials.com/userfiles/files/product-finder/spec/Zeodent 113 Precipitated Silica.pdf>.
50. Lubrizol. *Carbopol polymers: Overview*. [cited 2015 29th March ]; Available from: <https://www.lubrizol.com/Life-Science/Documents/Pharmaceutical/Bulletins/Bulletin-24---Formulating-Toothpaste-Using-Carbopol-Polymer.pdf>.
51. Nanotechnik, K., *MM3A Micromanipulator System Manual*. 2005.
52. Zheng, J., Z. R. Zhou, *Friction and wear behaviour of human teeth under various wear conditions*. . Tribology International, 2007. **40**(1): p. 278-284.
53. Da Silva, W.M., J. D. B. de Mello, *Using parallel scratches to simulate abrasive wear*. Wear, 2009. **267**(11): p. 1987-1997.
54. Evstigneev, K.M.a.P.R.M., *Modelling of nanoparticle manipulation by AFM: Rolling vs. sliding regimes*. EPL. **101**.
55. H. M. J. Keeling D. L., F.R.H.J., Beton P. H., Hobbs C. and Kantorovich L, *Nanoparticle manipulation*. Phys. Rev Lett, 2005: p. 94.
56. M. H. Sitti, H., *Controlled pushing of nanoparticles: modelling and experiments*. IEEE/ASME Transactions on Mechatronics. **5**.
57. Wright, J., *The Ethics of Economic Rationalism*. Business & Economics. 203: UNSW Press.
58. Berger, A., *A Strategic Analysis of Colgate's toothpaste product line: Marketing Strategy (Google eBook)*. 2011: GRIN Verlag.
59. Yongsong Xie, B.B., *Effects of particle size, polishing pad and contact pressure in free abrasive polishing*. Wear, 1996. **200**(1-2): p. 281-295.
60. El-Tayeb, N.S.M. and B.F. Yousif, *Evaluation of glass fiber reinforced polyester composite for multi-pass abrasive wear applications*. Wear, 2007. **262**(9-10): p. 1140-1151.
69. Ruijeven, M., G. Dalen, J.N., S. Regismond, *Imaging of Plant Materials for food Emulsion Structuring: Acryo-SEM and CSLM Study*. G.I.T. Imaging and Microscopy, 2009. **4**.
70. El-Tayeb, N.S.M. and B.F. Yousif, *Evaluation of glass fiber reinforced polyester composite for multi-pass abrasive wear applications*. Wear, 2007. **262**(9-10): p. 1140-1151.

71. Ashcroft, A.T., L.J. Brennan, and W.J. Wilson, *Oral care compositions*. 2014, Google Patents.
72. Meuramt, G., *ADVANCES IN FOOD RESEARCH*. 1964: Elsevier Science.
73. Bottenberg, P., *Development and Testing of Bioadhesive, Fluoride-containing Slow-release Tablets for Oral Use*. *Journal of Pharmacy and Pharmacology*, 1991. **43**(7): p. 457-464.



Table 16: Breakdown of ingredients for silica pastes

		B21	B22	B23	B24	J21	J22	J23	J24	J25	J26	J233	J236	J27	J28	J29
1	Abrasive silica	Zeodent 113	13	13	13	13	13	13	13	13	13	13	13	13	13	0
2	AC777	AC777	0	0	0	0	0	0	0	0	0	0	0	0	0	0
3	Thickening silica	Zeodent 165	6	6	6	6	6	6	6	6	6	6	6	6	6	6
4		Carrageenan	0	0	0	0	0	0	0	0	0	0	0	0	0	0
5		Xanthan gum	1.25	0	1.25	0	0	0	0	0	0	0	0	0	0	0
6		Carbomer2984	0	0	0.2	0.2	0.2	0	0	0.2	0.2	0.2	0.2	0	0	0.2
7	Structurants	Carbomer Ultraz 20	0	0	0	0	0	0.2	0	0	0	0	0	0	0	0
8		Carbomer Ultraz 21	0	0	0	0	0	0	0.2	0	0	0	0	0	0	0
9		Black Sheep Gel	0	0	0	0	0	0	0	0	0.2	0	0	0	0	0
10		SLS Gel	0	0	0	0	0	0	0	0	0.2	0	0	0	0	0
11		Easy Gel	0	0	0	0	0	0	0	0	0.2	0	0	0	0	0
12	Surfactant	steareth-30	3	3	3	3	3	3	3	3	3	3	3	3	3	3
13	Sweetener	Sodium Saccharin	0.1	0.1	0.1	0.1	0.1	0.1	0.1	0.1	0.1	0.1	0.1	0.1	0.1	0.1
14	Fluoride source	Sodium fluoride	0.32	0.32	0.32	0.32	0.32	0.32	0.32	0.32	0.32	0.32	0.32	0.32	0.32	0.32
15	Opacifier	Titanium Dioxide	0.5	0.5	0.5	0.5	0.5	0.5	0.5	0.5	0.5	0.5	0.5	0.5	0.5	0.5
16	Flavour	Mint flavour 17985667	0.7	0.7	0.7	0.7	0.7	0.7	0.7	0.7	0.7	0.7	0.7	0.7	0.7	0.7
17	Preservative	Sodium Benzoate	0.15	0.15	0.15	0.15	0.15	0.15	0.15	0.15	0.15	0.15	0.15	0.15	0.15	0.15
18		Acid Citric	0	0	0	0	0	0	0	0	0	0	0	0	0	0
19	Buffer system	Disodium Phosphate	0.41	0.41	0.41	0.41	0.41	0.41	0.41	0.41	0.41	0.41	0.41	0.41	0.41	0.41
20		Sodium phosphate	1	1	1	1	1	1	1	1	1	1	1	1	1	1
21		Aqua	41.62	41.62	41.62	41.62	41.62	41.62	41.62	41.62	41.62	41.62	41.62	41.62	41.62	41.62
22	Solvents	Glycerin 9091	5	5	5	5	5	5	5	5	5	5	5	5	5	5
23		Sorbitol 70/70	28	28	28	28	28	28	28	28	28	28	28	28	28	28

APPENDICES

Appendix A:

## **Appendix B:**

### **Information sheet:**

#### **Dental de-scaling and surface cleaning research**

You are being asked to participate in a research study. The research requires no involvement on your part, only your consent for removed teeth to be submitted for study before being destroyed. Before you give your consent, please read the following information.

#### **Investigators**

The primary researcher for this study is Chris Rose (MEng) of Sheffield University, Mechanical Engineering Dept. The project will be supervised by Professor Dwyer-Joyce (Head of Dept.) who will have access to findings and results.

#### **Purpose of the Study**

This study aims to better understand the effects of novel dental technology and aid in the development of more proficient de-scaling technology. Using real dental samples within trials will allow for representative results and a better appreciation of surface conditions via treatment.

#### **Confidentiality**

Donated samples will be dealt with anonymously; your dentist will not pass on any sensitive or personal information relating to the donor. By signing this form you give permission only for your age and sex to be made available to the researchers (Chris Rose/Raisa Karolia). Any photographs or videos of processed teeth will provide no information that may be traceable to the donor (recordings are used solely to highlight the efficacy of the cleaning process and provide a comparison between cleaning methods). After samples have been studied they will be destroyed.

#### **Voluntary Nature of Participation**

Participation in this study is voluntary. Your choice of whether or not to participate will not influence your future relations with Winfield, Rose and Woods Dental Practice or Sheffield University.

#### **Questions about the Study**

If you have any questions about the research which your Dentist is not able to satisfactorily answer you may contact Chris Rose/Raisa Karolia on 0114 2227897.

### **Sample donation consent form:**

#### **Agreement:**

Your signature below indicates that you have read the information in this agreement and have had a chance to ask any questions you have about the study. Your signature also indicates that you agree to the donation (for study) of the removed teeth.

You have been told that by signing this consent agreement you are not giving up any of your legal rights.

\_\_\_\_\_  
Name of Participant (please print)

\_\_\_\_\_  
Signature of Participant

\_\_\_\_\_  
Date

\_\_\_\_\_  
Signature of Investigator

\_\_\_\_\_  
Date



The University Of Sheffield.

Department Of Mechanical Engineering.

---

**- APPLICATION IS UNCONDITIONALLY APPROVED -**

\*\*\*\*\*

1 June 2011

Mr Chris Rose  
Mechanical Engineering

Dear Mr Rose,

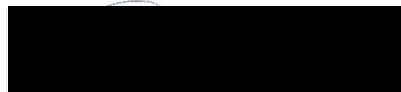
**PROJECT TITLE: 'Dental de-scaling and surface cleaning using acoustic waves'**

On behalf of the University ethics reviewers who reviewed your project, I am pleased to inform you that on 1 June 2011 the above-named project was unconditionally approved on ethics grounds, on the basis that you will adhere to the following document that you submitted for ethics review:

- University research ethics application form (*11 June 2011*)
- Participant information sheet (*11 June 2011*)
- Participant consent form (*to be signed by participant, 11 June 2011*)

If during the course of the project you need to deviate significantly from the above-approved document please inform me since written approval will be required. Please also inform me should you decide to terminate the project prematurely.

Yours sincerely



Mrs Galina Balikhin  
Ethics Administrator



THE QUEEN'S  
ANNIVERSARY PRIZES  
FOR HIGHER AND FURTHER EDUCATION  
1998 2000 2002

### Appendix C:

**Table 17:** Table showing modal, average and range of particle sizes obtained from laser diffraction and SEM (from 3 repeated tests and confirmed using a minimum of 10 SEM micrographs).

Particle Name	As Received		
	Modal Particle diameter (µm)	Range of particle size (µm)	Average particle size (µm)
CalEssence 70	0.70	0.50-0.98	0.67
Sturcal F	1.60	0.51-2.45	1.78
S2E	3.45	2.67-3.75	3.45
Albafil	3.60	3.56-3.67	3.65
Rods	6.02	1.34-6.55	6.00
Sturcal L	6.73	5.66-7.01	7.83
Omya 5AV	7.85	0.50-10.56	8.03

Table 17 shows there is little difference in size within each set of PCC particles as received, due to its regulated manufacture compared to GCCs.

### Appendix D:

**Table 18:** RDA of silica pastes, provided by the research team at Unilever Port Sunlight

Paste Name	RDA
BZ1	67.5
BZ2	64.5
BZ3	57.3
BZ4	78.7
JZ1	78.3
JZ2	100.8
JZ3	98.6
JZ4	92.4
JZ5	98.8
JZ26	70.6
JZ33	75.8
JZ36	77.8